Lecture Notes in Electrical Engineering 239

Ivan Zelinka
Pandian Vasant
Nader Barsoum
Editors

Power, Control and Optimization

Springer

Lecture Notes in Electrical Engineering

Volume 239

For further volumes:
http://www.springer.com/series/7818

Ivan Zelinka · Pandian Vasant
Nader Barsoum
Editors

Power, Control and Optimization

Springer

Editors
Ivan Zelinka
Department of Computer Science
Faculty of Electrical Engineering
and Computer Science VŠB-TUO
Ostrava-Poruba
Czech Republic

Nader Barsoum
Department of Engineering
and Information Technology
University Malaysia Sabah
Kota Kinabalu
Malaysia

Pandian Vasant
Department of Fundamental
and Applied Sciences
University Technology Petronas
Tronoh
Malaysia

ISSN 1876-1100 ISSN 1876-1119 (electronic)
ISBN 978-3-319-00205-7 ISBN 978-3-319-00206-4 (eBook)
DOI 10.1007/978-3-319-00206-4
Springer Cham Heidelberg New York Dordrecht London

Library of Congress Control Number: 2013937092

Printed on acid-free paper

Springer is part of Springer Science+Business Media (www.springer.com)

Foreword

Since the beginning of our technologies, we have been confronted with numerous technological challenges such as finding the optimal solution of various problems including control technologies, power sources construction, intelligent buildings, and energy distribution among others. The first electrical energy distribution network in USA, mechanical, electronical, or computational controllers can be mentioned as an example. Technological development of those and related areas has had and continues to have a profound impact on our civilization and life style.

Therefore, this book based on selected articles of international conference "Power, Control and Optimization", edited by Ivan Zelinka, Pandian Vasant, and Nader Barsoum, is a timely volume to be welcomed by the community focused on power control and optimization as well as computational intelligence community and beyond.

The book consists of 11 selected papers and starts with a very interesting papers about pseudo-gradient based particle swarm optimization method for nonconvex economic dispatch. Readers can also find another interesting papers about energy consumption impacted by climate, mathematical modeling of the influence of thermal power plant on the aquatic environment, investigation of cost reduction in residential electricity bill using electric vehicle at peak times or allocation, and size evaluation of distributed generation using ANN model and among the others.

Chapter authors are to the best of our knowledge the originators or closely related to the originators of presented ideas and its applications. Hence, this book certainly is one of few books discussing the benefit from intersection of those modern and fruitful scientific fields of research.

We hope that the book will be an instructional material for senior undergraduate and entry-level graduate students working in the area of power technologies, energy distribution or/and design of energy systems and its impact on environment. The book will also be a resource and material for practitioners who want to apply problems of power systems and energy distribution to solve real-life problems in their challenging applications.

The decision to write this book was based on few facts. The main one is that the research field on power systems and energy distribution, use and its impact on life is an interesting area, which is under intensive research by many other branches of

science today. This book is written to contain simplified versions of experiments with the aim to show how, in principle, problems about power systems can be solved.

It is obvious that this book does not encompass all aspects of power systems and energy distribution fields of research due to limited space. Only the main ideas and results of selected papers are reported here. The authors and editors hope that the readers will be inspired to do their own experiments and simulations, based on information reported in this book, thereby moving beyond the scope of the book.

This book is devoted to the studies of common and related subjects in intensive research fields of power technologies. For these reasons, we believe that this book will be useful for scientists and engineers working in the above-mentioned fields of research and applications.

January 2013

Ivan Zelinka
Pandian Vasant
Nader Barsoum

Contents

Pseudo-Gradient Based Particle Swarm Optimization Method for Nonconvex Economic Dispatch

Vo Ngoc Dieu, Peter Schegner and Weerakorn Ongsakul

Abstract This chapter proposes a pseudo-gradient based particle swarm optimization (PGPSO) method for solving nonconvex economic dispatch (ED) including valve point effects, multiple fuels, and prohibited operating zones. The proposed PGPSO is based on the self-organizing hierarchical particle swarm optimizer with time-varying acceleration coefficients (HPSO-TVAC) with position of particles guided by a pseudo-gradient. The pseudo-gradient here is to determine an appropriate direction for the particles during their movement so that they can quickly move to an optimal solution. The proposed method has been tested on several systems and the obtained results are compared to those from many other methods available in the literature. The test results have indicated that the proposed method can obtain less expensive total costs than many others in a faster computing manner, especially for the large-scale systems. Therefore, the proposed PGPSO is favorable for online implementation in the practical ED problems.

Keywords Economic dispatch · Multiple fuel options · Particle swarm optimization · Prohibited zones · Pseudo gradient · Valve point effects

V. N. Dieu (✉)
Department of Power Systems, Ho Chi Minh City University of Technology,
Ho Chi Minh, Vietnam
e-mail: vndieu@gmail.com

P. Schegner
Institute of Electrical Power Systems and High Voltage Engineering,
Technische Universität Dresden, 01069 Dresden, Germany
e-mail: schegner@ieeh.et.tu-dresden.de

W. Ongsakul
Energy Field of Study, Asian Institute of Technology,
Pathumthani 12120, Thailand
e-mail: ongsakul@ait.asia

I. Zelinka et al. (eds.), *Power, Control and Optimization*, Lecture Notes in Electrical Engineering 239, DOI: 10.1007/978-3-319-00206-4_1,

Nomenclature

a_i, b_i, c_i	fuel cost coefficients of unit i
e_i, f_i	fuel cost coefficients of unit i reflecting valve-point effects
a_{ij}, b_{ij}, c_{ij}	fuel cost coefficients for fuel type j of unit i
e_{ij}, f_{ij}	fuel cost coefficients for fuel type j of unit i reflecting valve-point effects
B_{ij}, B_{0i}, B_{00}	B-matrix coefficients for transmission power loss
c_{1i}, c_{1f}	initial and final values of cognitive acceleration factor, respectively
c_{2i}, c_{2f}	initial and final values of social acceleration factor, respectively
c_1, c_2	cognitive and social acceleration coefficients, respectively
DR_i	ramp down rate limit of unit i
$g_p\left(x_{id}^{(k)}\right)$	pseudo-gradient at point k for particle d of element i
N	total number of generating units
n_i	number of prohibited operating zones of unit i
N_p	number of particles
P_D	total system load demand
P_i	power output of unit i
$P_{i,\text{high}}$	highest possible power output of generator i
$P_{i,\text{low}}$	lowest possible power output of generator i
$P_{i,\max}$	maximum power output of generator i
$P_{i,\min}$	minimum power output of generator i
$P_{ij,\min}$	minimum power output for fuel j of generator i
P_L	total transmission loss
P_{ik}^{l}	lower bound for prohibited zone k of generator i
P_{ik}^{u}	upper bound for prohibited zone k of generator i
UR_i	ramp up rate limit of unit i
v_{id}	velocity of particle d for element i
x_{id}	position of particle d for element i
Ω	set of units with prohibited operating zones
$\delta(x_{id})$	direction indicator for position of element i in particle d

1 Introduction

The economic dispatch (ED) is used to determine the economical real power output of the online units so as their total production cost is minimized while satisfying the unit and system operating constraints [1, 2]. For mathematical convenience, the objective function of the ED problem was approximated by a single quadratic function [3], which is differentiable. Nevertheless, the input-output characteristics of thermal generating units are more complicated due to the effects of valve point loadings [4], multiple fuels [5], or prohibited zones [6].

Therefore, the practical ED problem should be formulated as a non-convex objective function subject to complex constraints, which cannot be directly solved by the mathematical programming techniques. Hence, more advanced techniques have to be developed to deal with the optimization problem with multiple minima.

Several conventional methods have been applied for solving ED problems such as gradient search, Newton's method, dynamic programming (DP) [3], hierarchical approach based on the numerical method (HNUM) [5], decomposition method (DM) [6], lambda iteration method [7], Maclaurin series-based Lagrangian (MSL) method [8], and novel direct search (NDS) [9]. Among these methods, the MSL and NDS methods can directly deal with a non-convex ED problem with non-differentiable objective. Although these methods can quickly find a solution for the problem, the obtained results are still the local optimum solution, especially for the large-scale systems. In general, the conventional methods are not effective for implementation on the ED problems with non-differentiable objective function. Recently, many methods based on artificial intelligence have been developed for solving ED problems such as Hopfield neural network (HNN) [10, 11], genetic algorithm (GA) [12], evolutionary programming (EP) [13], evolutionary algorithm (EA) [14, 15], differential evolution (DE) [16], artificial bee colony (ABC) algorithm [17], artificial immune system (AIS) [18], biogeography-based optimization (BBO) [19], and particle swarm optimization (PSO) [20–27]. Among of them, the HNN method which is based on the minimization of its energy function can be only applied to the convex optimization problems with differentiable objective function. Although this method can be implemented on large-scale problems, it suffers many drawbacks such as large number of iterations, linear constraint requirement, and local optimum solution. The others are the meta-heuristic search methods which are based on a population for searching an optimal solution for the problems. These search methods can overcome the drawbacks of the HNN and conventional methods due to their ability to find near optimal solution for non-convex optimization problems. However, for the large-scale and non-smooth problems with multiple minima these methods may suffer low solution quality and long computational time. Of all the meta-heuristic search methods, PSO is the most popular method implemented for solving different ED problems due to its powerful search ability, especially for nonconvex problems [21]. Several improvements for PSO method have been proposed for solving nonconvex ED problems such as quantum-inspired PSO (QPSO) [22], self-organizing hierarchical PSO (SOH_PSO) [23], modified PSO (MPSO) [24, 25], PSO with modified stochastic acceleration factors (PSO-MSAF) [26], new PSO with local random search (NPSO-LRS) [27], and simulated annealing like PSO (SA-PSO) [28]. These improved PSO-based methods can obtain higher solution quality than the conventional PSO method for complicated nonconvex optimization problems. In addition to the single methods, hybrid methods have been also developed for dealing with the nonconvex ED problems such as hybrid technique integrating the uniform design with the genetic algorithm (UHGA) [29], combining of chaotic differential evolution and quadratic programming (DEC-SQP) [30, 31], self-tuning hybrid differential evolution (self-tuning HDE) [32], and fuzzy adaptive particle swarm optimization algorithm with

Nelder–Mead simplex search (FAPSO-NM) [33]. These hybrid methods utilize the advantages of each element method to enhance their search ability for the complex problems. Consequently, they become powerful search methods for obtaining higher solution quality than the element methods. However, these hybrid methods may be more complicated and slower than the element methods due to combination of several operations.

In this chapter, a pseudo-gradient based particle swarm optimization (PGPSO) method is proposed for solving nonconvex ED problems considering valve point effects, multiple fuels, and prohibited operating zones. The proposed PGPSO is based on the self-organizing hierarchical particle swarm optimizer with time-varying acceleration coefficients (HPSO-TVAC) [34] with position of particles guided by a pseudo-gradient [35]. The pseudo-gradient here is to determine an appropriate direction for the particles during their movement so that they can quickly move to an optimal solution. The proposed method has been tested on several systems and the obtained results are compared to those from many other methods available in the literature.

The remaining organization the chapter is as follows. The formulation of nonconvex ED problems with valve point loading effects, multiple fuels, and prohibited operating zones are presented in Sect. 2. The PGPSO method is addressed in Sect. 3. The implementation of the PGPSO method to the nonconvex ED problems is described in Sect. 4. The numerical results are followed in Sect. 5. Finally, the conclusion is given.

2 Problem Formulation

The objective of an ED problem is to minimize the total cost of thermal generating units of a system over some appropriate period (1 h typically) while satisfying various constraints including system and unit operating constraints. Mathematically, the nonconvex ED problems are formulated as follows.

2.1 ED Problem with Valve Point Effects

The ED problem with valve point effects (VPE) is a non-smooth and non-convex problem with multiple minima due to taking into consideration of ripples in the heat-rate curve of boilers. The model of valve point loading effects has been proposed in Walter and Sheble [36] by introducing a sinusoidal function added to the quadratic fuel cost function. The objective of the problem is written as:

$$\text{Min } F = \sum_{i=1}^{N} F_i(P_i) \tag{1}$$

where the fuel cost function of unit i with VPE is represented by Sinha et al. [13]:

$$F_i(P_i) = a_i + b_i P_i + c_i P_i^2 + \left| e_i \times \sin(f_i \times (P_{i,\min} - P_i)) \right| \tag{2}$$

subject to

1. *Real power balance*: The total real power output of generating units satisfies total real load demand plus power loss:

$$\sum_{i=1}^{N} P_i = P_D + P_L \tag{3}$$

where the power loss P_L can be approximately calculated by Kron's formula [3]:

$$P_L = \sum_{i=1}^{N} \sum_{j=1}^{N} P_i B_{ij} P_j + \sum_{i=1}^{N} B_{0i} P_i + B_{00} \tag{4}$$

2. *Generator capacity limits*: The real power output of generating units should be within between their upper and lower bounds by:

$$P_{i,\min} \le P_i \le P_{i,\max} \tag{5}$$

2.2 ED Problem with Multiple Fuels

In the ED problem with multiple fuels (MF), the piecewise quadratic function is used to represent the multiple fuels which are available for each generating unit [5]. The fuel cost function of unit i is defined as [10]:

$$F_i(P_i) = \begin{cases} a_{i1} + b_{i1} P_i + c_{i1} P_i^2, \text{ fuel } 1, \ P_{i,\min} \le P_i \le P_{i1} \\ a_{i2} + b_{i2} P_i + c_{i2} P_i^2, \text{ fuel } 2, \ P_{i1} < P_i \le P_{i2} \\ \cdots \\ a_{ij} + b_{ij} P_i + c_{ij} P_i^2, \text{ fuel } j, \ P_{ij-1} < P_i \le P_{i,\max} \end{cases} \tag{6}$$

For generator i with j fuel options in (6), its cost curve is divided into j discrete segments between lower limit $P_{i,\min}$ and upper limit $P_{i,\max}$, in which each fuel type is represented by a quadratic function with lower power output limit P_{ij-1} and upper power output limit P_{ij}.

The objective of the ED problem with multiple fuels is to minimize total generator cost (1) with fuel cost function in (6) subject to the real power balance constraint (3) and generator capacity limits (5).

2.3 ED Problem with Both Valve Point Effects and Multiple Fuels

Thermal generating units can be supplied with multiple fuel sources and their boilers have also valve points for controlling their power outputs [12]. The fuel cost function of generating unit i is represented as:

$$F_i(P_i) = \begin{cases} F_{i1}(P_i), \text{ fuel } 1, \ P_{i,\min} \le P_i \le P_{i1} \\ F_{i2}(P_i), \text{ fuel } 2, \ P_{i1} < P_i \le P_{i2} \\ \cdots \\ F_{ij}(P_i), \text{ fuel } j, \ P_{ij-1} < P_i \le P_{i,\max} \end{cases} \tag{7}$$

where the fuel cost function for fuel type j of unit i is determined by:

$$F_{ij}(P_{ij}) = a_{ij} + b_{ij}P_{ji} + c_{ij}P_{ij}^2 + \left|e_{ij} \times \sin(f_{ij} \times (P_{ij,\min} - P_{ij}))\right| \tag{8}$$

The objective of the ED problem with both valve point effects and multiple fuels is to minimize total generator cost (1) with fuel cost function in (7) subject to the real power balance constraint (3) and generator capacity limits (5).

2.4 ED Problem with Prohibited Operating Zones

In some practical cases, thermal generating units may have prohibited operating zones (POZ) due to physical constraints on components of units. Consequently, the whole operating region of a generating unit with prohibited operating zones will be broken into several isolated feasible sub-regions [20].

The fuel cost function for each unit in the ED problem with POZ is a quadratic function as in (2) neglecting the sinusoidal term and the equality and inequality constraints for this problem include the real power balance constraint (3), generator capacity limits (5) for units having no POZ, and

1. *Prohibited operating zones*: For generating units with POZ, their entire feasible operating zones are decomposed in feasible sub-regions and their feasible operating points should be in one of the sub-regions as follows:

$$P_i \in \begin{cases} P_{i,\min} \le P_i \le P_{i1}^l \\ P_{ik-1}^u \le P_i \le P_{ik}^l,\ k = 2, \ldots, n_i \\ P_{in_i}^u \le P_i \le P_{i,\max} \end{cases} ; \forall i \in \Omega \tag{9}$$

2. *Ramp rate constraints:* The increased or decreased power output of a unit from its initial operating point to the next one should not exceed its ramp up and down rate limits. The ramp rate constraints are determined by:

$$P_i - P_{i0} \le UR_i, \text{ if generation increases} \tag{10}$$

$$P_{i0} - P_i \le DR_i, \text{ if generation decreases} \tag{11}$$

3 Pseudo-Gradient Based Particle Swarm Optimization

3.1 Self-organizing Hierarchical Particle Swarm Optimizer

PSO has become one of the most popular methods applied in various optimization problems due to its simplicity and capability to find near optimal solution, especially for complicated and non-convex problems [37]. Several improvements have been made to enhance the search ability of PSO to deal with more complicated and larger-scale problems [21]. In this chapter, the new improvement is based on the self-organizing hierarchical particle swarm optimizer with time-varying acceleration coefficients (HPSO-TVAC) [34]. For the implementation of the HPSO-TVAC on a n-dimension optimization problem, the position and velocity vectors of particle d are represented by $x_d = [x_{1d}, x_{2d}, \ldots, x_{nd}]$ and $v_d = [v_{1d}, v_{2d}, \ldots, v_{nd}]$, respectively. Suppose that the best previous position of particle d is represented by $pbest_d = [p_{1d}, p_{2d}, \ldots, p_{nd}]$ and the best particle among all particles is represented by $gbest$, the velocity and position of each particle in the next iteration $(k + 1)$ for are calculated as follows:

$$v_{id}^{(k+1)} = c_1^{(k)} \times rand_1 \times \left(pbest_d^{(k)} - x_{id}^{(k)}\right) + c_2^{(k)} \times rand_2 \times \left(gbest^{(k)} - x_{id}^{(k)}\right) \tag{12}$$

if $v_{id} = 0$ and $rand_3 < 0.5$ then

$$v_{id} = rand_4 \times v_{id,\max} \text{ else } v_{id} = -rand_5 \times v_{id,\max} \tag{13}$$

$$x_{id}^{(k+1)} = x_{id}^{(k)} + v_{id}^{(k+1)} \tag{14}$$

where $rand_i$, $i = 1, 2, \ldots, 5$ are randomly generated numbers in [0, 1] and the cognitive and social acceleration coefficients at iteration k are determined by:

$$c_1^{(k)} = (c_{1f} - c_{1i})\frac{k}{Iter_{\max}} + c_{1i} \tag{15}$$

$$c_2^{(k)} = (c_{2f} - c_{2i})\frac{k}{Iter_{\max}} + c_{2i} \tag{16}$$

where k is the iteration counter and $Iter_{\max}$ is the maximum number of iterations.

The upper and lower bounds for each particle position x_{id} are limited by the maximum and minimum limits of the variable represented by the particle, respectively. The velocity of each particle is limited in $[-v_{id,\max}, v_{id,\max}]$, $i = 1, \ldots, N$, $d = 1, \ldots, N_p$, where the maximum and minimum velocities for element i of particle d in the search space is determined by:

$$v_{id,\max} = R \times (x_{id,\max} - x_{id,\min}) \tag{17}$$

$$v_{id,\min} = -v_{id,\max} \tag{18}$$

where $v_{id,\max}$ and $v_{id,\min}$ are the maximum and minimum limits for element i of particle d and R is the limit coefficient for maximum velocity of particles.

3.2 Pseudo-Gradient Concept

Pseudo-gradient is to determine the search direction for each individual in population based methods [38]. The advantage of the pseudo-gradient is that it can provide a good direction in the search space of a problem without requiring the objective function to be differentiable. Therefore, the pseudo-gradient method is suitable for implementation on the meta-heuristic search methods for solving non-convex problems with multiple minima.

For a non-differentiable n-dimension optimization problem with objective function $f(x)$ where $x = [x_1, x_2, \ldots, x_n]$, a pseudo-gradient $g_p(x)$ for the objective function is defined as follows [35]: Supposed that $x_k = [x_{k1}, x_{k2}, \ldots, x_{kn}]$ is a point in the search space of the problem and it moves to another point x_l. There are two abilities for this movement.

1. If $f(x_l) < f(x_k)$, the direction from x_k to x_l is defined as the *positive direction*. The pseudo-gradient at point x_l is determined by:

$$g_p(x_l) = [\delta(x_{l1}), \delta(x_{l2}), \ldots, \delta(x_{ln})]^T \tag{19}$$

where $\delta(x_{li})$ is the direction indicator of element x_i moving from point k to point l defined by:

$$\delta(x_{li}) = \begin{cases} 1 & \text{if } x_{li} > x_{ki} \\ 0 & \text{if } x_{li} = x_{ki} \\ -1 & \text{if } x_{li} < x_{ki} \end{cases} \tag{20}$$

2. If $f(x_l) \geq f(x_k)$, the direction from x_k to x_l is defined as the *negative direction*. The pseudo-gradient at point x_l is determined by:

$$g_p(x_l) = 0 \tag{21}$$

The pseudo-gradient can also indicate a good direction similar to the conventional gradient in the search space based on the two last points. From the definition, if $g_p(x_l) \neq 0$, it implies that a better solution for the objective function could be found in the next step based on the direction indicated by the pseudo-gradient $g_p(x_l)$ at point l. Otherwise, the search direction at this point should be changed.

3.3 Proposed Pseudo-Gradient Based Particle Swarm Optimization

In this chapter, the proposed PGPSO is a combination of the HPSO-TVAC and pseudo-gradient. For implementation of the pseudo-gradient in the HPSO-TVAC, the two points considered here corresponding to x_k and x_l are $x^{(k)}$ and $x^{(k+1)}$, respectively. Therefore, the updated position for particles in (14) is rewritten as:

$$x_{id}^{(k+1)} = \begin{cases} x_{id}^{(k)} + \alpha \times \delta\left(x_{id}^{(k+1)}\right) \times \left|v_{id}^{(k+1)}\right| & \text{if } g_p\left(x_{id}^{(k+1)}\right) \neq 0 \\ x_{id}^{(k)} + v_{id}^{(k+1)} & \text{otherwise} \end{cases} \tag{22}$$

where $\alpha > 0$ is the acceleration factor for updating particle's position.

In (22), if the pseudo-gradient is non-zero, the position of the involved particle is quickly displaced to the global solution by its enhanced velocity; otherwise the position is normally updated as in (14). The value of α can be adjusted so that a particle can move faster or slower depending on the characteristic of each problem. In fact, too large value of α may lead to optimal solution ignored since the particles are at their limit positions while too small value of α may lead to particles trapped in local minima in the search space. In our experience, the proper values of α can be tuned in the range from 1 to 10.

The proposed PGPSO here is an improvement from the HPSO-TVAC method with its search capability enhanced by the pseudo-gradient. The advantage of the PGPSO is that its search capability is better than the HPSO-TVAC with the

support from the pseudo-gradient. During the search process, the particle's velocity will be accelerated if the pseudo-gradient indicates that the direction will lead to minimization of the objective function. Consequently, the particle can quickly move to the optimal position. In contrast, if the pseudo-gradient indicates that the direction will not lead to minimization of the objective function, the particle's position will be updated as the conventional PSO method. Moreover, the acceleration factor can be appropriately selected so that the particles can avoid ignoring optimal position or being trapped in local minima. Therefore, the PGPSO is a simple PSO method but more efficient than the HPSO-TVAC method, especially for nonconvex optimization problems with multiple minima.

4 Implementation of PGPSO to Nonconvex ED Problems

The proposed PGPSO here is implemented for the general problem which includes all the generator characteristics and constraints from the formulated problems. For properly handling the equality constraint of real power balance from the problem, the slack variable method is used. In addition, a heuristic search is also applied for a repairing strategy in case of prohibited zones violated. Other constraints for slack unit limits are handled in the fitness function for the problem. Therefore, all the constraints in the general problem are properly handled in the proposed PGPSO method.

4.1 Calculation of Power Output for Slack Unit

To guarantee that the equality constraint (3) is always satisfied, a slack generating unit is arbitrarily chosen and therefore its power output will be dependent on the power outputs of remaining $N - 1$ generating units in the system. The method for calculation of power output for the slack unit is given in Kuo [28].

4.2 Handling of Ramp Rate Constraints and POZ Violation

To handle the ramp rate limits, the highest and lowest possible power outputs of units are determined based on their power output limits, initial power output and ramp rate constraints as:

$$P_{i,\text{high}} = \min\{P_{i,\max}, P_{i0} + UR_i\} \tag{23}$$

$$P_{i,\text{low}} = \max\{P_{i,\min}, P_{i0} - DR_i\} \tag{24}$$

If the highest and lowest possible power outputs of a generating unit violate its POZ, the new limits should be redefined. Suppose that the highest or lowest possible power output of unit i violates its prohibited zone k, the new limit is redefined as follows:

$$P_{i,\text{high}}^{\text{new}} = \min\{P_{i,\text{high}}, P_{ik}^{l}\} \tag{25}$$

or

$$P_{i,\text{low}}^{\text{new}} = \max\{P_{i,\text{low}}, P_{ik}^{u}\} \tag{26}$$

When a unit operates in one of its prohibited zones, a repairing strategy is used to force the unit either to move toward the lower bound or upper bound of that zone. For making a decision based on the operating point of a unit located in one of its prohibited zones, the middle point of each prohibited zone P_{ik}^{m} is firstly determined by:

$$P_{ik}^{m} = \frac{P_{ik}^{l} + P_{ik}^{u}}{2} \tag{27}$$

This middle point divides a prohibited zone in two sub-zones, the left and right prohibited sub-zones with respect to the point. Therefore, the operating point P_i of unit i violating its prohibited zone k will be adjusted by:

$$P_i^{\text{new}} = \begin{cases} P_{ik}^{l} & \text{if } P_i \le P_{ik}^{m} \\ P_{ik}^{u} & \text{if } P_i > P_{ik}^{m} \end{cases} \tag{28}$$

However, when ramp rate constraints are included, the strategy for handling the POZ violation is more complicated. There are possibilities for adjusting the operating point of unit i when violating its prohibited zone k based on its initial power output P_{i0} and the violated position as follows:

- If $P_i > P_{ik}^{m}$ then

$$P_i^{\text{new}} = \begin{cases} \max\left\{P_{ik}^{u}, P_{i,\text{low}}\right\}, & \text{if } P_{i0} \ge P_{ik}^{u} \\ P_{ik}^{u}, & \text{if } P_{i0} \le P_{ik}^{l} \text{ and } P_{ik}^{u} \le P_{i,\text{high}} \\ \min\left\{P_{ik}^{l}, P_{i,\text{high}}\right\}, & \text{if } P_{i0} \le P_{ik}^{l} \text{ and } P_{ik}^{u} > P_{i,\text{high}} \end{cases} \tag{29}$$

- If $P_i < P_{ik}^{m}$ then

$$P_i^{\text{new}} = \begin{cases} \min\left\{P_{ik}^{l}, P_{i,\text{high}}\right\}, & \text{if } P_{i0} \le P_{ik}^{l} \\ P_{ik}^{l}, & \text{if } P_{i0} \ge P_{ik}^{u} \text{ and } P_{ik}^{l} \ge P_{i,\text{low}} \\ \max\left\{P_{ik}^{u}, P_{i,\text{low}}\right\}, & \text{if } P_{i0} \ge P_{ik}^{u} \text{ and } P_{ik}^{l} < P_{i,\text{low}} \end{cases} \tag{30}$$

4.3 Implementation of PGPSO

4.3.1 Initialization

A population of N_p particles is represented by $x = [x_1, x_2, \ldots, x_{Np}]$, where each particle's position $x_d = [P_{1d}, \ldots, P_{s-1d}, P_{s+1d}, \ldots, P_{Nd}]^T$ $(d = 1, \ldots, N_p)$ representing for power output of $N - 1$ generating units is initialized by:

$$x_{id}^{(0)} = (1 + rand) \times P_i^{(0)};\ i \neq s \tag{31}$$

where *rand* is a normally distributed stochastic number, $P_i^{(0)}$ is the initial operating point obtained by quadratic programming (QP) with quadratic objective function neglecting power loss, and s is the slack unit which is initially selected.

For the obtained initial solution, its upper and lower limits based on the generator limits should be satisfied:

$$x_{id} = \begin{cases} P_{i,\text{high}} & \text{if } x_{id} > P_{i,\text{high}} \\ P_{i,\text{low}} & \text{if } x_{id} < P_{i,\text{low}} \\ x_{id}^{(0)} & \text{otherwise} \end{cases};\ i \neq s \tag{32}$$

In addition, this initial solution should be also checked for POZ violation. If the violation is found, the repairing strategy in Sect. 4.2 is used to move the operating point to a feasible region. Based on the initial position of particles, the fitness function FT_d to be minimized corresponding to each particle for the considered problem is calculated:

$$FT_d = \sum_{i=1}^{N} F_i(x_{id}) + K_s \times \left(P_{sd} - P_s^{\text{lim}}\right)^2 \tag{33}$$

where K_s is the penalty factor for the slack unit, P_{sd} is the power output of the slack unit calculated from Sect. 4.1 corresponding to particle d in the population, and the power limits for the slack unit P_s^{lim} are determined based on its calculated output as follows:

$$P_s^{\text{lim}} = \begin{cases} P_{s,\text{high}} & \text{if } P_{sd} > P_{s,\text{high}} \\ P_{s,\text{low}} & \text{if } P_{sd} < P_{s,\text{low}} \\ P_{sd} & \text{otherwise} \end{cases} \tag{34}$$

where $P_{s,\text{high}}$ and $P_{s,\text{low}}$ are the highest and lowest possible power outputs of the slack unit.

The initial position is set to best value of each particle's position $pbest_d$ $(d = 1, \ldots, N_d)$ and the particle's position corresponding to the best fitness function in (33) is set to the best particle *gbest* among all particles in the population.

4.3.2 Calculation of Particle's Velocity and Position

The obtained initial position of particles is used for calculation of their velocity. The new velocity of particles is calculated as in (12–13) from the HPSO-TVAC method. The position of particles is then updated with the guidance of pseudo-gradient as in (22).

The new position of each particle should also satisfy their upper and lower limits as in (32) and the repairing strategy in Sect. 4.2 is used if any POZ violation is found. The new value of the fitness function is evaluated using (33) based on the new particle's position for determining the newly best position $pbest_d$ for each particle and best global position *gbest* among all particles.

4.3.3 Stopping Criteria

The algorithm of the proposed PGPSO is terminated when the predefined maximum number of iterations $Iter_{\max}$ is reached.

5 Numerical Results

The proposed PGPSO is tested on different systems corresponding to the formulated problems. The algorithm of the PGPSO is coded in Matlab platform and run 100 independent trials for each test case on a 2.1 GHz PC with 2 GB of RAM. In this chapter, the initial operating point is obtained by QP from optimization toolbox in Matlab.

5.1 Selection of Parameters

In the proposed PGPSO method, some parameters are predetermined for dealing with the systems such as cognitive acceleration and social factors, number of particles N_p, particle's velocity limit coefficient R, updating accelerator factor α, and maximum number of iterations $Iter_{\max}$. Among these parameters, the cognitive acceleration and social factors can be easily fixed by $c_{1i} = c_{2f} = 2.5$, $c_{2i} = c_{1f} = 0.2$ [23]. On the one hand, the penalty factor for the slack unit is large enough and set to 10^4 for all systems. On the other hand, the number of particles and maximum number of iterations depend on the dimension and complexity of problems. The number of particles is chosen in the range from twice to twenty times of the problem dimension while the maximum number of iterations is chosen in the range from 100 to 500 iterations. In this chapter, these parameters are chosen by experiments. For each problem, their value is first fixed at the low range and then increased. If the obtained result after one run is considerably improved in

Table 1 Additional parameters of PGPSO

System	No. of units	N_p	$Iter_{max}$	Initial R	α
Valve point effects	40	500	500	0.40	10.0
Multiple fuels	10	20	100	0.15	5.0
Prohibited operating zones	15	200	100	0.10	1.0
Valve point effects and multiple fuels	10	50	200	0.15	1.5
	20	50	500	0.15	2.5
	40	100	500	0.20	3.0
	80	200	500	0.10	2.0
	160	300	500	0.10	2.0

comparison with the previous one, their value will be increased. Otherwise, the obtained value is chosen as the proper value for multiple runs. In this chapter, the value of R will be reduced by 10 % from its initial value for every 100-iteration interval. By experiments, the values for the initial R and α can be chosen in a range of [0.1, 0.5] and [1, 10], respectively. For tuning R, its value is initially set to 0.1 and the step is set to 0.05 in the range [0.1, 0.25] and 0.1 in the range [0.3, 0.5].

Table 2 Solution for 40-unit system with VPE

Unit	P_{gi} (MW)	Unit	P_{gi} (MW)
1	110.8300	21	523.2797
2	110.8017	22	523.2841
3	97.4012	23	523.2808
4	179.7347	24	523.2798
5	92.6126	25	523.2801
6	139.9970	26	523.2837
7	259.6112	27	10.0000
8	284.6113	28	10.0000
9	284.6027	29	10.0037
10	130.0021	30	87.8077
11	168.8009	31	189.9993
12	168.7993	32	190.0000
13	214.7600	33	189.9986
14	304.5194	34	164.8063
15	394.2808	35	164.8018
16	394.2813	36	164.8468
17	489.2789	37	110.0000
18	489.2796	38	109.9999
19	511.2805	39	109.9994
20	511.2800	40	511.2830
Min cost ($/h)	121,415.2447		
Average cost ($/h)	121,998.6771		
Max cost ($/h)	122,746.9205		
Standard deviation ($/h)	329.0243		
Average CPU time (s)	5.895		

The value of α is also tuned by similar way by setting its initial value to 1.0 with the step of 0.5 in the range [1, 3] and 1.0 in the range [4, 10]. By experiments, the fine tuned parameters for each considered test system in this chapter are shown in Table 1.

5.2 Systems with Valve Point Effects

The proposed PGPSO is tested on a large-scale system from [13] comprising 40 generating units supplying to a load demand of 10,500 MW neglecting power loss. The optimal solution obtained by the proposed PGPSO method for this case is given in Table 2.

Table 3 shows a comparison of total cost and computational time from the proposed PGPSO method to those from improved fast EP (IFEP) [13], MSL [8], MPSO [24], evolutionary strategy optimization (ESO) [14], DEC-SQP [30, 31], self-tuning HDE [32], NPSO-LRS [27], NDS [9], SOH_PSO [23], QPSO [22], ABC [17], SA-PSO [28], BBO [19], UHGA [29], improved coordinated aggregation-based PSO (ICA-PSO) [39, 40], FAPSO-NM [33], DE [16], modified differential evolution (MDE) [41], and integration of the variable DE with the fuzzy adaptive PSO (FAPSO-VDE) [42]. Apparently, the PGPSO method obtains a less total cost of 121,415.2447 ($/h) than the total cost of the other methods except the MDE and FAPSO-VDE methods. Moreover, the PGPSO also obtains a higher

Table 3 Comparison of best total cost and CPU time for 40-unit system with VPE

Method	Total cost ($/h)	CPU time (s)
IFEP [13]	122,624.35	1,167.35
MSL [8]	122,406.10	0.078
MPSO [24]	122,252.27	–
ESO [14]	122,122.16	0.261
DEC-SQP [30, 31]	121,741.98	14.26
Self-tuning HDE [32]	121,698.51	6.07
NPSO-LRS [27]	121,664.43	20.74
NDS [9]	121,647.40	4.0471
SOH_PSO [23]	121,501.14	–
QPSO [22]	121,448.21	–
ABC [17]	121,441.03	32.45
SA-PSO [28]	121,430.00	23.89
BBO [19]	121,426.95	1.1749
UHGA [29]	121,424.48	333.68
ICA-PSO [39], [40]	121,422.10	139.92
FAPSO-NM [33]	121,418.30	40
DE [16]	121,416.29	72.94
MDE [41]	121,414.79	–
FAPSO–VDE [42]	121,412.56	22
PGPSO	121,415.24	5.895

quality solution in a faster manner with 5.895 s which is less than those from the other methods except MSL, ESO, NDS, and BBO methods. The computational time from IFEP, MSL, ESO, DEC-SQP, self-tuning HDE, NPSO-LRS, NDS, ABC, BBO, UHGA, ICA-PSO, DE, and FAPSO–VDE were from a Pentium-II 350 MHz with 128 MB of RAM PC, Pentium IV 1.5 GHz with 512 MB of RAM PC, Pentium IV PC, 1.1 AMD Athlon GHz with 112 MB of RAM, Pentium 1.5 GHz with 768 MB of RAM, Pentium IV 1.5 GHz with 128 MB of RAM, Pentium IV 2.6 GHz with 512 MB of RAM, 1.7 GHz with 1 GB of RAM, Pentium IV 2.3 GHz with 512 MB of RAM PC, Pentium IV 2.99 GHz PC, Pentium IV 1.4 GHz PC, Intel 1.67 GHz with 1 GB of RAM PC, and Pentium-IV 3.0 GHz PC, respectively. There is no computational time or computer processor reported for the other methods. In fact, it may not be directly comparable the computational time among the methods due to different computers and programming languages used. However, the comparison of computational time can be considered as a basis for estimation of their efficiency for dealing with the nonconvex ED problems.The test results have indicated that the PGPSO is effective for solving nonconvex ED with valve point effects.

5.3 System with Multiple Fuels

The test system from [10] comprises 10 generating units with multiple fuel options. Various load demands are considered for this system including 2,400, 2,500, 2,600, and 2,700 MW neglecting power loss. The solutions for different

Table 4 Results for 10-unit system with MF

Unit	Load demand of 2,400 MW		Load demand of 2,500 MW		Load demand of 2,600 MW		Load demand of 2,700 MW	
	F_i	P_i (MW)	F_i	P_i (MW)	F_i	P_i (MW)	F_i	P_i (MW)
1	1	189.7807	2	206.4667	2	216.2074	2	218.3351
2	1	202.3332	1	206.5038	1	210.8414	1	211.5971
3	1	253.8521	1	265.8326	1	278.5687	1	280.6878
4	3	233.1025	3	235.9293	3	238.9349	3	239.6504
5	1	241.8250	1	257.9819	1	275.7003	1	278.4149
6	3	232.9748	3	235.9461	3	239.0876	3	239.6019
7	1	253.4319	1	269.0991	1	286.0002	1	288.6804
8	3	233.0516	3	235.9656	3	239.1758	3	239.4526
9	1	320.3100	1	331.3439	1	343.3878	3	428.8039
10	1	239.3382	1	254.9309	1	272.0959	1	274.7759
Min total cost ($/h)		481.7227		526.2389		574.3814		623.8095
Average total cost ($/h)		485.3323		531.7085		576.9959		626.7308
Max total cost ($/h)		507.3870		571.6084		598.7630		646.2601
Standard deviation ($/h)		5.4601		7.9350		4.0521		4.3292
CPU (s)		0.228		0.228		0.229		0.233

Table 5 Comparison of best total costs and average CPU times for 10-unit system with MF

Method	2,400 MW		2,500 MW	
	Cost ($/h)	CPU (s)	Cost ($/h)	CPU (s)
HNUM [5]	488.50	1.08	526.70	1.08
HNN [10]	487.87	~60	526.13	~60
AHNN [11]	481.72	~4	526.230	~4
MPSO [24]	481.723	–	526.239	–
AIS [18]	481.723	–	526.240	–
ALHN [43]	481.723	0.042	526.239	0.043
PGPSO	481.723	0.228	526.239	0.228
Method	2,600 MW		2,700 MW	
	Cost ($/h)	CPU (s)	Cost ($/h)	CPU (s)
HNUM [5]	574.03	1.08	625.18	1.08
HNN [10]	574.26	~60	626.12	~60
AHNN [11]	574.37	~4	626.24	~4
MPSO [24]	574.381	–	623.809	–
AIS [18]	574.381	–	623.809	–
ALHN [43]	574.381	0.047	623.809	0.057
PGPSO	574.381	0.225	623.810	0.233

system load demands are given in Table 4. The total costs obtained by the PGPSO for the system with corresponding load demands of 2,400, 2,500, 2,600, and 2,700 are 481.7227 ($/h), 526.2389 ($/h), 574.3814 ($/h), and 623.8095 ($/h), respectively.

A comparison of the best total costs and average computational times of the PGPSO and HNUM [5], HNN [10], adaptive HNN (AHNN) [11], MPSO [24], AIS [18], and augmented Lagrange Hopfield network (ALHN) [43] is made as in Table 5. For this system, the best total costs from the PGPSO are less than those from HNUM and HNN for the load demand of 2,400 MW and HNUM, HNN, and AHNN for the load demand of 2,700 MW and close to those from the other methods for the remaining cases. For the computational times, the PGPSO is faster than HNUM, HNN, and AHNN and slightly slower than ALHN. The CPU times from the HNUM, HNN, AHNN, and ALHN methods were from a VAX 11/780, IBM PC-386, Compaq 90, and 2.1 GHz PC. There is no CPU time reported for the AIS method. From the obtained results, it has shown that the PGPSO can obtain the better solutions in a faster manner due to its powerful search ability. Accordingly, the proposed PGPSO is effective for solving nonconvex ED with multiple fuels.

Table 6 Results for 15-unit system with POZ

Unit	P_i (MW)	Unit	P_i (MW)
1	454.9644	9	43.2998
2	380.0000	10	160.0000
3	130.0000	11	80.0000
4	130.0000	12	80.0000
5	170.0000	13	25.0721
6	460.0000	14	15.6087
7	430.0000	15	15.7862
8	85.9332		
Power loss (MW)	30.6644		
Total power (MW)	2,660.6644		
Minimum total cost ($/h)	32,705.7533		
Average total cost ($/h)	32,716.8369		
Maximum total cost ($/h)	32,726.0751		
Standard deviation ($/h)	4.0221		
CPU time (s)	1.631		

Table 7 Comparison of best total cost and average CPU time for 15-unit system with POZ

Method	Power loss (MW)	Total power (MW)	Total cost ($/h)	CPU time (s)
GA [20]	38.2782	2,668.40	33,113.00	4.95
PSO [20]	32.4306	2,662.40	32,858.00	2.74
AIS 18	32.4075	2,662.04	32,854.00	–
SOH_PSO [23]	32.2800	2,662.29	32,751.00	0.0936
MPSO [25]	29.9780	2,661.62	32,738.42	–
PSO-MSAF [26]	30.4900	2,660.49	32,713.09	19.15
SA-PSO [28]	30.9080	2,660.90	32,708.00	10.37
PGPSO	30.6644	2,660.66	32,705.75	1.632

5.4 System with Prohibited Operating Zones

The test system consists of 15 units supplying to a load demand of 2,630 MW, considering ramp rate constraints and system power loss [20]. The results obtained by the proposed PGPSO for this system are given in Table 6.

The result obtained by the PGPSO is compared to that from GA and PSO in [20], AIS [18], SOH_PSO [23], MPSO [25], PSO-MSAF [26], and SA-PSO [28] as in Table 7. The proposed method obtains a less total cost of 32,705.7533 ($/h) than the best total cost from the other methods. In addition, the proposed method is faster than GA, PSO, PSO-MSAF, and SA-PSO and slightly slower than SOH_PSO. The GA and PSO, SOH_PSO, and PSO-MSAF methods were implemented on a Pentium III 550 with 256 MB of RAM, Pentium IV 2.8 GHz with 512 MB of RAM, and Pentium IV 2.60 GHz with 512 MB of RAM, respectively. There is no computational time reported for the AIS and MPSO methods. The result

Table 8 Results for 10-unit system with VPE and MF

Unit	F_i	P_i (MW)
1	2	218.5941
2	1	210.9690
3	1	280.6574
4	3	240.1769
5	1	279.6374
6	3	240.1769
7	1	290.0615
8	3	239.3707
9	3	427.7234
10	1	272.6326
Min total cost ($/h)		623.8431
Average total cost ($/h)		624.0979
Max total cost ($/h)		626.5191
Standard deviation ($/h)		0.5428
CPU time (s)		1.494

Table 9 Comparison of best total cost and average CPU time for 10-unit system with VPE and MF

Method	Total cost ($/h)	CPU time (s)
CGA_MU [12]	624.7193	26.64
IGA_MU [12]	624.5178	7.32
PSO-LRS [27]	624.2297	1.81
NPSO [27]	624.1624	0.76
NPSO-LRS [27]	624.1273	1.60
RGA [15]	624.5081	4.1340
DE [15]	624.5146	2.8236
PSO [15]	624.5074	3.3852
PGPSO	623.8431	1.494

comparison has indicated that the PGPSO can obtain better solution quality than many other methods for the nonconvex ED with POZ.

5.5 Systems with Both Valve Point Effects and Multiple Fuels

5.5.1 10-unit System

The test system from [12] comprises 10 units with VPE and MF. This system supplies to a load demand of 2,700 MW neglecting power loss. Table 8 shows the result obtained by the proposed PGPSO for this system.

The best total cost and average computational time from the proposed method are compared to those from other methods such as conventional GA with multiplier updating (CGA_MU) and improved GA with multiplier updating (IGA_MU) in Chiang [12], PSO with local random search (PSO-LRS), new PSO (NPSO), and NPSO-LRS in Selvakumar and Thanushkodi [27], and real-coded GA (RGA), PSO, and DE in Manoharan et al. [15] as in Table 9. Obviously, the total cost obtained from the proposed method for this system is less than that from the other methods. The proposed PGPSO is also faster than the CGA_MU, IGA_MU, PSO-LRS, NPSO-LRS, RGA, PSO, and DE methods and slightly slower than the NPSO method. The computational times for the CGA_MU and IGA_MU methods were from a PIII-700 PC, the computational times for the PSO-LRS, NPSO, and NPSO-LRS methods from a Pentium IV 1.5 GHz with 128 MB of RAM, and the computational times for the CGA, PSO, and DE method from a Pentium IV 1.8 GHz with 1 GB of RAM PC. Test result indicates that the PGPSO can obtain better solution quality than many other methods for nonconvex ED problem with valve point effects and multiple fuels.

Table 10 Results for large-scale systems with VPE and MF

No. of units	20	40	80	160
Min total cost ($/h)	1,247.7326	2,495.6162	4,994.2781	10,004.7260
Average total cost ($/h)	1,248.9623	2,499.6127	5,003.0250	10,032.4883
Max total cost ($/h)	1,259.2242	2,512.9091	5,021.0196	10,107.1708
Standard deviation ($/h)	2.0378	3.8971	6.2272	17.0031
CPU time (s)	4.078	18.645	43.191	91.570

Table 11 Comparison of average total cost and average CPU time for large-scale systems with VPE and MF

Method	No. of units	Total cost ($)	CPU time (s)
CGA_MU [12]	20	1,249.3893	80.48
	40	2,500.9220	157.39
	80	5,008.1426	309.41
	160	10,143.7263	621.30
IGA_MU [12]	20	1,249.1179	21.64
	40	2,499.8243	43.71
	80	5,003.8832	85.67
	160	10,042.4742	174.62
PGPSO	20	1,248.9623	4.078
	40	2,499.6127	18.645
	80	5,003.0250	43.191
	160	10,032.4883	91.570

5.5.2 Large-Scale Systems

The large-scale systems here consisting of 20, 40, 80, and 160 units are based on the basic 10-unit system above. The considered systems are created by duplicating the basic 10-unit system with the load demand adjusted proportionally to the system size. The results obtained by the proposed method for these systems including minimum costs, average costs, maximum costs, standard deviations, and computational times are given in Table 10. For all systems, the difference between the maximum and minimum costs obtained the proposed method is small and the ratio between the standard deviation and the minimum cost is less than 0.17 %. In Table 11, the average total costs and computational times from the PGPSO method are compared to those from CGA_MU and IGA_MU methods in Chiang [12]. The result comparison has shown that the proposed PGPSO can obtain better average total costs with faster average computational times than both CGA_MU and IGA_MU. Therefore, the proposed method is also effective for solving large-scale nonconvex ED problems with valve point effects and multiple fuels.

6 Conclusion

In this chapter, the newly proposed PGPSO method has been efficiently implemented for solving different nonconvex ED problems. The PGPSO method is a novel improvement of PSO by combining the HPSO-TVAC method with the pseudo-gradient to improve its search capability. The pseudo-gradient is efficient for guiding the search direction for each individual in population based methods. In addition, an efficient repairing strategy is also used for handling POZ violation considering ramp rate constraints. With the new improvement, the proposed PGPSO method is more effective than many other methods in solving nonconex ED problems with multiple minima. The proposed method has been tested on different systems with nonconvex generator's characteristics including valve point effects, multiple fuels, and prohibited operating zones. Test results have shown that the proposed PGPSO can obtain better solution quality than many other methods, leading substantial cost savings.

Appendix

The unit data for 40-unit system with valve point effects are given in Table A1.

The unit data for 10-unit system with multiple fuels is given in Table A2.

The unit data for 15-unit system with prohibited zones is given in Table A3 and prohibited zones are given in Table A4.

The unit data for 10-unit system with valve pint effects and multiple fuels is given in Table A5.

Table A1 Unit data for 40-unit system with valve point effects

Unit	a_i ($/h)	b_i ($/MWh)	c_i ($/MW^{2}h)	e_i ($/h)	f_i (1/MW)	P_{imin} (MW)	P_{imax} (MW)
1	94.705	6.73	0.0069	100	0.084	36	114
2	94.705	6.73	0.0069	100	0.084	36	114
3	309.54	7.07	0.02028	100	0.084	60	120
4	369.03	8.18	0.00942	150	0.063	80	190
5	148.89	5.35	0.0114	120	0.077	47	97
6	222.33	8.05	0.01142	100	0.084	68	140
7	287.71	8.03	0.00357	200	0.042	110	300
8	391.98	6.99	0.00492	200	0.042	135	300
9	455.76	6.6	0.00573	200	0.042	135	300
10	722.82	12.9	0.00605	200	0.042	130	300
11	635.2	12.9	0.00515	200	0.042	94	375
12	654.69	12.8	0.00569	200	0.042	94	375
13	913.4	12.5	0.00421	300	0.035	125	500
14	1,760.4	8.84	0.00752	300	0.035	125	500
15	1,728.3	9.15	0.00708	300	0.035	125	500
16	1,728.3	9.15	0.00708	300	0.035	125	500
17	647.85	7.97	0.00313	300	0.035	220	500
18	649.69	7.95	0.00313	300	0.035	220	500
19	647.83	7.97	0.00313	300	0.035	242	550
20	647.81	7.97	0.00313	300	0.035	242	550
21	785.96	6.63	0.00298	300	0.035	254	550
22	785.96	6.63	0.00298	300	0.035	254	550
23	794.53	6.66	0.00284	300	0.035	254	550
24	794.53	6.66	0.00284	300	0.035	254	550
25	801.32	7.1	0.00277	300	0.035	254	550
26	801.32	7.1	0.00277	300	0.035	254	550
27	1,055.1	3.33	0.52124	120	0.077	10	150
28	1,055.1	3.33	0.52124	120	0.077	10	150
29	1,055.1	3.33	0.52124	120	0.077	10	150
30	148.89	5.35	0.0114	120	0.077	47	97
31	222.92	6.43	0.0016	150	0.063	60	190
32	222.92	6.43	0.0016	150	0.063	60	190
33	222.92	6.43	0.0016	150	0.063	60	190
34	107.87	8.95	0.0001	200	0.042	90	200
35	116.58	8.62	0.0001	200	0.042	90	200
36	116.58	8.62	0.0001	200	0.042	90	200
37	307.45	5.88	0.0161	80	0.098	25	110
38	307.45	5.88	0.0161	80	0.098	25	110
39	307.45	5.88	0.0161	80	0.098	25	110
40	647.83	7.97	0.00313	300	0.035	242	550

Table A2 Unit data for 10-unit system with multiple fuels

Unit	Fuel type	a_{ij} ($/h)	b_{ij} ($/MWh)	c_{ij} ($/MW^{2}h)	$P_{ij\min}$ (MW)	$P_{ij\max}$ (MW)
1	1	26.97	−0.3975	0.002176	100	196
	2	21.13	−0.3059	0.001861	196	250
2	2	1.865	−0.03988	0.001138	50	114
	3	13.65	−0.198	0.00162	114	157
	1	118.4	−1.269	0.004194	157	230
3	1	39.79	−0.3116	0.001457	200	332
	3	−2.876	0.03389	0.000804	332	388
	2	−59.14	0.4864	1.18E-05	388	500
4	1	1.983	−0.03114	0.001049	99	138
	2	52.85	−0.6348	0.002758	138	200
	3	266.8	−2.338	0.005935	200	265
5	1	13.92	−0.08733	0.001066	190	338
	2	99.76	−0.5206	0.001597	338	407
	3	−53.99	0.4462	0.00015	407	490
6	2	1.983	−0.03114	0.001049	85	138
	1	52.85	−0.6348	0.002758	138	200
	3	266.8	−2.338	0.005935	200	265
7	1	18.93	−0.1325	0.001107	200	331
	2	43.77	−0.2267	0.001165	331	391
	3	−43.35	0.3559	0.000245	391	500
8	1	1.983	−0.03114	0.001049	99	138
	2	52.85	−0.6348	0.002758	138	200
	3	266.8	−2.338	0.005935	200	265
9	3	14.23	−0.01817	0.000612	130	213
	1	88.53	−0.5675	0.001554	213	370
	3	14.23	−0.01817	0.000612	370	440
10	1	13.97	−0.09938	0.001102	200	362
	3	46.71	−0.2024	0.001137	362	407
	2	−61.13	0.5084	4.16E-05	407	490

Table A3 Unit data for 15-unit system with prohibited zones

Unit	a_i ($/h)	b_i ($/MWh)	c_i ($/MW^{2}h)	$P_{i\min}$ (MW)	$P_{i\max}$ (MW)	$S_{i\max}$ (MW)	UR_i (MW)	DR_i (MW)	P_{i0} (MW)
1	671	10.1	0.000299	150	455	50	80	120	400
2	574	10.2	0.000183	150	455	0	80	120	300
3	374	8.8	0.001126	20	130	30	130	130	105
4	374	8.8	0.001126	20	130	30	130	130	100
5	461	10.4	0.000205	150	470	0	80	120	90
6	630	10.1	0.000301	135	460	0	80	120	400
7	548	9.8	0.000364	135	465	50	80	120	350
8	227	11.2	0.000338	60	300	50	65	100	95
9	173	11.2	0.000807	25	162	30	60	100	105

(continued)

Table A3 (continued)

Unit	a_i ($/h)	b_i ($/MWh)	c_i ($/MW^{2}h)	$P_{i\min}$ (MW)	$P_{i\max}$ (MW)	$S_{i\max}$ (MW)	UR_i (MW)	DR_i (MW)	P_{i0} (MW)
10	175	10.7	0.001203	25	160	30	60	100	110
11	186	10.2	0.003586	20	80	20	80	80	60
12	230	9.9	0.005513	20	80	0	80	80	40
13	225	13.1	0.000371	25	85	20	80	80	30
14	309	12.1	0.001929	15	55	40	55	55	20
15	323	12.4	0.004447	15	55	40	55	55	20

Table A4 Prohibited zones for 15-unit system

Unit	Prohibited zone 1	Prohibited zone 2	Prohibited zone 3
2	(185 225)	(305 335)	(420 450)
5	(180 200)	(305 335)	(390 420)
6	(230 255)	(365 395)	(430 455)
12	(30 40)	(55 65)	

Table A5 Unit data for 10-unit system with valve point effects and multiple fuels

Unit	Fuel type	a_{ij} ($/h)	b_{ij} ($/MWh)	c_{ij} ($/MW^{2}h)	e_{ij} ($/h)	f_{ij} (1/MW)	$P_{ij\min}$ (MW)	$P_{ij\max}$ (MW)
1	1	26.97	−0.3975	0.002176	0.02697	−3.975	100	196
	2	21.13	−0.3059	0.001861	0.02113	−3.059	196	250
2	2	1.865	−0.03988	0.001138	0.001865	−0.3988	50	114
	3	13.65	−0.198	0.00162	0.01365	−1.98	114	157
	1	118.4	−1.269	0.004194	0.1184	−12.69	157	230
3	1	39.79	−0.3116	0.001457	0.03979	−3.116	200	332
	3	−2.876	0.03389	0.000804	−0.00288	0.3389	332	388
	2	−59.14	0.4864	1.18E-05	−0.05914	4.864	388	500
4	1	1.983	−0.03114	0.001049	0.001983	−0.3114	99	138
	2	52.85	−0.6348	0.002758	0.05285	−6.348	138	200
	3	266.8	−2.338	0.005935	0.2668	−23.38	200	265
5	1	13.92	−0.08733	0.001066	0.01392	−0.8733	190	338
	2	99.76	−0.5206	0.001597	0.09976	−5.206	338	407
	3	−53.99	0.4462	0.00015	−0.05399	4.462	407	490
6	2	1.983	−0.03114	0.001049	0.001983	−0.3114	85	138
	1	52.85	−0.6348	0.002758	0.05285	−6.348	138	200
	3	266.8	−2.338	0.005935	0.2668	−23.38	200	265
7	1	18.93	−0.1325	0.001107	0.01893	−1.325	200	331
	2	43.77	−0.2267	0.001165	0.04377	−2.267	331	391
	3	−43.35	0.3559	0.000245	−0.04335	3.559	391	500

(continued)

Table A5 (continued)

Unit	Fuel type	a_{ij} ($/h)	b_{ij} ($/MWh)	c_{ij} ($/MW^{2}h)	e_{ij} ($/h)	f_{ij} (1/MW)	$P_{ij\min}$ (MW)	$P_{ij\max}$ (MW)
8	1	1.983	−0.03114	0.001049	0.001983	−0.3114	99	138
	2	52.85	−0.6348	0.002758	0.05285	−6.348	138	200
	3	266.8	−2.338	0.005935	0.2668	−23.38	200	265
9	3	14.23	−0.01817	0.000612	0.01423	−0.1817	130	213
	1	88.53	−0.5675	0.001554	0.08853	−5.675	213	370
	3	14.23	−0.01817	0.000612	0.01423	−0.1817	370	440
10	1	13.97	−0.09938	0.001102	0.01397	−0.9938	200	362
	3	46.71	−0.2024	0.001137	0.04671	−2.024	362	407
	2	−61.13	0.5084	4.16E-05	−0.06113	5.084	407	490

References

1. Chowdhury, E.H., Rahrnan, S.: A review of recent advances in economic dispatch. IEEE Trans. Power Syst. **5**, 1248–1259 (1990)
2. Xia, X., Elaiw, A.M.: Optimal dynamic economic dispatch of generation: a review. Electr. Power Syst. Res. **80**, 975–986 (2010)
3. Wood, A.J., Wollenberg, B.F.: Power Generation, Operation, and Control, 2nd edn. Wiley, New York (1996)
4. Fink, L.H., Kwatny, H.G., Mcdonald, J.P.: Economic dispatch of generation via valve-point loading. IEEE Trans. Power Appar. Syst. **88**, 805–811 (1969)
5. Lin, C.E., Viviani, G.L.: Hierarchical economic dispatch for piecewise quadratic cost functions. IEEE Trans. Power Appar. Syst. **103**, 1170–1175 (1984)
6. Lee, F.N., Breipohl, A.M.: Reserve constrained economic dispatch with prohibited operating zones. IEEE Trans. Power Syst. **8**, 246–254 (1993)
7. Fan, J.Y., McDonald, J.D.: A practical approach to real time economic dispatch considering unit's prohibited operating zones. IEEE Trans. Power Syst. **9**, 1737–1743 (1994)
8. Hemamalini, S., Simon, S.P.: Maclaurin series-based Lagrangian method for economic dispatch with valve-point effect. IET Gener. Transm. Distrib. **3**, 859–871 (2009)
9. Lin, W.-M., Gowa, H.-J., Tsai, M.-T.: Combining of direct search and signal-to-noise ratio for economic dispatch optimization. Energy Conver. Manag. **52**, 487–493 (2011)
10. Park, J.H., Kim, Y.S., Eom, I.K., Lee, K.Y.: Economic load dispatch for piecewise quadratic cost function using Hopfield neural network. IEEE Trans. Power Syst. **8**, 1030–1038 (1993)
11. Lee, K.Y., Sode-Yome, A., Park, J.H.: Adaptive Hopfield neural networks for economic load dispatch. IEEE Trans. Power Syst. **13**, 519–526 (1998)
12. Chiang, C.-L.: Improved genetic algorithm for power economic dispatch of units with valve-point effects and multiple fuels. IEEE Trans. Power Syst. **20**, 1690–1699 (2005)
13. Sinha, N., Chakrabarti, R., Chattopadhyay, P.K.: Evolutionary programming techniques for economic load dispatch. IEEE Trans. Evol. Comput. **7**, 83–94 (2003)
14. Pereira-Neto, A., Unsihuay, C., Saavedra, O.R.: Efficient evolutionary strategy optimization procedure to solve the nonconvex economic dispatch problem with generator constraints. IEE Proc. Gener. Transm. Distrib. **152**, 653–660 (2005)
15. Manoharan, P.S., Kannan, P.S., Baskar, S., Iruthayarajan, M.W.: Penalty parameter-less constraint handling scheme based evolutionary algorithm solutions to economic dispatch. IET Gener. Transm. Distrib. **2**, 478–490 (2008)
16. Noman, N., Iba, H.: Differential evolution for economic load dispatch problems. Elec. Power Syst. Res. **78**, 1322–1331 (2008)

17. Hemamalini, S., Simon, S.P.: Artificial bee colony algorithm for economic load dispatch problem with non-smooth cost functions. Elec. Power Comp. Syst. **38**, 786–803 (2010)
18. Panigrahi, B.K., Yadav, S.R., Agrawal, S., Tiwari, M.K.: A clonal algorithm to solve economic load dispatch. Elec. Power Syst. Res. **77**, 1381–1389 (2007)
19. Bhattacharya, A., Chattopadhyay, P.K.: Biogeography-based optimization for different economic load dispatch problems. IEEE Trans. Power Syst. **25**, 1064–1077 (2010)
20. Gaing, Z.L.: Particle swarm optimization to solving the economic dispatch considering the generator constraints. IEEE Trans. Power Syst. **18**, 1187–1195 (2003)
21. Mahor, A., Prasad, V., Rangnekar, S.: Economic dispatch using particle swarm optimization: a review. Renew. Sustain. Energy Rev. **13**, 2134–2141 (2009)
22. Meng, K., Wang, H.G., Dong, Z.Y., Wong, K.P.: Quantum-inspired particle swarm optimization for valve-point economic load dispatch. IEEE Trans. Power Syst. **25**, 215–222 (2010)
23. Chaturvedi, K.T., Pandit, M., Srivastava, L.: Self-organizing hierarchical particle swarm optimization for nonconvex economic dispatch. IEEE Trans. Power Syst. **23**, 1079–1087 (2008)
24. Park, J.-B., Lee, K.-S., Shin, J.-R., Lee, K.Y.: A particle swarm optimization for economic dispatch with nonsmooth cost functions. IEEE Trans. Power Syst. **20**, 34–42 (2005)
25. Neyestani, M., Farsangi, M.M., Nezamabadi-pour, H.: A modified particle swarm optimization for economic dispatch with non-smooth cost functions. Eng. Apps. AI **23**, 1121–1126 (2010)
26. Subbaraj, P., Rengaraj, R., Salivahanan, S., Senthilkumar, T.R.: Parallel particle swarm optimization with modified stochastic acceleration factors for solving large scale economic dispatch problem. Electr. Power Energy Syst. **32**, 1014–1023 (2010)
27. Selvakumar, A.I., Thanushkodi, K.: A new particle swarm optimization solution to nonconvex economic dispatch problems. IEEE Trans. Power Syst. **22**, 42–51 (2007)
28. Kuo, C.-C.: A novel coding scheme for practical economic dispatch by modified particle swarm approach. IEEE Trans. Power Syst. **23**, 1825–1835 (2008)
29. He, D.-K., Wang, F.-L., Mao, Z.-Z.: Hybrid genetic algorithm for economic dispatch with valve-point effect. Elec. Power Syst. Res. **78**, 626–633 (2008)
30. dos Santos Coelho, L., Mariani, V.C.: Combining of chaotic differential evolution and quadratic programming for economic dispatch optimization with valve-point effect. IEEE Trans. Power Syst. **21**, 989–996 (2006)
31. dos Santos Coelho, L., Mariani, V.C.: Correction to Combining of chaotic differential evolution and quadratic programming for economic dispatch optimization with valve-point effect. IEEE Trans. Power Syst. **21**, 1465 (2006)
32. Wang, S.-K., Chiou, J.-P., Liu, C.-W.: Non-smooth/non-convex economic dispatch by a novel hybrid differential evolution algorithm. IET Gener. Transm. Distrib. **1**, 793–803 (2007)
33. Niknam, T.: A new fuzzy adaptive hybrid particle swarm optimization algorithm for non-linear, non-smooth and non-convex economic dispatch problem. Appl. Energy **87**, 327–339 (2010)
34. Ratnaweera, A., Halgamuge, S.K., Watson, H.C.: Self-organizing hierarchical particle swarm optimizer with time-varying acceleration coefficients. IEEE Trans. Evol. Comput. **8**, 240–255 (2004)
35. Wen, J.Y., Wu, Q.H., Jiang, L., Cheng, S.J.: Pseudo-gradient based evolutionary programming. Electron. Lett. **39**, 631–632 (2003)
36. Walter, D.C., Sheble, G.B.: Genetic algorithm solution of economic load dispatch with valve point loading. IEEE Trans. Power Syst. **8**, 1325–1332 (1993)
37. Kennedy, J., Eberhart, R.: Particle swarm optimization. In: Proceedings of the IEEE Conference Neural Networks (ICNN'95), vol. 4, pp. 1942–1948 (1995)
38. Pham, D.T., Jin, G.: Genetic algorithm using gradient-like reproduction operator. Electron. Lett. **31**, 1558–1559 (1995)

39. Vlachogiannis, J.G., Lee, K.Y.: Economic load dispatch: a comparative study on heuristic optimization techniques with an improved coordinated aggregation-based PSO. IEEE Trans. Power Syst. **24**, 991–1001 (2009)
40. Vlachogiannis, J.G., Lee, K.Y.: Closure to discussion on Economic load dispatch: a comparative study on heuristic optimization techniques with an improved coordinated aggregation-based PSO. IEEE Trans. Power Syst. **25**, 591–592 (2010)
41. Amjady, N., Sharifzadeh, H.: Solution of non-convex economic dispatch problem considering valve loading effect by a new modified differential evolution algorithm. Int. J. Electr. Power Energy Syst. **32**, 893–903 (2010)
42. Niknam, T., Mojarrad, H.D., Meymand, H.Z.: A novel hybrid particle swarm optimization for economic dispatch with valve-point loading effects. Energy Convers. Manage. **52**, 1800–1809 (2011)
43. Dieu, V.N., Ongsakul, W., Polprasert, J.: The augmented Lagrange Hopfield network for economic dispatch with multiple fuel options. Math. Comp. Model. **57**, 30–39 (2013)

Energy Consumption Impacted by Climate Change Application: Case Study Astara

Mostafa Jafari

Abstract To study past climate conditions, main climatic factor related to the energy consumption namely temperature and precipitation were considered. Heating degree days (HDD), cooling degree days (CDD) and sunshine hours were analyzed. According to all reports in different scales temperature of Astara region, in last half century has been increased. In the longer future time period, the study area will face with higher values of increasing temperature. HDD with base temperature of 18 °C reduced in last 18 years. HDD in January which is cold month also reduced. Meanwhile CDD increased. CDD in July which is warm month also increased. This is in harmony with increasing the number of sunshine hours in the same time slice. By changing HDD and CDD in cool and warm seasons, it means the pattern of energy consumption in the region has changed. Astara location is included in both of Central Asia and West Asia sub-regions in IPCC AR4. Projection for temperature change in Central Asia sub-region is not in agreement with national and local downscaling results.

Keywords Climate change · Energy consumption · Local application · Astara

1 Introduction

The Intergovernmental Panel on Climate Change (IPCC) published the Fourth Assessment Report (AR4) in 2007 and stated that recent climate change and variation are induced by increases in the atmospheric greenhouse gases (GHGs)

M. Jafari (✉)
Head of TPS for LFCCs (UN-IGO), and Member of Academic Board of Research Institute of Forests and Rangeland, LA/AR4 & AR5/IPCC Nobel Peace Prize winner, P.O. Box 13185-16, Tehran, I.R. Iran
e-mail: mostafajafari@rifr-ac.ir; mostafajafari@libero.it
URL: http://www.lfccsandclimatechange.pbworks.com

I. Zelinka et al. (eds.), *Power, Control and Optimization*, Lecture Notes in Electrical Engineering 239, DOI: 10.1007/978-3-319-00206-4_2,

concentration due to anthropogenic activities. The report includes the results of impact assessments on a wide range of sectors. These assessments have been conducted based on future climate projections, which refer to aspects of the future climate evaluated by Atmosphere-Ocean Coupled General Circulation Models (CGCMs) [1]. In climate change studies context; international, regional and national research institutes according to the available data and scenarios analyze past conditions and will provide projection for the future climate changes [2–4]. Estimates for the likelihood of future climate changes in different country were made based on the projection from the IPCC climate models [5]. Therefore, provided results are different in time scales, scenarios and study areas and may not be adapted precisely. With the set of models showing increasing agreement in their simulations of twentieth-century trends in climate and of projected changes in climate on sub-continental to continental scales, the climate scenarios that were generated seem likely to provide a plausible representation of the types of climatic conditions that could be experienced during the 21st century [6].

2 Methods

Astara forest, from geographical, topographical and climatic points of views is an especial and unique ecosystem (Fig. 1, Table 1). In this investigation, past climate conditions, main climatic factor related to the energy consumption namely temperature and precipitation were considered. Heating degree days, cooling degree days and sunshine hours were analyzed.

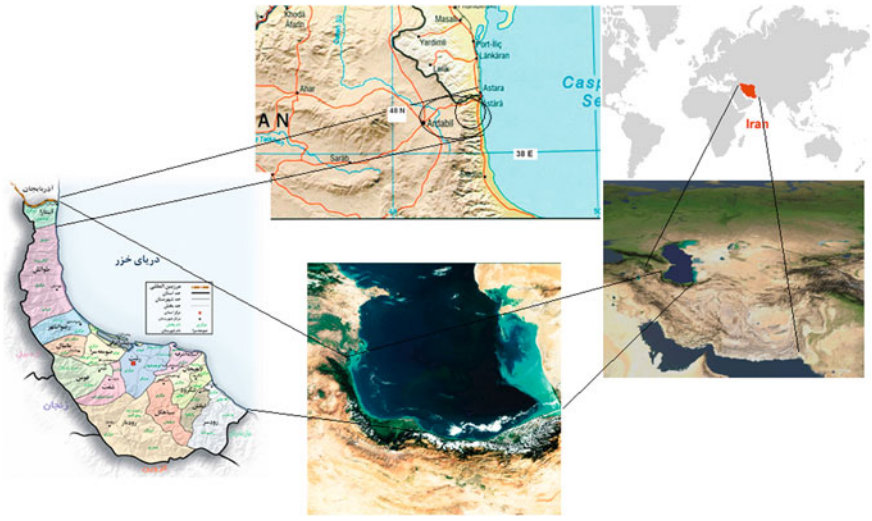

Fig. 1 Astara study location map (maps from different sources)

Table 1 Forest study zone in Astara and location of meteorology stations in Astara and Ardebil

Region/stations	Elevation from sea level (m)	Longitude E	Latitude N	Stations code
Astara chay forest—No. 1	Minimum 0 and Maximum 1,750 m and majority of forest in 100–1,000 m	48 51 45 E and 48 34 E	38 26 30 N and 38 17 30 N	(Region no. 1)
Astara synoptic	−18.0	48 52 E	38 25 N	40709
Astara climatology	+25	48 52 E	38 26 N	
Ardebil	+1,350	48 17 E	38 15 N	

2.1 What are Annual and Monthly Heating and Cooling Degree Days?

The Heating Degree Days (HDDs) and Cooling Degree Days (CDDs) are based on daily temperature observations, with each month having at least 25 records and no less than 15 years of data between [7]. Heating and Cooling Degree Days, which indicate the level of comfort, are based on the average daily temperature. The average daily temperature is calculated as follows:

$$[\text{Maximum daily temperature} + \text{minimum daily temperature}]/2.$$

If the average daily temperature falls below comfort levels, heating is required and if it is above comfort levels, cooling is required. The HDDs or CDDs are determined by the difference between the average daily temperature and the BASE (comfort level) temperature. The BASE values used are 12 and 18 °C for heating and 18 and 24 °C for cooling [7]. In this case, base degrees for heating are 18 °C and for cooling is 21 °C.

Examples 1. If heating is being considered to a temperature BASE of 18 degrees, and the average daily temperature for a particular location was 14 degrees, then heating equivalent to 4 degrees or 4 HDDs would be required to maintain a temperature of 18 degrees for that day. However if the average daily temperature was 20 degrees then no heating would be required, so the number of HDDs for that day would be zero.

2. If cooling is being considered to a temperature BASE of 21 degrees, and if the average temperature for a day was 27 degrees, then cooling equivalent to 6 degrees or 6 CDDs would be required to maintain a temperature of 21 degrees for that day. However if the average temperature was 20 degrees, then no cooling would be required, so the number of CDDs for that day would be zero.

3. In Nebraska-USA one base used for both cooling and heating degrees like: Hot days, which may require the use of energy for cooling, are measured in cooling degree-days. On a day with a mean temperature of 80 °F, for example, 15 cooling degree-days would be recorded (80–65 base = 15 CDD). Cold days are measured in heating degree-days. For a day with a mean temperature of 40 °F, 25

heating degree-days would be recorded (65 base–40 = 25 HDD). Two such cold days would result in a total of 50 heating degree-days for the 2 days period [8].

CDD Cost calculation in USA: Degree days: A degree day gauges the amount of heating or cooling needed for a building using 65 degrees as a baseline. To compute heating/cooling degree-days, it needs to take the average temperature for a day and subtract the reference temperature of 65 °F (18 °C). If the difference is positive, it is called a "Cooling Degree Days". If the difference is negative, it is called a "Heating Degree Days". The magnitude of the difference is the number of days. For example, if your average temperature is 50 degrees for a day in September, the difference of the average temperature for that day and the reference temperature of 65 degrees would yield a −15. Therefore, you know that you are going to have Heating Degree Days that day. Since the magnitude of the difference is 15, you know that you are going to have 15 Heating Degree Days. Electrical, natural gas, power, and heating, and air conditioning industries utilize heating and cooling degree information to calculate their needs [9].

In USA, following formula is using for calculation of HDD cost:

$$\text{HDD monthly cost} = \text{HDD} \times 30\,(\text{days of month}) \times 20\,\text{US\$}$$

To calculate the CDD, take the average of a day's high and low and subtract 65. For example, if the day's average temperature is 80 °F, its CDD is 15. If everyday in a 30-day month had an average temperature of 80 °F, the month's CDD value would be 450 (15 × 30). The nominal settlement value for its month's weather derivative contract would therefore be $9,000 (450 × $20).

To calculate HDD, take the average of a day's high and low temperatures and subtract from 65. For example, if the day's average temperature is 50 °F, its HDD is 15. If every day in a 30-day month had an average temperature of 50 °F, the month's HDD value would be 450 (15 × 30). The nominal settlement value for this month's weather derivative contract would therefore be $9,000 (450 × $20) [10].

- 1 °C = 33.8 °F
- To convert °F HDD to °C HDD: (5/9) × (Temperature in Fahrenheit)
- To convert °C HDD to °F HDD: (9/5) × (Temperature in Celsius).

Note that, because HDD are relative to a base temperature (as opposed to being relative to zero), it is incorrect to add or subtract 32 when converting degree days from Celsius to Fahrenheit or vice versa.

HDD can be added over periods of time to provide a rough estimate of seasonal heating requirements. In the course of a heating season, for example, the number of HDD for New York City is 5,050 whereas that for Barrow, Alaska is 19,990. Thus, one can say that, for a given home of similar structure and insulation, around four times the energy would be required to heat the home in Barrow than in New York. Likewise, a similar home in Los Angeles, California, whose heating degree days for the heating season is 2,020, would require around two fifths the energy required to heat the house in New York City [11].

2.2 Global Projections

IPCC used different models (HadCM3, CSIRO, NCAR-PCM, ECHAM4, CGCM2, GFDL, CCSRNIES) and scenarios (A1FI, A2, B2, B1) to provide climate projection in global, continental and regional levels [12]. According to provided projection by IPCC, changes in precipitation and temperature could be considered in different scales from global to local levels.

2.3 Temperature

Based upon data provided in the map for the changes in surface temperature by IPCC [12], surface temperature in whole Iran except small area in south for the period of 1970–2004 between 1 and 2 °C was increased.

According to the map of geographical pattern of surface warming; projected surface temperature changes for the late 21st century (2090–2099), relative to the period 1980–1999, surface temperature in north of Iran based upon AOGCM and A1B SRES will increase between 3 and 3.5 °C and central and southern part will experience increase of 4 °C and more [12]. While, global mean of temperature depend on scenarios and region will experience of 1.1–6.4 degrees increase which will cause sea level rise of 0.18–0.59 m (source: Table 3.1 SPM, IPCC [12]).

According to the Atmosphere-Ocean General Circulation Model (AOGCM) projections of surface warming; projected surface temperature changes for the early and late 21st century relative to the period 1980–1999, show the multi-AOGCM average projections for the A2, A1B and B1 SRES scenarios averaged over decades 2020–2029 and 2090–2099 (Source: WGI 10.4, 10.8 Figs. 10.28, 10.29, SPM and Fig. 3.2, IPCC [12]), provided by IPCC [12], Iran's surface temperature will increase 1–2 °C for 20 s and 4–5.5 for 90 s. The rates are increasing from B1 to A2 [12].

2.4 Future Climate Projection for Asia Sub Regions

Projected changes in surface air temperature and precipitation for sub-regions of Asia under SRES A1FI (highest future emission trajectory) and B1 (lowest future emission trajectory) pathways for three time slices, namely 2020s (2010–2039), 2050s (2040–2069) and 2080s (2070–2099) was provided by IPCC for seasonal (Table 2) and annual mean (Table 3) [12]. Astara study area is part of both Central Asia and also West Asia sub-regions (Table 2).

With comparison of two sub-regions of Central Asia and West Asia (Fig. 2), which both include and cover Astara region, it could be extracted, that temperature in both sub-regions and based on both scenarios, and in four seasons, and for all tree time slices will increase.

Table 2 Projected changes in surface air temperature and precipitation for sub-regions of Asia under SRES A1FI (highest future emission trajectory) and B1 (lowest future emission trajectory) pathways for three time slices, namely 2020s, 2050s and 2080s (*Source* Table 10.5, [2])

Sub-region	Season	2010–2039				2040–2069				2070–2099			
		Temperature °C		Precipitation %		Temperature °C		Precipitation %		Temperature °C		Precipitation %	
		A1FI	B1	A1FI	B1	A1FI	B1	A1FI	B1	A1FI	B1	A1FI	B1
Central Asia (30 N–50 N; 40 E–75 E)	DIF	1.82	1.52	5	1	3.93	2.50	8	4	6.22	3.44	10	6
	MAM	1.53	1.52	3	−2	3.71	2.58	0	−2	6.24	3.42	−11	−10
	JJA	1.86	1.89	1	−5	4.42	3.12	−7	−4	7.50	4.10	−13	−7
	SON	1.72	1.54	4	0	3.96	2.74	3	0	6.44	3.72	1	0
West Asia (12 N–42 N; 27 E–63 E)	DIF	1.26	1.06	−3	−4	3.1	2.9	−3	−5	5.1	2.8	−11	−4
	MAM	1.20	1.24	−2	−8	3.2	2.2	−8	−9	5.6	3.0	−25	−11
	JJA	1.55	1.53	13	5	3.7	2.5	13	20	6.3	2.7	32	13
	SON	1.48	1.35	18	13	3.6	2.2	27	29	5.7	3.2	52	25

Table 3 Annual mean (four seasons) of projected changes in surface air temperature (°C) and precipitation (%) for West and Central sub-regions of Asia under SRES A1FI (highest future emission trajectory) and B1 (lowest future emission trajectory) pathways for three time slices, namely 2020s, 2050s and 2080s (*Source* Table 10.5, [2])

Sub-region ▼	Annual mean (4 seasons)	2010–2039				2040–2069				2070–2099			
		Precipitation (%)		Temperature (°C)		Precipitation (%)		Temperature (°C)		Precipitation (%)		Temperature (°C)	
Scenarios ▶		A1FI	B1	A1FI	B1	A1FI	B1	A1FI	B1	A1FI	B1	A1FI	B1
West Asia	Mean	6.5	1.5	1.39	1.29	7.25	8.75	3.4	2.22	12	5.75	5.67	2.92
Central Asia	Mean	3.25	(−) 1.5	1.73	1.61	1	(−) 0.5	4.00	2.76	(−) 3.25	(−) 2.75	6.6	3.67

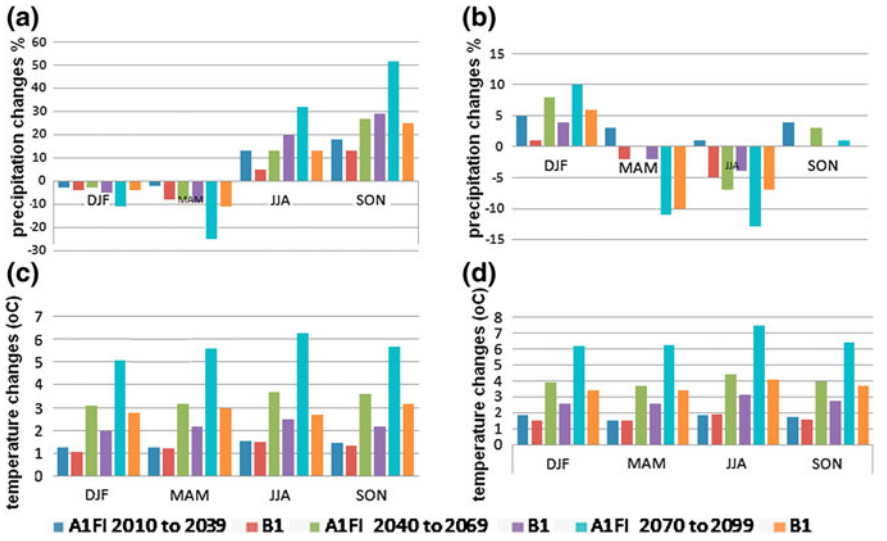

Fig. 2 Comparison of changes in precipitation (*top* graphs a and b) and temperature (*bottom* graphs c and d) in West Asia (*left* graphs a and c) and Central Asia (*right* graphs b and d) sub-regions projected under B1 and A1FI scenarios in four seasons (DJF, MAM, JJA, SON) in three 30 years periods namely 2010–2039, 2040–2069 and 2070–2099, (Graphs produced by author according to the IPCC data)

2.5 Past Climate Changes in Middle East

According to the results obtained from a study with using data for 52 stations in 15 countries including Iran, temperature increased significantly during 1950–2003 [13]. Also some changes observed in the amount of precipitation. Along with the IPCC report, for the West Asia and Middle East region including Iran, according to the climatology stations data, from 1951 to 2003 because of increase of temperature the number of frozen days significantly reduced.

2.6 Climate Projections in Middle East

Future projections for precipitation (%) and temperature (°C) changes has been provided by IPCC in the Middle East region for three time slices, namely 2010–2039, 2040–2069 and 2070–2099. Temperature in all four season according to the different scenarios (A1FI, A2, B2, B1) and using various models (HadCM3, CSIRO, NCAR-PCM, ECHAM4, CGCM2, GFDL, CCSRNIES) will increase (Figs. 3, 4, and 5). Possible precipitation changes could be summarized as follow:

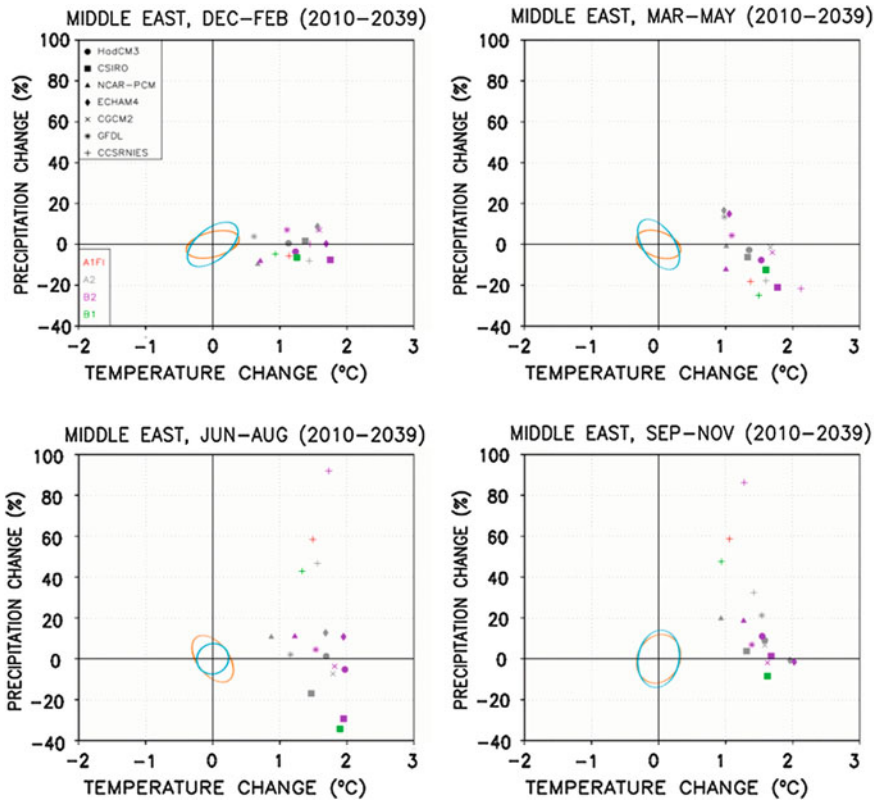

Fig. 3 Future projection of precipitations (%) and temperature (°C) changes in Middle East, for four seasons in 2010–2039 based upon 4 scenarios (A1FI, A2, B2, B1) and 7 models (HadCM3, CSIRO, NCAR-PCM, ECHAM4, CGCM2, GFDL, CCSRNIES) (*Source* IPCC [12]; Tim Carter, IPCC projections expert)

2.7 Past Climate Changes in Iran

According to the recorded data in synoptic stations (IRIMO report) significant increase in minimum, maximum and mean of temperature in most regions observed. In some region like Central, North West, North East of Iran significant decrease observed. In some station increasing pattern and in some other decreasing pattern for precipitation observed.

In Hyrcanian forest region in southern part of Caspian Sea [14] temperature pattern most often increased in last half century [15] and precipitation pattern in the same region mostly showed a decreasing pattern in the same period (Table 4) [15].

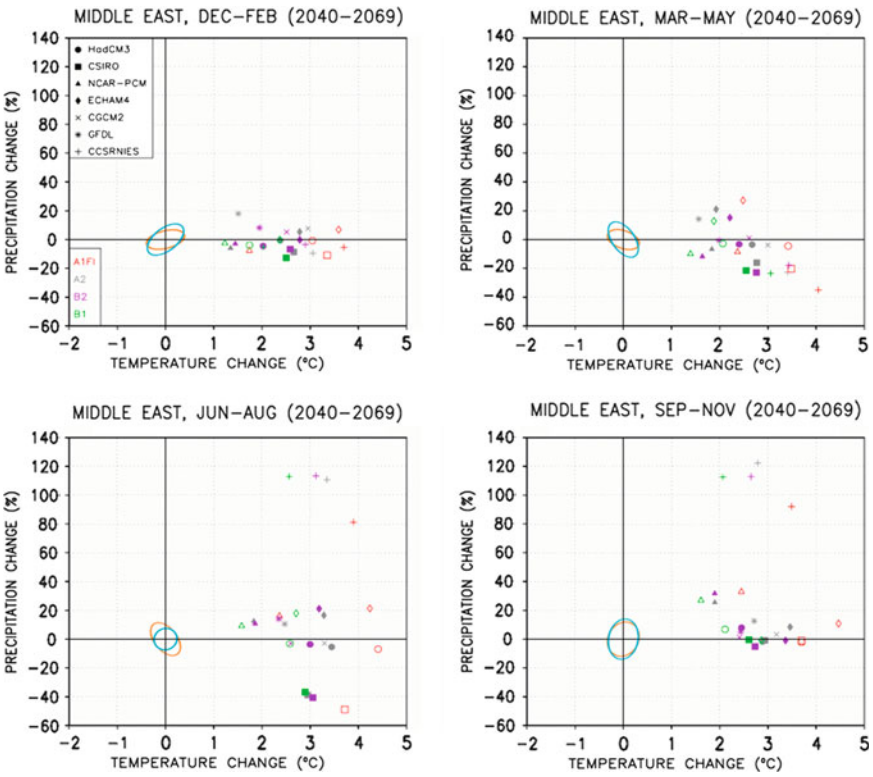

Fig. 4 Future projection of precipitations (%) and temperature (°C) changes in Middle East, for four seasons in 2040–2069 based upon 4 scenarios (A1FI, A2, B2, B1) and 7 models (HadCM3, CSIRO, NCAR-PCM, ECHAM4, CGCM2, GFDL, CCSRNIES) (*Source* IPCC [12]; Tim Carter, IPCC projections expert)

Changes in temperature and precipitation patterns could cause climate conditions change and have impacts on forests, rangelands and deserts ecosystems [15].

2.8 Past Climate Changes in Astara

Past climate condition in the region analyzed by consideration of main climatic factors such as temperature and precipitation in synoptic and climatology stations. Also parameters like humidity and wind fluctuation were investigated. Two important factors, heating degrees and cooling degrees, together with sunshine hours in Astara, were considered. Climatology and synoptic stations data were for a time period of 40 and 18 years respectively.

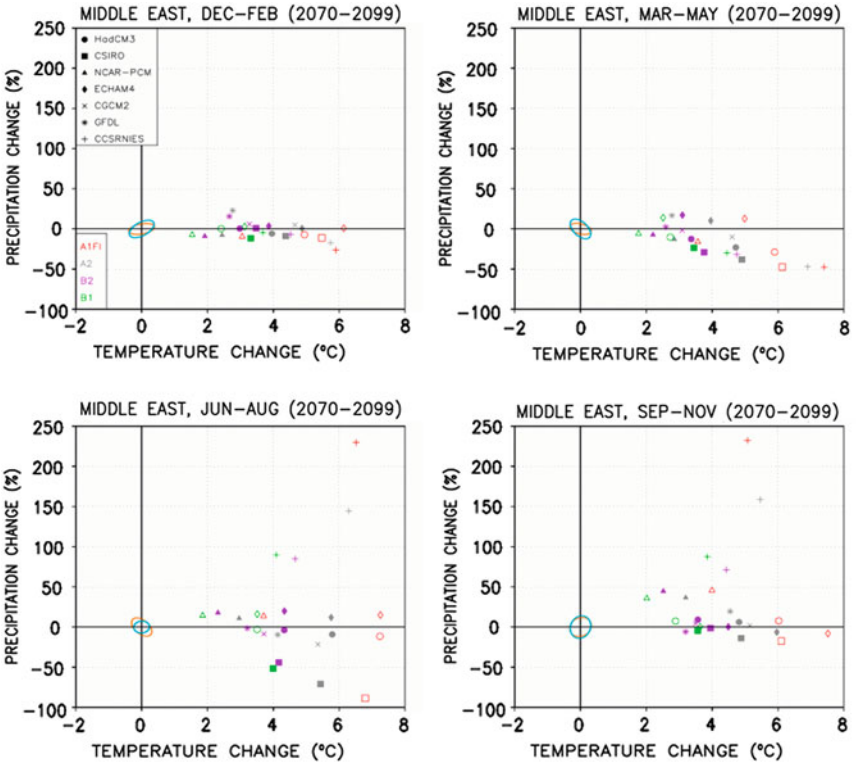

Fig. 5 Future projection of precipitations (%) and temperature (°C) changes in Middle East, for four seasons in 2070–2099 based upon 4 scenarios (A1FI, A2, B2, B1) and 7 models (HadCM3, CSIRO, NCAR-PCM, ECHAM4, CGCM2, GFDL, CCSRNIES) (*Source* IPCC [12]; Tim Carter, IPCC projections expert)

Table 4 Trend of temperature and precipitation changes in last 50 years of Caspian region [15]

Station (year)	Precipitation change (mm)		Temperature change (°C)			
			Minimum	Maximum		Mean
	Increase	Decrease	Increase	Increase	Decrease	Increase
Rasht (49)	56.4		2.45	0.08		1.28
Anzali (54)		509.4	2.10		1.18	0.40
Baboulsar (54)	184.6		1.80	1.10		1.44
Gorgan (53)		55.6	0.11	0.31		0.09

Precipitation pattern in last 40 years in Astara with annual changes were studied, (126.17 mm mean of 40 years of climatology and 1,378.81 mm mean of 18 synoptic stations). Trend of precipitation changes in Astara has an increasing rate.

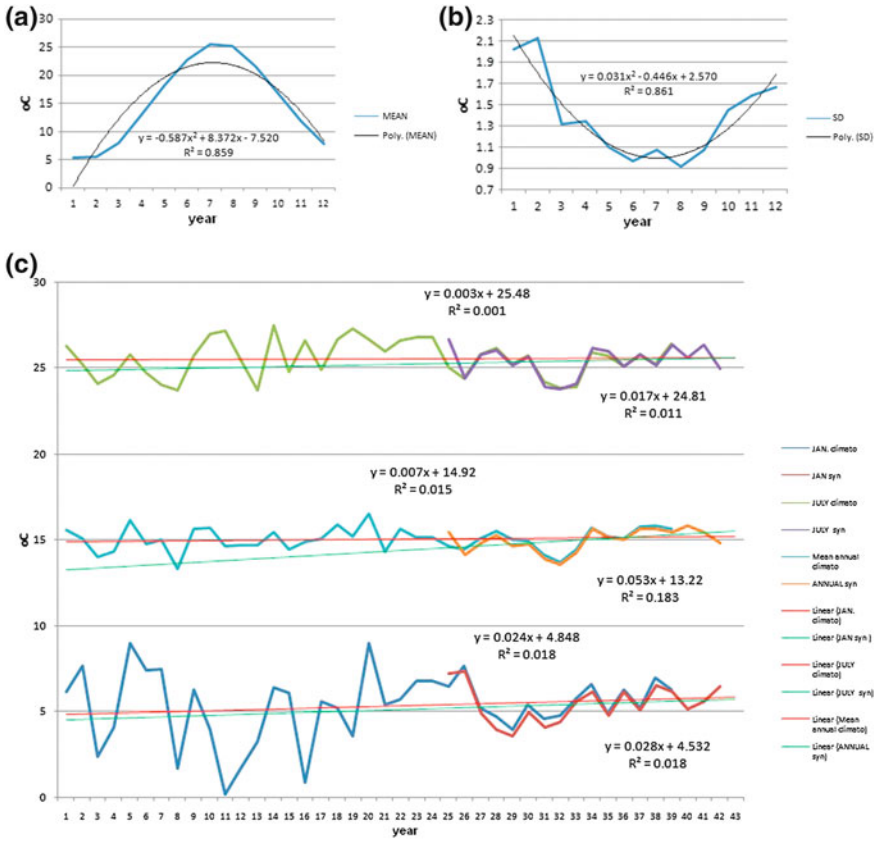

Fig. 6 Past changes of temperature in Astara. **a** Mean of daily average (monthly) temperature (*top left*). **b** Standard deviation of mean of daily average (monthly) temperature (*top right*) in Astara climatology station, 1961–2000. **c** Mean of daily temperature of January (*bottom*), July (*top*), and annual mean (*middle*) in Astara climatology station (+25 m), 1961–2000; and Synoptic station (−18 m), 1986–2003 (*bottom*)

In Fig. 6, past changes in temperature pattern in two climatology (mean of 15.09 °C in climatology and 15.02 °C in synoptic stations) (Fig. 6a), and synoptic (Fig. 6c), stations are presented, adaptation of data in cold (January) and warm (July) months and annual mean (Fig. 6c) give high level of confidence of available data. Mean annual daily temperature the same as mean annual minimum temperature has an increasing pattern, while mean annual maximum temperature has a decreasing trend. With attention to the differences of elevation between two stations, small different of trends are interesting. Standard deviation of mean daily average (monthly) temperature in Astara' climatology station showed that, temperature fluctuation in cold months in the region are much higher than warm months (Fig. 6a, b).

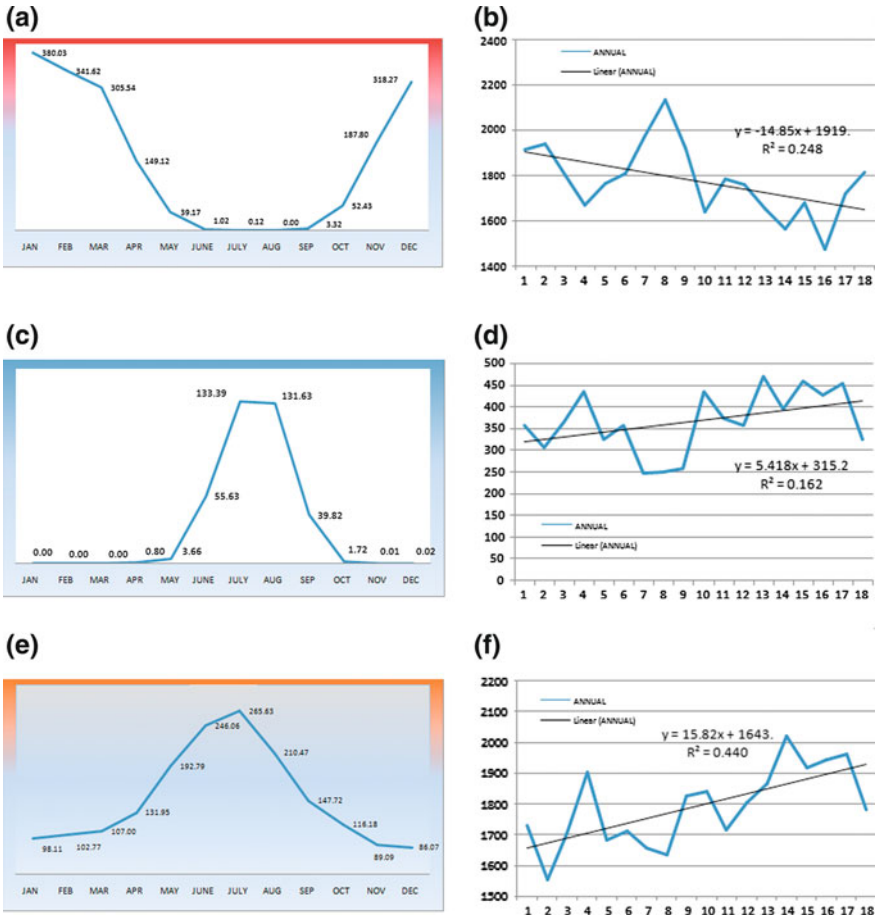

Fig. 7 Astara synoptic station, 1986–2003, total monthly mean. **a** Mean heating degrees °C (based upon 18 °C). **b** Linear trend of mean heating degrees, °C. **c** Mean cooling degrees, °C (based upon 21 °C). **d** Linear trend of mean cooling degrees, °C. **e** Mean monthly total sunshine (hour). **f** Linear trend of total annual sunshine (hour) (*Source* [15])

Changes in humidity trends and wind fluctuation in Astara are presented separately [16].

Heating degrees trend decreased in last 18 years (Fig. 7a, b), while in the same time cooling degrees trend increased (Fig. 7c, d), and this is in the same line of increasing sunshine hours (Fig. 7e, f), and total of these three factors certified warming trend in the Astara region.

2.9 Investigation on Climate Change Projections in Astara and Ardebil

Based on IPCC data and models in global scale and national data and information, downscaling maps in national and regional scales (Fig. 8) produced [17]. National and regional climate projections have some agreement and disagreement with global, continental region and sub-regions projections.

According to the downscaled outcome maps, regional distribution of mean precipitation in future (2010–2039) comparing with the past (1976–2005), Astara region between 1 and 8.7 mm (mean of +4.85 mm) will increase (will reach to 1,265.02 mm according to the climatology and 1,383.61 mm according to the synoptic stations). While in near western part of Astara in the way to Ardebil, a small area will face with reduction of 5.8–23.3 mm (mean of −14.55 mm) rainfall.

Mean precipitation of Gilan province for the time slice of 1976–2005 was about 1,569.9 mm and projected for the period of 2010–2039 precipitation will increased by 10.63 % (amount of +167 mm) and will reach to 1,736.9 mm.

Based on the same results, projections for future, the number of wet days in Astara region between 0 and 3 days will reduce, but in the same climatic area

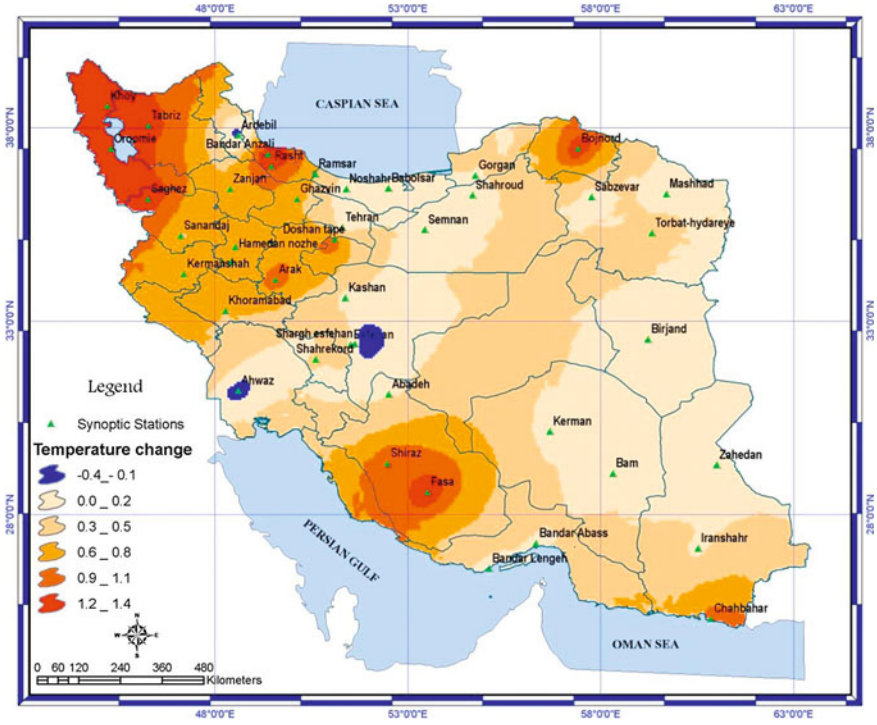

Fig. 8 Mean different distribution of temperature in 2010–2039 compare with 1976–2005 according to the downscaling ECHO-G model [17]

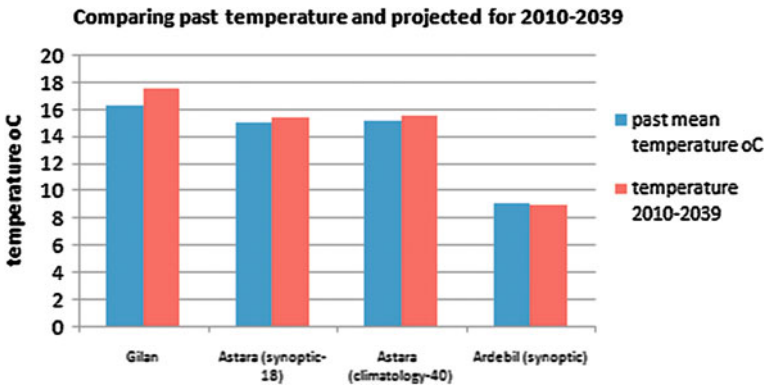

Fig. 9 Temperature changes in projected period (2010–2039), comparing with time slice of (1976–2005), in Gilan province, Astara (synoptic and climatology stations) and Ardebil forests

(west southern) will face with 1–7 days increase of wet days. Mean of dry days will increase between 4 and 9 days. Also temperature in study area of Astara between 0.3 and 0.5 °C (mean of +0.4 °C) will increase (will reach to 15.49 °C according to the climatology and 15.42 °C according to the synoptic stations) (Fig. 8).

Mean temperature of Gilan province for the time slice of 1976–2005 was about 16.2 °C and projected for the period of 2010–2039 temperature will increased by 1.3 °C and will reach to 17.5 °C (Fig. 9). It is needed to be noted that: based on downscaling produced maps in national and regional scales for 1979–2005, Astara region is in a category with temperature of 9.1–12 °C. While based upon my data calculation obtained from climatology and synoptic stations mean temperature is about 15.02 °C (Fig. 9). Probably this rose from using Ardebil synoptic station with mean of temperature of 9.1 °C for downscaling program.

Based on the same results, projections for future, the number of hot days in Astara region between 5 and 10 days will increase, and the number of freezing days will decrease between 0 and 5 days.

2.10 Climate Condition in Astara Especial Forest Ecosystem (District 1)

For assessment of past climatic condition of Astara region data from climatology and synoptic stations were considered (Table 1 and Figs. 6 and 7). To analysis of higher elevation changes, data from nearest station of Ardebil has been used. Ardebil station which is in high mountain in the west part of Astara, despite of difference in elevation (1,325 m) which cause difference in temperature (5.2–8.3 °C), have good correlation in trend of temperature changes (Fig. 10). A detail of stations' characteristics is presented in Table 1.

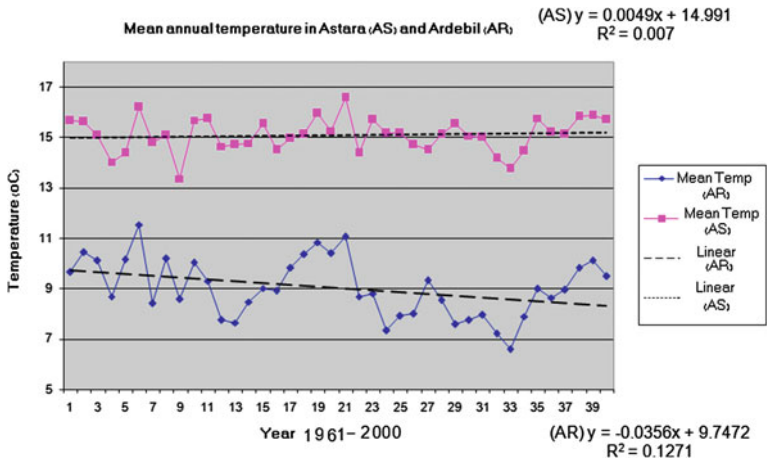

Fig. 10 Mean annual temperature in Ardebil and Astara stations

In 40 years ago, in Astara region with each 252.95 m going upward, temperature was reducing by 1 °C. At the present condition (year 2000) because of increasing trend of temperature in Astara and decreasing trend in Ardebil with changing elevation of 193.04 m temperature will reduce by 1 °C.

Climatology curves (amberotermic graphs) for different stations in Caspian region including Astara stations which are located in southern part of Caspian Sea from west to east were considered (Fig. 11). In produced graphs climatic differences clearly can be distinguished from wet in west to drier condition in the east. To this extend, can be conclude that main difference in climatic conditions in Caspian region raise form differences of the amount of precipitation, and temperature has a secondary effect.

Geographical situation in Astara district. Astara district is situated on western part of Albourz Range Mountain, with north-south direction. Therefore forest covers are on the west-east slops. This region is among those limited areas which from west are affected from Mediterranean (European) climate and from east north from Caspian currents.

Forest conditions and topography of Astara district. Total area of Astara district is about 22,481.25 ha including 18,328.13 ha forests (total Gilan province 511,306 ha), 545.31 ha cool condition rangelands (total Gilan province 467,167 ha), and 3,607.81 ha of farmlands and villages areas. 60 % of forest natural regeneration is from seed sources and 40 % from seeds and copies [18]. Astara forest canopy classification according to the volume is from less than 100 to more than 350 m^3/ha. Astara, land classification of forest area according to the volume per hectare is about 85.92 up to 350 m^3/ha and about 14.07 % with more than 350 m^3/ha. Mean volume per hectare is about 157.17 ± 8.8 (m^3).

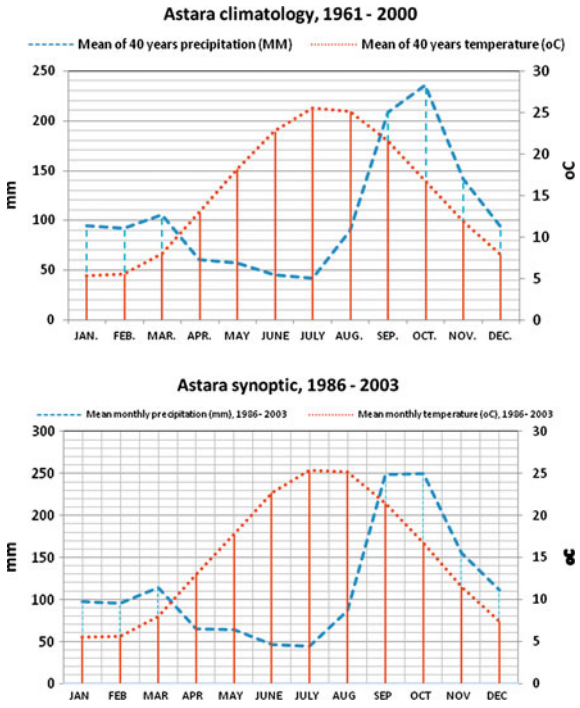

Fig. 11 Climatology curves (amberotermic graphs) for Astara stations in Caspian region for climatology (1961–2000) (*top*) and synoptic (1986–2003) (*bottom*)

3 Results

3.1 Precipitation Changes

Last 40 years of recorded climatology station's data showed an increasing trend in Astara total annual precipitation. Seasonal distributions of rainfall in last 40 years are: fall (Oct., Nov. and Dec.) 38 %, summer 26 %, winter 23 % and spring 13 %. It means two seasons of autumn and summer received main percentage (64 %) of annual precipitation. Warm seasons (summer and spring) received 39 % of annual precipitation while cool season (autumn and winter) received 61 %. In above mentioned time slice October received maximum (240 mm) and July minimum (40 mm) amount of rainfalls.

3.2 Temperature Changes

Based on recorded data in climatology station, in Astara during last 40 years differences of daily maximum and minimum of temperature as a 2nd degree curve first showed increasing and then decreasing patterns. Trend on linear pattern showed a little decrease.

Trend of average daily mean temperature (monthly), showed increasing from January, and in July–August reach to its warmest position and then decline to minimum amount in December (Fig. 6a). Data approved that temperature fluctuation changes in cold months are greater than warm months. Standard deviation (SD) of temperature in cold months is about 2 °C and in warm months about 1 °C (Fig. 6b). Changes in daily mean temperature (annual) in Astara station in last 40 years as linear and 2nd degree curves trends showed increasing patterns. According to the recorded data, mean of annual minimum temperature in cold month (January), warm month (July) and annul mean had increasing trends (Fig. 6c). Mean of annual maximum temperature in warm month (July), slightly in cold month (January), and for annul mean had decreasing trends (Fig. 6c). Hot days which started from May, continue up to October and reach its maximum values in July–August showed a decreasing trend both in linear and 2nd degree curves. According to the data recorded in the synoptic station, mean annual temperature, January and July temperature (Fig. 6c), had increasing patterns in last 18 years.

Freezing days which started from November, continue to May next year, and reach its maximum values in January and February presented decreasing trend both in linear and 2nd degree curves.

Heating Degree Days (HDD) with base temperature of 18 °C reduced in last 18 years (Fig. 7a, b). HDD in January which is cold month also reduced. In the same time Cooling Degree Days (CDD) increased (Fig. 7c, d). CDD in July which is warm month also increased. This is in the same line of increasing the number of sunshine hours in the same time slice (Fig. 7e, f).

Temperature changes recorded for 18 years in synoptic station for cold season (January), warm season (July) and annual mean are in a harmony with last 18 years of changes which recorded for 40 years in climatology station. This can be interpreted of high level of confidence for the precise data (Fig. 6c).

3.3 Other Climatic Factors Changes

As consequence of temperature and precipitation changes, other climatic factors also will change. Relative humidity and thunder and storm are presented and discussed elsewhere [15, 19].

4 Discussion

As a fact, Iran is located on dry belt of the earth and its vegetation cover and forest ecosystems are valuable resources [20, 21]. Also there are limited of adequate research on climate change [2]. So consideration of past climatic changes and investigation on future climate projection have very important role in development

Table 5 Comparison of past changes on Astara temperature in different scales

Scale of study	Temperature (past)
Global	1–2 °C increase (1970–2004)
Asia	
Central Asia	
West Asia	Increase (1951–2003)
Middle East	Increase (1951–2003)
National	
Gilan	Increase
Ardebil	Decrease
Astara	Increase

programs [16, 22]. Even though, the changes in temperature and precipitation are consistent with the other factors [5].

Assessment of all data, document and reports on the past climate changes in the region confirmed that, temperature in last half century increased (Table 5). Studies on the past temperature changes related to the Astara region in global, continental, national and local levels do not have significant differences, except small variation in seasonal changes. Temperature changes had a reducing trend in Ardebil region, which is in the high mountains of western part of Astara. Projections for future temperature changes in Astara are mainly documented for increasing temperature and its amount are different based on employed scenarios (Table 6). Elsewhere, research outcome show that all the IPCC scenarios have similar patterns and only differ in amplitude [23]. From time slices point of view, longer time will experience higher degrees of temperature changes. Astara is located in both Central Asia and West Asia sub-regions in IPCC assessments [2]. Based on the projection for Central Asia sub-region, the region will face with higher degrees of temperature changes, which this is not in the same line as national and local downscaled projections. Downscaled projections in local level prove that Gilan province as whole will have higher degree of temperature changes than Astara which is in the western part of the province, and going more westwards, which is mountainous area of Ardebil; this will change to reduction of temperature. Downscaling and projection of seasonal extreme daily precipitation has been studied elsewhere [24].

Precipitation trend in Middle East region decreased in last half century with some seasonal increase. Precipitation in Gilan province decreased in Anzali station and increased in Rasht station, precipitation showed a seasonal changes pattern (Table 4). Astara experienced in increase of precipitation for last 50 years with some reduction in seasonal levels. Based on global projection with A1B scenario in time period of (2090–2099) Astara which is in the western part of Caspian Sea, in winter season despite of reduction of precipitation in west part of the country, will have 10 % increase of rainfall, and in summer will face with 20 % reduction of precipitation, which these are in the same line of IPCC projection for the Central Asia sub-region and against its projection for the West Asia sub-region. Projections for Middle East region and downscaled projection in national and local levels are more or less in harmony with these projections.

Table 6 Comparison of future projections changes on Astara temperature in different scales

Scale of study	Temperature (projections)
Global	3–3.5 °C increase in 90s (2090–2099, scenario A1B)
	1–2 °C increase in 20s (2020–2029, scenarios B1, A1B, A2)
	4–5.5 °C increase in 90s (2090–2099, scenarios B1, A1B, A2)
Asia	
Central Asia	Increase (in 4 seasons, 2 scenarios—B1, A1F1-, 330 years time slices from 2010 to 2099) From 1.6 to 6.6 °C increase
West Asia	Increase (in 4 seasons, 2 scenarios—B1, A1F1-, 330 years time slices from 2010 to 2099) From 1.2 to 5.6 °C increase
Middle East	Increase up to 2 °C (2010–2039)
National	
Gilan	Increase 1.3 °C (2010–2039)
Ardebil	Decrease 0.1 °C
Astara	Increase 0.3–0.5 °C (2010–2039)

It seems for future projection on precipitation changes in the Astara region it is possible to benefit of global, Central Asia sub-region, Middle East and downscaled national level projections.

5 Conclusion: Astara Climate Change and Energy Balance

Energy balance can be considered from climate change points of views. Energy optimization solution also could be considered, as it has been studied in Nigeria for a given GSM Base Station Site and location in rural area [25].

The theoretical model even could be improved for the reduction in energy consumption, as it has been studied in Greece for the improvement of building energy performance (17). Heating degrees, cooling degrees and total sunshine are factors which are effective on energy consumptions. These data are recorded in Astara synoptic station in period of 1986–2003.

In Astara case study, total monthly heating degrees recorded in winter season reached up to 380.03 °C (January) which is about 12.66 degrees per day. In the same time cooling degree is zero and total monthly sunshine is 98.11 h (January) which is about 3.27 h per day.

Total monthly cooling degrees recorded in summer season reached up to 133.39 °C (July) which is about 4.44 degrees per day. In the same time heating degree is about zero and total monthly sunshine is 265.63 h (July) which is about 8.85 h per day.

Total annual heating degrees in 18 years ago in Astara station was 1,919 °C and total annual cooling degrees was recorded as 315 °C and total annual sunshine was about 1,643 h. During this 18 years period of time trend of mean annual temperature increased from 14.51 °C by about 0.954–15.46 °C.

This warming caused decrease of total annual heating degrees by about 267.3 °C per year down to total annual of 1,651.7 °C. Total annual cooling degrees increased by about 97.38 °C per year up to total annual of 412.38 °C. Total annual sunshine in creased by about 284.76 h per year up to total annual of 1,927.76 h.

Decrease of 267.3 °C per year of heating degrees and increase of 97.38 °C of cooling degrees gives a difference of total of 169.92 °C (267.3–97.38 =169.92 °C) of energy saving in 18 years time.

The price of weather derivatives traded in the summer are based on an index made up of monthly CDD and HDD values. The settlement price for a weather futures contract is calculated by summing a month's CDD and HDD values and multiplying by $20.

$$\text{HDD monthly cost} = \text{HDD} \times 30\,(\text{days of month}) \times 20\,\text{US\$}$$

In Astara case study a difference of annual total of 169.92 °C calculated for energy saving in 18 years time. If we want to calculate cost as a rate of $20 similar to USA conditions, after converting Celsius to Fahrenheit, it would be about $6,117.12 as follow:

$$169.92 \times 9/5 = 305.856$$
$$305.856 \times \$20 = \$6,117.12$$

References

1. Maleviti, E.: The development of a theoretical model for optimizing energy consumption in buildings. Int. J. Energ. Optim. Eng. **1**(4), 1–14 (2012). doi:10.4018/ijeoe.2012100101
2. Cruz, R.V., Harasawa, H., Lal, M., Wu, S., Anokhin, Y., Punsalmaa, B., Honda, Y., Jafari, M., Li, C., Huu Ninh, N.: Asia climate change 2007: impacts, adaptation and vulnerability. In: Parry, M.L., Canziani, O.F., Palutikof, J.P., van der Linden, P.J., Hanson, C.E. (eds.) Contribution of Working Group II to the Fourth Assessment Report of the Intergovernmental Panel on Climate Change, pp. 469–506. Cambridge University Press, Cambridge (2007)
3. Jafari, M.: Climate change and IPCC assessments abstract of keynote lecture of the symposium. In: The Final Report of ICCAP, the Research Project on the Impact of Climate Changes on Agricultural Production System in Arid Areas, pp. 315–317. ICCAP Publication 10-Japan, ISBN 4-902325-09-8 (2007)
4. Okada, M., Iizumi, T., Nishimori, M., Yokozawa, M.: Mesh climate change data of Japan Ver. 2 for climate change impact assessments under IPCC SRES A1B and A2. J. Agric. Meteorol. **65**(1), 97–109 (2009)
5. Hsu, H.H., Chen, C.T.: Observed and projected climate change in Taiwan. Meteorol. Atmos. Phys. **79**(1–2), 87–104 (2002)
6. MacCracken, M.C., Barron, E.J., Easterling, D.R., Felzer, B.S., Karl, T.R.: Climate change scenarios for the US national assessment. Bull. Am. Meteorol. Soc. **84**(12), 1711 (2003)
7. Australian Government, Bureau of Meteorology. http://www.bom.gov.au/index.shtml (2008)
8. Nebraska Public Power District. http://www.nppd.com/ (2008)
9. NOAA: The National Oceanic and Atmospheric Administration. http://www.noaa.gov (2008)

10. The free dictionary. http://financial-dictionary.thefreedictionary.com/Heating+Degree+Day+-+HDD (2008)
11. Wikipedia, the free encyclopedia. http://en.wikipedia.org/wiki/Heating_degree_day (2012)
12. IPCC, climate change 2007: Impacts, adaptation and vulnerability. In: Parry, M.L., Canziani, O.F., Palutikof J.P., van der Linden, P.J., Hanson, C.E. (eds.) Contribution of Working Group II to the Fourth Assessment Report of the Intergovernmental Panel on Climate Change, pp. 469–506. Cambridge University Press, Cambridge (2007)
13. Zhang, X.B., Aguilar, E., Sensoy, S., Melkonyan, H., Tagiyeva, U., Ahmed, N., Kutaladze, N., Rahimzadeh, F., Taghipour, A., Hantosh, T.H., Albert, P., Semawi, M., Ali, M.K., Al-Shabibi, M.H.S., Al-Oulan, Z., Zatari, T., Khelet, I.A., Hamoud, S., Sagir, R., Demircan, M., Eken, M., Adiguzel, M., Alexander, L., Peterson, T.C., Wallis, T.: Trends in middle east climate extreme indices from 1950 to 2003. J. Geophys. Res. Atmos. **110**(D22): Art. No. D22104 NOV 24 (2005)
14. Jafari, M.: Forests and forestry research in I.R. of Iran. J. Trop. For. (in Japanese) **44**, 14–20, Journal code L 1235A, ISSN: 0910-5115, Japanese Publisher (1999)
15. Jafari, M.: Investigation and analysis of climate change factors in Caspian Zone forests for last fifty years (in Persian). Iran. J. For. Poplar Res. **16**(2), 314–326 (2008a)
16. Jafari, M.: An overview on sustainable forest management (SFM) with an introduction to monitoring and evaluation (in Persian) ISBN: 964-6931-80-4, pp. 170. Pouneh Publisher, Tehran, Iran (2006)
17. CC IRIMO: National Centre of Climatology. Islamic Republic of Iran Meteorological Organization. Downscaling report (2008)
18. TFB, Technical Forestry Bureau: Integrated Plan of Northern Forest, primary phase, vol. 1, Districts 1, 2 and 3. Technical Forestry Bureau (TFB), Forests, Ranges and Watershed management Organization (FRWO), Ministry of Jihad -e- Agriculture (1987)
19. Jafari, M.: Thunder and storm fluctuations in the Caspian region over the last half century (in Persian). Iran. J. For. Poplar Res. **16**(4), 583–598 (2008b)
20. Jafari, M.: The present status of forestry research in I.R. Iran. In: Four articles on forests, Technical Publication No. 176-1997, pp. 121, Research Institute of Forests and Rangelands (1997a)
21. Jafari, M.: Present status of afforestation research in I.R. Iran. In: Four articles on forests, Technical Publication No. 176-1997, pp. 121, Research Institute of Forests and Rangelands (1997b)
22. Jafari, M.: Review on needfulness for plant ecophysiological study and investigation on climate change's effects on forest, rangeland and desert ecosystems presented. In: Workshop; Climate Change in South-Eastern European Countries: Causes, Impacts, Solutions, Orangerie, Burggarten, Graz, Austria, 26–27 March 2007 (2007a)
23. Boulanger, J.P., Martinez, F., Segura, E.C.: Projection of future climate change conditions using IPCC simulations, neural networks and Bayesian statistics. Part 1: temperature mean state and seasonal cycle in South America. Clim. Dyn. **27**(2–3), 233–259 (2006)
24. Wang, J.F., Zhang, X.B.: Downscaling and projection of winter extreme daily precipitation over North America. J. Clim. **21**(5), 923–937 (2008)
25. Anayochukwu, A.V., Ndubueze, N.A.: Energy optimization at GSM base station sites located in rural areas. Int. J. Energy Optim. Eng. **1**(3), 1–31 (2012). doi:10.4018/ijeoe.2012070101

Computer Tools for Modelling and Evaluating the Potential of Energy Storage Systems with Reference to the Greek Islands Case

Christos Sbiliris and Vassilis Dedoussis

Abstract In the effort to meet climate change targets the share of renewable energy in electricity market has to be increased. The augmented penetration of renewable sources in the electricity grids could be destabilizing and may create barriers to their future expansion. Energy storage technologies are being regarded as a potential solution to deal with the intermittent nature of renewable energy sources. Introduction of energy storage systems in a future Smart Grid is definitely a complex problem and requires the technological analysis of the energy system itself. The purpose of this paper is to present an up-to-date critical examination of the state of the art of different computer tools that can be used to analyse the integration of energy storage systems utilized in conjunction with distributed generation. Particular emphasis is given to the case of isolated Greek islands.

Keywords Energy storage systems · Energy tools · Energy systems modelling · Microgrids · Isolated islands

1 Introduction

The transition from conventional grid network with central stations in future networks with high penetration of decentralized production, dispersed/distributed generation (DG), mainly from renewable energy sources, involves the development and application of new technologies and the appropriate institutional

C. Sbiliris (✉) · V. Dedoussis
Department of Industrial Management and Technology,
University of Piraeus, Piraeus, Greece
e-mail: xsbiliri@webmail.unipi.gr

V. Dedoussis
e-mail: vdedo@unipi.gr

I. Zelinka et al. (eds.), *Power, Control and Optimization*, Lecture Notes in Electrical Engineering 239, DOI: 10.1007/978-3-319-00206-4_3,

framework [1]. Moving towards large penetration of renewable sources into the electricity grid could be destabilizing, mainly due to the intermittent nature of renewable energies (namely solar and wind); thus showing their unsuitability to be dispatchable. In order to overcome this deficiency of renewable energy sources one has to introduce energy storage devices [1–3]. Energy storage is expected to play a very important role in ensuring safety, reliability and overall efficiency of a low or zero CO_2 emission electricity grid [1]. Electrical energy storage offers the potential to store electrical energy once generated from low and zero carbon sources and to subsequently match supply and demand as required. The augmented penetration of renewable energy sources as well as the trend towards a network transformation into Smart Grid, supports the storage concept more than ever before. Another attractive feature towards energy storage utilisation is the appearance of newer and cost-effective technology options which makes it likely that energy storage will finally become a reality in the near future [4, 5]. Nowadays, the microgrid concept is under development and is being examined as a completely new approach in order to integrate Distributed Energy Resources (DER) to the grids and specially isolated areas such as small islands. The proper design, simulation and optimization a microgrid in order to integrate the distributed energy resources for the management of energy distribution within it, will not only assist managers responsible for capital investment decisions to value different technologies combination but also system operators to develop better integration control strategies for a more efficient operation of future hybrid power systems. A systematic investigation and evaluation of current energy storage technologies in conjunction with both centralized and distributed renewable sources electrical power generation [6], as well as analysis and computational simulation of various case studies [7] is, therefore, imperative.

In this paper an evaluation of energy tools used for analysing power systems is provided so as to assist the process of selecting the appropriate energy storage technology. The paper begins by describing the promising energy storage technologies for large and small scale applications and the current status of modelling these principal energy storage devices. Subsequently, the paper outlines the need for energy storage in microgrids and especially in isolated areas such as islands. A comparison and a brief discussion of some of the energy tools and studies available is carried out. Finally the main characteristics, that a power system design tool incorporating energy storage modules are presented and critically discussed.

2 Energy Storage Technologies-Modeling and Evaluation

Energy storage technologies, utilized in conjunction with distributed generation and the Grid can be divided into two categories. The first category includes those technologies related to direct storage of electricity (e.g. supercapacitors, superconducting magnetic energy storage-SMES, etc.). The second one is associated with the indirect storage of electrical energy, namely storing electricity to another

form of energy (e.g. electrochemical, thermal, mechanical, potential or kinetic energy storage), which can be converted back to electrical, whenever there is a need to meet, an expected or unexpected high overall energy demand [3, 4]. The following sub-sections describe the promising energy storage technologies for application in large scale and in distributed generation with renewable energy sources, as well as the current status of modelling the principal energy storage devices.

2.1 Battery Energy Storage System

A Battery Energy Storage System (BESS) has energy stored in chemical form and produces electricity through an electrochemical reaction. Batteries can be found in many sizes, power ratings, various types [e.g. lead-acid (L/A), sodium-sulfur (NaS), Vanadium Redox (VRB), Zinc-Bromine (ZnBr), ion Lithium (Li-ion), Nickel Cadmium (NiCd) and Nickel Metal Hybrid (NiMH) etc.] and their technologies are in various stages of research and development. They have numerous advantages, such as high discharge depth, high capacity and reduced maintenance requirements. However, many battery types have only limited market penetration, are expensive, or have short lifetimes [2, 4, 5]. Several papers have been published on stand-alone renewable energy systems and the problem of a better integration of the energy produced by them. In work [8] three stand alone photovoltaic power systems using different energy storage technologies as hybrid systems were optimized and compared. An example of an isolated renewable energy-diesel system in conjunction with energy storage technologies is presented in Sebastian and Alzola [9]. Where a Wind Diesel Hybrid System (WDHS) has been modelled and simulated using a Matlab-Simulink Model, in order to investigate the improvement in the system dynamics by using the BESS. Another use of battery energy storage systems seems to be small scale applications such as the integration of renewable energy sources into commercial and residential buildings. Four battery energy storage technologies have been discussed and evaluated techno-economically, by using two different software tools Matlab-Simulink and HOMER in the work of Nair and Garimella [10]. In order to design hybrid energy systems, a complex problem with high number of parameters, researchers have already used available commercial simulation/software tools or have developed new tools, such as HOGA, presented in Dufo-Lopez and Bernal-Agustin [11]. The design tool HOGA has been developed in C++, uses Genetic Algorithms, can be used for different control strategies and can simulate energy storage technologies such as batteries.

2.2 Thermal Energy Storage

This technology is based on storing energy by changing the temperature of certain materials from a relatively low temperature to a higher one. The heat of the

material is used to produce steam which in turn drives a steam turbine coupled to an electrical generator producing electricity. Thermal energy storage systems are efficient, robust, and relatively inexpensive. In work [12] thermal storage was evaluated for applications including concentrating solar power using the GCAM model. Gil et al. [13] discuss the materials used in concentrated solar thermal power generation along with modeling of thermal energy storage systems, pointing out that in order to properly design, simulate and analyze these systems the corresponding software tools should include detailed information on the materials used at high temperature operation.

2.3 Pumped Hydro Energy Storage

Pumped storage hydropower is currently the most widely implemented storage technology especially for large scale applications. It is also the most mature technology, as it is being utilized since the early twentieth century. This energy storage technology is reliable, has a long lifetime and the operating cost is low. However, there are some limitations, such as suitable geographic siting and facility size/capacity. Furthermore, there are environmental concerns related to the construction of artificial water reservoirs and their impact on ecosystems [2, 3, 14]. In work [15] the current trends for new PHES plants in EU are pointed out. Bueno and Carta [16] present the case of an isolated power system, proposing an appropriate wind powered pumped hydro storage system to be installed on Gran Canaria island (Canarian Archipelago) in order to deal with the problem of the penetration of renewable sourced energy in their conventional electrical grid system. An algorithm for the selection of the optimum economic renewable system has been developed and evaluated. Another example on pumped storage systems introduction in isolated power production systems is presented in Katsaprakakis et al. [17] where two case studies for Crete and Rhodes island have been evaluated using a single criterion optimization algorithm.

2.4 Compressed Air Energy Storage

As an alternative to pumped hydro storage is considered to be CAES, which also seems to be a good solution for large scale applications. This system stores energy in the form of compressed air in high pressure tanks or underground geological cavities such as aquifers or mines. Advantages of this energy storage system are: low storing losses, fast start-up time response and applications versatility to both large and small scale distributed generation. The main disadvantage is the existence of the appropriate geological structures, such as mines [2, 3, 14]. CAES could also be used for small and medium scale applications [14]. In paper [18] a deterministic model has been used to perform an evaluation of a compressed air energy storage

(CAES) plant in the Danish electricity system, in order to investigate the integration of wind power. EnergyPLAN computer model has been used as an analysis tool of the specific national energy system since it provides the ability to perform both system-economic and business-economic evaluations. An example of small scale application is that of wind–compressed air energy storage (Wind–CAES) systems in islanded electricity networks. A dual-mode CAES configuration in conjunction with wind farms is evaluated by Zafirakis and Kaldellis [19] using a developed simulation algorithm for the dual-mode CAES system.

2.5 Flywheel Energy Storage

Flywheels store energy in the form of mechanical-kinetic energy. The energy is saved via the turning of a mass spinning at high speed. It can be converted back to electrical energy by connecting the spinning mass to the rotor of a generator. Flywheels have long lifetime, high energy density and are relatively environmental friendly [2]. A flywheel farm approach, where several devices are networked together, could also be used for large-scale energy management. However, flywheels are a relatively "new" electrical energy storing technology, they require maintenance because of the moving mechanical parts involved, and have a high cost. Further development of the flywheel construction materials and improvement of the semiconductors seem to provide new possibilities for flywheels energy storage implementations, in renewable applications as well as transport systems [5, 20, 21]. In renewable energy systems, flywheels can serve as energy storage devices in islanded power systems where wind plants and diesel hybrid systems provide electricity, or in other isolated renewable energy distributed systems. A variety of different flywheels configurations have been studied simulated and compared to find the optimal for a given application in the work by Carrillo et al. [22].

2.6 Superconducting Magnetic Energy Storage

SMES systems store energy in a magnetic coil of superconducting material which is cooled in very low temperature via a very cold liquid such as liquid helium [3]. The absence of moving parts in a SMES system, the limited maintenance requirement and the long lifetime are some of this storage technology advantages. Flywheels respond at microseconds with excellent voltage regulation and are environmental friendly [2, 3]. The cooling requirements and the high manufacturing cost are considered the main disadvantages of SMES [2, 3, 14]. One of the most important parts, when designing and selecting a SMES, is the size of the superconducting magnetic coil. In work [23] Genetic Algorithms have be used to identify the optimal SMES controller configuration considering both coil size and system uncertainties.

2.7 Super Capacitor Energy Storage

Super capacitor is actually a double layer capacitor, energy is stored in the electric field between two electrodes by applying a DC voltage. The principle of supercapacitors operation is the same as capacitors, though improved materials with higher dielectric constants offer higher storage capacity. Supercapacitors can be charged and discharged really fast, have long cycle life and are environmental friendly. Depending on the application supercapacitor may require a DC/AC converter and control equipment which affects adversely their efficiency and cost [2, 3, 24]. The improvements of the materials used in the construction of supercapacitors will lead to further integration of these energy storage devices to a variety of hybrid power generation systems [5]. A variety of mathematical models and equivalent circuits of supercapacitors have been proposed, the simplest equivalent circuit to model a supercapacitor is the classic RC model, a capacitor C with an equivalent series resistance (ESR) to represent the Joule losses. Other equivalent circuits are the RC parallel branch model, the RC branches series-parallel model, RC transmission line model. For these more detailed supercapacitor RC models is harder to experimentally obtain the characteristic parameters, so the simplest model is usually preferred as it is explained in work [25], where supercapacitor is modelled using Matlab/Simulink. A new supercapacitor model is introduced in Tironi and Musolino [26] able to obtain the parameters by a simple constant current charge test, providing a better representation of the dynamics of the storage device.

2.8 Hydrogen Energy Storage-Fuel Cells

Hydrogen produced via large or small scale electrolysis of water, is not a renewable energy source and maybe regarded more as an (electrical) energy storage agent. Fuel cells can be used to generate electricity for the grid or in transport applications. Hydrogen fuel cells are environmental friendly provided that the electricity required for electrolysis is produced via renewable energy sources [2]. Fuel cells technology is rather new and quite expensive and compared to batteries, fuel cells can produce electricity in a continuous way [27]. Decentralised power systems based on photovoltaic or wind generators can use electrolytic production of hydrogen (H_2) as a mean to store the excess energy produced by them [14]. Using H_2 as storage system can be used not only for load management but also for wind power fluctuations smoothing. Different control strategies for electrolytic production of H_2 may also maximize the utilization of wind power in weak systems. Simulation models and implementation of different control strategies for systems as described above have been developed as MATLAB-function and the power flow toolbox MATPOWER has been employed in the work by Korpaas et al. [28]. Avril et al. [29], have developed a multi-objective code

using swarm optimization, which was used to compare batteries and Hydrogen storage in a distributed generation system (PV), for an isolated real case, in order to evaluate the storage technologies for a given period of time.

3 Microgrids and Distributed Energy Storage

Nowadays rapid changes in the power industry, augmenting distributed generation and the trend towards a network transformation into Smart Grids show the need to develop new power systems [7]. Research to identify the electric grid of the future is currently underway and the main goal is the wide utilisation of renewable energy sources. As the number of distributed solar photovoltaic (PV) installations and wind farms are growing rapidly [24] it seems that integration of significant quantities of distributed renewable energy, combined with storage, will lead to a new power network design allowing higher penetration of renewable sources [30], such as microgrid. A microgrid can be perceived as a group of dispersed generators, dispersed storages (DS) and a mixture of load consumers [31] (for extended review on definitions of the microgrid concept see [32]). A microgrid may be operated in grid mode, meaning interconnected to the main grid, or in islanded mode [33]. In general, islanding happens when dispersed generating units provide part of the energy needed disconnected from the main grid distribution system. One of the most important challenges faced when operating such DG system is not only the coordinated operation of the numerous generators and their power flow but also controlling the frequency and voltage of such a system. Designing an optimal microgrid is a complex task mainly because of the intermittent nature of distributed renewable sources (solar, wind) where traditional design and optimisation tools cannot be used [34]. Energy storage used in conjunction with renewable energy has been suggested as a means to increase the use of renewable energy while maintaining system stability [6]. The increase of small generation units, mainly including renewable energy sources, connected to Low Voltage (LV) networks has lead to the need of further development of microsource modelling and control strategies definition. The analysis of these microgrids demands appropriate dynamic models for simulation purposes. In work [35] a management and control strategy for optimally operating a microgrid in standalone mode is proposed. According to the authors a central controller is receiving data from a communication facility and with the help of an optimal function a suitable generation value for each one of the DG units is determined. Microgrid is considered to be a new concept but it is believed that research has reached the point where demonstration of practical operating systems is achievable. A stand alone mode system exists in Kythnos island, in Greece whose power system is not connected to the main Greek power grid exhibiting the main characteristics of a microgrid [32, 36].

According to Hanley et al. [37] new energy storage modelling tools, tools for further analysis of the power systems and business decision models will be needed for the optimal integration of energy storage systems. These modelling and

simulation tools will help designers to evaluate the needs and effects of various storage technologies. When selecting the most appropriate storage technology, the most relevant criteria characteristics are capital cost, energy capacity, power capacity, lifetime (or cycling capacity), efficiency, self discharge rates, environmental impact, storage duration and technical maturity [4, 14, 24]. In work [14] the storage technologies have been divided in four categories based on their applications, (a) low power applications, (b) medium power applications, (c) network connection application with peak levelling and (d) power quality applications. A series of reports from Sandia National Laboratories [38] is providing useful information on the energy storage technologies evaluation, from the techno-economic point of view. In these reports another categorisation of has been proposed: (a) Grid System, (b) End-user/Utility Customer, (c) Renewables. Research shows that the choice of an energy storage technology depends on the application in either the conventional grid or in the DG grid and therefore a detailed techno-economic evaluation of different systems is difficult to be achieved [2, 3]. Energy storage technologies can provide a variety of services to the benefit of the electricity network [7]. Details on the subject can be found in Sandia National Laboratories report [39].

4 Energy Storage for Greek Island Electrification

Isolated systems, mainly islands, have felt the pressure for higher penetration of renewable sources. The pressure is becoming even stronger and the reasons are mainly the excessive fuel costs caused by the additional costs of shipment but also to the relatively small system size. These isolated systems have often considerable renewable sources available, but the extensive utilization of these renewable resources, such as solar and wind, is often limited due to security reasons. The network must be operated within tight margins of voltage as well as frequency, though wind and solar plants and other renewable sources are not capable to support and maintain the system at the desired operating condition and may sometimes lead to a negative overall effect mainly due to the intermittent nature of these resources [30, 34, 37]. Most non interconnected Greek islands are depended on their autonomous (including both conventional and renewable) generation systems to cover the demand. It is expected that introduction of energy storage technologies in these systems will be considered an economic and reliable solution helping in the further augmentation of the penetration of renewable sources [40].

Wind and PV systems with storage consideration has been investigated for feasibility purposes for a number of scattered islands in the Aegean archipelagos [41]. Pumped hydro energy storage combined with wind sources looks promising for the island of Lesbos [42] and other islands with medium or large grid systems which are geologically suitable. In islands (either inhabited or deserted) renewable resources can also be used for hydrogen production which is another form of energy storage. Hydrogen can be used as fuel for cars or ferries as described in

paper [28] for a case study of a Norwegian island. Gondal and Sahir [43] discuss modelling tools of hydrogen in conjunction with renewables in order to assist the decision makers to invest in this technology. Prodromidis and Coutelieris [44] investigate the utilisation of batteries and flywheels for autonomous renewable energy based systems for the case of the Greek island of Naxos concluding that these hybrid power systems seems to be economically competitive, while flywheels commercialization is expected in near future. Energy storage could also be used in hybrid renewable based power systems, which are not only responsible for electrification but also for desalination and production of potable water. An example of anhydrous areas or islands is the one presented by Karellas et al. [45] for the Greek island of Chalki.

5 Analysis Tools for Energy storage Impact in Micro-grid Applications

Developing an appropriate flexible tool for the design and capacity planning of renewable energy generation units combined with storage devices will help to localize the energy storage benefits to an intermittent renewable system. Therefore, various strategies for increasing renewable energy source penetration into the grid using storage technologies have to be studied. One of the main reasons for the limited implementation in practice of the energy storage technologies, is the lack of appropriate tools to investigate the operational cost and evaluation of the benefits using market models when planning the power system including the storage devices. Furthermore, the lack of a formal mechanism for calculating the value of the benefits and savings brought by energy storage is a major constraint for wider storage implementation [46–48].

Kuldeep and Bharti [3] defined the major factors to be considered when designing and implementing energy storage technologies both for grid connected and off-grid application. These characteristics should be included in an appropriate design and planning tool to obtain an optimized model of energy storage for use in a microgrid environment or in a smart grid. Very useful information concerning energy storage software tools is also included in a special purpose report prepared for the U.S. Department of Energy [49]. It is interesting to note that neither pumped hydro power nor compressed air energy storage systems due to siting limitations have been addressed in this report. It is evident that new tools or new modules within existing tools should be developed in order to help energy systems designers to appreciate quantitatively the value of storage introduction in the modern power grid.

Combining the results from work [3] and [49] the factors that should be considered while developing an energy storage optimisation and evaluation tool can be summarised as follows:

- Power plant generation capacity optimization.
- Identification of the application the storage technology is being used and its suitability.
- Modeling of the energy storage technology, optimal sizing of the storage system and optimization for specific use, such as ancillary services, renewable integration etc.
- Development of an energy storage dispatch algorithm.
- The interconnection requirements and constraints of energy storage in conjunction with distributed generation.
- Control strategies to ensure power system reliability, power quality and efficient planning functionality.
- Analysis of the investment effectiveness of the energy storage technology under evaluation, from techno-economical perspective such as the return of the investment on the end user costumer or the utility.

In order to examine the introduction of energy storage modules in energy tools, a thorough investigation was conducted considering studies, models and planning software tools. The investigation was based on the work of Hoffman et al. [49], and Connolly et al. [50] and on internet sources [51–58]. For the sake of comparison purposes the results of the investigation are summarized and presented in tabular form in Table 1 below.

The energy tool characteristics evaluated are:

- Energy storage modeling availability.
- The energy tool is able to perform arbitrage involving the purchase of inexpensive electricity available during periods when demand for electricity is low, to charge the storage plant, so that the low priced energy can be used or sold at a later time when the price for electricity is high.
- As operation optimization tool it provides the option to optimize the system solution around particular uses.
- The tool is able to provide information on the impact of round trip efficiency of the energy technology used.
- An investment return optimisation tool is capable to financially optimize and provide information on the return of the investment.
- The energy tool as simulation tool simulates the energy power system under study for a one year period time using a time step, usually hourly.
- The energy tool as scenario tool can operate the results for multitime-period, combining the results into scenarios for a longer period of time usually 20–50 years.

For the sake of completeness simplified flow charts/diagrams from the user manuals for two of the most important energy tools evaluated in this study, RETScreen and EnergyPLAN, are presented below in Figs. 1 and 2, respectively [52, 58] and are briefly discussed.

RETScreen is a clean energy project analysis software which is used for the evaluation of energy production, life cycle costs, and greenhouse gas emissions,

Table 1 Characteristics of energy storage in the tools investigated

Tool	Energy storage technologies (modules)	Arbitrage	Operation optimisation	Round trip efficiency	Investment return optimisation	Simulation	Scenario
DIgSILENT	(batteries, fuel cells, flywheel (in PowerStore), Matlab Integration)	No	N/A	Yes	No	Yes	N/A
EnergyPLAN	(pumped hydro, hydrogen, CAES, thermal storage)	No	Yes	Yes	Yes	Yes	No
HOMER	(batteries, hydrogen, flywheels)	N/A	Yes	N/A	Yes	Yes	No
NEMS	(storage technologies to model load shifting)	N/A	N/A	N/A	Yes	N/A	Yes
PowerWorld	(possible)	No	N/A	No	No	Yes	N/A
PSAT	(batteries, fuel cell)	No	Yes	Yes	Yes	Yes	No
ReEDS	(pumped hydropower, compressed air, batteries, thermal storage)	Yes	Yes	Yes	Yes	N/A	Yes
RETScreen	(batteries)	No	No	Yes	N/A	No	Yes

N/A: Not explicitly information is available

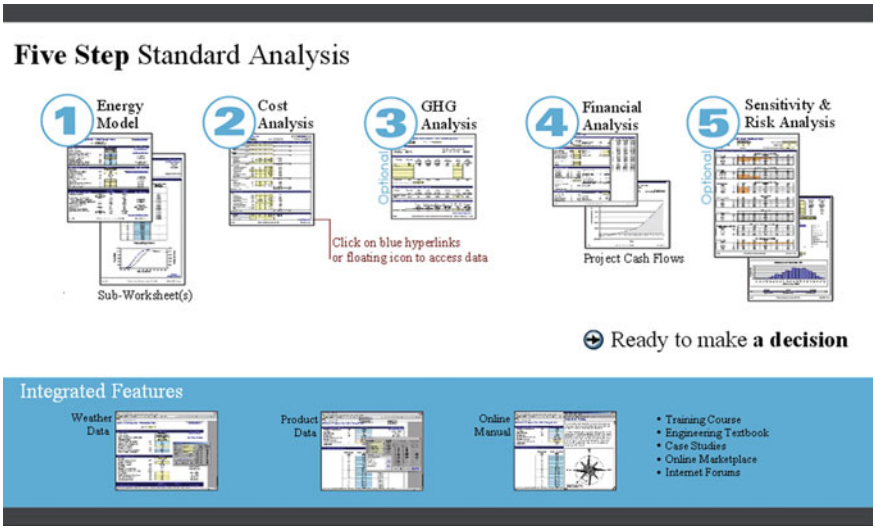

Fig. 1 RETScreen model flow chart

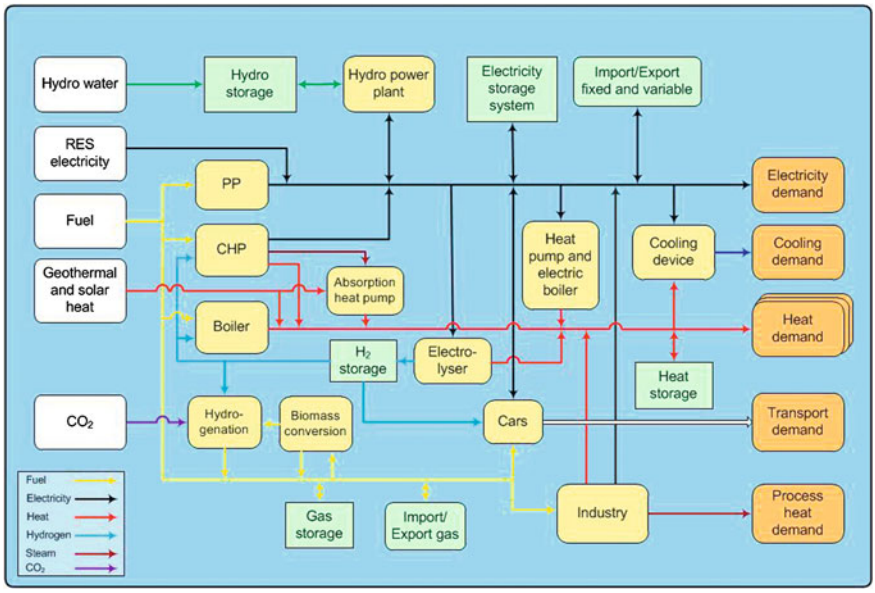

Fig. 2 EnergyPLAN diagram

which has been developed as a Microsoft Excel spreadsheet file. It also has embedded data, such as product, weather and cost databases. In order to perform the analysis the software processes the input data from five worksheets. In the Start worksheet general information about the project is provided by the user such as

title, location, weather condition etc. In the first step the Energy Model worksheet is used to define the basic technological parameters of the proposed case study such as the technology selected, the size etc., which then will be used, in combination with the internal databases, to perform the requested simulation to extract results. In step two, Cost Analysis is used to help the user estimate costs or/and credits of the case studied. Input data for initial cost, investment, cost standpoint etc. are inserted in this worksheet. In step three GHG analysis, Emission Analysis is provided to help in the evaluation of the emission reduction potential of the proposed project compared with the base case scenario. In step four Financial Summary, or Financial Analysis worksheet includes financial parameters input items of the project (e.g. discount rate, debt ratio, etc.), and its calculated financial viability output items (e.g. IRR, simple payback, NPV, etc.), which allows the decision-maker to evaluate the economic viability of the project. In step five the software includes the Sensitivity and Risk Analysis, this feature of the software shows the relationship between the key parameters and the financial indicators, as well as the risk of the investment.

EnergyPLAN is a user friendly energy analysis software tool, designed in a series of tab sheets. The main goal of the model is to assist the design of national or regional energy planning strategies implementing different energy systems and investments. EnergyPLAN considers, actually three primary sectors of any national energy system, namely electricity, heat, and transport sectors. The model is hourly simulation deterministic input/output model. In the front page a holistic view of the energy system as shown in Fig. 2 is provided. In the Input tab, information of the energy system is inserted in the model such as, energy demands (heat, electricity, transport, etc.), energy production units and resources (wind turbines, power plants, oil boilers, storage, etc.). In the Cost tab fuel costs, taxes, variable and fixed operational (maintenance) costs, investment costs and lifetime are introduced in the model according to the technology selected by the user. In the Regulation tab, the regulation and operation of each plant and the system including technical limitations are defined. In the Output tab the output results of the analysis can be shown and/or exported from the model in the three following ways: View on the screen, Print or see in Graphics. Finally, in the Setting tab, user has the option to define the energy units and monetary units.

It should be noted finally, that various ‘real world’ case studies have been carried out world-wide using the available energy analysis software tools. EnergyPLAN has been used for simulation of a renewable energy system for the case of Mljet island in Croatia [59]. Additionally EnergyPLAN has been used to model the Chinese energy system in order to study the large-scale integration of wind power in their system [60]. HOMER software has been used to find the optimal energy solution for a given GSM Base Station Site in Nigeria [61], the software has also been employed to evaluate a stand-alone PV system comprising of batteries as described in the work of Nair and Garimella [10] from the technoeconomical point of view. In another work by Castañeda et al. [62], HOMER is used as a sizing tool for a stand-alone hybrid generation system integrating renewable energies for comparative purposes. The latter case study concerns a load, located in Álora

(Málaga), Spain and the system has batteries and fuel cells. NEMS is used to create the annual energy output of USA [50]. RETScreen has been used to evaluate the cost of a stand-alone photovoltaic system for a 4-person residential house in Malaysia [63].

6 Discussion and Concluding Remarks

It can be seen that *none* of the eight tools presented has *all* the storage technology models or the important characteristics. None is also absolutely dedicated to energy storage optimisation. In addition there is no single software tool suitable for the investigation of evaluating the various energy storage technologies in conjunction with renewable energy sources, in terms of a micro or smart grid [49, 64]. In order to define the role and amount of storage, research should be focused on the determination of an evaluation method to monetize the benefits provided by energy storage technologies. There has been a number of projects aiming at this development of an energy storage evaluation tool such as RESET (Renewable Energy Storage Engagement Tool), which calculates the maximum economic value of excess renewable generation by optimally sizing energy storage systems allowing comparison and evaluation of the economic profitability of multiple energy storage technologies at their site [65]. One of the most sophisticated, energy storage evaluation tool is the one produced from the partnership between the Sandia National Laboratories and KEMA funded from the DOE's Energy Storage Program, the ES-Select^{TM} Tool [66]. The aforementioned tool has been released for public download which will help utilities, developers and regulators to select the best storage option based on the application studied. It provides a graphical comparison of statistical distributions for characteristics of feasible energy storage technologies, such as installed cost and payback, to help users make informed final decisions. It is a preliminary investigation tool which will help users to decide whether or not a further detailed simulation run and site specific analysis should be conducted.

It can be concluded, therefore, that the selection of an energy storage technology depends on the specifications of the application to be addressed. Also, even though there is a wide range of energy tools only a limited number includes energy storage modelling. It is obvious that there is no single software package able to deal with the optimal sizing, sitting and operation of energy storage in distributed renewable energy generation that would be useful to managers responsible for capital investment decisions to value energy storage technologies and introduce these technologies in present grid infrastructure development. Adopting energy storage technologically will require appropriate modelling tool offering system analysis, information on the economic and operational benefits and most important including a methodology of evaluation of the different energy storage technologies to determine the suitability and selection for specific application such as the integration of various renewable energy resources.

Electric storage is expected to play a larger role in islanded systems not only by helping to stabilize generation and load variations but also minimise the operation cost of the existing systems. Greek islands which are isolated and exhibit tremendous amount of wind and solar power potential do indeed present a suitable field of applying such energy storage technology analysis and evaluation tools.

References

1. Naish, C., McCubbin, I., Edberg, O., Harfoot, M.: Outlook of energy storage technologies. Technical report, European Parliament's committee on industry, research and energy (ITRE) (2006)
2. Cole, S., Van Hertem, D., Meeus, L., Belmans, R.: Energy storage on production and transmission level: a SWOT analysis. WSEAS Trans. Power Syst. **1**, 31–38 (2006)
3. Kuldeep, S., Bharti, D.: Energy storage technology for performance enhancement of power systems. Electr. Power Qual. Utilization Mag. **4**, 1–9 (2009)
4. Baker, J.: New technology and possible advances in energy storage. Energy Policy **36**, 4368–4373 (2008)
5. Hall, P.J., Bain, E.J.: Energy-storage technologies and electricity generation. Energy Policy **36**, 4352–4355 (2008)
6. Hall, P.J.: Energy storage: the route to liberation from the fossil fuel economy? Energy Policy **36**, 4363–4367 (2008)
7. Wade, N.S., Taylor, P.C., Lang, P.D., Jones, P.R.: Evaluating the benefits of an electrical energy storage system in a future smart grid. Energy Policy **38**, 7180–7188 (2010)
8. Li, C.H., Zhu, X.J., Cao, G.Y., Sui, S., Hu, M.R.: Dynamic modeling and sizing optimization of stand-alone photovoltaic power systems using hybrid energy storage technology. Renew. Energy **34**, 815–826 (2009)
9. Sebastian, R., Alzola, R.P.: Simulation of an isolated wind diesel system with battery energy storage. Electr. Power Syst. Res. **81**, 677–686 (2011)
10. Nair, N.K., Garimella, N.: Battery energy storage systems: assessment for small-scale renewable energy integration. Energy Buildings **42**, 2124–2130 (2010)
11. Dufo-Lopez, R., Bernal-Agustin, J.L.: Design and control strategies of PV-Diesel systems using genetic algorithms. Sol. Energy **79**, 33–46 (2005)
12. Zhang, Y., Smith, S.J., Kyle, G.P., Stackhouse, J.: Modeling the potential for thermal concentrating solar power technologies. Energy Policy **38**, 7884–7897 (2010)
13. Gil, A., Medrano, M., Martorell, I., Lázaro, A., Dolado, P., Zalba, B., Cabeza, L.F.: State of the art on high temperature thermal energy storage for power generation. Part 1: concepts, materials and modellization. Renew. Sustain. Energy Rev. **14**, 31–55 (2010)
14. Ibrahim, H., Ilinca, A., Perron, J.: Energy storage systems-characteristics and comparisons. Renew. Sustain. Energy Rev. **12**, 1221–1250 (2008)
15. Deane, J.P., O Gallachoir, B.P., McKeogh, E.J.: Techno-economic review of existing and new pumped hydro energy storage plant. Renew. Sustain. Energy Rev. **14**, 1293–1302 (2010)
16. Bueno, C., Carta, J.A.: Wind powered pumped hydro storage systems, a means of increasing the penetration of renewable energy in the Canary Islands. Renew. Sustain. Energy Rev. **10**, 312–340 (2006)
17. Katsaprakakis, D.A., Christakis, D.G., Zervos, A., Papantonis, D., Voutsinas, S.: Pumped storage systems introduction in isolated power production systems. Renew. Energy **33**, 467–490 (2008)
18. Lund, H., Salgi, G.: The role of compressed air energy storage (CAES) in future sustainable energy systems. Energy Convers. Manage. **50**, 1172–1179 (2009)

19. Zafirakis, D., Kaldellis, J.K.: Autonomous dual-mode CAES systems for maximum wind energy contribution in remote island networks. Energy Convers. Manage. **51**, 2150–2161 (2010)
20. Murakami, K., Komori, M., Mitsuda, H., Inoue, A.: Design of an energy storage flywheel system using permanent magnet bearing (PMB) and superconducting magnetic bearing (SMB). Cryogenics **47**, 272–277 (2007)
21. Bolund, B., Bernhoff, H., Leijon, M.: Flywheel energy and power storage systems. Renew. Sustain. Energy Rev. **11**, 235–258 (2007)
22. Carrillo, C., Feijóo, A., Cidrás, J.: Comparative study of flywheel systems in an isolated wind plant. Renew. Energy **34**, 890–898 (2009)
23. Ngamroo, I.: An optimization of robust SMES with specified structure H[infinity] controller for power system stabilization considering superconducting magnetic coil size. Energy Convers. Manage. **52**, 648–651 (2011)
24. Beaudin, M., Zareipour, H., Schellenberglabe, A., Rosehart, W.: Energy storage for mitigating the variability of renewable electricity sources: an updated review. Energy Sustain. Dev. **14**, 302–314 (2010)
25. Zhan-li, C., Wei-rong, C., Qi, L., Zhi-ling, J., Zhi-han, Y.: Modeling and dynamic simulation of an efficient energy storage component supercapacitor. In: Power and Energy Engineering Conference (APPEEC), 2010 Asia-Pacific, pp. 1–4 (2010)
26. Tironi, E., Musolino, V.: Supercapacitor characterization in power electronic applications: proposal of a new model. In: 2009 International Conference on Clean Electrical Power, pp. 376–382 (2009)
27. Edwards, P.P., Kuznetsov, V.L., David, W.I.F., Brandon, N.P.: Hydrogen and fuel cells: towards a sustainable energy future. Energy Policy **36**, 4356–4362 (2008)
28. Korpaas, M., Greiner, C.J., Holen, A.T.: A logistic model for assessment of wind power combined with electrolytic hydrogen production in weak grids. In: 15th Power Systems Computation Conference. Liege, Belgium (2005)
29. Avril, S., Arnaud, G., Florentin, A., Vinard, M.: Multi-objective optimization of batteries and hydrogen storage technologies for remote photovoltaic systems. Energy **35**, 5300–5308 (2010)
30. Toledo, O.M., Oliveira Filho, D., Diniz, A.n.S.n.A.C.: Distributed photovoltaic generation and energy storage systems: a review. Renew. Sustain. Energy Rev. **14**, 506–511 (2010)
31. Lidula, N.W.A., Rajapakse, A.D.: Microgrids research: a review of experimental microgrids and test systems. Renew. Sustain. Energy Rev. **15**, 186–202 (2011)
32. Mitra, I., Degner, T., Braun, M.: Distributed generation and microgrids for small island electrification in developing countries: a review. SESI J. **18**, 6–20 (2008)
33. Xuan, L., Bin, S.: Microgrids: an integration of renewable energy technologies. In: International conference on electricity distribution, CICED 2008, China (2008)
34. Biczel, P., Michalski, L.: Simulink models of power electronic converters for DC microgrid simulation. In: 6th International Conference-Workshop, Power Quality, Alternative Energy and Distributed Systems, Compatibility and Power Electronics. CPE '09, pp. 161–165 (2009)
35. Ghadimi, A.A., Rastegar, H.: Optimal control and management of distributed generation units in an islanded microgrid. In: 2009 CIGRE/IEEE PES Joint Symposium Integration of Wide-Scale Renewable Resources into the Power Delivery System (2009)
36. Rikos, E., Tselepis, S., Hoyer-Klick, C., Schroedter-Homscheidt, M.: Stability and power quality issues in microgrids under weather disturbances. IEEE J. Sel. Top. Appl. Earth Observations Remote Sens. **1**, 170–179 (2008)
37. Hanley, C., Peek, G., Boyes, J., Klise, G., Stein, J., Dan, T., and Tien, D.: Technology development needs for integrated grid-connected PV systems and electric energy storage. In: Photovoltaic Specialists Conference (PVSC), 34th IEEE, pp. 1832–1837 (2009)
38. Eyer, J.M., Iaunnucci, J.J., Corey, G.P.: Energy storage benefits and market analysis handbook a study for the doe energy storage systems program. Technical report SAND2004-6177, Sandia National Laboratories (2004)

39. Eyer, J., Corey, G.: Energy storage for the electricity grid: benefits and market potential assessment guide. Technical report SAND2010-0815, Sandia National Laboratories (2010)
40. Tsikalakis, A., Tassiou, I., Hatziargyriou, N.: Impact of energy storage in the secure and economic operation of small islands. In: Proceedings of the Medpower04, Larnaca, Cyprus (2004)
41. Kaldellis, J.K., Zafirakis, D.: Optimum sizing of stand-alone wind-photovoltaic hybrid systems for representative wind and solar potential cases of the Greek territory. J. Wind Eng. Ind. Aerodyn. **107–108**, 169–178 (2012)
42. Kapsali, M., Anagnostopoulos, J.S., Kaldellis, J.K.: Wind powered pumped-hydro storage systems for remote islands: a complete sensitivity analysis based on economic perspectives. Appl. Energy **99**, 430–444 (2012)
43. Gondal, I.A., Sahir, M.H.: Review of modelling tools for integrated renewable hydrogen systems. In: 2nd International Conference on Environmental Science and Technology, pp. 355–359. IACSIT Press, Singapore (2011)
44. Prodromidis, G.N., Coutelieris, F.A.: Simulations of economical and technical feasibility of battery and flywheel hybrid energy storage systems in autonomous projects. Renew. Energy **39**, 149–153 (2012)
45. Karellas, S., Terzis, K., Manolakos, D.: Investigation of an autonomous hybrid solar thermal ORC-PV RO desalination system. The Chalki island case. Renew. Energy **36**, 583–590 (2011)
46. Mazhari, E., Zhao, J., Celik, N., Lee, S., Son, Y.J., Head, L.: Hybrid simulation and optimization-based design and operation of integrated photovoltaic generation, storage units, and grid. Simul. Model. Pract. Theory **19**, 463–481 (2011)
47. Solomon, A.A., Faiman, D., Meron, G.: Properties and uses of storage for enhancing the grid penetration of very large photovoltaic systems. Energy Policy **38**, 5208–5222 (2010)
48. Divya, K.C., Ostergaard, J.: Battery energy storage technology for power systems: an overview. Electr. Power Syst. Res **79**, 511–520 (2009)
49. Hoffman, M., Sadovsky, A., Kintner-Meyer, M., et al.: Analysis tools for sizing and placement of energy storage in grid applications: a literature review. Technical report, Pacific Northwest National Laboratory (2010)
50. Connolly, D., Lund, H., Mathiesen, B.V., Leahy, M.: A review of computer tools for analysing the integration of renewable energy into various energy systems. Appl. Energy **87**, 1059–1082 (2010)
51. DIgSILENT GmbH Software and Consulting Company: http://www.digsilent.de/index.php/products-powerfactory.html
52. EnergyPLAN home page: http://energy.plan.aau.dk
53. HOMER energy modeling software: http://www.homerenergy.com
54. The National Energy Modeling System (NEMS): http://www.eia.gov/oiaf/aeo/overview
55. Power World Corporation: http://www.powerworld.com
56. Power System Analysis Toolbox (PSAT): http://www.uclm.edu/area/gsee/Web/Federico/psat.htm
57. Regional Energy Deployment System (ReEDS): http://www.nrel.gov/analysis/reeds
58. RETScreen international home page: http://www.retscreen.net
59. Lund, H., Duić, N., Krajačić, G., Graça Carvalho, M.D.: Two energy system analysis models: a comparison of methodologies and results. Energy **32**, 948–954 (2007)
60. Liu, W., Lund, H., Mathiesen, B.V.: Large-scale integration of wind power into the existing Chinese energy system. Energy **36**, 4753–4760 (2011)
61. Anayochukwu, A.V., Ndubueze, N.A.: Energy optimization at GSM base station sites located in rural areas. Int. J. Energy Optim. Eng. **3**, 1–31 (2012)
62. Castañeda, M., Fernández, L.M., Sánchez, H., Cano, A., Jurado, F.: Sizing methods for stand-alone hybrid systems based on renewable energies and hydrogen. In: Proceedings of the Mediterranean Electrotechnical Conference, MELECON, pp. 832–835 (2012)

63. Applasamy, V.: Cost evaluation of a stand-alone residential photovoltaic power system in Malaysia. In: 2011 IEEE symposium on business, engineering and industrial applications, ISBEIA 2011, pp. 214–218 (2011)
64. Tan, X., Li, Q., Wang, H.: Advances and trends of energy storage technology in microgrid. Int. J. Electr. Power Energy Syst. **44**, 179–191 (2013)
65. Renewable Energy Storage Engagement Tool (RESET): http://fiesta.bren.ucsb.edu/~aecom-energy/index.html
66. ES-Select™ Tool: http://www.sandia.gov/ess/esselect.html

Particle Swarm Intelligence Based Optimization Controller Applied to Two Area Interconnected Power Systems

V. Jeyalakshmi and P. Subburaj

Abstract This paper presents the optimal performance of Load Frequency control (LFC) in interconnected two-area power systems. Proportional–Integral (PI) controllers are commonly used for LFC systems in power industry. But the dynamic behaviors in the presence of variations in load changes with different operating conditions are needed to be improved. This paper proposes Particle Swarm Optimization (PSO) based Load Frequency Control for improving the dynamic performance of the system. A two area interconnected power system, having different generating units is considered to be equipped with Proportional Integral and Derivative (PID) controller. PSO algorithm is implemented to search the optimal controller parameters by minimizing the time domain objective function. The performance of the proposed PID controller has been evaluated by the performance of the conventional controller and the controller tuned by Genetic algorithm (GA) in order to demonstrate the superior efficiency of the proposed PSO algorithm. Simulation results proved that the proposed algorithm is moderately fast algorithm and yields true optimal gains with minimum overshoot, minimum undershoot, minimum rise time and minimum settling time for any power system. Furthermore, the dynamic behavior of the proposed controller under variations of system parameters and load changes are better than that of conventional and GA controllers.

Keywords Load frequency control · Genetic algorithm · Optimization technique · Power system · Particle swarm optimization

V. Jeyalakshmi (✉)
PSN College of Engineering and Technology, Tirunelveli, India
e-mail: jey_guru2005@yahoo.co.in

P. Subburaj
National Engineering College, Kovilpatti, India
e-mail: subbuneceee@yahoo.com

I. Zelinka et al. (eds.), *Power, Control and Optimization*, Lecture Notes in Electrical Engineering 239, DOI: 10.1007/978-3-319-00206-4_4,

1 Introduction

It is well known that three-phase alternating current (AC) is generally used to transmit the electricity. During the transmission, both the active power balance and the reactive power balance must be maintained between the generation and utilization of the AC power. The power balances correspond to two equilibrium points: frequency and voltage. A good quality of the electric power system requires both the frequency and the voltage to be remain at constant values during operation. It will be impossible to maintain the balances of both the active and reactive powers without proper compensation. As a result of the imbalance, the frequency and the voltage levels will be varied with the change of variations in the loads. Thus a control system is essential to cancel the effects of the random load changes and to keep the frequency and the voltage at the constant values [1]. The active power and frequency control is referred to as load frequency control (LFC). The foremost task of LFC is to keep the frequency constant against the randomly varying active power loads, which are also referred to as unknown external disturbance. Another task of the LFC is to regulate the tie-line power exchange error [2]. A typical large-scale power system is composed of several areas of generating units interconnected together and power is exchanged between utilities. A major problem in the parallel operation of interconnected power systems is the control of frequency and inter-area tie-line power flow control. The objective of the LFC in interconnected power systems is to maintain the frequency of each area and to keep tie-line power flows within some pre-specified tolerances by adjusting the outputs of the high capacity generators when fluctuations occur in the load demands [3]. There have been increasing interest in designing load frequency controllers with better performance during the past years and many control strategies have been developed for LFC. The first proposed control strategy was a proportional integrator (PI) controller, which is nowadays widely used in the industry [4]. The main drawback of this controller is that the dynamic performance of the system is limited by its integral gain.

Despite the potential of the modern control techniques with different structure, Proportional Integral Derivative (PID) type controller is still widely used for solution of the LFC problem [4]. This is because due to it's performed well for a wider class of process. Also, it gives robust performance for a wide range of various operating conditions and easy to implement. The PID controller parameters tuning are usually done by trial and error methods based on the conventional experiences. Hence, they are not capable of providing good robust performance for power system subjected to different kinds of uncertainties and disturbances. An appropriate selection of PID controller parameters results in satisfactory performance during system upsets. Thus, the optimal tuning of a PID gain is required to get the desired level of robust performance [5, 6]. Since the optimal setting of PID controller gains is a "multimodal" optimization problem (i.e., there exists more than one local optimum) and more complex due to nonlinearity, complexity and

time-variability of the real world power systems operation. Hence, the local optimization techniques, which are well elaborated upon, are not suitable for such a problem. Many studies have been carried out in the past on this important issue in power systems such as linear feedback, optimal control and variable structure control [7–9] have been proposed in order to improve the robust performance. These controllers may be improper in some operating conditions. This could be due to the complexity of the power systems such as nonlinear load characteristics with variable operating points. The availability of an accurate model of the system under study plays a crucial role in the development of the most control strategies like optimal control. However, an industrial process, such as a power system, contains different kinds of uncertainties due to changes in the system parameters and its characteristics, loads variations and errors in the modeling.

Recently, a global optimization technique like Genetic Algorithm has attracted the attention in the field of controller parameter optimization [10–12]. Unlike other techniques, GA is a population based search algorithm, which works with a population of strings that represent different solutions. Therefore, GA has implicit parallelism that enhances its search capability and the optima can be located swiftly when applied to the complex optimization problems. Unfortunately recent research has found some drawbacks in GA performance [13] such as the parameters being optimized are highly correlated. They need to run several times to obtain the best optimal solution [14, 15]. Also, the premature convergence of GA degrades its performance and reduces its search capability resulting in sub-optimal solutions with revisiting the same solutions. To overcome this problem of sub-optimal convergence, powerful computational intelligent evolutionary techniques as Particle Swarm Optimization is proposed by the authors [16–18] to optimize the PID gains of the controller for the Automatic Generation Control problem in power systems. PSO is a computational intelligence-based technique that is not largely affected by the size and the nonlinearity of the problem, and can converge to the optimal solution in many problems where most analytical methods fail to converge. PSO has been applied to various fields of power system including economic dispatch problems as well as in optimization problems in electric power systems [19]. It can therefore be effectively applied to different optimization problems in power systems.

In this work, different controllers such that, Conventional PID, Genetic Algorithm based PID (GAPID) and Particle Swarm Optimization based PID (PSOPID) are developed. The comparative study has been made between these controllers by varying the system parameters with different load conditions. In this simulation study, two area power systems with two different parameters are chosen and load frequency control of this system is made based on optimal tuning of PID controller parameters. Simulation results show that the overshoots, undershoots and settling times with the proposed PID controller are better than the outputs of the conventional and GA controllers under a wide range of changing load conditions with different system parameter changes occurred.

2 Dynamic Model of the System

A two-area interconnected power systems with different units are considered here. Figure 1 shows the representation of the two-area interconnected power systems. The two areas may have the combinations of different units. (Thermal—Hydro units). The detailed transfer function models of speed governors, thermal non-reheat turbines and hydro turbines are developed. Governors are the units that are used in power systems to sense the frequency bias caused by the load change and it can be cancelled by varying the inputs of the turbines. The transfer function of governor unit is given by [20]:

$$G_g(S) = \frac{\Delta P_e(s)}{\Delta P_v(s)} = \frac{1}{T_{g1}s + 1}$$

where ΔPe—change in electrical power; ΔP_v—Change in gate/valve position; T_{g1}—Governor time constant.

A turbine unit in power systems is used to transform the natural energy, such as the energy from steam or water, into mechanical power that is supplied to the input of the generator. In LFC model, there are three kinds of commonly used turbines: non-reheat, reheat and hydraulic turbines, all of which can be modeled by transfer functions. The transfer function of the non-reheat turbine is represented as follows:

$$G_{NR}(S) = \frac{\Delta P_m(s)}{\Delta P_v(s)} = \frac{1}{T_{t1}s + 1}$$

where ΔPm—change in mechanical power; T_{t1}—Time delay.

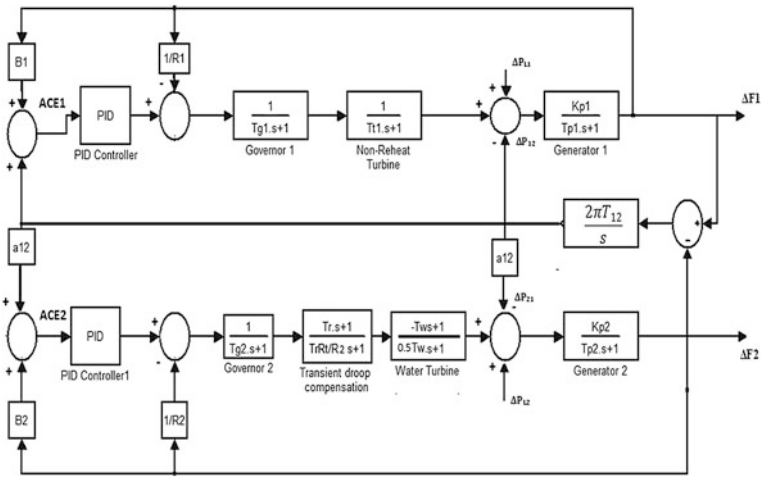

Fig. 1 Two area interconnected power system for test case B1

A generator unit in power systems converts the mechanical power (ΔPm) received from the turbine into electrical power (Δf). The transfer function of the generator is represented as follows:

$$G(S) = \frac{\Delta f(s)}{\Delta P_m(s)} = \frac{K_{pi}}{T_{pi}s + 1}$$

where K_{pi}—System gain for area i; T_{pi}—Generator time constant for area i.

Hydraulic turbines are non-minimum phase units due to the water inertia. In the hydraulic turbine, the water pressure response is opposite to the gate position change at first and recovers after the transient response. Thus the transfer function of the hydraulic turbine is in the form of,

$$G_H(S) = \frac{\Delta P_m(s)}{\Delta P_v(s)} = \left(\frac{-T_w s}{0.5T_w s + 1}\right)$$

where T_w—water starting time.

For stability concern, a transient droop compensation part in the governor is needed for the hydraulic turbine. The transfer function of the transient droop compensation part is given by

$$G_{TD}(S) = \left(\frac{T_r s + 1}{T_r\left(\frac{R_t}{R_2}\right)s + 1}\right)$$

where T_r—reset time; R_t and R_2—temporary droop and permanent droop respectively.

2.1 Problem Description

The LFC problem considered here is the perturbations in small load and system parameter changes which continuously disturb the normal operation of a power system. To overcome the above difficulty we propose an optimal controller to provide better performance when disturbances are occurring. In practical cases we are having different units are interconnected together to meet the increasing demand. Interconnection established increases the overall system reliability. Even if some generating units in one area fail, the generating units in the other area can compensate to meet the load demand [21]. In this work, the frequency and tie line power deviation among different units are observed and the dynamic performance of the system is also analyzed. Since the two areas are interconnected by tie-lines, a single PID controller whose input contains the error signal and their changes in both areas are used. The PID controller has the following structure [22]:

$$\mathrm{K}(s) = K_p + \frac{K_i}{s} + K_d s \tag{1}$$

where K_p is the proportional gain, K_i is the integral gain and K_d is the derivative gain. The control signal for PID controller can be given in the following equation.

$$U_i(s) = -K(s) * ACE_i(s) \tag{2}$$

The control action which depends upon the Area Control Error (ACE) which is a linear combination of net tie-line power error (ΔP_{tie}) and frequency error (Δf) and represented as [14]:

$$ACE_i = \Delta P_{tie,i} + b_i \Delta f_i \tag{3}$$

where b_i is frequency bias coefficient, $\Delta P_{tie,i}$ is the tie-line interchange error and Δf_i is the frequency error component. This signal is used to regulate the generator output power based on network load demand. The objective is to obtain the better transient response under varying system parameters with various load conditions. The transient response can be optimized that means minimum undershoot, minimum overshoot and minimum settling time of DF1, DF2 and Delta P_{tie} for area 1 and area 2 respectively. This is achieved through optimization of PID Gains of the PID controllers by any of the optimization techniques. A performance index can be defined by the Integral of Time multiply Absolute Error (ITAE) of the frequency deviation of both areas and tie line power. The objective function J is set to be

$$J(K_P, K_i, K_d) = \int_0^t t(|\Delta f_1| + |\Delta f_2| + |\Delta P_{tie}|)dt \tag{4}$$

It is clear that the controller with lower ITAE is better than the other controllers. To compute the optimum parameter values, 10 and 25 % step change in ΔP_{L1} and ΔP_{L2} is assumed and the performance index is minimized using optimization algorithms.

3 Optimization Techniques

Proper selection of PID controller parameters is necessary for the satisfactory operation of the system. In this work, the problem of PID controller parameter selection is formulated as an optimization problem, the objective function of which is given by Eq. (4). Optimization techniques such as GA and PSO are applied to the above optimization problem to search for the optimum value of the controller parameters. The implementations of these algorithms are given in the following sections.

3.1 Genetic Algorithm

Genetic algorithm (GA) is one of the optimization methods based on the mechanics of natural selection and genetics. An implementation of genetic algorithm begins with a population of chromosomes [23]. The major steps involved are the generation of population of solutions, finding the objective function and fitness function and the application of genetic operators. There are four operators such as, selection, reproduction, crossover and mutation. In nature, the individual can have better survival traits that will survive for a longer period of time. This in turn provides it a better chance to produce offspring with its genetic material. Therefore, after a long period of time, the entire population will consist of lots of genes from the superior individuals and less from the inferior individuals. In a sense, the fittest survived and the unfit died out. This force of nature is called natural selection. Changes occur during reproduction. The chromosomes from the parents exchange randomly by a process called crossover. Therefore, the offspring exhibit some traits of the father and some traits of the mother. A rare process called mutation also changes some traits.

An important characteristic of genetic algorithm is the coding of variables that describes the problem. The most common coding method is to transform the variables into a binary string or vector; GA performs best when the solution vectors are binary. Just like natural genetics a chromosome (a string) will contain some genes (binary bits). A population size is chosen which consists of several parent strings. The strings are then subjected to an evaluation of fitness function and its least fitness value will be selected for the next generation. The selected strings will produce new off springs by reproduction, cross over and mutation operation. Hence a new population which is different from old population is produced in each cycle of iteration. The whole process is repeated for several iterations till or near optimal solution is reached.

While applying GA to obtain optimal PID controller parameters, the following factors are needed to be considered.

1. Representation of Decision variables
2. Formation of Fitness function

Variable Representation

Each individual in the genetic population represents a candidate solution. In the binary-coded GA, the solution variables are represented by a string of binary alphabets. For tuning of PID controller, the elements of the solution consist of Proportional gain (Kp), Integral gain (Ki) and Derivative gain (K_d). These variables are represented as binary strings in the GA population. With binary representation, an individual in the GA population for computing optimal controller parameters will look like the following:

$$\underbrace{1011100111}_{K_p} \quad \underbrace{101101101}_{K_i} \quad \underbrace{1011100101}_{K_d}$$

Evaluation of the individuals in the population is accomplished by calculating the objective function of the problem using the parameter set. The result of the objective function is used to calculate the fitness value of the individual. Fitter chromosomes have higher probabilities of being selected for the next generation. The fitness function is a reciprocal of the performance criterion as in (4). Hence, the minimization of objective function given by (4) is transformed to a fitness function to be maximized as follows:

$$F_{fitness} = \frac{1}{1 + F_{cost}} \tag{5}$$

For designing the controller, cost function (F_{cost}) can be assumed as minimization of "Integral time Absolute Error" (ITAE), as shown in Eq. (4).

In this research work, the PID Controller gains K_p, K_i, and K_d are represented by a string of 32 binary bits. Then binary coded value is converted to decimal value which gives the corresponding gain values. Now the problem is the optimization of dynamic performance of the system with respect to undershoot, overshoot and settling time. We choose the fitness function as the sum of the absolute value of the error signal multiplied with time (ITAE). Population size is chosen as 100. The fitness function is computed for each string of the population, the string which gives less value of fitness function is considered as the better one. The better strings survive in the next population and 50 % of the strings are selected on the basis of their fitness function value and the remaining 50 % are selected from the first generation on the basis of their best value to make the population size of 100 for the next generation. After performing GA operations such as selection, cross over and mutation new off spring strings are produced for the controller gains. Then the system performance characteristics and the fitness values are evaluated for each string. The continuous process of evaluation of fitness function, selection, crossover and mutation represents one complete cycle of iteration. In such a way that within 100 iteration cycles the PID controller gains reach its optimal value to obtain the desired performance characteristics.

3.2 Particle Swarm Optimization

Particle Swarm Optimization (PSO) is a population based stochastic optimization technique developed by Eberhart and Kennedy [22], inspired the social behavior of bird flocking or fish schooling. PSO shares many similarities with evolutionary computation techniques such as Genetic Algorithms (GA). The system is initialized with a population of random solutions and searches for optimal by updating generations [24]. However, unlike GA, PSO has no evolution operators such as crossover and mutation. The population of solution candidates is called a "swarm", while each candidate is called a "particle". It uses a number of particles that constitute a swarm moving around in the D-dimensional search space looking

for the best solution. The particles have memory and each particle keeps track of its previous best position, called *pbest* with its fitness value. When a particle takes all the population as its topological neighbors, the best value is a global best called *gbest*. The PSO concept consists of changing the velocity of each particle toward its pbest and gbest locations at every iteration. The flow chart of PSO Algorithm employing is shown in Fig. 2.

Further investigation describes the implementation of PSO algorithm in this work. Let a swarm of n particles be considered for population. In a physical D-dimensional search space, the position and the velocity of individual ith *particle is* represented as the vectors $X_i = (x_{i,1}, x_{i,2},\ldots, x_{i,D})$ and $V_i = (v_{i,1}, v_{i,2} \ldots v_{i,D})$ respectively. The pbest is the best previous position yielding the best fitness value for the ith particle and is represented as $pbest_i = (pbest_{i,1}, pbest_{i,2},\ldots pbest_{i,D})$ and gbest is the best position in the whole swarm population and is represented as $gbest_i = (gbest_{i,1}, gbest_{i,2},\ldots gbest_{i,D})$. The PSO algorithm updates its velocity and its position by the using the following Equation [13]:

$$V_{i,d}{}^{k+1} = W * V_{i,d}{}^{k} + c_1 * rand_1 \times (pbest_{i,d}{}^{k} - X_{i,d}{}^{k}) + c_2 * rand_2 \times (gbest_{i,d}{}^{k} - X_{i,d}{}^{k}) \quad (6)$$

$$X_{i,d}{}^{k+1} = X_{i,d}{}^{k} + V_{i,d}{}^{k+1} \quad (7)$$

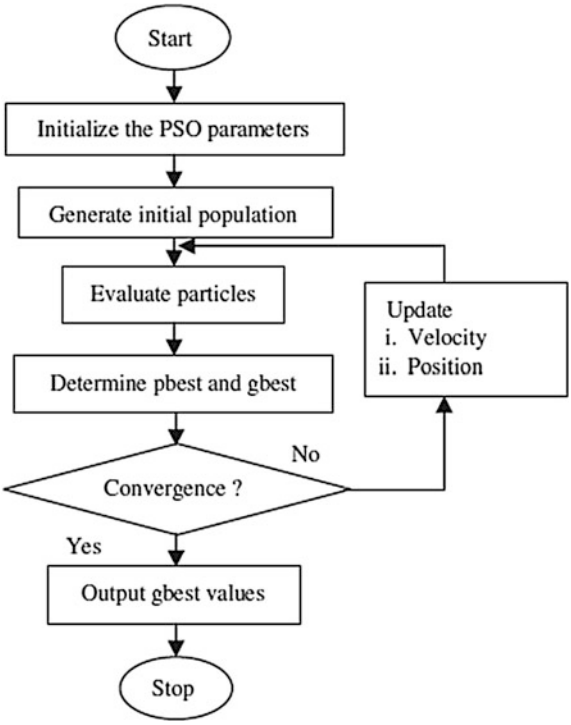

Fig. 2 Flow chart of PSO algorithm

where $C_1 = 1.5$ and $C_2 = 1.5$ are the learning factors which determines the relative influence of cognitive and social component to update the position and velocity respectively. $rand_1$ and $rand_2$ are two random numbers in the range of [0,1]. $V_{i,\,d}{}^k$ and $X_{i,\,d}{}^k$ are the velocity and position of *i*th particle in *d*th dimension till *k*th iteration respectively. The $gbest_{i,d}{}^k$ is the global best of *i*th particle in *d*th dimension till *k*th iteration and $pbest_{i,d}{}^k$ is the personal best of *i*th particle in *d*th dimension till *k*th iteration. The inertia weight parameter W, which controls the exploration and exploitation of the search space. In general, the weight W is set according to the following equation [13]:

$$W = W_{max} - (W_{max} - W_{min}) \times Iter/Iter_{max} \tag{8}$$

where W_{max} and W_{min} are the initial and final weight respectively. Iter is the current iteration number and $Iter_{max}$ is maximum iteration number. The principle of a particle displacement in the swarm is graphically shown in Fig. 3, for a two dimensional design space.

The velocity is restricted to a certain dynamic range. v_{max} is the maximum allowable velocity for the particles, i.e., in case the velocity of the particle exceeds v_{max}, then it is reduced to v_{max}. Thus, the resolution and fitness of search depend upon v_{max}. If v_{max} is too high, then the particles will move beyond good solution, and if v_{max} is too low, then the particles will be trapped in local minima. The learning factors (c1 and c2) which change the velocity of a particle towards $pbest_i$ and $gbest_i$.

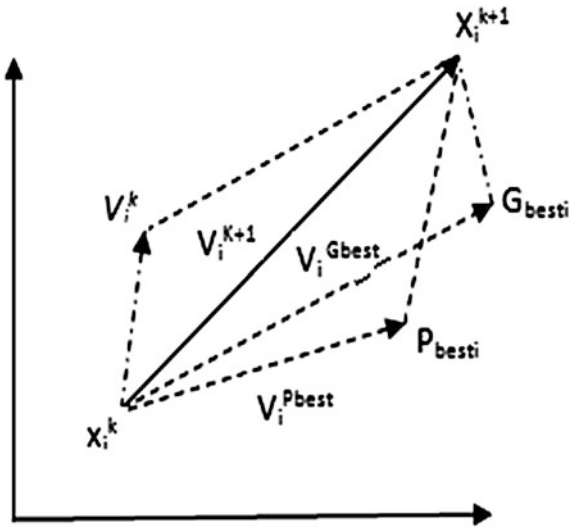

Fig. 3 Particle's position from one instant k to another instant k + 1

4 Simulation Results

Simulation studies were performed on an interconnected power system that explained in Sect. 2. Typical data for the system parameters and algorithm parameters are given in Appendix. To start GA algorithm, a decision has to be made about the GA parameters which include population size, crossover probability, mutation probability, and number of generations. The proper choice of these parameters will ensure sufficient diversity in the population, which prevents the GA from being trapped in a local minimum. Moreover, random initial population will prevent premature convergence, and does not bias the performance of the GA. General guide lines available in the literature can be used in the selection process. After so many trials, a population size, a crossover probability, and a mutation probability are used as given in Appendix are chosen. The algorithm is terminated when there is no significant improvement in the value of the performance index as shown in Fig. 4.

The PSO parameters given in Appendix are used. After updating the position and the velocity of each particle the performance index is evaluated and the convergence is verified. The algorithm is also terminated when there is no significant improvement in the value of the performance index as shown in Fig. 5.

From Figs. 4 and 5 it is clearly understand that the PSO algorithm will provide better performance in reducing the performance index value. After 30 generations only GA provides the saturated value of ITAE. But in case of PSO from initial condition also the value of ITAE is very much reduced as compared to GA.

The performances of three controllers (Conventional, GA and PSO) are tested with the power system having different combinations of units such as thermal and hydro units. The main objective of this paper is to establish that the PSO algorithm is the best optimization algorithm for complex system when there are system parameters and load changes are frequently occurred. For that different test cases in the power system at different conditions are considered Table 1 shows 18 test cases of two area interconnected power systems.

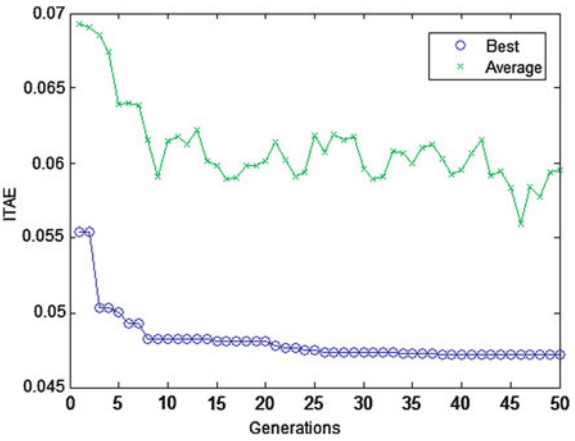

Fig. 4 Performance Index for the test case A3 using GA

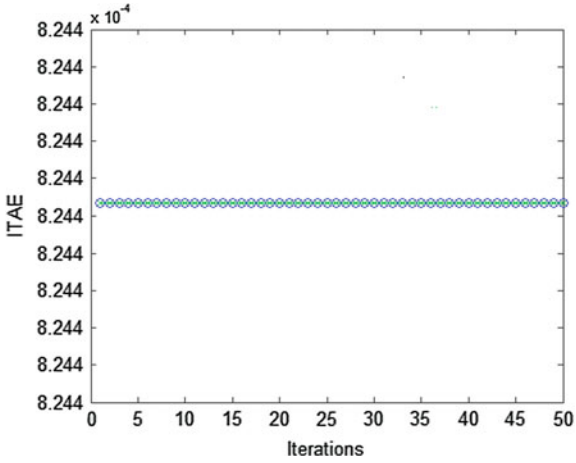

Fig. 5 Performance Index for the test case B5 using PSO

Table 1 Test cases of interconnected two-area power systems

Test case	System parameters	Area 1 Unit I	Area 2 Unit II	Load conditions
Case A1	$T_{p1} = 20$;	Thermal	Thermal	10 % increase in area 1
Case A2	$T_{12} = 0.0866$	Thermal	Thermal	25 % increase in area 1
Case A3	B1 = 0.4166	Thermal	Thermal	10 % increase in area 2
Case A4	$T_{p2} = 20$;	Thermal	Thermal	25 % increase in area 2
Case A5	$T_{12} = 0.0549$	Thermal	Thermal	10 % increase in area 1 and 2
Case A6	$B_2 = 0.275$	Thermal	Thermal	25 % increase in area 1 and 2
Case B1	$T_{p1} = 10$;	Thermal	Hydraulic	10 % increase in area 1
Case B2	$T_{12} = 0.0549$	Thermal	Hydraulic	25 % increase in area 1
Case B3	$B_1 = 0.275$	Thermal	Hydraulic	10 % increase in area 2
Case B4	$T_{p2} = 20$;	Thermal	Hydraulic	25 % increase in area 2
Case B5	$T_{12} = 0.0866$	Thermal	Hydraulic	10 % increase in area 1 and 2
Case B6	$B_1 = 0.4166$	Thermal	Hydraulic	25 % increase in area 1 and 2
Case C1	$T_{p1} = 10$;	Hydraulic	Hydraulic	10 % increase in area 1
Case C2	$T_{12} = 0.0549$	Hydraulic	Hydraulic	25 % increase in area 1
Case C3	$B_1 = 0.275$	Hydraulic	Hydraulic	10 % increase in area 2
Case C4	$T_{p2} = 10$;	Hydraulic	Hydraulic	25 % increase in area 2
Case C5	$T_{12} = 0.0549$	Hydraulic	Hydraulic	10 % increase in area 1 and 2
Case C6	$B_2 = 0.275$	Hydraulic	Hydraulic	25 % increase in area 1 and 2

For analyzing purpose the load in the two areas are changed as 10 and 25 % and with transient responses are observed. Simulation analytical results conclude that the PSO algorithm could rapidly converge to the best optimal solution. In this section different comparative cases are examined to show the effectiveness of the proposed PSO Algorithm method for optimizing PID controller parameters. The performance index is calculated for the given power system using various techniques are tabulated in Table 2.

Table 2 ITAE Value for various load conditions

The calculated ITAE							
Test cases	PSO	GA	CONV	Test Cases	PSO	GA	CONV
Case A1	0.0012	0.0112	0.0405	Case B4	0.0024	0.0314	0.6775
Case A2	0.0052	0.0235	0.6275	Case B5	0.0008	0.0415	0.4454
Case A3	0.0065	0.0471	0.7501	Case B6	0.0021	0.0612	0.5125
Case A4	0.0046	0.0884	0.1123	Case C1	0.0065	0.1221	0.2010
Case A5	0.0044	0.0556	0.2245	Case C2	0.0054	0.0067	0.0221
Case A6	0.0051	0.0088	0.0334	Case C3	0.0056	0.0545	0.0112
Case B1	0.0087	0.0234	0.4231	Case C4	0.0263	0.0615	0.1125
Case B2	0.0056	0.0887	0.3345	Case C5	0.0003	0.0511	0.0123
Case B3	0.0011	0.0445	0.1152	Case C6	0.0004	0.0061	0.0812

The dynamic performances of the system under varying load conditions when the system parameter changes are compared for three different controllers. For different values of ΔP_{L1} are applied to both areas, at the same time the system parameters such as T_{Pi}, T_{ij} and B_i are also changed to show the effectiveness of the control strategy optimized by the PSO Algorithm. A step load disturbance of control area 1 is increased by 10 and 25 % of nominal loading and the transient response of the system is observed. The same disturbances are applied to control area 2 and the response of the system is also observed. Then the increased load disturbance 10 and 25 % of nominal loading is applied to both areas simultaneously. As a result, it is found that the PSO based controller drastically reduces the overshoot by a large value as shown in Figs. 6, 7 and 8. Settling time, Rise Time and Peak Time have also improved. All these analytical results have been validated by executing MATLAB SIMULINK with proper values of input parameters, variable parameters and optimal PID gains.

4.1 Performance Analysis

The optimal objective function evaluations are made 50 times for each technique with all the test cases. The Matlab 7.0 software is used for simulation purpose. Figures 6, 7 and 8 shows the plots of Change in FI (DF1), Change in F2 (DF2) and Change in Ptie (Delta Ptie) versus time for all three algorithms for test cases A1, B4 and C5 respectively.

4.2 Parameter Variations

A parameter variation test is also applied to assess the robustness of the proposed controller. Figure 6 shows the response of the system with variations in T_{ij}. It is

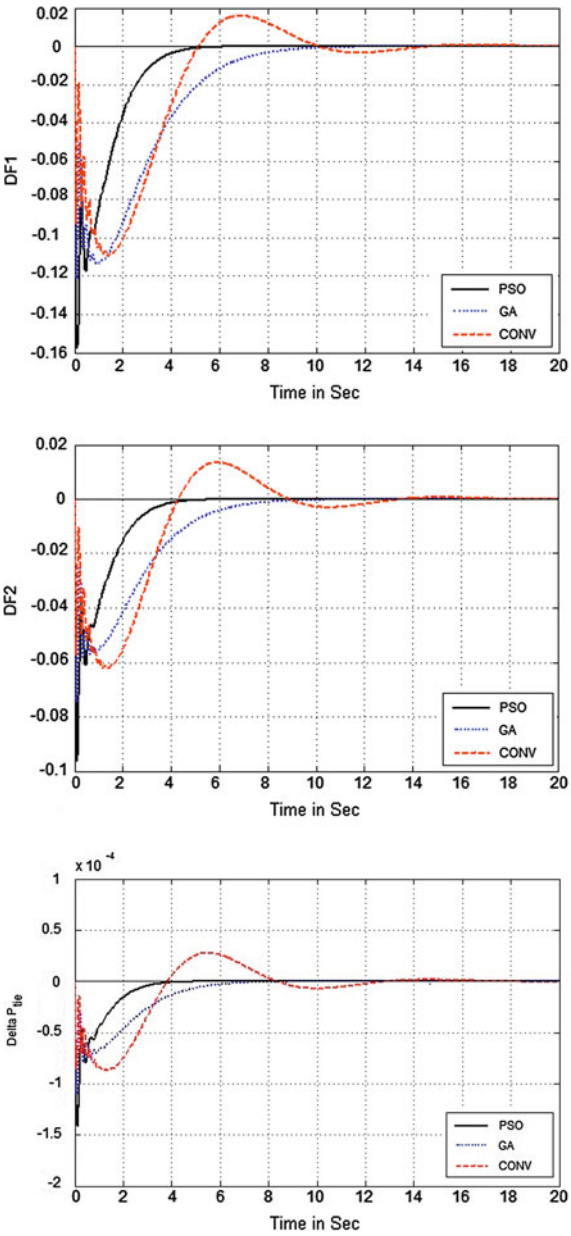

Fig. 6 Change in frequency DF1, DF2 and Tie-line power flow for the test case A1

clear that the system is stable with the proposed controller. Another parameter variation test is also applied to validate the effectiveness of the proposed controller. The response of the system with variations in generator time constant (Ti)

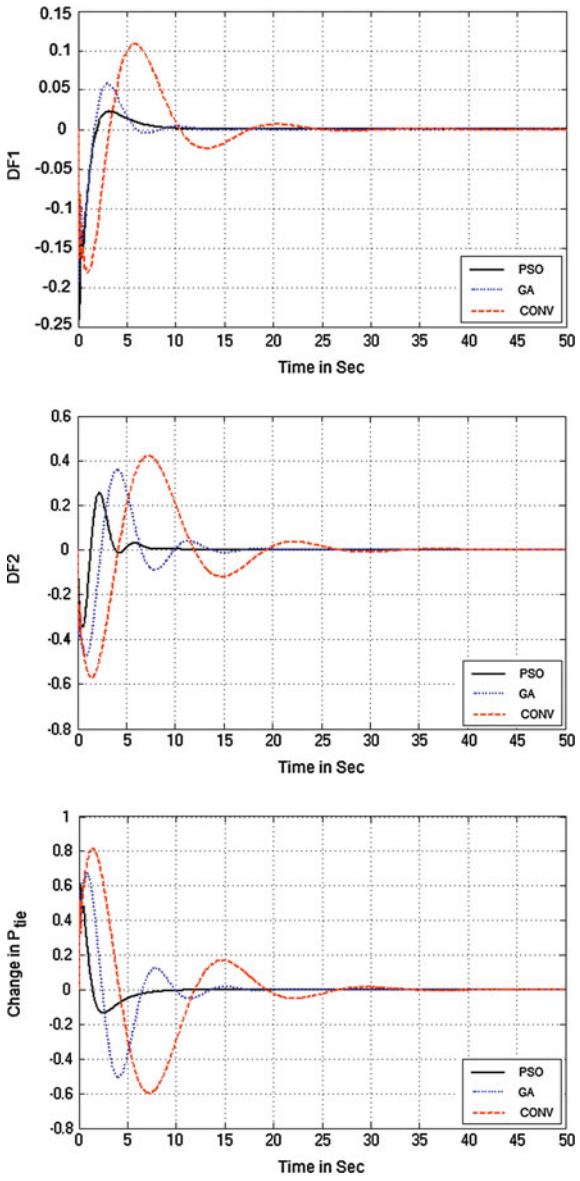

Fig. 7 Change in frequency DF1, DF2 and Tie-line power flow for the test case B4

is shown in Fig. 7. The designed controller is capable of providing sufficient damping to the system oscillatory modes under different operating conditions. Hence, the robustness of the proposed controller are verified.

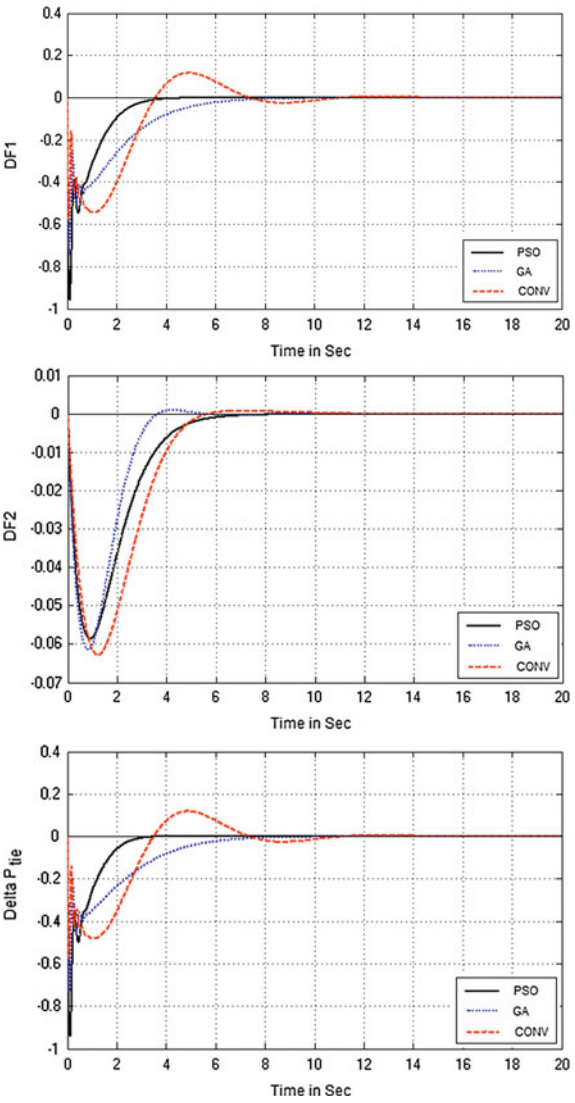

Fig. 8 Change in frequency DF1, DF2 and Tie-line power flow for the test case C5

5 Conclusions

The proposed PSO Algorithm is applied to tune the parameters of the load frequency controller in two area interconnected power systems. The proposed controller was applied to the power systems with the considerations of system parameter changes and various load conditions. To demonstrate the robustness of the proposed method, comparative study has been made between Conventional, GA and PSO controller. The optimal gain values of PID Controller are obtained by

applying Genetic Algorithm while considering the ITAE as performance index. The performance measures such as the settling time, rise time, maximum overshoot, and undershoot are being observed from the response curve. The optimal gain values are also obtained using proposed PSO algorithm and it provides better performance than GA under dynamic condition. The simulation results show that the proposed method is robust when changes in the parameter of the system occurred. Therefore, the proposed PSO-PID controller is recommended to generate good quality and reliable electric energy. In addition, the proposed controller is very simple and easy to implement since it does not require more information about system parameters. Many real world optimization problems can be modeled with multiple and even conflicting objectives. Hybrid metaheuristics technique can provide a more efficient behavior and a higher flexibility when dealing with multi objective problems. In future, multi objective design of load frequency controller using hybrid metaheuristics technique will be considered.

6 Appendix

The typical values of parameters of the system are shown below:

$$TP_1 = TP_2 = 20 \text{ s};\ T_{T1} = T_{T2} = 0.3 \text{ s};\ T_{12} = 0.545 \text{ p.u};$$
$$T_{G1} = T_{G2} = 0.08 \text{ s};\ Kp_1 = Kp_2 = 120 \text{ Hz/p.u MW};\ a12 = -1;$$
$$R1 = R2 = 2.4 \text{ Hz/p.u MW};\ B_1 = B_2 = 0.425 \text{ p.u MW/Hz};$$

GA Parameters:

No of variables = 3; No of generation = 50;
Population size = 20; Cross over probability = 0.6;
Mutation probability = 0.06.PSO Parameters:

Population Size = 20; $C_1 = C_2 = 2$; $rand_1 = rand_2 = 0.5$;
$\omega_{max} = 0.9$ and $\omega_{min} = 0.4$; $Iter_{max} = 50$.

References

1. Kundur, P.: Power System Stability and Control. Tata McGraw-Hill Publication, New York (1994)
2. Malik, P., Kumar, A., Hope, G. S.: A load frequency control algorithm based on a generalized approach. IEEE Trans. Power Syst. **3**(2), 375–382 (1988)
3. Ai-Hamouz, Z.M., Abdel-Magid, Y.L.: Variable structure load-frequency controllers for multi area power systems. Int. J. Electr. Power Energy Syst. **15**(5), 23–29 (1993)
4. Sharifi, A., Sabahi, K., Aliyari Shoorehdeli, M., Nekoui, M.A., Teshnehlab, M.: Load frequency control in interconnected power system using multi-objective PID controller. In: IEEE Conference on Soft Computing in Industrial Applications, Muroran, Japan, pp. 217–221 (2008)

5. Tan, W.: Tuning of PID Load frequency controller for power systems. J. Energy Conv. Manage. **50**, 1465–1472 (2009)
6. Roy, R., Bhatt, P., Ghoshal, S.P.: Evolutionary computation based three-area automatic generation control. Int. J. Electr. Power Energy Syst. **37**(8), 5913–5924 (2010)
7. Lili, D., Yao, Z.: On design of a robust load frequency controller for interconnected power systems. In: 2010 American Control Conference Marriott Waterfront, Baltimore, pp. 1731–1736 (2010)
8. Sadeh, J., Rakhshani, E.:Multi-area load frequency control in a deregulated power system using optimal output feedback method. In: 5th International Conference on European Electricity Market (EEM), pp. 1–6 (2008)
9. Tan, W.: Unified tuning of PID load frequency controller for power systems via IMC. IEEE Trans. Power Syst. **25**(1), 341–350 (2010)
10. Ghoshal, S.P.:Application of GA/GASA based fuzzy automatic generation control of a multi-area thermal generating system. Int. J. Electr. Power Syst. Res. **70**(2), 115–128 (2004)
11. Hsu, C.C., Yamada, S., Fujikawa, H., Shida, K.: A Fuzzy self-tuning parallel genetic algorithm for optimization. J. Comput. Ind. Eng. **30**(4), 883–893 (1996)
12. Mariano, S., Ferreira, L.: Optimal control: load frequency control of a large power system. In: IEEE Conference on Power Electronics and Motion Control, pp. 2076–2081 (2008)
13. Bhatt, P., Roy, R., Ghoshal, S.P.: GA/particle swarm intelligence based optimization of two specific varieties of controller devices applied to two-area multi-units automatic generation control. In. Int. J. Electr. Power Energy Syst. **32**, 299–310 (2010)
14. Farhangi, R., Boroushaki, M., Hosseini, S.H.: Load–frequency control of interconnected power system using emotional learning-based intelligent controller. Int. J. Electr. Power Energy Syst. **36**(1), 76–83 (2012)
15. Dieu, V.N., Schegner, P.: Real power dispatch on large scale power systems by augmented lagrange hopfield network. Int. J. Energy Optim. Eng, **1**(1), 19–38 (2012)
16. Ghoshal, S.P.: Optimizations of PID Gains by particle swarm optimizations in fuzzy based automatic generation control. Electr. Power Syst. Res. **70**(3), 203–212 (2004)
17. del Valle, Y., Ganesh Kumar, V., Mohagheghi, S., Hernandez, J.-C., Ronald, G.H.: Particle swarm optimization: basic concepts, variants and applications in power systems. IEEE Trans. Evol. Comput. **12**(2), 171–195 (2008)
18. Naka, S., Genji, T., Yuru, T., Fukuyama, Y.A.: Hybrid particle swarm optimization for distribution state estimation. IEEE Trans. Power Syst. **18**, 60–68 (2003)
19. Ganesan, T., Vasant, P., Elamvazhthi, I.: Hybrid neuro-swarm optimization approach for design of distributed generation power system. Int. J. Neural Comput. Appl. (2012)
20. Wood, A.J., Wollenberg, B.F.: Power Generation, Operation and Control, 2nd edn. Wiley, New York (1994)
21. Ismail, M.M., Mustafa Hassan, M.A.: Load frequency control adaptation using artificial intelligent techniques for one and two different areas power system. Int. J. Control Autom. Syst. **1**(1), 12–23 (2012)
22. Khodabakhshian, A., Edrisi, M.: A new robust PID load frequency controller. Int. J. Control Eng. Practice **16**, 1069–1080 (2008)
23. Ramesh, S., Krishnan, A.: Modified genetic algorithm based load frequency controller for interconnected power system. Int. J. Electr. Power Eng. **3**(1), 26–30 (2009)
24. Kennedy, J., Eberhart, R.C.: Particle swarm optimization. In: Proceedings of IEEE International Conference on Neural Networks (ICNN'95), Vol. 4, Perth, Australia, pp. 1942–1948 (1995)

Allocation and Size Evaluation of Distributed Generation

Partha Kayal and C. K. Chanda

Abstract Recently technological innovation, environmental concerns and market liberalization help to penetrate Distributed Generation (DG) of significant number and capacity into power distribution system. This paper represents technique to minimize power losses in a distribution feeder by optimizing DG model in terms of size and location. A novel Voltage Stability Indicator (VSI) is proposed that can identify critical buses in distribution system. Based on VSI, the suitable location of distributed generator is identified. Desired size of DG is evaluated by simulating ANN model with proper training. The proposed methodology is tested by checking through 15 bus radial distribution and 52 bus practical distribution systems. There are considerable improvements of voltage profiles of the buses after appropriate allocation of DG. Appreciable reductions of distribution power losses for both the systems are also obtained.

Keywords Voltage stability indicator · ANN model · Priority list · DG size

1 Introduction

Worldwide there is growing interest in Distributed Generation (DG) for supplying electrical power to consumers. Integration of DG can have an impact on the practices used in distribution systems, such as the voltage profile, power flow, power quality, stability, reliability, and protection. In addition, with the small scale

P. Kayal (✉) · C. K. Chanda
Department of Electrical Engineering, Bengal Engineering and Science University, Shibpur, Howrah, India
e-mail: partha_kayal@yahoo.co.in

C. K. Chanda
e-mail: ckc_math@yahoo.com

I. Zelinka et al. (eds.), *Power, Control and Optimization*, Lecture Notes in Electrical Engineering 239, DOI: 10.1007/978-3-319-00206-4_5,

capacity, time of DG installment and some uncertainties in economic planning and construction are reduced. Therefore, the DG projects contain less risk compared with central power plant ones. Most of the radial distribution systems suffer with voltage stability [1, 2] problems at feeders. DG can provide voltage support to boost up the low voltage at the end of feeder. Additionally, DG also promotes greater competition in electricity supply market, because of its short payback period in comparison with transmission and central generation station projects, and its supply power directly to the local distribution network and the local utility. But, unplanned uses of DG while solving some problems may cause additional problem. Therefore some tools or techniques [3–6] are needed to be examined for allocation and sizing of DG.

Recent researches focus on selection of best places for installation and preferable size of DG units in large distribution system. Kashem and Ledwich [7] have discussed about optimal use of voltage support distributed generation to support voltage in distribution feeders. They have applied sensitivity analysis to determine appropriate size of DG. Analytical approaches to choose optimal location for DG in radial network with an objective of loss minimization have been presented by Caisheng and Nehrir [8]. Rafidah and Rahim [9] have discussed about methodology to evaluate DG size and its impact on power losses and voltage profile in distribution system. Acharya et al. [10] have derived an expression to calculate appropriate size and location for DG placement to minimize distribution losses. A G.A based optimal sizing and placement of DG considering the system energy loss minimization in different loading condition have been presented by Singh et al. [5]. However, this method needs extensive calculations. A method for placement of DG units using continuation power flow analysis has been proposed by Hedayati et al. [11]. Devi and Subramanyam [12] have discussed about optimal DG unit placement using fuzzy logic. Ganesan and Subramanyam [6] have optimized cost, emission and reliability of DG using Hopfield Neural Networks (HNN), Particle Swarm Optimization (PSO) and HNN-PSO techniques. These methods take longer time for calculation. Roy and Mandal [13] have studied optimal reactive power dispatch using Quasi Oppositional Biogeography Based Optimization (QOBBO) technique. The methodology determines control variable settings such as generator terminal voltages, tap positions of the regulating transformer and the VAR injection of the shunts compensator, for real power loss minimization in the transmission system.

In this paper, optimal allocation of DG based on determination of most sensitive buses to the voltage collapse in distribution network is analyzed. A Voltage Stability Indicator (VSI) is developed from conventional power flow equation to determine stability condition of buses. Artificial Neural Network (ANN) technique is used to determine the proper capacity of DG to ensure the static voltage of each node within permissible limit. Proposed method is tested on 15 bus and 52 bus radial distribution systems. Through simulation, the impact of DG on static voltage profile is illustrated. The influence of DG on voltage stability and system power losses are also quantified here.

2 Location Selection for DG

In developing countries most of the distribution systems are operated with radial structure. Larger voltage drop in these types of systems are obvious. By analyzing voltage sensitivity of lines, weakness of network voltage may be identified and opportunities for improvement with real or reactive power compensation via DG can be examined.

2.1 Voltage Stability Indicator

Power network are becoming heavily stressed to meet ever increasing load demand. This situation has resulted into deterioration of voltage magnitudes at buses. One of the major problems that may associate with such a stressed system is voltage collapse. From the necessity of accurate analysis of voltage stability a number of analytical and computational tools have been discussed [1, 2, 7]. In this section a simple VSI is formulated for radial distribution system to get a estimation of the distance to voltage collapse. The indicator uses the bus voltage and network information provided by load flow program.

Any branch $r_i + jx_i$ connected between bus:i and bus:i + 1 of the radial distribution system may be represented by an equivalent circuit model as in Fig. 1.

$$I^2 = (P_{i+1}^2 + Q_{i+1}^2)/V_{i+1}^2 \tag{1}$$

Again

$$I^2 = \frac{P_L^2 + Q_L^2}{(V_i - V_{i+1})^2} \tag{2}$$

Here P_L and Q_L are the active and reactive power loss of the line connected between two nodes.

So, from Eqs. (1) and (2) equating I^2 it becomes,

$$\frac{P_{i+1}^2 + Q_{i+1}^2}{V_{i+1}^2} = \frac{P_L^2 + Q_L^2}{(V_i - V_{i+1})^2} \tag{3}$$

Now

$$P_{i+1} = P_i - P_L \tag{4}$$

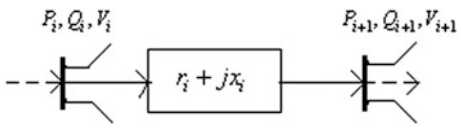

Fig. 1 Two bus power system network

$$Q_{i+1} = Q_i - Q_L \tag{5}$$

$$P_L = r_i\left(\frac{P_{i+1}^2 + Q_{i+1}^2}{V_{i+1}^2}\right) \tag{6}$$

$$Q_L = x_i\left(\frac{P_{i+1}^2 + Q_{i+1}^2}{V_{i+1}^2}\right) \tag{7}$$

As the value of P_L and Q_L from Eqs. (6) and (7) have used in Eq. (3)

$$\left(V_i \cdot V_{i+1} - V_{i+1}^2\right)^2 = \left(P_{i+1}^2 + Q_{i+1}^2\right).\left(r_i^2 + x_i^2\right) \tag{8}$$

Since the positive root of the Eq. (8) is taken,

$$V_{i+1}^2 - V_{i+1}.V_i + \sqrt{\left(\left(P_{i+1}^2 + Q_{i+1}^2\right).\left(r_i^2 + x_i^2\right)\right)} = 0 \tag{9}$$

The roots of the Eq. (9) are real if

$$V_i^2 - 4 \cdot \sqrt{\left(\left(P_{i+1}^2 + Q_{i+1}^2\right).\left(r_i^2 + x_i^2\right)\right)} \geq 0 \tag{10}$$

From Eq. (10) the developed Voltage Stability Index (VSI) is given as

$$L_{i+1} = \frac{4 \cdot \sqrt{\left(\left(P_{i+1}^2 + Q_{i+1}^2\right).\left(r_i^2 + x_i^2\right)\right)}}{V_i^2} \leq 1 \tag{11}$$

In practice, distribution system operators are always try to maintain the system within a given voltage stability margin; so that small contingencies do not make the system unstable. Therefore, L_{i+1} must be less than threshold value for maintaining stability at that bus. The more the value of the indicator nearer to zero the system is more stable.

2.2 Priority List

Voltage stability level of each bus is calculated using the proposed VSI. The buses are ranked in descending order according to their values of VSI to form a priority list. The top ranked bus has chosen first for allocation of DG. Subsequently lower ranked buses are fed with power from DG units. How many number of DG units would be installed depend on sizing issues of DG units. After installation of each DG unit, load flow solution is performed to monitor voltage magnitude of buses, network power losses and voltage stability condition of the system.

3 Sizing of DG

DG is small scale power generation ranging from multi-kW to few MW and usually connected to distribution system. The impact of DG on distribution system may be positive or negative depending upon the size and operating condition of DG. The size at most should be such that it is consumable within the distribution substation boundary. Further increase of size can cause reverse flow of power through substation which will lead to high system losses.

3.1 ANN Model

For a particular bus as the size of DG is increased beyond optimal DG size network losses starts increasing rather than decreasing. So, appropriate size evaluation of DG has become very significant. The use of ANN can capable to indicate the best solution for a given distribution system. This is because of the advantage of high computation rate provided by three layered feed forward ANN in approximating a complex nonlinear mapping. A feed forward ANN works on the basis of propagation of signal in only one direction from an input stage to an output stage through intermediate neurons. Number of hidden layer is chosen to match the complexity of the function. Error Back Propagation Learning algorithm (EBPL) is used as training algorithm for ANN due to faster learning and reliable convergence. The error function chosen for learning process is Mean Square Error (MSE) of outputs. The architecture of three layered ANN is shown in Fig. 2.

Appropriate size of DG unit for a particular bus can be determined for desired voltage profile of that bus. With random change of DG unit at that bus, values of voltage magnitudes are determined from power flow solutions. Feed forward ANN is trained rigorously with DG size correspond to voltage magnitudes at poor voltage stable bus obtained from load flow solution. Then, for any required bus voltage the optimal size of DG unit (MVA) for that particular bus evaluated.

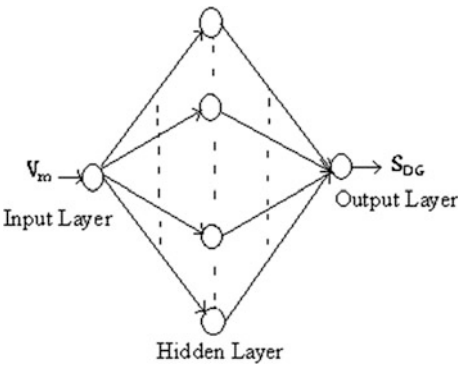

Fig. 2 Architecture of three layered feed forward ANN

3.2 Computational Procedure

Installation of DG of non-optimal size can result in an increase of system losses; implying reduction of voltage magnitudes at buses of network. Computational procedure for proposed methodology is as follows (Fig. 3).

1. Run the power flow solution at base case of the system.
2. Calculate VSI of each bus and store.
3. Arrange VSI of buses in descending order to form priority list.
4. Place DG at top ranked bus.
5. Change size of DG randomly within certain limit and calculate voltage magnitude of the highest priority bus to form training data set.
6. Train three layered feed forward ANN properly with training data set.
7. Evaluate appropriate DG size (MVA) for desired voltage profile at the bus from ANN model.
8. Repeat step-5 to step-7 to allocate DG units subsequently at other weak voltage stable buses till desired voltages at all buses are obtained.

4 Test System

The proposed technique has been tested on 15 bus [14] and 52 bus radial distribution system. Single line diagram of 15 bus system is as shown in Fig. 4.

Load data of the system is given in Table 1.

There are three main feeders of 11 kV, 52 bus practical distribution system supplying a total load of 4.184 + j2.025 MVA [15]. The schematic diagram of the test system is shown in Fig. 5.

Line impedance of the system is 0.0086 + j0.0037 Ω/km.

A Newton–Raphson algorithm based load flow solution program is written in MATLAB 7 to solve power flow problem.

5 Simulation Results

VSI of each bus is calculated with system data of base configuration. Priority list is prepared and presented in Table 2.

Obtaining the data from power flow solution, total branch power losses are calculated for 15 bus. Total distribution loss incurred is 79 + j75 kVA. The size of distribution system in term of load (MVA) will play an important role to select the size of DG. To obtain a reasonable solution; the size of DG unit should not be so small or so high with respect to load value. Therefore DG range is chosen as 10 %

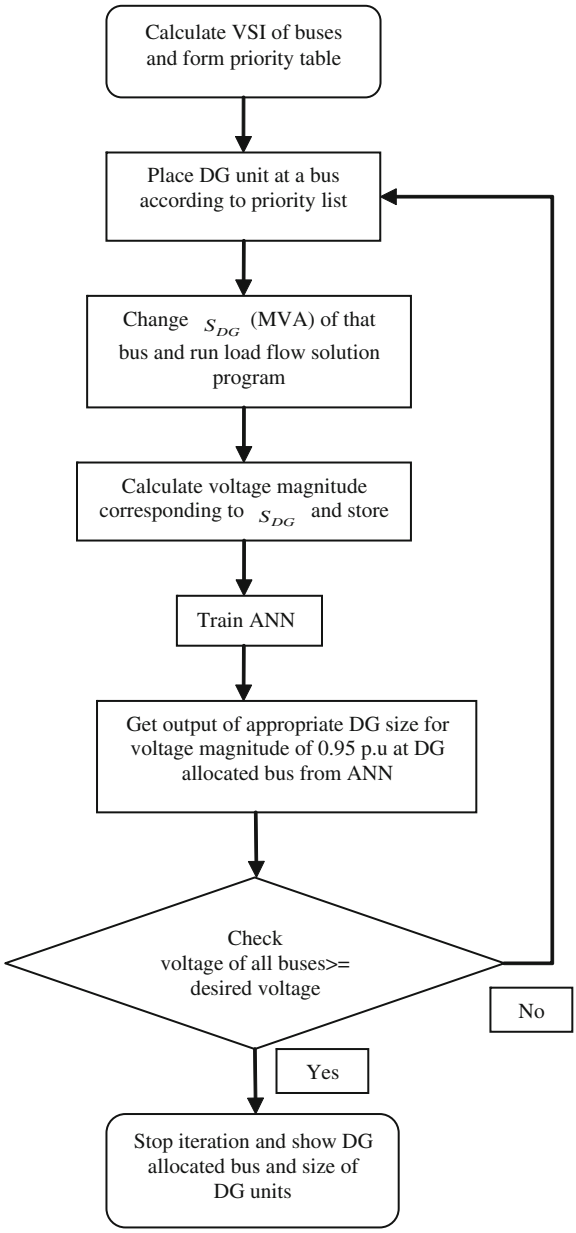

Fig. 3 Flow chart for allocation and sizing of DG units

of total load $\leq S_{DG} \leq 30$ % of total load for this system. Optimal size of DG unit is quantified through raising the voltage magnitude of ill voltage stable bus to 0.95 p.u. According to priority list DG is installed at Bus-10. Appropriate size of DG is obtained from ANN model. Figure 6 shows that ANN estimated size of DG is 0.2454 MVA.

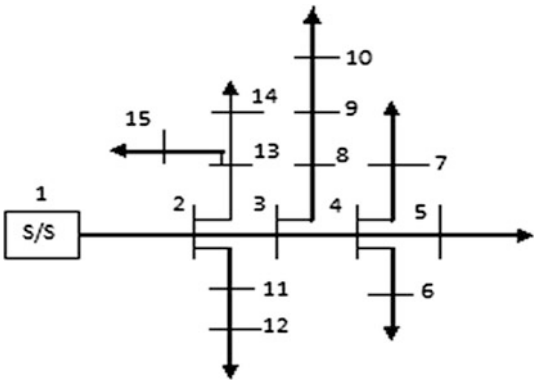

Fig. 4 Single line diagram of 15 bus radial distribution system

Table 1 Load and generation data of 15 bus distribution system

Bus number	Load		Generation	
	Active (kW)	Reactive (kVAR)	Active (kW)	Reactive (kVAR)
1	–	–	1,305	1,325
2	44	45	–	–
3	70	71	–	–
4	140	143	–	–
5	44	45	–	–
6	140	143	–	–
7	70	71	–	–
8	140	143	–	–
9	70	71	–	–
10	140	143	–	–
11	70	71	–	–
12	44	45	–	–
13	44	45	–	–
14	140	143	–	–
15	70	71	–	–

For 15 bus system one DG is sufficient to boost up the voltage magnitudes of all the lower voltage buses near to 0.95 p.u as shown in Fig. 7.

For 52 bus system active and reactive power losses of the network are obtained as 741 kW and 307 kVAR respectively. Table 3 shows rank of buses to allocate DG.

According to priority list first DG unit is placed at Bus-44 because it is the most sensitive bus to voltage collapse. DG range is chosen as 0.4648 MVA $\leq$ $S_{DG} \leq$ 1.3944 MVA i.e. 10 % of total load $\leq S_{DG} \leq$ 30 % of total load for this system. Based on the proposed methodology, optimum size of DG unit at Bus-44 is calculated using ANN. Figure 8 obtained from simulation of ANN model shows training and target output data at Bus-44. Very low Mean Square Error (MSE = 0.00069) confirms the validation of the proposed model.

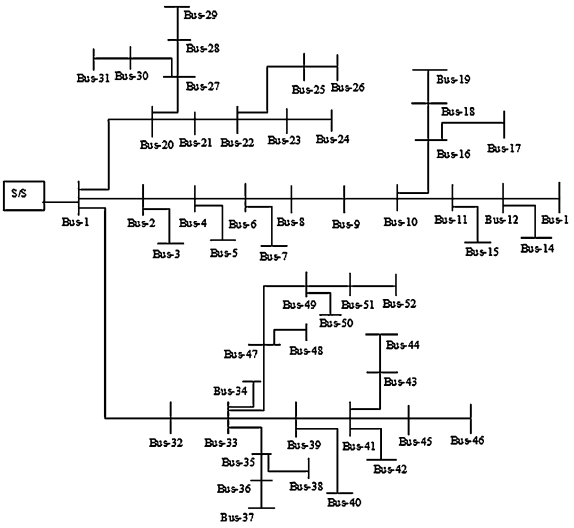

Fig. 5 Single line diagram of 52 bus radial distribution system

Table 2 Priority list of 15 bus radial system

Rank	Bus number	Value of VSI
1	10	0.222
2	8	0.190
3	9	0.132
4	6	0.124
5	7	0.121
6	11	0.112
7	14	0.107
8	4	0.101
9	13	0.082
10	3	0.067
11	15	0.064
12	12	0.056
13	5	0.051
14	2	0.046
15	1	–

Appropriate DG size at Bus-44 is 0.7123 MVA i.e. 15.06 % of total load.

In the same way another two DG units are installed consecutively at Bus-36 and at Bus-13.

Minimum size of DG i.e. 0.4648 MVA is sufficient to raise the voltage beyond 0.95 p.u at Bus-36.

For Bus-13, size of DG is determined from ANN simulation as shown in Fig. 9.

Appropriate sizes of DG units along with MSEs are tabulated in Table 4.

After installation of three DG units, it is seen that voltage profile of all the buses are raised above 0.90 p.u and that is shown in Fig. 10.

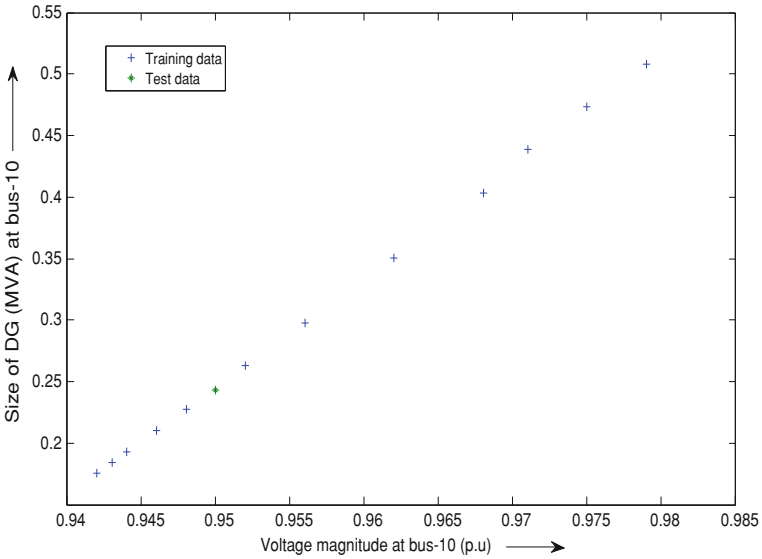

Fig. 6 Training and testing output of ANN for 15 bus radial system

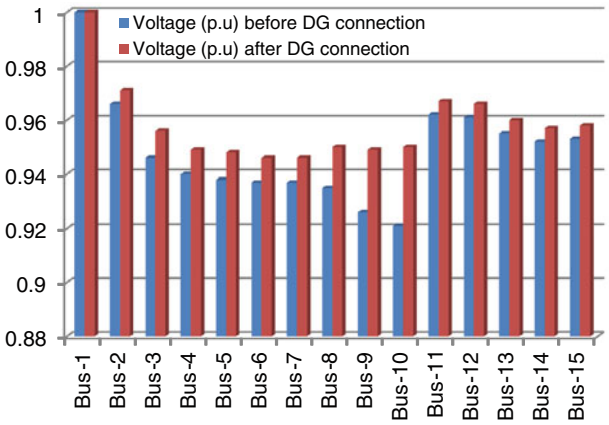

Fig. 7 Comparison of voltage profiles of different buses of 15 bus distribution system

Active and reactive power losses for both the systems are reduced significantly as shown in Tables 5 and 6.

Total power loss is reduced about 76.55 % for 52 bus system and 33.06 % for 15 bus system after proper allocation of DG units.

The optimization techniques for sizing of DGs are iterative process with repetitive solution of power flow problem. So, the processes are time consuming. A number of times, optimization techniques are needed to obtain size of DGs for different required voltage profile at load buses. Once the training has done, ANN

Table 3 Priority list of 52 bus system

Rank	Bus number	Value of VSI
1	44	0.4323
2	36	0.3483
3	13	0.3433
4	18	0.3365
5	03	0.3102
6	33	0.2993
7	15	0.2969
8	47	0.2801
9	17	0.2537
10	23	0.2390
11	50	0.2230
12	19	0.2084
13	31	0.2061
14	46	0.1960
15	42	0.1927
16	10	0.1873
17	08	0.1628
18	39	0.1467
19	40	0.1415
20	14	0.1354
21	37	0.1338
22	25	0.1327
23	09	0.1243
24	24	0.1200
25	30	0.1148
26	28	0.0968
27	45	0.1040
28	22	0.1021
29	34	0.1019
30	02	0.0982
31	28	0.0968
32	35	0.0896
33	38	0.0875
34	43	0.0825
35	26	0.0724
36	05	0.0722
37	29	0.0718
38	04	0.0692
39	32	0.0671
40	41	0.0670
41	49	0.0653
42	16	0.0585
43	21	0.0556
44	07	0.0524
45	27	0.0419
46	20	0.0410
47	48	0.0394
48	52	0.0265
49	11	0.0235
50	12	0.0156
51	06	0.0119
52	1	_

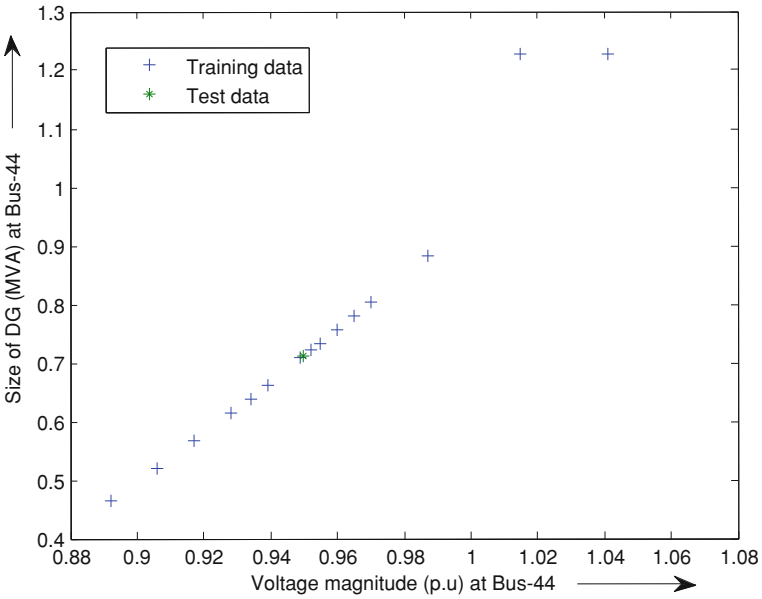

Fig. 8 Graph of test output along with training data for different voltage magnitudes at Bus-44

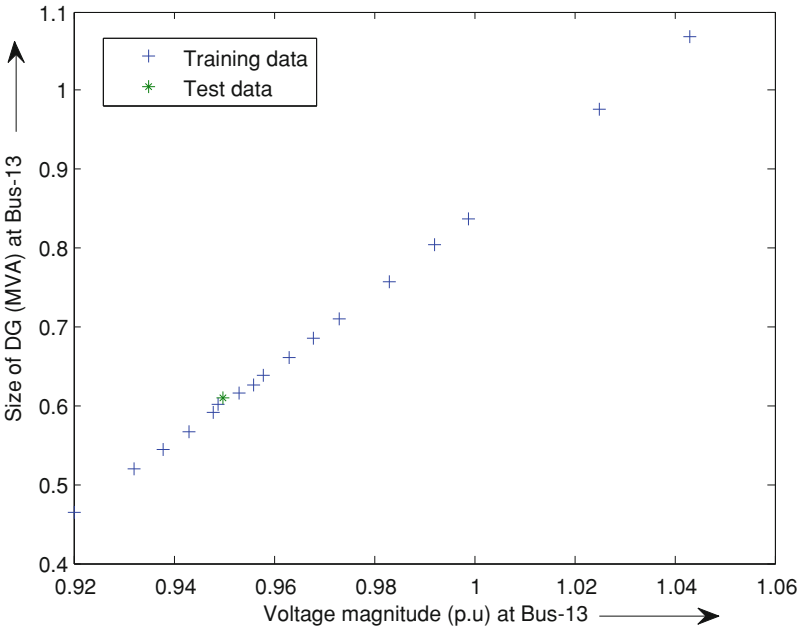

Fig. 9 Graph of training and test output data with respect to voltage magnitudes at Bus-13

Table 4 Size of DG at three vulnerable buses

Bus number	Size of DG		MSE
	(kW)	(kVAR)	
Bus-44	641.4	309.8	0.00069
Bus-36	418.4	202.5	–
Bus-13	547.1	264.3	0.00028

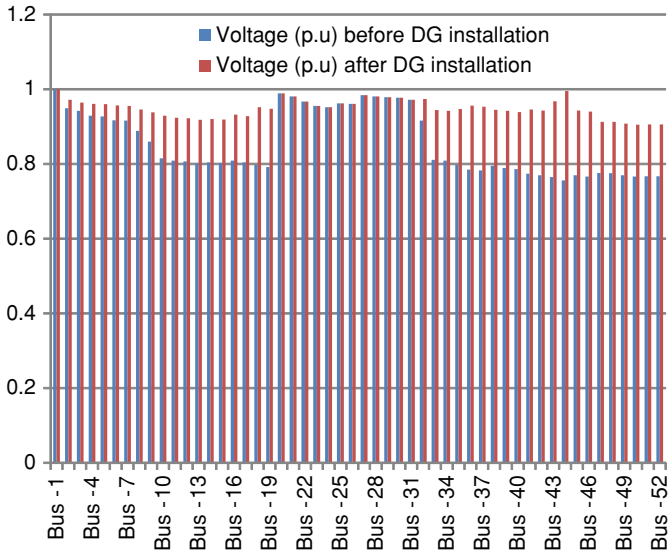

Fig. 10 Comparison of voltage magnitudes of buses before and after DG installation for 52 bus system

Table 5 Losses of the 15 bus system before and after DG installation

	Active power loss (kW)	Reactive power loss (kVAR)
Before DG installation	79	75
After DG installation	53	50

Table 6 Comparative study of power losses before and after DG installation of 52 node network

	Active power loss (kW)	Reactive power loss (kVAR)
Before DG installation	741	307
After DG installation	176	70

technique can directly estimate the size of DG unit for any required voltage profile. So, the technique is quite fast. But, sometimes it may generate sub-optimal solution. The optimization techniques used for the study are complex and difficult to understand. The proposed methodology is rather simple in nature.

6 Conclusion

Priority table is used for easy selection of best location for single or multiple DG units. The buses are ranked using VSI which make priority Table. Appropriate size of DG for desired voltage profile has been evaluated by ANN technique. The proposed algorithm is tested on 15 bus and practical 52 bus radial distribution system. The process is simple and low time demanding. From results obtained, it can be concluded that the optimal sizes of DG units vary from bus to bus, depending on connected loads. Different optimal sizes and locations of DG units are required for different systems depending on their configurations. The results reveal that the integration of DG is highly effective in reducing power losses in the distribution network. Placing DG of appropriate size at optimum location also permit an increase of voltage magnitudes at buses.

References

1. Dey, S., Chanda, C.K., Chakraborti, A.: Development of global voltage security indicator (VSI) and role of SVC on it in longitudinal power supply (LPS) system. Elsevier, Electr. Power Syst. Res. **68**, 1–9 (2004)
2. Gubina, F., Strmcnik, B.: A simple approach to voltage stability assessment in radial network. IEEE Trans. Power Syst. **12**(3), 1121–1128 (1997)
3. Ismail, K.S.: Neural network based load balancing and reactive power control by Static VAR compensator. Int. J. of Computer and. Int. J. Comput. Electr. Eng. **1**(1), 1793–8198 (2009)
4. Shin, J.R.: A new optimal routing algorithm for loss minimization and voltage stability improvement in radial power systems. IEEE Trans. Power Syst. **22**(2), 648–657 (2007)
5. Singh, D., Singh, D., Verma, K.S.: GA based energy loss minimization approach for optimal sizing and placement of distributed generation. Int. J. Knowl.-Based Intell. Eng. Syst. **12**, 147–156 (2008)
6. Ganesan, T., Vasant, P., Elamvazuthi, I.: Hybrid neuro-swarm optimization approach for design of distributed generation power systems. Springer, Neural Comput. Appl. (2012). doi:10.1007/s00521-012-0976-4
7. Kashem, M.A., Ledwich, G.: Multiple distributed generators for distribution feeder voltage support. IEEE Trans. Energy Convers. **20**(3), 676–684 (2005)
8. Caisheng, W., Nehrir, M.H.: Analytical approaches for optimal placement of distributed generation sources in power system. IEEE Trans. Power Syst. **19**(4), 2068–2076 (2004)
9. Rafidah, S., Rahim, A.: Implementation of DG for loss minimization and voltage profile in distribution system. In: 4th International Power Engineering and Optimization Conference, 23–24 June, Selangor, Malaysia (2010)
10. Acharya, N., Mahat, P., Mithulananthan, N.: An analytical approach for DG allocation in primary distribution network. Elect. Power Energy Syst. **28**, 669–678 (2006)
11. Hedayati, H., Nabaviniaki, S.A., Akbarimajd, A.: A method for placement of DG units in distribution networks. IEEE Trans. Power Deliv. **23**(3), 1620–1628 (2008)
12. Devi, A.L., Subramanyam, B.: Optimal DG unit placement for loss reduction in radial distribution system-a case study. ARPN J. Eng. Appl. Sci. **2**(6), 57–61 (2007)
13. Roy, P.K., Mandal, D.: Optimal reactive power dispatch using quasi-oppositional biogeography-based optimization. Int. J. Energy Optim. Eng. (IJEOE) **1**(4), 38–55 (2012)

14. Das, D., Kothari, D.P., Kalam, A.: Simple and efficient method for load flow solution of radial distribution networks. Elsevier, Electr. Power Energy Syst. **17**(5), 335–346 (1995)
15. Thukaram, D., Khincha, H.P., Vijaynarasimha, H.P.: Artificial neural network and support vector machine approach for locating faults in radial distribution system. IEEE Trans. Power Deliv. **20**(2), 710–721 (2005)

Multiperiod Economic Dispatch: A Decomposition Approach

Antonio Marmolejo and Igor Litvinchev

Abstract This work presents a decomposition algorithm to solve a multiperiod optimal economic dispatch (MOED) which determines the start up and shutdown schedules of thermal units. The transmission network considers capacity limits and line losses. The mathematical model is presented using mixed integer non linear problem (MINLP) with binary variables. A generalized cross decomposition algorithm has been implemented to minimize the dispatch cost while satisfying generating units and powerflow limits. This algorithm exploits the structure of the problem to reduce solution time. The original problem is decomposed into a primal subproblem, which is a non linear problem (NLP), a dual subproblem, which is a mixed integer non linear problem, and a mixed integer problem (MIP) called master problem. Two test systems are presented to evaluate the performance of the proposed decomposition strategy. Numerical results show the superiority of the cross decomposition approach.

Keywords Economic dispatch · Lagrangean relaxation · Benders decomposition · Cross decomposition

1 Introduction

A definition of economic dispatch is the operation of generation facilities to produce energy at the lowest cost to reliably serve consumers, recognizing any operational limits of generation and transmission facilities.

A. Marmolejo (✉) · I. Litvinchev
Autonomous University of Nuevo Leon,
San Nicolás de los Garza, México
e-mail: marmolejo.antonio@hotmail.com

I. Litvinchev
e-mail: igor@yalma.fime.uanl.mx

I. Zelinka et al. (eds.), *Power, Control and Optimization*, Lecture Notes in Electrical Engineering 239, DOI: 10.1007/978-3-319-00206-4_6,

An electric network consists of many generation nodes with various generating capacities and cost functions, lines of transmission and nodes of power demand. The MOED problem is made up by unit commitment problem [1] and optimal power flow that is seen as an economic dispatch (ED) [2–4]. Both subproblems have been studied for many years and there are many algorithms to found good solutions with different complexity. Most of the authors consider both problems separately. In the typical unit commitment (UC), the transmission network is not considered and in ED, the transmission network is modeled in but only a single time period is considered.

Since the MOED problem is a NP-hard MINLP, for large power systems, it is extremely difficult to obtain the exact optimal solution [1]. Because of this, we present an alternative to solve a MOED based on a generalized cross decomposition (GCD) [5] strategy in order to reduce the computational effort.

This decomposition simultaneously utilizes primal and dual subproblems by exploiting the advantages of lagrangean relaxation [6] and generalized benders decomposition (GBD) [7]. The practical motivation of Cross Decomposition is to replace the hard primal master problem with the easier dual subproblem to the largest possible extent.

The proposed decomposition strategy shows good convergence properties for this application, the number of iterations required to attained convergence is typically low, so the computation time is less.

2 Problem Description

MOED problem is defined as determining the mix of generators and their estimated output level to meet the expected demand of electricity over a given time horizon (a day or a week), while satisfying the load demand, spinning reserve requirement and transmission network constraints.

In this work we addresses a MOED problem based on [8] notation, where network constraints are represented through a DC model [2] and considers a multiperiod time horizon.

2.1 Nomenclature

Constants

A_j	Start up cost of power plant j
B_{nm}	Susceptance of line $n-m$
C_{nm}	Transmission capacity limit of line $n-m$
D_{nk}	Load demand at node n during period k

$E_j(t_{jk})$ Nonlinear function representing the operating cost of power plant j as a function of its power output in period k
E_{j1} Linear coefficient of operating cost for the plant j
E_{j2} Quadratic coefficient of operating cost for the plant j
F_j Fixed cost of power plant j
V_{jk} Parameter which is equal to 1 when plant j is committed in period k after dual subproblem is solved in φ iteration
Y_{jk} Parameter which is equal to 1 when plant j is started up at the beginning of period k after dual subproblem is solved in φ iteration
K_{nm} Conductance of line $n-m$
R_k Spinning reserve requirement during period k
$\overline{T_j}$ Maximum power output of plant j
$\underline{T_j}$ Minimum power output of plant j
nr Reference node with angle cero

Variables

t_{jk} Power output of plant j in period k
v_{jk} Binary variable, which is equal to 1 when plant j is committed in period
y_{jk} Binary variable, which is equal to 1 when plant j is started up at the beginning of period k
δ_{nk} Angle of node n in period k
λ_{nk} Lagrangean multiplier associated to a power balance constraint
μ_k Lagrangean multiplier associated to a spinning reserve requirement
γ_{nk}, β_{nk} Lagrangean multipliers associated to transmission capacity limits

Sets

J Set of indices of all plants
K Set of period indices
N Set of indices of all nodes
Λ_n Set of indices of the power plants j at node n
Ω_n Set of indices of nodes connected and adjacent to node n
Φ Set of Generalized Cross Decomposition iterations

The objective is minimises a function that includes fixed cost, start up cost and operating cost. A second order polynomial describes the variable costs as a function of the electric power.

$$Min\, Z = \sum_{k \in K} \sum_{j=J} [F_j v_{jk} + A_j y_{jk} + E_j(t_{jk})] \tag{1}$$

There is a power balance constraint per node and time period. In each period, the production has to satisfy the demand and losses in each node. Line losses are modeled through cosine approximation and it is assumed that the demand for electric energy is known and is discretized into t periods.

$$\sum_{j\in\Lambda_n} t_{jk} + \sum_{m\in\Omega_n} B_{nm}[\delta_{mk} - \delta_{nk}] - \sum_{m\in\Omega_n} K_{nm}[1 - \cos(\delta_{mk} - \delta_{nk})] = D_{nk} \quad \forall n \in N, \forall k \in K \tag{2}$$

Spinning reserve requirements are modeled. In each period the running units have to be able to satisfy the demand and the prespecified spinning reserve.

$$\sum_{j\in J} \overline{T}_j v_{jk} \geq \sum_{\mathrm{n}\in\mathrm{N}} \mathrm{D_{nk}} + R_k \quad \forall k \in K \tag{3}$$

Each unit has a technical lower and upper bound for the power production.

$$\underline{T}_j v_{jk} \leq t_{jk} \leq \overline{T}_j v_{jk} \quad \forall j \in J, \forall k \in K \tag{4}$$

Transmission capacity limits of lines avoid dynamic stability system problems.

$$-C_{nm} \leq B_{nm}[\delta_{mk} - \delta_{nk}] \leq C_{nm} \quad \forall n \in N, \forall k \in K, \forall m \in \Omega_n \tag{5}$$

This constraint holds the logic of running, start-up and shut-down of the units. A running unit cannot be started-up.

$$y_{jk} \geq v_{jk} - v_{jk-1} \quad \forall j \in J, \forall k \tag{6}$$

Angle in all buses has a lower and upper bound.

$$-\pi \leq \delta_{nk} \leq \pi \quad \forall n \in N/\{nr\}, \forall k \in K \tag{7}$$

3 Solution Approach

Because the MOED is a MINLP Np-hard problem, there is an exponential increase in solution time with the number of time periods as well as with the number of generation nodes. Therefore, in order to solve this problem in better solution time than other methods, we apply GCD strategy.

The basic GCD [5] consists of two phases, that is the primal and dual subproblem phase (phase I), and the master problem phase (phase II), and appropriate convergence tests. In phase I the primal subproblem provides an upper bound of the optimal solution for the MOED (1-7) and lagrange multipliers for the dual subproblem. The dual subproblem provides lower bound on the solution of MOED and supplies binary variables for the primal subproblem.

Both, the primal and the dual subproblem generate cuts for the master problem in phase II. At each iteration of the GCD, primal and dual subproblems are solved, and a primal convergence test is applied on binary variables, while a dual convergence test is applied on lagrange multipliers. If any convergence test fails, then we enter phase II that features the solution of master problem and return subsequently to phase I. The convergence tests of the GCD provide information about

an upper bound improvement and a lower bound improvement. Upper bound improvement corresponds to a decrease in the upper bound obtained by the primal subproblem. A lower bound improvement corresponds to an increase in the lower bound obtained by the dual subproblem.

In this work we present a strategy for the implementation of the GCD that avoid the use of master problem. This is because the master problem is known to be a more difficult and cpu time consuming problem, than the primal and dual subproblems of phase I. The key idea is to make extensive use of phase I (primal and dual subproblems). For this, we use a MINLP and NLP solvers to solve primal and dual subproblems respectively. These solvers ensure the convergence of each subproblem solution in less time than the solution of master problem.

Therefore, the MOED is divided into one primal problem (9) and one dual subproblem (8), which is a classic economic dispatch. The algorithm initialized with a set of lagrange multipliers, which are defined heuristically as a result of the knowledge of the original problem. Then, the dual subproblem is solved and provides integer variables for the primal subproblem and a lower bound of the original problem (MOED) in the φ iteration of GCD.

Later, the primal subproblem is solved and provides the lagrangean multipliers (that are fixed in the next dual subproblem) and an upper bound for the MOED problem in the φ iteration of GCD.

To conform the dual subproblem we used a nodal decomposition of the original problem [9] to relax the system constraints power balance (2), spinning reserve (3) and transmission capacity limits of lines (5). Dualizing these constraints produces a dual subproblem that is less expensive to solve and speed up the solution of this subproblem.

A primal convergence test and dual convergence test are used to check a bound improvement and to verify when an optimal solution is reached. We describe the dual subproblem and primal subproblem for MOED.

Dual subproblem

$$\begin{aligned}
&\min_{t_{jk},v_{jk},y_{jk},\delta_{nk}} D_{sub}^{\varphi}\Big\{\sum_{k\in K}\sum_{j\in\lambda_n}[F_j v_{jk}+A_j y_{jk}+E_j(t_{jk})]\\
&+\sum_{k\in K}\lambda_k\Big[D_{nk}-\sum_{j\in\lambda_n}t_{jk}-\sum_{m\in\omega_n}B_{nm}(\delta_{mk}-\delta_{nk})+\sum_{m\in\omega_n}K_{nm}(1-\cos(\delta_{mk}-\delta_{nk})\Big]\\
&+\sum_{k\in K}\mu_k\Big[D_{nk}+R_k-\sum_{j\in J}\overline{T}_j v_{jk}\Big]+\sum_{k\in K}\gamma_k\Big[C_{nm}-\sum_{m\in\omega_n}B_{nm}(\delta_{mk}-\delta_{nk})\Big]\\
&+\sum_{k\in K}\beta_k\Big[-\sum_{m\in\omega_n}B_{nm}(\delta_{mk}-\delta_{nk})-C_{nm}\Big]\Big\}
\end{aligned} \tag{8}$$

subject to constraints (2), (4) and (6).

Primal subproblem

$$
\begin{aligned}
&\underset{t_{jk},\delta_{nk}}{Min}\, P^{\varphi}_{sub} = \sum_{k\in K}\sum_{j=J}[E_j(t_{jk})] \\
&subject\ to: \\
&\sum_{j\in\Lambda_n} t_{jk} + \sum_{m\in\Omega_n} B_{nm}[\delta_{mk}-\delta_{nk}] - \sum_{m\in\Omega_n} K_{nm}[1-\cos(\delta_{mk}-\delta_{nk})] = D_{nk} \\
&\qquad \forall n\in N, \forall k\in K \\
&\underline{T_j} v_{jk} \le t_{jk} \le \overline{T_j} v_{jk} \qquad \forall j\in J, \forall k\in K \\
&-C_{nm} \le B_{nm}[\delta_{mk}-\delta_{nk}] \le C_{nm} \qquad \forall n\in N, \forall k\in K, \forall m\,\Omega_n \\
&-\pi \le \delta_{nk} \le \pi \qquad \forall n\in N/\{nr\}, \forall k\in K \\
&v_{jk} = V^{\varphi}_{jk} \\
&y_{jk} = Y^{\varphi}_{jk}
\end{aligned}
\tag{9}
$$

In all cases available solution data include total generation costs, on/off status of every thermal unit per hour, power output of every plant per hour, angle of every node per hour.

4 The Computational Tool

Two test systems are presented to evaluate the performance of the proposed decomposition strategy. The IEEE 24 bus test system with 24 nodes, 24 thermal units and 38 transmission lines [10], and a portion of bus electric energy system of Mainland Spain with 104 nodes, 62 thermal units and 160 transmission lines [8].

The mathematical model of MOED and the decomposition strategy were implemented in GAMS [11] using the solver DICOPT [12] for solving the MINLP problems (dual subproblems).

DICOPT solves a series of NLP and MIP subproblems. These subproblems can be solved using any NLP or MIP solver that runs under GAMS, for this case we use CONOPT [13] for solving the NLP problems (primal subproblems) and CPLEX 12 [14] for MIP problems. All the models have been solved on an AMD Phenom ^{TM} II N970 Quad-Core with a 2.2 GHz processor and 8 GB RAM.

5 Results

The graphics in the Figs. 1 and 2 show GCD iterations were needed to solve IEEE 24 bus test system, and 104 nodes system. E-optimum corresponds to optimal value of the full scale model (MOED) obtained directly with DICOPT solver. Additionally, the graphics present total CPU time required for solving two test systems. We compared direct solution with DICOPT true GAMS with the GCD strategy. The decomposition strategy proposed yield better solutions to the addressed problem (Table 1).

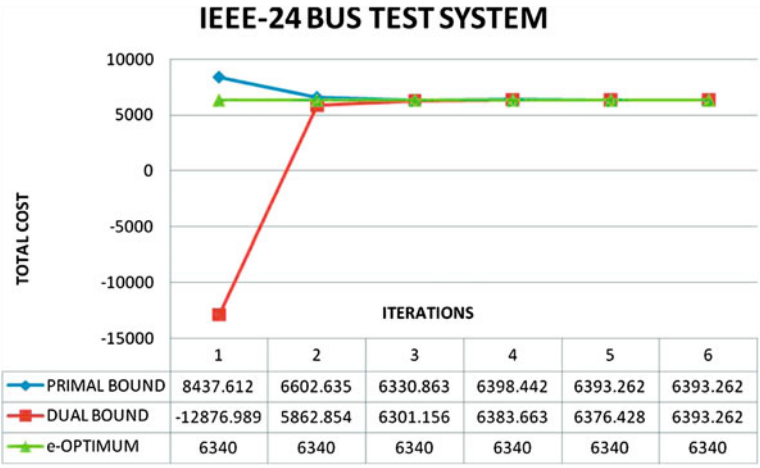

	1	2	3	4	5	6
PRIMAL BOUND	8437.612	6602.635	6330.863	6398.442	6393.262	6393.262
DUAL BOUND	-12876.989	5862.854	6301.156	6383.663	6376.428	6393.262
e-OPTIMUM	6340	6340	6340	6340	6340	6340

Fig. 1 Generalized cross decomposition of the IEEE 24 bus test system

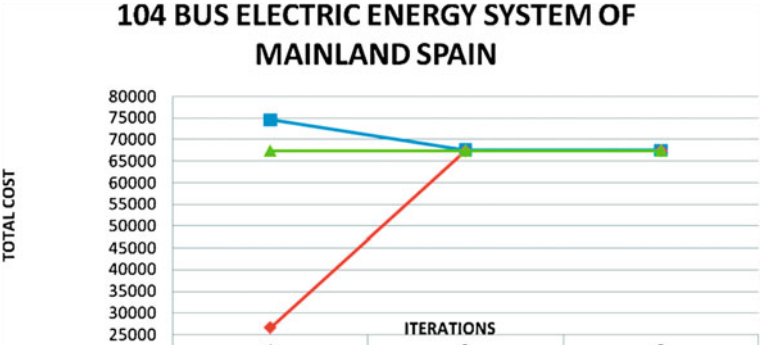

	1	2	3
PRIMAL BOUND	74567.3453	67501.0183	67457.80877
DUAL BOUND	26614.57448	67393.67098	67449.32997
e-OPTIMUM	67450	67450	67450

Fig. 2 Generalized cross decomposition of the 104 nodes electric energy system of Mainland Spain

Table 1 Solution time results obtained by generalized cross decomposition strategy and by DICOPT solver

System	GCD strategy	Solver DICOPT
24-nodes	00′18″	07′54″
104-nodes	2′54″	18′34″

6 Conclusions

Several works revealed that the computational effort of multiperiod optimal economic dispatch models grows exponentially with the number of time periods and nodes. Therefore, in order to reduce the computational effort of the problem special techniques must be employed. The proposal was to apply generalized cross decomposition strategy, which exploits the structure of the problem, to reduce solution time by decomposing the model (MOED). It was not necessary to solve a master problem since in the subproblem phase, NLP and MINLP solvers were tuned to obtain solutions with a 10 % of optimality. In case the primal subproblem (NLP subproblem) are very difficult, using a combination of NLP solvers under GAMS has been found to be effective. The solution of proposed strategy showed a significant reduction in computational effort with respect to the full-scale MINLP solver.

References

1. Tseng, C.L.: On power system generation unit commitment problems. Dissertation, UC Berkeley, December (1996)
2. Wood, A. J., Wollenberg, B.F.: Power Generation, Operation and Control. Wiley, London (1996)
3. Ngoc Dieu, V., Schegner, P.: Real power dispatch on large scale power systems by augmented lagrange hopfield network. Int. J. Energy Optim. Eng. (IJEOE), 1(1), 19–38. doi:10.4018/ijeoe.2012010102
4. Hopfield Lagrange Network for Economic Load Dispatch. In: P. Vasant, N. Barsoum, and J. Webb (eds.), Innovation in Power, Control, and Optimization: Emerging Energy Technologies (pp. 57–94). Engineering Science Reference, Hershey, PA. doi:10.4018/978-1-61350-138-2.ch002
5. Holmberg, K. MINLP: Generalized cross decomposition. Encycl. Optim. 2148–2155 (2009)
6. Geoffrion, A.M.: Lagrangean relaxation for integer programming. Math. Program. Study **2**, 82–114 (1974)
7. Geoffrion, A.M.: Generalized benders decomposition. J. Optim. Theor. Appl. **10**(4), 237 (1972)
8. Alguacil, N., Conejo, A.: Multiperiod optimal power flow using benders decomposition. IEEE Trans. Power Syst. **15**(1), 196–201 (2000)
9. Marmolejo, J.A., Litvinchev, I., Aceves R.: Programación Multiperiodo de Unidades Térmicas. Presented in XIV Latin Ibero-American Congress on Operations Research (CLAIO 2008). Book of Extended Abstracts
10. Charman, P., Bhavaraju, P., Billington, R.: IEEE reliability test system. IEEE Trans. Power Apparatus Syst. **98**(6), 2047–2054 (1979)
11. Brooke, A., Kendrick, D., Meeraus, A.: GAMS: A User's Guide. The Scientific Press, San Francisco (1998)
12. Brooke, A., Kendrick, D., Meeraus, A.: GAMS/DICOPT. User Notes. GAMS Development Corporation (2010)
13. Drud, A.S.: CONOPT: A large scale GRG code. ORSA J. Comput. **6**(2), 207–216 (1994)
14. Brooke, A., Kendrick, D., Meeraus, A.: GAMS/Cplex 12. User Notes. GAMS Development Corporation (2010)

Developing a Framework for Energy Technology Portfolio Selection

Hamid Davoudpour and Maryam Ashrafi

Abstract Today, the increased consumption of energy in world, in addition to the risk of quick exhaustion of fossil resources, has forced industrial firms and organizations to utilize energy technology portfolio management tools viewed both as a process of diversification of energy sources and optimal use of available energy sources. Furthermore, the rapid development of technologies, their increasing complexity and variety, and market dynamics have made the task of technology portfolio selection difficult. Considering high level of competitiveness, organizations need to strategically allocate their limited resources to the best subset of possible candidates. This paper presents the results of developing a mathematical model for energy technology portfolio selection at a R&D center maximizing support of the organization's strategy and values. The model balances the cost and benefit of the entire portfolio.

1 Introduction

Today, the problems of energy are considered as topic discussions around the world and a brief look at energy consumption shows that the progress of a country is directly related to it. Nowadays, most of the world's energy is provided by fossil sources, but some problems such as limitations on fossil sources forced companies to use their energy resources more effectively. Many researches focused on the best energy options by which the choice of the most energy optimized solution are possible in different areas [1–3]. To achieve this objective, they plan to manage energy technology.

H. Davoudpour · M. Ashrafi (✉)
Industrial Engineering and Management Systems Department,
Amirkabir University of Technology, No 424, Hafez Avenue, Tehran, Iran
e-mail: ashrafi.mm@aut.ac.ir, ashrafi.mm@gmail.com

I. Zelinka et al. (eds.), *Power, Control and Optimization*, Lecture Notes in Electrical Engineering 239, DOI: 10.1007/978-3-319-00206-4_7,

Industrial and academic interest to manage technology especially energy technology more effectively is growing as the complexity, cost and rate of technological innovation increase. Furthermore, firm equipment with the best technologies doesn't guarantee success anymore; but it has to be in support of the firm technology strategies.

A technology strategy is an organization's overall objectives, principles and tactics relating to the technologies that the organization uses. It explains how technology should be utilized as part of an organization's overall corporate strategy [4].

It is clear that for success in research and development (R&D), it is critical to decide about right technologies in the related context of organization. The normal process for doing this is through the development of a technology strategy and technology portfolio [5]. The resource limitation, increasing intensity of competition and fast technology changes make firms to move towards technology portfolio paradigm.

Developing technology strategy needs selecting a proper portfolio of technologies. The main concept of portfolio of technology is to allocate a limited set of resources to projects in a way that balances risk, reward, and is in alignment with corporate strategy [6].

Technology portfolio managers often select their portfolio using a mixture of different methods. Many early selection models were based on linear programming, scoring models and checklists [7, 8]. These models usually involved the conversion of the attributes of a technology/project into a single monetary value [5]. Reviewing technology/project portfolio selection models, we have identified three schools of thoughts on how to classify the approaches for project portfolio selection: (1) quantitative methods; (2) qualitative methods and (3) hybrid methods which is an integrated and synthesis of the first two schools of thought.

Iamratanakul et al. [9] argued that the first school of thought is mainly influenced by Baker, Freeland, and Pound providing quantitative approaches to project selection and resource allocation up to the early 1990s. Heidenberger and Stummer break quantitative technology portfolio selection methods in R&D centers into six categories [10]:

1. Benefit measurement methods: they arrange projects according to the benefit they provide within overall budget constraints.
2. Mathematical programming: the objective is to optimize the expected benefits to be realized from a portfolio of R&D projects, while recognizing limits to the available resources.
3. Decision and game theory: in these approaches uncertain future events or firm's reactions to environmental changes are taken into account.
4. Simulation models: they represent real world systems and usually are used when experiments cannot be applied in real world because of cost or time.
5. Heuristics: increasing complexity make it difficult to find best solutions. Heuristic modeling finds acceptable but not necessarily optimal answers.

6. Cognitive emulation: these methods use pervious experiences to help decision making processes.

The second classification of technology/project portfolio selection methodologies is influenced by Souder, Mandakovic, and Gupta tackling the problem by qualitative techniques, such as using bubble diagrams, scoring models for project ranking and selection [9].

Introducing an integrated and synthesis of these two schools of thought, many researchers apply hybrid methods of technology/project portfolio selection such a graphical methods, conjoint analysis, data envelopment analysis (DEA) and scenario planning.

Energy R&D centers usually deal with technology development projects so it is highly recommended to use project portfolio planning and management techniques to ensure an effective energy technology management. Project portfolio selection includes methods for analyzing and collectively managing a group of current or proposed projects based on numerous key characteristics such as total expected cost, consumption of scarce resources (human or otherwise) expected timeline and schedule of investment, expected nature, magnitude and timing of benefits to be realized, and relationship or inter-dependencies with other projects in the portfolio.

In recent years, some complicated models were developed to capture the actual situation of energy technology portfolio selection. Applications of this concept to energy investment can be seen in [11–14]. Yu [15] presented a model to assess risks in a multi-pool setting. A comprehensive review of the state-of-the-art in energy portfolio can be found in Kienzle et al. [16]. Oldenburger [17] developed a hybrid model to evaluate technology portfolio. The model is comprised of two phases: the first phase is dedicated to general filtering of technologies and the technology comparison is done in the next phase using 52 risk and return criteria via bubble diagrams. Chen et al. [18] utilized scenario analysis approach for renewable energy technology portfolio. They developed four scenarios based on results of future studies and expert views.

In this paper, benefit measurement models, mathematical programming and heuristic modeling are used to provide a framework to select the best possible set of projects related to energy technology development. The framework is designed in a way that maximizes the support of the organization's strategy considering related failure risk.

This paper presents a framework to quantify the support of organization's strategy while selecting a portfolio of energy technologies. The model selects if, and when, to start funding energy technology project over a scheduling period. The effectiveness of a project is influenced by whether or not it is in alignment with the overall strategy in the organization. The optimization model identifies the funding strategy that maximizes the support of the strategy, subject to budgetary and portfolio balance constraints such as expected timeline and schedule of investment, strategic requirements, magnitude of portfolio, and relationship or interdependencies with other projects in the portfolio.

The energy technology portfolio selection framework is proposed in Sect. 2. Furthermore, a list of technology portfolio evaluation criteria is introduced in this section. This list is used to develop a mathematical programming model for energy technology portfolio selection which maximizes the support of the organization's strategy in Sect. 3. In Sect. 4, a Tabu Search algorithm and its computational results of problem solving are presented. Finally, the conclusions derived from the analysis of energy technology portfolio selection are presented.

2 Technology Portfolio Evaluation Framework

Ideally, firms wish to accurately translate their needs into technology portfolio selection models.

Technology portfolio management is basically a decision process to find and modify the best resource allocation among various technology candidates of an organization. Technology portfolio selection should be considered as a process that includes several related steps, rather than just evaluating or scoring technologies, or solving an optimization problem [19].

In order to develop an integrated framework using the technology strategy and roadmap outputs, we utilized system theory approach. Based on system theory approach, we construct a systemic framework for technology portfolio planning and management in which each system component provides other components with required inputs through a multi stage process. This framework provides steps, from collection technology roadmap results and suggested technologies to individual technologies evaluation, ranking and developing a balanced technology portfolio. Figure 1 illustrates the proposed framework consisting of 4 stages.

Preparing org technology roadmap and identifying appropriate technology candidates, organizations should apply technology portfolio selection methods to

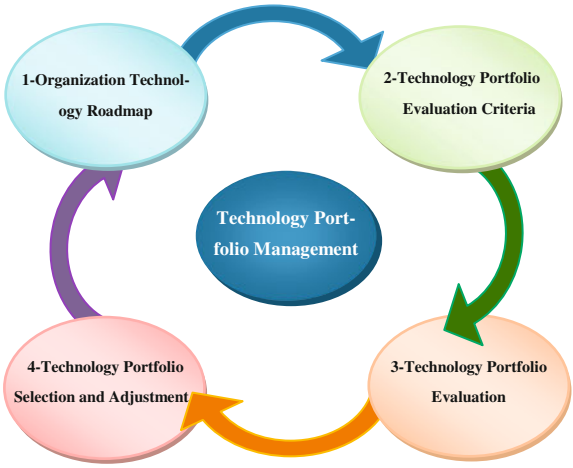

Fig. 1 A framework for technology portfolio selection

choose among their candidate pool. Technology portfolio selection involves multiple interrelated criteria, resources and uncertain and qualitative factors that are difficult to measure [20].

Since the objective of the project portfolio selection is to select a portfolio of technologies that brings the most value to the firm, the portfolio selection criteria are developed in two fundamental areas.

Technology portfolios allow for the definition of a clear dichotomy between two families of elements. There are things that are mainly under the firm's control, assets that depend on the firm's behavior and decisions; these factors are referred as "the company's technological competitiveness". And, there are things that do not depend on the firm's actions, that are beyond its control; these elements are referred as the "the attractiveness of the technology". Assessing the situation of a firm regarding these factors is also useful for strategy formulation because they offer guidance to the resource allocation process and by combining these two dimensions (the company's technological competitiveness and technological attractiveness), resource allocation strategies for technology programs could be derived [21].

Hence, the first step is to provide a list of important technology evaluation criteria (technological competitiveness and technological attractiveness) in technology or project selection process. This list of criteria should be prioritized according to the importance of each factor in portfolio selection process. The result of this step is used to develop a linear integer program which maximizes the estimated support of firm's strategy subject to portfolio balance and budget constraints.

2.1 List of Technology Evaluation Criteria

R&D project and technology portfolio selection involve multiple interrelated criteria, resources and uncertain and qualitative factors that are difficult to measure [20]. Miller and Lessard [22] believe that project failure usually appears due to decision makers' inability to identify management challenges rather than technical problems, and management challenges are seen as a result of lack of awareness about the nature, characteristics and related uncertainties of projects. So it is very critical to consider correct and comprehensive measures in technology portfolio selection. The measures used for this model are adapted from several sources. The primary list of evaluation criteria is drawn out of related literature. The initial list of the criteria extracted from related literature is presented in Table 1.

Then the primary list is revised and changed based on the organization's culture and special needs. Some criteria may be added to list and some of them may be considered as unimportant and be eliminated. Once the list is completed, the company should determine importance of each criterion regarding the strategy of the organization. The acceptable results can be achieved by the help of panel of experts in the related field. In this research, Analytical Hierarchy Process (AHP)

Table 1 List of important criteria in technology portfolio selection

Attractiveness	Competitiveness
Market volume opened by technology	Experience accumulated in the field
Span of applications opened by technology	Registered patents
Market sensitivity to technical factors	Value of laboratories and equipment
Future products or services which will be achieved by use of this technology	Fundamental research team competencies
Added value	Applied research team competencies
Key technology	Development team competencies
Number of stake-holders	Capability to keep up with fundamental scientific and technical knowledge
Competitors' level of involvement	Financing capacity
Competitive intensity	Quality of relationships between R&D and Production
Impact of technology on competitive issues	Quality of relationships between R&D and Marketing
Barriers to copy or imitation	Capacity to protect against imitation
Dominant design	
Technical factors	
Position of the technology in its own life-cycle	
Potential for progress Performance gap *vis-a-vis* alternative technologies	
Threat of substitution technologies	
Ability to transfer the technology from one unit to another	
Ability of integration with other systems in company	
Flexibility to technical changes	
Difficulty of implementation	
Supporting strategy of company	
Societal stakes	
Public support for development	
Green technology	

has been used to prioritize criteria and a group of experts were asked to compare pair wise of criteria based on their importance in energy technology selection process regarding the strategy of the organization. We used Expert Choice to process and analyze criteria ranking. Finally, ten most important criteria, according the computed weights, were selected to be used in the mathematical model of energy technology portfolio selection. Table 2 shows the energy technology evaluation final criteria and their relative weights final list based on AHP results with overall inconsistency rate of 0.02.

Table 2 Criteria prioritizing results

Criteria	Relative weight
Competitive situation in market	0.205
Added value	0.187
Potential of commercialization	0.129
Position of the energy technology in its own life-cycle	0.078
Threat of substitution technologies	0.078
Key of technology	0.057
Supporting national related strategies	0.052
Impact on environmental factors and energy consumption improvement	0.048
Ability to result in technical Know-How	0.032
Successful Experience accumulated in the field	0.030
Registered patents	0.030
Ability to use international cooperation potentials	0.022
Span of applications opened by technology	0.021
Value of laboratories	0.012
Alignment with organization objective and capability	0.011
Value of equipments	0.006

2.2 Constructing a Mathematical Model for Energy Technology Portfolio Selection

The next step is to provide an optimization model that integrates the portfolio management's existing tools into a linear, integer program. The model incorporates data from the experts and the estimated financial performance to directly calculate the total performance of any portfolio. The optimization model then maximizes the estimated support of firm's strategy which the portfolio provides, subject to technology portfolio balance and budget constraints.

The energy technology portfolio selection problem is to select a set of energy technology from a pool of candidate technologies to maximize the expected benefits during the planning horizon. Each candidate technology has specific lifecycle and its execution requires the exclusive use of a number of resources (e.g., budget, human resources, etc.). However, the availability of each resource type is usually limited. Unlike money, there is limited transferability for human resources from one technology to another technology, due to the specialization of skills. To effectively utilize limited resources, it is important to link technology portfolio selection decisions to the key corporate strategies and to maintain the balance of technology portfolio [15]. Below model constraints and objective function are presented.

Timing: x_{itj} is the decision variable, i is the technology index, t is the enumerated year in the planning horizon (from year 1 to year n) and j is the year in which the related project starts receiving fund. The project can only be started once. To model this constraint, another binary variable, y_i, is presented in which $y_i = 1$ when project i is slated to receive funding in calendar years and is subject to the constraint:

$$\sum_{t=1}^{n}\sum_{j=1}^{t} x_{ijj} = y_i \quad i = 1, 2, \ldots, p \tag{1}$$

$$y_i \leq 1 \quad i - 1, 2, \ldots, p \tag{2}$$

Portfolio size: There may be some restrictions according to limited human resources to number of technologies to be selected in calendar years. This number is usually estimated by experts and it is based on previous experiences.

$$\sum_{i=1}^{p} y_i \leq Q \tag{3}$$

Portfolio cost: a total yearly cost includes capital expenditures, the cost of implementation and sustaining costs. It is assumed that cost is dependent of the year in which a technology project is launched. The technology project costs for the entire portfolio are captured in a matrix where each element represents the incremental cost of project related to implementation phase of project, which is based on number of years spent since start of the technology project. This matrix is based on the predicted costs. The budget represents the maximum amount of money available to spend on the portfolio of energy technology project for each calendar year. The cost in any given year cannot exceed the budget available.

$$\sum_{i=1}^{p}\sum_{j=1}^{t} C_{(t-j+1)} x_{itj} \leq B_t \quad t = 1.2, \ldots, n \tag{4}$$

where $C_{(t-j+1)}$ is the predicted cost of technology project i from its start date through the current year.

Strategic requirements: This constraint sets the number of projects that must support each of the strategic objectives (M_m). N_{im} is a matrix that each element of it is equal to one if project i supports objective m.

$$\sum_{i=1}^{p} N_{im} y_i \geq M \tag{5}$$

Dependency: the last constraint is focused on the prerequisite rules and dependencies between projects. P is a matrix in which $P_{ij} = 1$ where project i is dependent to project j, and if project i is selected then project j should be selected too.

$$y_i \geq p_{ij} y_i \quad i, j = 1, 2, \ldots, p \tag{6}$$

Model Objective Function: The relative importance weights of criteria and sub-criteria were determined in previous section. In this section we use those sub-criteria and their relative weights to calculate the selected portfolio support of firm's strategy (sup) as model objective function:

$$Max \sum_{i=1}^{p} Sup_i \, y_i \tag{7}$$

$$Sup_i = \sum_{k=1}^{10} W_k S_{ik}, \quad i = 1, 2, \ldots, p \tag{8}$$

where W_k shows the weight of the *kth* sub-criterion and S_{ik} is the representative of the *ith* technology score in relation to the *kth* sub-criterion.

3 Problem Solving and Computational Results

The optimization model may be solved by any mathematical method and tools such as solver, lingo or heuristic methods regarding the size of the problem. As the size of the problem increases, the search-space of candidate solutions grows exponentially which makes an exhaustive search for the optimal solution inadequate regarding time and cost, but exact methods may be used when the size of the problem is small.

In this research Tabu Search is developed to solve the optimization model. Decision makers can easily and quickly use these programs and update them over time periods. This algorithm needs a primary solution. Starting from a good primary solution would improve the quality of the algorithm. In this case to obtain a primary (but not necessarily feasible) solution, if the strategy of company is competition-based, core technologies are selected and if it is resource-based, leftover technologies could be selected.

In order to verify Tabu Search algorithm, the test problems were classified into two main groups based on their size: (1) small size problems and (2) medium and large size problems. Lingo was used to solve small size problems. The results then compared to the results achieved by using Tabu Search algorithm. It seems that algorithm results in optimal solution in small size problems.

In medium and large size problems, the optimization model cannot be solved in polynomial time, so linear programming relaxation method was used to get information about the original problem. The linear programming relaxation of a 0-1 integer program is the problem that arises by replacing the constraint that each variable must be 0 or 1 by a weaker constraint, that each variable belong to the interval [0,1].

$$x_i \in \{0, 1\} \rightarrow 0 \leq x_i \leq 1 \tag{9}$$

The resulting relaxation is a linear program. In all cases, the solution quality of the linear program is at least as good as that of the integer program, because any integer program solution would also be a valid linear program solution. That is, in a maximization problem, the relaxed program has a value greater than or equal to that of the original program (upper bound) [23]. So the difference between the best

Table 3 Results of test problems

	Tabu Search		Lingo Solution	Upper bound	Tabu Search Percentage of error
	Best solution	Run time			
n = 4 p = 5	1.9201	0.003669	1.9201	–	0.0000
n = 4 p = 7	2.0859	0.005074	2.0859	–	0.0000
n = 4 p = 10	3.0043	0.007108	3.0043	–	0.0000
n = 4 p = 15	3.2650	0.008918	3.2650	–	0.0000
n = 4 p = 20	3.8769	3.3105	–	3.9502	1.855602
n = 5 p = 10	3.1283	0.008493	3.1283	–	0.0000
n = 5 p = 15	3.7612	5.7384	–	3.8069	1.200452
n = 5 p = 20	3.7935	11.0604	–	3.8964	2.640899
n = 5 p = 25	4.4202	11.5203	–	4.5366	2.565798
n = 5 p = 30	4.4831	17.1393	–	4.5708	1.918701
n = 5 p = 35	4.8604	19.2843	–	4.9184	1.179245
n = 5 p = 40	5.2880	22.5413	–	5.3719	1.561831
n = 5 p = 45	5.9933	30.1813	–	6.1058	1.84251
n = 5 p = 50	6.233	36.27433	–	6.93	10.06
n = 10 p = 10	3.8474	7.35199	–	4.0281	4.486
n = 10 p = 15	4.8176	41.63098	–	5.0216	4.06

solution achieved by algorithm and the upper bound can be calculated as the percentage of error for each problem. The instances have been carried out on a personal computer with CPU 2.66 GHz and 2 GB of RAM and the Tabu Search algorithm has been implemented and compiled using MATLAB (R2010b). The results of sixteen test problems are summarized in Table 3.

Analyzing the percentage of error shows that the quality of solution achieved by Tabu Search algorithm is usually acceptable. Figures 2 and 3 show the algorithm run times and the percentage of error respectively.

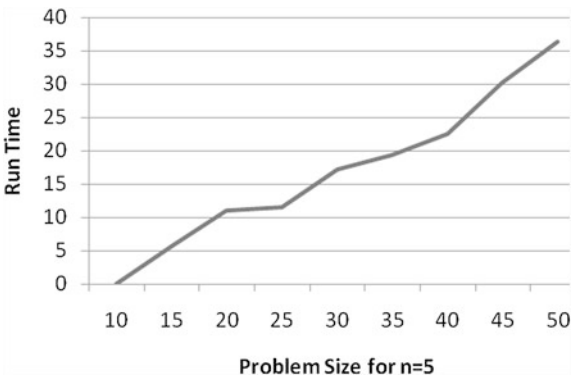

Fig. 2 Run time of Tabu Search algorithm

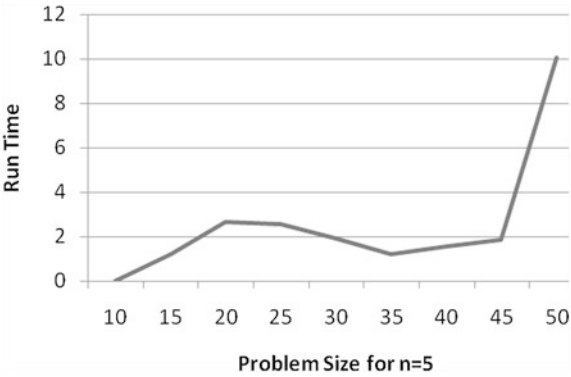

Fig. 3 Percentage of error of Tabu Search algorithm

4 Conclusions

The diffusion and effective usage of energy technologies has been hampered by lack of efficient management, maintenance and capacity to construct and purchase the right technology portfolio.

Managing technology portfolio is one of the critical firms' tools to deal with the increasing complexity of technologies and maintain in global markets. Technology portfolio selection is a rather complex task using various models to choose among the high number of candidate technologies considering various criteria and constraints.

This work proposes a quantitative method that enables a team to evaluate and optimize an energy technology portfolio where the projects are dependant and the cost of implementation is highly related to the phase of implementation.

The Optimization Model utilizes existing data and integrates the existing portfolio management tools. The model's format provides flexibility to evaluate performance of alternative solutions. The mathematical nature of the model requires the input data to be numerically quantifiable.

The model can quickly answer some questions about addition of new technologies or changes of amount of budget. The model also minimizes the time required to evaluate the portfolio or reevaluate it when technologies metrics were updated.

In order to solve the proposed model, a Tabu Search algorithm is applied to the constrained energy technology portfolio selection problem. We test the robustness of the algorithm with 16 different classes of problems with various time horizons. The proposed algorithm is especially suited for large scale instances, when exact approaches are doomed to fail.

Finally the model balances the portfolio in alignment with the overall objectives of the company. The model effectively provides a means to optimize and balance technologies over multiple periods in a technology portfolio.

References

1. Anayochukwu, A.V., Ndubueze, N.A.: Energy optimization at GSM base station sites located in rural areas. Int. J. Energy Optim. Eng. (IJEOE) **1**(3), 1–31 (2012)
2. Maleviti, E.: The development of a theoretical model for optimizing energy consumption in buildings. Int. J. Energy Optim. Eng. (IJEOE) **1**(4), 1–14 (2012)
3. Fahim, A.A., Khalil, E.E.: Energy efficient operation of university hostel buildings under indoor environmental quality requirements. Int. J. Energy Optim. Eng. (IJEOE) **1**(2), 96–109 (2012)
4. David, F.: Strategic Management. Merrill Publishing Company, Columbus (1989)
5. Doctor, R.N., Newton, D.P., Pearson, A.: Managing uncertainty in research and development. Technovation **21**, 79–90 (2001)
6. Dickinson, M.W., Thornton, A.C., Graves, S.: Technology portfolio management: optimizing interdependent projects over multiple periods. IEEE Trans. Eng. Manage. **48**(4), 518–527 (2001)
7. Tidd, J., Bessant, J., Pavitt, K.: Managing Innovation Integrating Technological, Market and Organizational Change, 3rd edn. Wiley, London (2009)
8. Coldrick, S., Longhurst, Ph, Ivey, P., Hannis, J.: An R&D options selection model for investment decisions. Technovation **25**, 185–193 (2005)
9. Iamratanakul, S., Patanakul, P., Milosevic, D.: Project portfolio selection: from past to present. In: Proceedings of the 2008 IEEE ICMIT, pp. 287–292 (2008)
10. Heidenberger, K., Stummer, C.: Research and development project selection and resource allocation: a review of quantitative modelling approaches. Int. J. Manage. Rev. **1**(2), 197–224 (1999)
11. Awerbuch, S., Berger, M.: Energy Security and Diversity in the EU: A Mean- Variance Portfolio Approach, International Energy Agency, Paris, Report no. EET/2003/03 (2003)
12. Awerbuch, S., Berger, M.: EU Energy Diversity and Security: Applying Portfolio Theory to Electricity Planning and Policy-making. International Energy Agency, Paris (2003)
13. Awerbuch, S., Jansen, J.C., Beurskens, L., Dre, T.: The Cost of Geothermal Energy in the Western US Region: A Portfolio-Based Approach, Sandia National Laboratories, SAND-2005-5173, (2005)
14. Awerbuch, S.: Portfolio-based electricity generation planning: policy implications for renewable and energy security. Mitig. Adapt. Strat. Glob. Change **11**(3), 693–710 (2006)
15. Yu, O.S.: Technology Portfolio Planning Management. Star Strategy Group Los Altas, California (2006)
16. Kienzle, F., Koeppel, G., Stricker, P., Anders, G.: Efficient electricity production portfolios taking into account physical boundaries. In: Proceedings of the 27th USAEE/IAEE North American Conference, Houston, pp. 16–19 (2007)
17. Oldenburger, N.: Technology Portfolio Management. Faculty of Technology Policy and Management, Delft (2004)
18. Chen, T.Y., Yu, O.S., Hsue, G.J., Hsu, F.M., Sung, W.M.: Renewable energy technology portfolio planning with scenario analysis: a case study for Taiwan. Energy Policy **37**, 2900–2906 (2009)
19. Ghasemzadeh, F., Archer, N.P.: Project portfolio selection through decision support. Decis. Support Syst. **29**, 73–88 (2000)
20. Huang, C.H.C.H., Chub, P.Y., Chiang, Y.H.: A fuzzy AHP application in government-sponsored R&D project selection. Omega **36**, 1038–1052 (2008)
21. Jolly, D.: The issue of weightings in technology portfolio management. Technovation **23**, 383–391 (2003)
22. Miller, R., Lessard, D.: The Strategic Management of Large Engineering Projects; Shaping Institutions, Risks and Governance. Massachusetts Institute of Technology Press, Cambridge (2000)
23. Aardal, K., Weismantel, R.: Polyhedral Combinatory: An Annotated Bibliography, Annotated Bibliographies in Combinatorial Optimization. Wiley, London (1997)

Investigation of Cost Reduction in Residential Electricity Bill using Electric Vehicle at Peak Times

Onur Elma and Ugur Savas Selamogullari

Abstract The use of electric vehicles (EVs) is becoming more common in the world. Since these vehicles are equipped with large battery capacity, they can be used as energy provider when they are parked and have enough charge level. This study investigates the possibility of Vehicle to Home (V2H) concept using EV as energy provider for a residential house in Istanbul, Turkey. High resolution residential electrical demand data is obtained to characterize the residential demand. Then, case studies are completed in MATLAB/Simulink to evaluate the cost reduction in residential electricity bill when the EV is used to supply the residential demand at peak times. It is assumed that the EV will be fully charged at off-peak hours when the energy cost is lower. Savings are calculated by finding the difference between residential electricity cost at peak times and EV charging cost at off-peak hours. Results will provide more realistic prediction of cost savings since residential demand dynamics are taken into account. In addition, the advantages of shifting peak demand to off-peak hours through the use of EV for existing grid infrastructure is discussed in terms of reduced losses and increased transmission capability.

Keywords: Vehicle to home (V2H) · Electric vehicle · Demand management · Cost analysis

1 Introduction

With the increased environmental concerns all around the globe, many countries have been offering incentives for EVs. Therefore, vehicle producers in many countries focus on this topic and have manufactured various prototypes of EVs [1].

O. Elma (✉) · U. S. Selamogullari
Electrical Engineering Department, Yıldız Technical University, Esenler, Istanbul, Turkey
e-mail: onurelma@yildiz.edu.tr

U. S. Selamogullari
e-mail: ugursavas@yahoo.com, selam@yildiz.edu.tr

I. Zelinka et al. (eds.), *Power, Control and Optimization*, Lecture Notes in Electrical Engineering 239, DOI: 10.1007/978-3-319-00206-4_8,

Since EVs are equipped with large energy backup capacity, they can be used to provide power to both grid and houses. These modes can be identified as Vehicle to Grid (V2G) and Vehicle to Home (V2H). The grid-connected electric vehicles can be used to meet the peak energy demand [2, 3]. It can be said that widespread use of EVs and the evolution of smart grid will lead to dramatic changes in existing electrical power systems in near future.

Overall, the residential electrical demand constitutes high percentage of total demand. This becomes important especially at peak hours when everybody is at home and using electricity. Thus, the effect of residential demand response (DR) on the peak loading has been investigated [4–7]. Several methods have been suggested in the literature for DR [8]. Most common method is shifting peak demand to off-peak hours by using smart control methods. Shifting load demand to off-peak hours offers benefit to both customer and to utility companies as well. In conventional grid structure, transmission and distribution losses contribute large percentage of total losses due to the distance between generation and customers. An optimization study for the cost of power loss and congestion of transmission services are given in [9].

If the residential demand can be reduced at peak hours or shifted to off-peak hours with proper control algorithms, then transmission losses can be minimized and optimal use of existing grid can be achieved. The EV will be an enabling technology to move towards such operation in the existing grid structure [10–13]. The feasibility of V2H technology is discussed in [10]. A simulation model is developed to investigate the peak demand reduction using the EV. Various case studies are completed and it is shown that the peak demand can be reduced with the use of EV battery. The use of plug-in hybrid electrical vehicles (PHEVs) together with renewable energy sources for energy and comfort management in large smart building is studied in [11]. Multi-agent control method with particle swarm optimization is used in control algorithm and it is shown that about 7 % savings can be achieved without affecting customer comfort. A general framework for analyzing Vehicle to Grid and Vehicle to Home applications of PHEVs is given in [12]. Daily load profiles for various house types and distribution transformer are obtained using probabilistic approach and national database on electricity consumption for various domestic electrical devices. Vehicle to building (V2B) operation of electrical vehicles are analyzed in [13]. It is stated that V2B mode of operation is much easier to implement within a 3–5 year time frame compared to Vehicle to Grid operation. Both demand side management under peak load and outage management under grid faults using EVs are analyzed. Case studies are used to demonstrate the feasibility of the demand side management and outage management strategies.

This study mainly focuses on the use of an EV to supply residential electrical demand at peak times and its effect on residential electricity bill for a house in Istanbul, Turkey. In order to obtain realistic saving estimates, high resolution residential demand characteristics are obtained through measurements, which is missing in the literature. Then, possible cost benefits of using EV for demand management in a residential house is investigated by considering daily energy tariffs in Turkey. A three level energy tariff is used in Turkey and the peak time

pricing is about 2.5 times higher than off-peak time pricing. Thus, it would be highly economical to use the EV to supply the load demand at peak hours. In the demand management algorithm, the EV is used as much as possible to provide peak residential demand. It is assumed that the EV will be fully charged at off-peak hours when the energy cost is lower. This will result in savings in residential electricity bill since the EV will be charged at off-peak hours. Savings can be found by finding the difference between residential electricity cost at peak times and EV charging cost at off-peak hours where the cost is lower. Since the available energy from the EV depends on the driving conditions during the day, case studies are completed by considering different EV battery state of charge conditions. In addition, the advantages of shifting peak demand to off-peak hours through the use of EV as backup on for existing grid infrastructure is discussed in terms of reduced losses and increased transmission capability.

This paper is organized as follows: in Sect. 2, the measurement result of the residential electrical demand is given. In Sect. 3, details of energy tariffs in Turkey are given. In Sect. 4, basic information on EVs is given. In Sect. 5, case studies on the topic are completed and results are summarized. In Sect. 6, conclusions are given.

2 Residential Load Demand

Numerous parameters affect the energy use in a residential house. Mainly, user's habits, such as attitudes and opinions, determine the residential demand characteristics. In Maleviti [14], a theoretical model is given to analyze user's attitudes and opinions and to improve energy performance of a hotel building.

In this study, electrical power consumption data at a 4-person residential house in Istanbul, Turkey are measured with a sampling rate of seconds. Selected 4-person family structure represents large percent of family structure in Turkey.

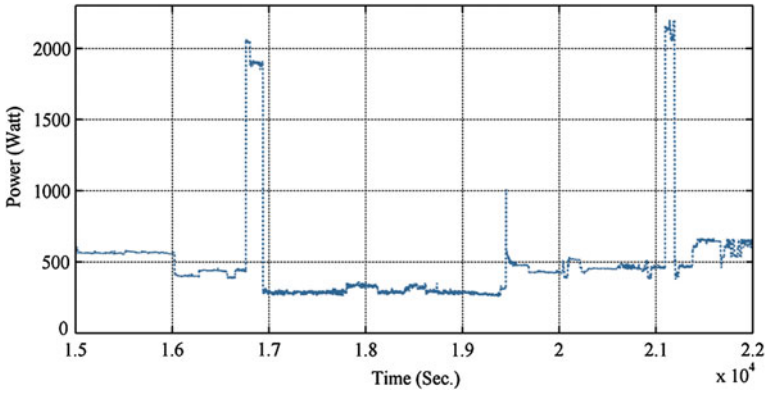

Fig. 1 A portion of measured residential load data

Table 1 Turkish electricity tariff for active power

	Day ($/kWh)	Peak ($/kWh)	Night ($/kWh)
Residential buildings	0.139	0.217	0.083
Commercial buildings	0.142	0.217	0.087
Industry	0.135	0.212	0.078

No demand management is applied during the data collection to obtain real electricity use of a typical Turkish family. The data is collected for a week [15]. During data collection, voltage and current measurements at the house main electrical panel are measured and stored with high resolution. A portion of the measured data is shown in Fig. 1 as an example. It is assumed that the residential demand has a periodic characteristic and weekly measurements can capture this periodicity.

3 Electricity Tariffs in Turkey

Since the cost of electricity depends on many parameters such as the type of source used, location, government policies, etc., each country has different tariffs for electricity. Mainly two tariffs are used for electricity pricing: fixed pricing and dynamic pricing. In fixed pricing, the electricity cost is fixed and does not depend on the time of use of electricity. In dynamic pricing, the electricity cost changes within a day based on the time of use of electricity [16].

In addition to fixed pricing, a 3-level tariff is employed in Turkey. In this tariff, a day is divided into three time frames (day-time, peak-time, and night-time) and each time frame priced differently:

- Hours between 06:00 and 17:00 are defined as day-time,
- Hours between 17:00 and 22:00 are defined as peak-time,
- Hours between 22:00 and 06:00 are defined as night-time.

Cost of electricity for each time frame, updated in April 2012, is given in Table 1 [17]. The values in Table 1 are raw prices which does not include costs such as tax, maintenance, transmission and distribution, meter reading, etc. When author's residential electricity bills are analyzed, it is found that final electricity cost per kWh is approximately 60 % more than the prices given in Table 1.

4 Electric Vehicles (EVs)

Although EVs were first developed in 1800s, they were not commercially available due to driving distance limitation and cost issues compared to internal-combustion engine powered vehicles. However, there has been growing interest in electrical vehicles in recent years due to mainly environmental concerns.

Table 2 A sample list of manufactured or planned to be manufactured EVs

Company	Model	Date of sale
Renault	Fluence ZE, Twizy, ZOE, Kongoo Express ZE	Fluence, Twizy, Kangoo: 2011 ZOE: 2012
Audi	E-tron, A1 E-tron	2012
BMW	MINI-E, Active-E, Megacity	2013
Chrysler-Fiat	Fiat 500	2012
Daimler	Smart ED For two	2012
Ford	Transit Connect Electric, Focus BEV	Transit Connect: 2011 FocusBEV: 2011
Honda	N/A	2012
Nissan	LEAF, NV200, Infiniti EV	LEAF: mass-production
Tesla	Roadster, Model S	Roadster: mass-production Model S: 2012
THINK	City EV	Mass-production
Toyota	Pirius PHEV	2012
Volkswagen	Golf Twin Drive	2013

EVs can broadly be divided into two groups: electric vehicles based on only battery power (BEV) and hybrid electrical vehicles (HEV) based on both internal combustion engine power and battery power. Recently, plug-in hybrid vehicles (PHEV) with the possibility of charging/discharging from an electrical outlet have been developed. A sample list of manufactured or planned to be manufactured EVs is given in Table 2 [18].

5 Case Studies

Since EVs are equipped with large battery capacity, they can be used as energy provider when they are parked and have enough charge level. This study investigates the possibility of V2H concept using EV as energy provider for a residential house in Istanbul, Turkey. V2H concept is also being studied by electrical vehicle manufacturers. Toyota City Low-carbon Verification project started in 2010 by Toyota and Leaf-to-Home project by Nissan are examples of such studies.[1,2]

First, high resolution residential electrical demand data is obtained to characterize the residential demand. Then, case studies are completed in MATLAB/Simulink to evaluate the cost reduction in residential electricity bill when the EV is used to supply the residential demand at peak times. The block diagram of the considered system is given in Fig. 2.

[1] http://www2.toyota.co.jp/en/news/11/06/0630.html

[2] http://www.nissan-global.com/EN/NEWS/2012/_STORY/121001-01-e.html

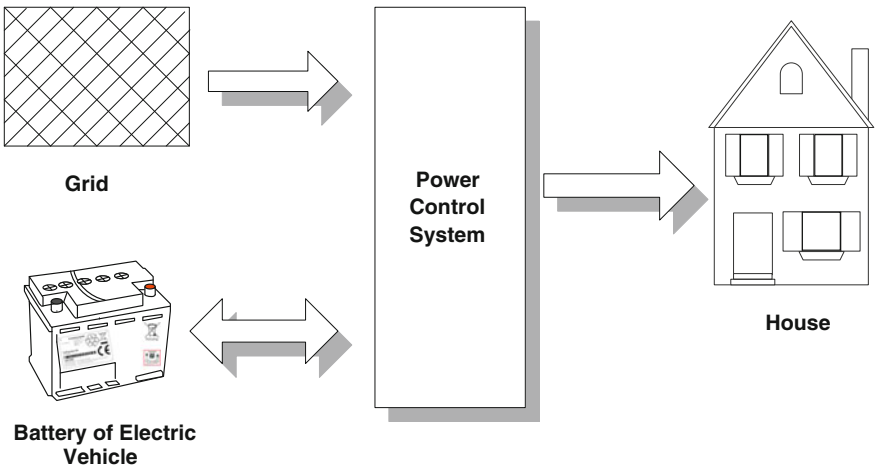

Fig. 2 Considered vehicle/grid hybrid power system

Renault Fluence ZE with battery capacity of 20 kWh is selected as the electrical vehicle for case studies since this vehicle is already on sale in Turkey. Renault Company owns the battery pack in its EVs and rent this battery pack to EV owner. This provides easy handling of recycling and battery maintenance.

A demand management algorithm is used to shift peak residential demand to off-peak hours by using the EV battery. It is assumed that the EV will be fully charged during off-peak hours when the energy cost is lower. The flowchart of the used algorithm is given in Fig. 3.

The algorithm uses the price of electricity and EV battery state of charge (SOC) as decision criteria. If the electricity price is high (between 17:00 and 22:00 h) and the EV is at home with enough battery capacity, then the demand is supplied by the EV until the predetermined minimum SOC level is reached. Here, minimum SOC level is chosen as 30 %. The EV is charged after peak hours with lower energy cost. If the required demand between at peak hours cannot be supplied with the EV at any instant, the demand is supplied through the grid. The proposed algorithm is implemented in MATLAB/Simulink as shown in Fig. 4.

Using the measured weekly residential demand data, minimum and maximum loaded days between 17:00 and 22:00 h within a week are found. The demand data for these two days are used as input to system simulations. Since the battery SOC level in the EV is depend on driving habits and the traffic during a day, available energy from the EV will vary. Thus, three different starting SOC levels (50, 75 and 100 %) are considered for the EV battery to consider daily driving effects on the battery SOC.

Simulation results are given in Fig. 5. As seen, when minimum loaded day is considered, the electrical vehicle can supply the demand at peak hours for each considered SOC level (Fig. 5a). When maximum loaded day is considered, the

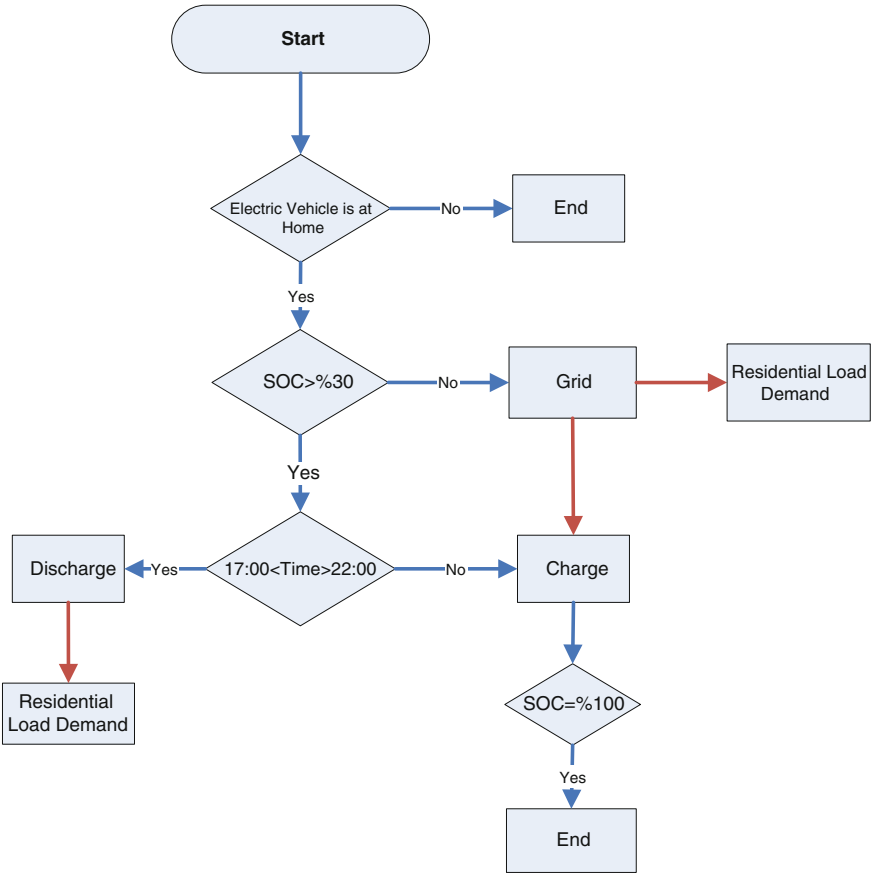

Fig. 3 Flowchart of EV use for demand management

demand between 17:00 and 22:00 h can be supplied by the EV for SOC levels of 75 and 100 %. However, when SOC level is 50 %, only a part of the demand can be supplied through the EV as SOC level goes below 30 % (Fig. 5b).

Economic savings can be found by finding the difference between residential electricity cost at peak times and EV charging cost at off-peak hours where the cost is lower. Savings for both minimum loaded day and maximum loaded day at peak times in a week are calculated. Then, using the calculated amounts as base values, monthly and yearly savings are calculated. Obtained results are summarized in Table 3. In these calculations, 60 % increased electricity price per kWh is used since in final billing the unit prices per kWh is about 60 % more than what is given in Table 1 due to addition of tax, maintenance, meter reading, transmission and distribution costs, etc.

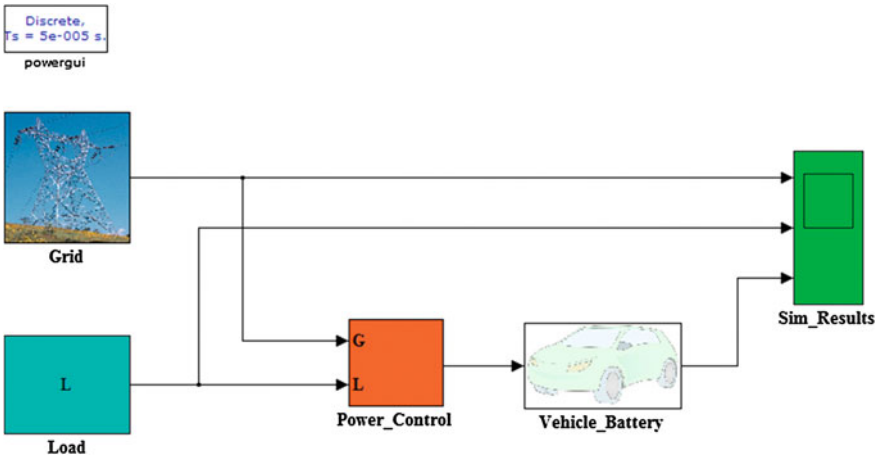

Fig. 4 System simulation block diagram

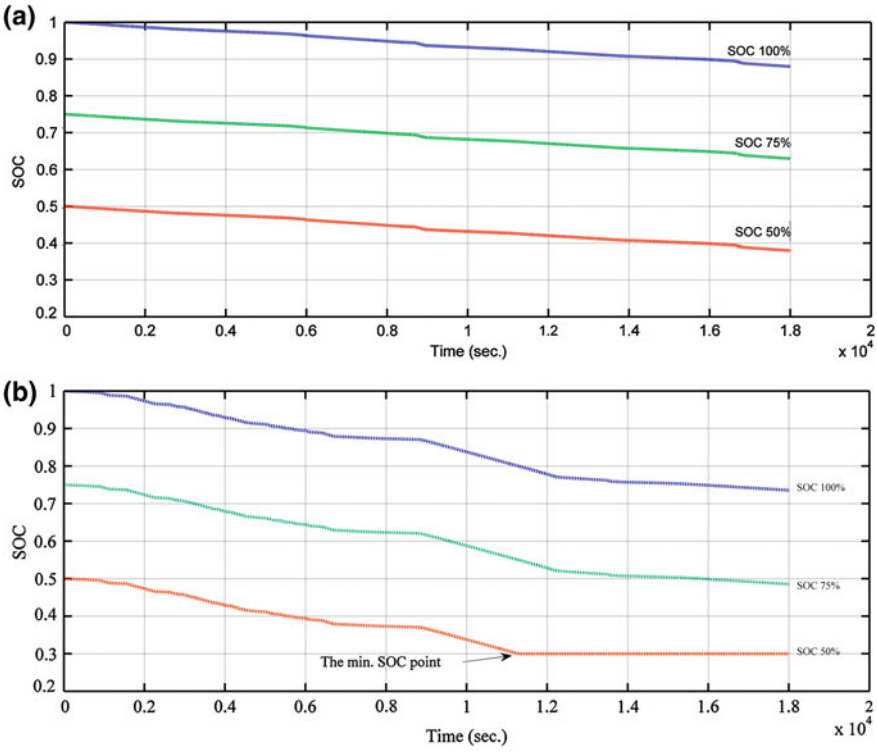

Fig. 5 Vehicle battery SOC values between 17:00 and 22:00 h for three different initial SOC levels. **a** Minimum loaded day between 17:00 and 22:00. **b** Maximum loaded day between 17:00 and 22:00

Table 3 Savings with the use of EVs at peak hours in a residential house

	Savings with the use of EV at peak hours ($) [minimum loaded day]		Savings with the use of EV at peak hours ($) [maximum loaded day]	
	Monthly	Yearly	Monthly	Yearly
Normal bill	25.1	305.1	55.33	673.3
Using EV at peak times	9.6	116.8	21.24	258.4
The price difference	15.5	188.3	34.1	414.9

6 Conclusions

In this study, the use of EV for demand management in a residential house is considered. Since EVs have large storage capacity, they can be used to supply residential demand at peak times when the vehicle is at home with enough battery capacity. The EV can be fully charged when the cost of electricity is lower.

Potential savings are assessed for a residential house by considering three different initial EV battery SOC levels, which emulate the driving conditions throughout the day. Based on minimum and maximum loaded days between 17:00 and 22:00 h within a week, it is found that between $15.5 and $34.1 can be saved in a month and $188.3 and $414.9 can be saved in a year.

In case studies, high resolution residential demand data is used. Since our focus in this study is to analyse the effect of the proposed demand management algorithm on residential electricity bill, analyses are completed based on required residential energy demand and available EV battery energy. This greatly simplifies analyses without going into details in component models such as battery model, control system model, etc. The results provides realistic upper limit on the savings with EV use for residential demand management. More detailed analyses will be completed in a future study.

The use of EVs in supplying residential peak demand provides benefits to utility as well. Although a single residential house is considered in this study, potential benefits to utility side will be more pronounced with increasing number of EVs. This is due to peak shaving offered by EV battery. The results can be summarized as less CO_2 emissions, reduced electricity unit cost, avoiding new installment of transmission and distribution lines, reduction in current ratings thus more efficient use of existing grid structure with lower losses, etc. However, careful planning of EV charging must be done in order to prevent another peak hour. Renewable energy integration together with charge/discharge scheduling of PHEVs will be subject of future research.

There are 2 million houses and 2.5 million cars in Istanbul, Turkey.[3] Using the measured data, the peak demand between 17:00 and 22:00 h can be approximated as 4.812 GWh for minimum loaded day and 10.596 GWh for maximum loaded

[3] http://www.ibb.gov.tr/sites/ks/trTR/0IstanbulTanitim/konum/Pages/Sayilarla_Istanbul.aspx

day in a week. If 10 % of houses have EVs and use the proposed demand management algorithm, between 0.4812 and 1.059 GWh energy demand can be shifted to off-peak hours. This means that utility does not have to use additional gas turbine to supply these peak demands. Thus, considerable savings on CO_2 emissions could be achieved with the use of EVs for demand management. The saved CO_2 amount can be used in carbon trading between countries.

References

1. Masoum, A.S., Deilami, S., Moses, P.S., Masoum, M.A.S., Abu-Siada, A.: Smart load management of plug-in electric vehicles in distribution and residential networks with charging stations for peak shaving and loss minimization considering voltage regulation. IET Gener. Transm. Distrib. **5**, 877–888 (2011)
2. Saber, A.Y., Venayagamoorthy, G.K.: Intelligent unit commitment with vehicle-to-grid a cost emission optimization. J. Power Source **195**, 898–911 (2010)
3. Berthold, F., Blunier, B., Bouquain, D., Williamson, S., Miraoui, A.: PHEV control strategy including vehicle to home (V2H) and home to vehicle (H2V) functionalities. In: IEEE Vehicle Power and Propulsion Conference (VPPC), pp. 1–6 (2011)
4. Ghosh, S., Sun, X.A., Xiaoxuan Z.: Consumer profiling for demand response programs in smart grids. In: Innovative Smart Grid Technologies—Asia (ISGT Asia) (2012)
5. Fuller, J.C., Schneider, K.P., Chassin, D.: Analysis of residential demand response and double-auction markets. In: IEEE Power and Energy Society General Meeting (2011)
6. Saele, H., Grande, O.S.: Demand response from household customers: experiences from a pilot study in Norway. Smart Grid IEEE Trans. **2**(1), 102–109 (2011)
7. Shao, S., Pipattanasomporn, M., Rahman, S.: Grid integration of electric vehicles and demand response with customer choice. Smart Grid IEEE Trans. **3**(1), 543–550 (2012)
8. Albadi, M.H., El-Saadany, E.F.: A summary of demand response in electricity markets. Electr. Power Syst. Res. **78**(11), 1989–1996 (2008)
9. Shooshtari, A.T., Joorabian, M., Milani, A.E.: Transmission service cost calculation with power loss and congestion consideration. Int. J. Energy Optim. Eng. **1**(1), 39–58 (2012)
10. Haines, G., McGordon, A., Jennings, P.: The simulation of vehicle-to-home systems—using electric vehicle battery storage to smooth domestic electricity demand. In: Ecologic Vehicle and Renewable Energies International Conference and Exhibition, Monaco (2009)
11. Wang, Z., Wang, L., Dounis, A.I., Yang, R.: Integration of plug-in hybrid electric vehicles into energy and comfort management for smart building. Energy Buildings **47**, 260–266 (2012)
12. Turker, H., Bacha, S., Chatroux, D., Hably, A.: Modelling of system components for vehicle-to-grid (V2G) and vehicle-to-home (V2H) applications with plug-in hybrid electric vehicles (PHEVs). In: IEEE PES Innovative Smart Grid Technologies (ISGT), pp. 1–8 (2012)
13. Pang, C., Dutta, P., Kezunovic, M.: BEVs/PHEVs as Dispersed Energy storage for V2B uses in the smart grid. Smart Grid IEEE Trans. **3**(1), 473–482 (2012)
14. Maleviti, E.: The development of a theoretical model for optimizing energy consumption in buildings. Int. J. Energy Optim. Eng. **1**(4), 1–14 (2012)
15. Elma, O., Selamoğulları, U.S.: A comparative sizing analysis of a renewable energy supplied stand-alone house considering both demand side and source side dynamics. Appl. Energy **96**, 400–408 (2012)
16. Moholkar, A., Klinkhachorn, P. and Feliachi, A.: Effects of dynamic pricing on residential electricity bill. In: Power Systems Conference and Exposition, vol. 2, pp. 1030–1035. IEEE PES (2004)

17. http://www.epdk.org.tr/web/elektrik-piyasasi-dairesi/ulusal-tarifeler. Last accessed on 01.05.2012
18. Ugur, E.: Application of energy management on a prototype electric vehicle. MSc Thesis, Yıldız Technical University, Department of Electrical Engineering, Istanbul (2011)

Wind Prediction in Malaysia

S. W. Lee, B. C. Kok, K. C. Goh and H. H. Goh

Abstract The wind speed prediction in Kudat, Malaysia had been done by using Mycielski-1 approach and K-mean clustering statistical method. There is some improvement in obtaining the random number of Mycielski-1. Besides, the comparison of K-means clustering with the optimal number of K is presented in this paper. The wind prediction is important to study a favorable site's wind potential. The prediction is based on 3 years history data provided by Meteorology Department of Malaysia and 1 year data as the reference to check the accuracy of both algorithms. The basic concept of Mycielski-1 algorithm is to predict the next value by looking to history data. Meanwhile, the K-means clustering can group the values with similar mean into the same group, and the prediction can be done by getting the probability of occurrence. The result shows the prediction of Mycielski-1 algorithm and K-means clustering are promising. The wind speed is predicted in order to obtain the mean power for energy planning.

Keywords Wind prediction · Mycielski-1 · K-means clustering · Wind power in Malaysia · Energy planning

1 Introduction

The growth of renewable energy around the world became significant since last decade. The existences of renewable energy enable mankind to harness and convert it to electricity to reduce the dependency on fuel. There are various kinds of energy resources. Wind energy is one of the renewable energies which has high

S. W. Lee · B. C. Kok · K. C. Goh · H. H. Goh (✉)
Department of Electrical Power Engineering, Faculty Electrical and Electronic Engineering, Universiti Tun Hussein Onn Malaysia, Parit Raja, 86400 Batu Pahat, Johor, Malaysia
e-mail: hhgoh@uthm.edu.my

I. Zelinka et al. (eds.), *Power, Control and Optimization*, Lecture Notes in Electrical Engineering 239, DOI: 10.1007/978-3-319-00206-4_9,

possibility to be harnessed in Malaysia. Malaysia is a country without four seasons. However, Malaysia encounters two monsoon seasons. Southwest Monsoon starts from late May to September, meanwhile Northeast Monsoon starts from November to March [1]. Due to the Northeast Monsoon, there will be a heavy downpour in the east coast area of Peninsular Malaysia and West Sarawak. During the raining season, the wind speed in certain states will be relatively high.

According to the Ministry of Energy, Green Technology and Water Malaysia, it is targeted to install 350 MW of renewable energy in Malaysia which is 300 MW in West Peninsular Malaysia and 50 MW from Sabah under Ninth Malaysia Plan. Unfortunately, wind speed in Malaysia is not consistence. For the very beginning stage on developing the wind power plant in Malaysia, wind prediction is necessary in order to have a well energy planning in a potential site. Estimation of the wind power generated can be obtained when the wind speed is predicted.

One of the cities in Sabah was chosen for this research purpose. Kudat has a population of 33,378 people with the geographical location at latitude of 6.9°N and longitude of 116.84°E. Kudat is located at 131 km from Kota Kinabalu, the capital of Sabah. By using the 3TIER software, the wind speed at the seaside faced to South China Sea in Kudat is relatively high if compared with other states [2]. Previously, there was a study about wind energy potential in Kudat and Labuan [3]. Weibull distribution function is used to determine the wind profile. Yearly wind power density of the particular places were obtained. Besides, the Perhentian Island in peninsular of Malaysia also can be used as the location to harness the solar and wind energy [4]. The hybrid power generation had been also studied by Onar et al. [5].

In addition, there are a lot of studies regardless to wind turbine and energy utilisation [6, 7]. For instance, load frequency control can be fully utilised to a grid connected wind farm. Apart from that, the wind power system reliability is very important in the context of harnessing wind power [8, 9]. The system reliability should be known before the alternative energy could be utilised due to the big amount of expenses on wind farm maintenance. Hence, wind map or wind capacity of a location is important so that the investment and efforts put on it is worthy [10, 11]. In terms of energy planning, the output prediction of wind power generated can be predicted so that the proper wind site can be decided [12, 13].

2 Background of Study

Wind prediction is important before any wind power plant project can be started. Potential benefit of a wind site can be retrieved by manufacturers even there was no local data for a particular site. Estimation of that particular site can be done by obtaining the data from the nearest wind measuring station. Beccali et al. [14] Serporta had used a neural network method, which called Generalized Mapping Regressor (GMR) to generate the wind velocity through the training to the neurons for Sicily. So, the wind speed behaviour must be obtained in order to utilise this approach. Authors used Matlab to generate coding for the estimation [14].

In terms of wind speed analysis, Bivona et al. [15] analyzed hourly wind speed in Sicily by using Weibull distribution function. They used the meteorology department's wind data to study on the characteristics of wind speed at nine locations in Sicily. In that particular research, the fitness of the Weibull distribution function to the wind speed was clearly be seen.

Apart of that, Louka et al. [16] introduced some modelling that applied in Greece. For instance, University of Athens used SKIRON modeling to forecast the wind speed for 5 days ahead. At the same time, Regional Atmospheric Modeling System (RAMS) was developed at Colorado State University and Mission Research Inc. ASTeR Division. RAMS can forecast the wind in 48 h later. In addition, adaptive fuzzy neural network (F-NN) also applied for the wind power prediction for 120 h ahead. However, these methods cannot handle the systematic errors which are caused by the local adaptation problems. The authors proposed Kalman filtering to improve the performance of aforementioned methods. It is one of the statistical optimal sequential estimation procedures for dynamic systems. Results show that the systematic errors can be eliminated by using Kalman filtering.

For this paper, the prediction of the wind speed is done by using Mycielski algorithm and K-mean clustering statistical method. Mycielski approach is a data compression method which has been widely used in communication engineering. This method fully utilises the history data as the reference for the prediction value. Mycielski method is actually the advance version of the Limpel Ziv (LZ). The research on hourly wind speed prediction in Turkey had been done by Hocaoglu et al. by using Mycielski approach [17]. It is a new approach in wind power prediction. Authors had analysed and predicted the wind speed in Kayseri, Izmir and Antalya. The result of prediction is promising and very close to the actual data. The comparison of data fitting for both actual and predicted data had been done by using Weibull distribution function. The comparison had proven the accuracy of the predicted result.

In 2011, same group of researchers had modified the algorithm in order to solve the looping problem by adding the random number into the predicted data [18]. The modified algorithm called Mycielski-1 and Mycielski-2. In Mycielski-1, the random number in between -0.4 and 0.4 is added into the predicted value. This random number can be changed according to the requirement of the research. Meanwhile, the history data were rounded to the nearest integer number and divided into a few cluster in Mycielski-2. The prediction is done by randomly select the history data from different cluster. In addition, authors also made the comparison between the modified Mycielski approach and Markov chain.

On the other hand, the K-mean clustering is a statistical method that arranges all data into few clusters. The number of cluster is determined by the user. However, there was a research shown that the optimal number of clusters is 4. This is due to the quantization error for 4 number of clusters is reduced dramatically if compare with 1–3 clusters [19]. J. Asamer and K. Din used K-mean clustering to predict the velocities on motorways. In the particular paper, the cluster is divided into

4 cluster centre. Besides, there are some researchers like Bishnu and Bhattacherjee [20] used the K-means clustering together with neural network algorithm to predict the software fault.

Once the prediction of the wind speed had been done, the suitable wind turbine for Malaysia can be chosen by referring to the international wind turbine specification. So, government can seek for the professional opinion from the wind turbine providers regarding the suitable wind turbine. According to the international wind turbine specification, there are IECI, II, and III which means high, medium and low wind respectively.

3 Methodology

According to the meteorological data obtained from the meteorology department Malaysia, the anemometer at Kudat was placed at latitude 6°55′N and longitude 116°50′E. It is also equivalent to latitude 6.916N and longitude 116.83E. By using FirstLook software provided by 3TIER, the actual place of the location of the anemometer can be found. The location of the anemometer in Kudat is shown in Table 1. The global wind rank calculated by FirstLook software is 66 %. 3TIER claims that 80 % of the wind project can be done if the wind rank is higher than 65 %. In addition, most of the wind projects can be found at the area which has the wind rank from 80 to 90 % (Fig. 1).

The location of anemometer is facing the Sulu Sea. However, the wind speed is higher at the coast face to South China Sea. The global wind rank at the coast facing South China Sea is 80 %. Hence, some amendments are needed to be done on the mean wind speed provided by the Meteorology Department Malaysia. Table 2 shows the higher global wind rank obtained by using Firstlook software (Fig. 2).

According to the wind profile power law, the wind speed listed in Table 1 can be further adjusted to height of 100 m. This is because the wind speed is higher at higher altitude. The adjustment is based on the formula:

$$\frac{u_x}{u_r} = \left(\frac{z_x}{z_r}\right)^{\alpha} \tag{1}$$

Table 1 The adjusted wind speed (ms^{-1}) to 80 % global wind rank over 4 years

Mth	Jan	Feb	Mar	Apr	May	Jun	Jul	Aug	Sep	Oct	Nov	Dec	Annual
Year													
2007	2.9	3.5	3.0	2.6	2.2	2.3	2.6	2.5	3.2	2.5	3.3	2.4	2.7
2008	2.9	3.0	2.4	2.3	2.9	2.2	2.5	2.1	2.9	2.2	2.1	2.3	2.5
2009	3.0	2.7	2.4	3.0	2.5	2.5	2.9	3.4	3.6	3.2	2.4	3.3	3.0
2010	3.5	3.9	3.4	2.9	2.5	2.3	2.2	2.7	2.3	2.7	2.2	2.3	2.7

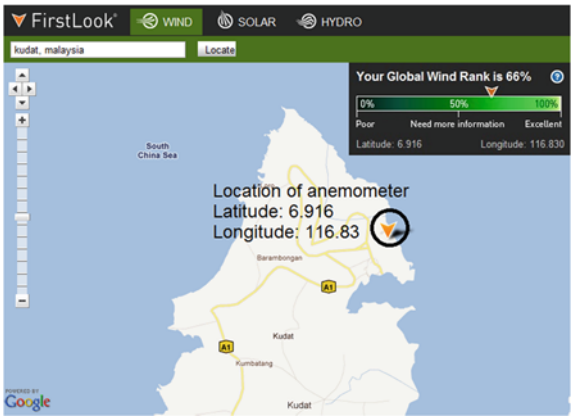

Fig. 1 The location of anemometer in Kudat

where u_x is the wind speed (ms^{-1}) at height of z_x (m). u_r denotes the reference wind speed (ms^{-1}) at reference height z_r (m). α denotes the constant of wind assessment during neutral stability which is approximately $\frac{1}{7}$ or 0.143.

3.1 Mycielski Algorithm

First of all, the recorded wind data has to be rounded into nearest wind states before proceeds to the Mycielski algorithm. This step is purposely making the searching process simpler. The rounding is based on the Eq. (2).

$$|x - y_i| \leq 0.2; x = y_i, i \geq 0 \tag{2}$$

where x denotes the wind speed; y denotes the value of wind state i is positive integer represents the iteration of wind state.

For the requirement of this research, there are 12 wind states in total. The wind state can be tabulated in Table 2.

After the rounding process had done, Mycielski algorithm can be preceded. Mycielski is an algorithm which performs the prediction on the time series data. By using the history data, the prediction is done based on the data. The prediction starts with searching the latest history data back to the earlier history data. The algorithm will keep searching the exact same history data until the pattern of searched data never appear in the history data set. Hence, the prediction is done by taking the data before the algorithm stop. For instance, let the data that need to be predicted $\hat{x}[n+1]$, where n represents the number of time series data sample.

In order to predict the data precisely, the difference of predicted $\hat{x}[n+1]$ and the actual value of $\hat{x}[n+1]$ should be minimum. The history data, f_n can be expressed as the function as shown in Eq. (3)

Table 2 The iteration of wind state

i	0	1	2	3	4	5	6	7	8	9	10	11	12
y_i (ms^{-1})	0	0.5	1.0	1.5	2.0	2.5	3.0	3.5	4.0	4.5	5.0	5.5	6.0

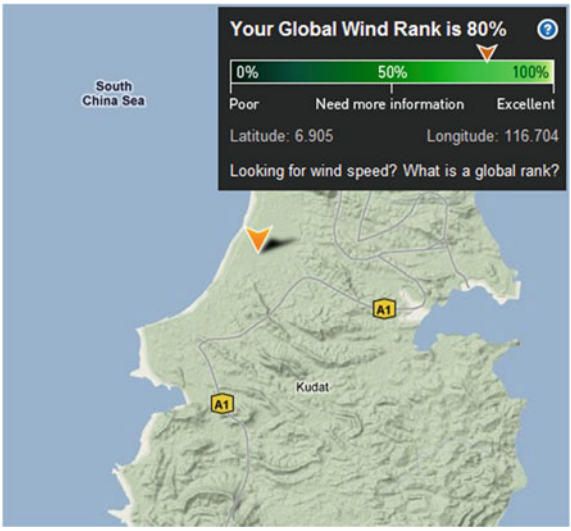

Fig. 2 The proposed location of wind turbine

$$f_n = (x[1], x[2], \ldots, x[n-1], x[n]) \tag{3}$$

The searching process of the algorithm is started from the latest data $x[n]$ back to $x[1]$. The main objective of this algorithm is to find the longest pattern of the history data which match the pattern of current data. Hence, the pattern searching is started from the shortest history data, in this case will be $x[n]$. If the value of $x[n]$ was happened in the history data, the algorithm will continue to search the pattern of ($x[n-1]$, $x[n]$). The algorithm will make a prediction when there is no same pattern can be found in the remaining history data sample. For example, the pattern of ($x[n-1]$, $x[n]$) was happened in ($x[5]$, $x[6]$) before, and there is no pattern of ($x[n-2]$, $x[n-1]$, $x[n]$) can be found in the history data. Hence, the algorithm will halt. The prediction will be done by taking the value of $x[7]$, since the pattern after ($x[5]$, $x[6]$) is $x[7]$. This can be explained by the main philosophy of this algorithm, which is how the pattern of the data in history is, and then the current data will be the same pattern. Referring to the previous works which had done by Fidan et al. [17, 18], they had created an equation to express the aforementioned prediction process. The particular equation is shown in Eq. (4):

$$\begin{aligned} m &= \arg\max_{L}\{x[k] = x[n], x[k-1] = x[n-1], \\ f_{n+1} &= \hat{x}[n+1] = x[m] \end{aligned} \tag{4}$$

Although it was not written in the papers published, it is believed that the symbol L in the equation represents the location of the longest pattern found in the history. Due to the prediction value will be the data after the longest pattern. Hence, the prediction value can be expressed as $\arg\max_L[n - L + 1]$. As mentioned earlier, the prediction value is $\hat{x}[n + 1]$, so the prediction value can be expressed as in Eq. (5).

$$\hat{x}[n + 1] = \arg\max_L[n - L + 1] \tag{5}$$

There was a cyclic fault happened in the earlier version of Mycielski approach. Hence, Mehmet Fidan, Fatih Onur Hocaoğlu and Ömer N. Gerek had modified the approach by adding the random number range from −0.4 to +0.4 to the predicted value and make it Mycielski-1 approach. However, the randomness of the number will cause the predicted result become unreliable. Due to this reason, authors had figured out another solution which is obtaining the average difference, d_{avg} from the history data in this paper. The principle of obtaining the d_{avg} is same as the principle of Mycielski, which is the transitional behaviour of wind speed. Basically, the d_{avg} can be obtained by taking the difference between the months and find the average for past few years depends on the available data. The result shown this kind of random number finding is more reliable than the original Mycielski-1 approach. The details of findings will show in next section.

Then, the random number will be added into the predicted value. Once the prediction had done, the predicted value will be updated in the history data. Then the next prediction $\hat{x}[n + 2]$ can be done based on the updated history data.

3.2 K-Means Clustering

K-means clustering is one of the data mining methods by grouping all the data with the similar mean into a cluster. There may be a lot of clusters in a certain analysis. However, the optimal cluster number with the least error is 4 [19]. For this research, the optimal cluster been found from the hierarchical analysis by using Ward's method is 2. Due to the comparison purpose, 4 clusters analysis will be presented in this paper also.

In order to compare the efficiency of Mycielski and K-means clustering, the same data is used for the wind speed prediction computation. The wind speed data ranges from 2007 to 2009 are used for algorithm training. Meanwhile, the wind speed in 2010 will be used as the tester.

First of all, the optimal clusters solution must be identified before the computation started. The number of cluster might affect the accuracy at the end of the prediction. Once the number of cluster had been determined, the initial center of cluster of the data should be obtained. For this paper, the initial centers of clusters were chosen based on the largest and the lowest values. The classification of the

initial center of cluster might be varied for different research. The most of important part of the K-means clustering is the distance between the data and the center of cluster. The algorithm will stop when the shortest distance between the data and the center of cluster is achieved. The distance is calculated by using Euclidean distance. The Euclidean distance is formulated as in Eq. (6).

$$D_n = \sqrt{(x_n - x_i)^2 + (y_n - y_i)^2} \tag{6}$$

where D_n represents the distance between nth data and the center of cluster;

x_i and y_i denote the coordinate of the ith center of cluster;
x_n and y_n denote the coordinate of the nth center of cluster.

The process of finding the shortest distance will stop when the distances of all data for two consequences are met.

The wind speed prediction is done by obtained the probability of the occurrence of wind speed in that particular time. The wind speed data is first to be clustered by using K-means clustering. Then, the trend of the wind speed is studied. Last but not least, the probability of the wind speed either go upper cluster or lower cluster or maintain in the same cluster is obtained. In order to have a better prediction result, the K-means clustering of the wind speed for each month in different years is obtained. Finally, the prediction is done by using the probability tree method.

4 Results and Analysis

Table 3 shows the wind speed obtained from meteorology department Malaysia after apply wind profile power law and rounded up process. The wind data in year 2010 is purposely shown for reference. After round up process, the Mycielski approach is applied in order to obtain the prediction for year 2010. The random number for each month is shown in Table 4.

Mycielski approach is applied in order to make the prediction for the wind speed in year 2010. The random number as shown in Table 5 is added into the predicted wind speed.

The graph of obtained wind speed and predicted wind speed can be illustrated in Fig. 3. As shown in the graph, the shape of the graph is look alike for obtained

Table 3 The round up wind speed in Kudat

Mth	Jan	Feb	Mar	Apr	May	Jun	Jul	Aug	Sep	Oct	Nov	Dec
Year												
2007	3.5	4.5	3.5	3.5	2.5	3.0	3.5	3.0	4.0	3.0	4.0	3.0
2008	3.5	3.5	3.0	3.0	3.5	2.5	3.0	3.5	2.5	2.5	2.5	3.0
2009	3.5	3.5	3.0	3.5	3.0	3.0	3.5	4.5	4.5	4.0	3.0	4.0
2010	4.5	5.0	4.5	3.5	3.0	3.0	2.5	3.5	3.0	3.5	2.5	3.0

Table 4 The average difference (d_{avg}) for each month from 2007 to 2009

Mth	Jan	Feb	Mar	Apr	May	Jun	Jul	Aug	Sep	Oct	Nov	Dec
d_{avg}	0.3	0.3	−0.7	0.2	−0.3	−0.2	0.5	0	0.7	−0.8	0	0.2

Table 5 The rounded up prediction wind speed in 2010 after add in d_{avg}

Mth	Jan	Feb	Mar	Apr	May	Jun	Jul	Aug	Sep	Oct	Nov	Dec
Prediction (ms^{-1})	3.5	5.0	4.5	4.0	2.5	3.0	4.0	3.5	5.5	4.5	4.0	2.5

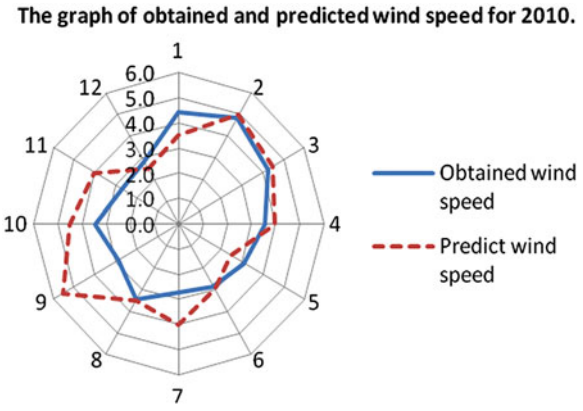

Fig. 3 The graph of *obtained* and *predicted wind speed* for 2010 using Mycielski-1

and predicted wind speed. However, there is much difference in September. This will be considered as the prediction error.

For K-means clustering, the wind speed data for 2007–2009 were sorting in ascending order. As in Fig. 4, the minimum wind speed is 2.1 ms^{-1} in August 2008 whereas the highest wind speed is 3.6 ms^{-1} in September 2009.

By using the wind speed data in Table 1, the center of clusters for 2 clusters and 4 clusters methods are shown in Tables 6 and 7 respectively. Meanwhile, the wind prediction by using K-means clustering is shown in Table 8. Result as shown in Table 8 can be illustrated in Fig. 5 (Table 8).

5 Discussion

The Mycielski algorithm delivers a good prediction for the mean wind speed in Kudat, Malaysia. By using Mycielski-1 approach, the wind speed for year 2010 is predicted. From the result in Fig. 6, the lowest accuracy is about 55 %. In terms of the monthly comparison, the prediction results for February, March, June, and August are perfectly matched with the obtained data. The smallest percentage of difference is in April whereas the largest difference is in September. However, by looking into the history data for September in 2007, 2008 and 2009 respectively,

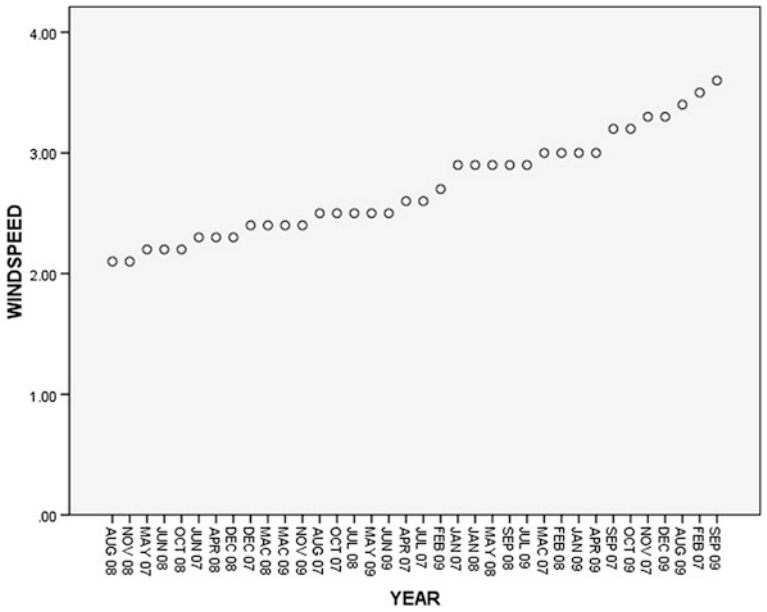

Fig. 4 The wind speed from 2007 to 2009 in ascending order

Table 6 The K-means clustering using 2 clusters

Cluster	1	2
Center of cluster (ms^{-1})	2.39	3.12

Table 7 The K-means clustering using 4 clusters

Cluster	1	2	3	4
Center of cluster (ms^{-1})	2.21	2.5	2.99	3.42

Fig. 5 The comparison between *actual* and *predicted wind speed*

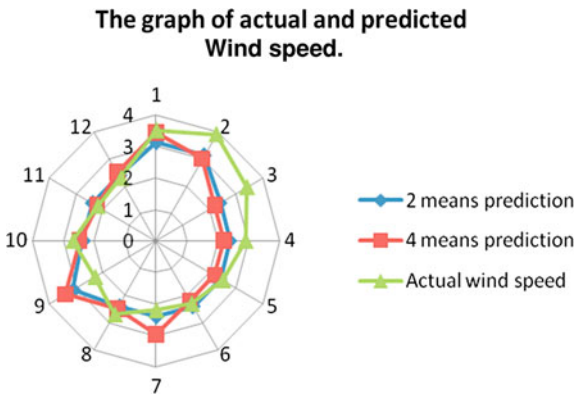

Table 8 The predicted wind speed by using K-means clustering

Mth (ms^{-1})	Jan	Feb	Mar	Apr	May	Jun	Jul	Aug	Sep	Oct	Nov	Dec
2 Clusters	3.12	3.12	2.39	2.39	2.39	2.39	2.39	2.39	3.12	2.39	2.39	2.39
4 Clusters	3.42	2.99	2.21	2.21	2.21	2.21	2.99	2.5	3.42	2.5	2.21	2.5

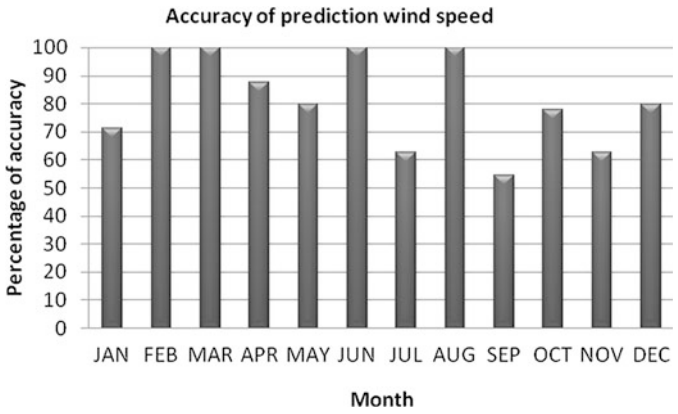

Fig. 6 The graph of accuracy for wind prediction using Mycielski-1 in 2010

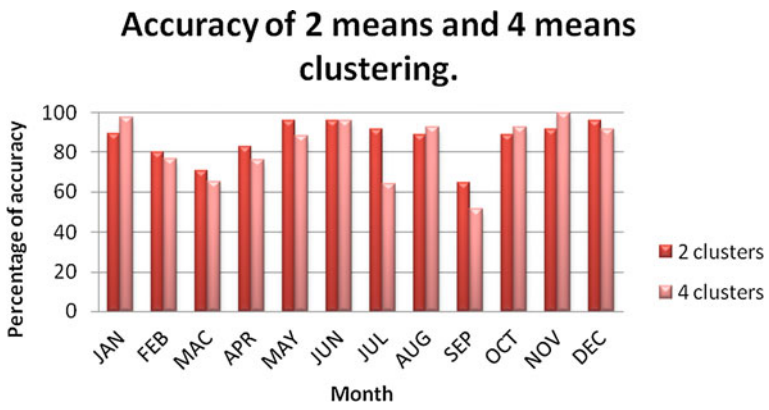

Fig. 7 The accuracy of wind prediction using 2 and 4 clusters

the wind speed is relatively high in this month. Mycielski approach assumes that 2010 is having higher wind speed in September. Same goes to July and November. The large difference of the obtained and predicted wind speed is considered as the computing error. However, the overall result shows that Mycielski-1 approach is successful to predict the wind speed in 2010. This prediction algorithm is suitable for hourly, monthly, and yearly wind speed prediction. For the future work, it is recommended to consider the capacity factor of the wind site as well.

On the other hand, in terms of accuracy of the prediction, the comparison of 2-means clustering and 4-means clustering is done as shown in Fig. 7.

From Fig. 7, the accuracy of each month is more than 70 % except in September 2010. The same reason applied in this error. By looking into the comparison of accuracy between 2-means and 4-means clustering, the 2-means clustering has higher overall accuracy if compared with the latter. In 2-means clustering, the average accuracy for 2010 wind speed prediction is 86.14 % whereas 4-means clustering is 3.51 % less than that, which is 82.63 %. Although the different of accuracy is not significant, the efficiency of determining the number of means is determined.

6 Conclusion

In conclusion, the Mycielski algorithm has average accuracy of 81.35 %. It means that this algorithm can predict well on the wind speed of Kudat. The wind speed for year 2010 is predicted and there are 9 out of 12 months have accuracy more than 70 %. On the other hand, for the 2-means clustering and 4-means clustering, the average accuracy is 86.14 % and 82.63 % respectively. In terms of prediction value, the 2-means clustering has 92 % of predicted wind speed is more than 70 %. Meanwhile, 4-means clustering has same amount of month that predicted the wind speed which accuracy achieved more than 70 %. Hence, the result shown that the prediction methods presented in this paper are reliable especially K-means clustering with the number of cluster obtained by using Ward's cluster analysis. In order to get more reliable result, it is better to have a huge history data as the database. The algorithm can be more precise due to the search process has more data to be compared. In the Mycielski-1 algorithm, the random number is added to the prediction value purposely to eliminate the recurrence error in predicting the wind speed. The proposed algorithm in finding the random number gives promising result. In order to analyze using K-means clustering, the computation tools are necessary in order to calculate a large number of Euclidean distances. Last but not least, the wind speed in Kudat shows that Malaysia can develop the wind energy as the mean wind speed is beyond the cut in speed of most of the wind turbines. However, the selection of the wind turbine is actually the key of success of this planning. In a nutshell, the utilization of wind speed prediction can lead to a good development in green energy Malaysia.

Acknowledgments Authors would like to thank the Ministry of Higher Education Malaysia (MOHE) for giving the scholarship to the author in order to accomplish this research. Furthermore, the authors would like to thank Ministry of Energy, Green Technology and Water Malaysia (KeTTHA), Ministry of Higher Education, Malaysia (MOHE) and The Office for Research, Innovation, Commercialization, Consultancy Management (*ORICC*), UTHM for financially supporting this research under the Fundamental Research Grant Scheme (FRGS) grant No.0905 in funding this research.

References

1. MOSTI: Monsoon. [cited 2011 28 December]; Available from: http://www.met.gov.my/index.php?option=com_content&task=view&id=69&Itemid=160&lang=english
2. FirstLook: Renewable energy risk analysis: Wind, solar, hydro data, 3TIER (2011)
3. Islam, M.R., Saidur, R., Rahim, N.A.: Assessment of wind energy potentiality at Kudat and Labuan, Malaysia using Weibull distribution function. Energy **36**(2), 985–992 (2011)
4. Zuhairuse, M.D.: The development of hybrid renewable energy system (wind and solar) for sustainable living at Perhentian Island Malaysia. Eur. J. Soc. Sci. **9**(4), 557–563 (2009)
5. Onar, O.C., Uzunoglu, M., Alam, M.S.: Dynamic modeling, design and simulation of a wind/fuel cell/ultra-capacitor-based hybrid power generation system. J. Power Sources **161**(1), 707–722 (2006)
6. Badmasti, B., Bevrani, H., Naghshbandy, A.H.: Impacts of high wind power penetration on the frequency response considering wind power reserve. Int. J. Energy Optimization Eng. (IJEOE) **1**(3), 32–47 (2012). doi:10.4018/ijeoe.2012070102
7. Fahim, A.A., Khalil, E.E.: Energy efficient operation of university hostel buildings under indoor environmental quality requirements. Int. J. Energy Optimization Eng. (IJEOE) **1**(2), 96–109 (2012). doi:10.4018/ijeoe.2012040106
8. Hahn, B., Durstewitz, M., and Rohrig, K., Wind Energy (Reliability of Wind Turbines Experiences of 15 Years with 1,500 W), ed J Peinke et al, Springer, Berlin, pp. 329–332, 2007
9. Karki, R.: Renewable energy credit driven wind power growth for system reliability. Electr. Power Syst. Res. **77**(7), 797–803 (2007)
10. Jewer, P., Iqbal, M.T., Khan, M.J.: Wind energy resource map of labrador. Renewable Energy **30**(7), 989–1004 (2005)
11. Khan, M.J., Iqbal, M.T., Mahboob, S.: A wind map of Bangladesh. Renewable Energy **29**(5), 643–660 (2004)
12. Focken, U., et al.: Short-term prediction of the aggregated power output of wind farms—a statistical analysis of the reduction of the prediction error by spatial smoothing effects. J. Wind Eng. Ind. Aerodyn. **90**(3), 231–246 (2002)
13. Landberg, L.: Short-term prediction of the power production from wind farms. J. Wind Eng. Ind. Aerodyn. **80**(1–2), 207–220 (1999)
14. Beccali, M., et al.: Estimation of wind velocity over a complex terrain using the generalized mapping regressor. Appl. Energy **87**(3), 884–893 (2010)
15. Bivona, S., Burlon, R., Leone, C.: Hourly wind speed analysis in Sicily. Renewable Energy **28**(9), 1371–1385 (2003)
16. Louka, P., et al.: Improvements in wind speed forecasts for wind power prediction purposes using Kalman filtering. J. Wind Eng. Ind. Aerodyn. **96**(12), 2348–2362 (2008)
17. Hocaoglu, F.O., Fidan, M., Gerek, O.N.: Mycielski approach for wind speed prediction. Energy Convers. Manage. **50**(6), 1436–1443 (2009)
18. Fidan, M., Hocaoğlu, F.O., Gerek, Ö.N.: Improved synthetic wind speed generation using modified Mycielski approach. Int. J. Energy Res. **36**(13), 1226–1237 (2012)
19. Asamer, J., Din, K.: Prediction of velocities on motorways by k-means clustering. In: 7th Mexican International Conference on Artificial Intelligence MICAI'08 (2008)
20. Bishnu, P.S., Bhattacherjee, V.: Software fault prediction using quad tree-based k-means clustering algorithm. IEEE Trans. Knowl. Data Eng. **24**(6), 1146–1150 (2012)

Genetic Algorithm Based Multi Objective Optimization of Building Design

Faranak Ebrahimnejad Farahani and Armin Ebrahimi Milani

Abstract Cost of materials using to build any structure such as residential, commercial or even industrial buildings is one of the most major concerns of architectures and civil engineers which it mainly affects their design in recent years. Beside this important fact on optimal designing, one can consider more optimizations for his/her design in reducing the cost of energy. In this chapter a new procedure is proposed to optimize the buildings' design considering a balance between different spends including materials and annual energy consumption to reduce the overall cost of construction and proper permanent service providing respectively, with an acceptable saving. Genetic Algorithm (GA) is used to overcome this multi objective optimization problem which it is considered to be one of the proper solutions due to existing limitations and its advantages. Proposed GA is fully discussed and the effectiveness of the procedure is examined through different numerical results and experimentations.

Keywords Building design · Multi-objective optimization · Construction material cost · Air conditioning cost · Lighting cost · Genetic algorithm

1 Introduction

The building design involves the use of various types of systems, which can vary depending on the specific design objectives, the project location, the knowledge of the designer, etc., all of which lead to many different design configurations.

F. E. Farahani
Abnieh Betonie Co., Tehran, Iran
e-mail: chestnut7fa@yahoo.com

A. E. Milani (✉)
Young Researchers Club, Science and Research Branch,
Islamic Azad University, Tehran, Iran
e-mail: a.milani@srbiau.ac.ir

I. Zelinka et al. (eds.), *Power, Control and Optimization*, Lecture Notes in Electrical Engineering 239, DOI: 10.1007/978-3-319-00206-4_10,

This can be observed by examining low energy building demonstration projects from around the world [1].

These projects depended on trial and error optimization using dynamic energy simulation tools, coupled with the knowledge of the designers. Simulations are normally used in a scenario by scenario basis, with the designer generating one design and subsequently having a computer evaluate it. This can be a slow and tedious process and typically only a few scenarios are evaluated from a large range of possible choices. Although a reduction in the energy use of residential buildings can be achieved by relatively simple individual measures, very high levels of performance require the coherent application of measures, which together optimize the performance of the complete building system [2].

The use of design guidelines is one way that designers try to optimize building performance. There are various books and papers that give specific guidelines on how to design energy efficient houses.

The difficulty of using design guidelines is that they are generally dependent on the climate where they were developed and the specific technologies that were used in their development. Another drawback of using guidelines is that they are generally developed assuming ideal conditions. There may be situations where a solar house is built on a property that is not directly facing south or that is partially shaded, where existing design guidelines would perform poorly [3].

Early most related studies refers to Gero and Radford [4] which they suggested the use of dynamic programming to select window size and glazing materials in order to minimize energy consumption in 1978.

Wilcox [5], O'Neill et al. [6], Sander et al. [7] and Sullivan et al. [8] in 1993 used regression analysis on data created by parametric Department of Energy (Developed by the DOE) building simulation software several runs to optimize design parameters of buildings in 1993.

Simplified procedures such as LT method [9], a way of estimating the combined energy usage of lighting, heating, cooling and ventilation systems to enable the designer to make comparisons between options, use energy graphs to explore the impact of a few key building design parameters but are unable to handle the high level of detail and complexity.

GAs have been used in building applications related to energy consumption, mostly to optimize the sizing and control of Heating, Ventilation and Air Conditioning (HVAC) systems [10–12].

However, Caldas and Norford [13, 14] described the development and testing of a new generative design system during the years 1999 and 2000. Their Generative System consists of a method for creating new designs, a procedure to evaluate them, and a mechanism to evolve solutions towards an improved performance in terms of the selected criteria. It uses a Genetic Algorithm as a search engine and also the DOE-2.1E software to assess the use of natural lighting, thermal performance and yearly energy consumption.

Furthermore, in 2001, they investigated the possibility of encoding architectural design intentions into a generative design system [15], while in 2003, their studies

using Genetic Algorithm not only showed successful results in designing and controlling of HVAC Systems but also in optimization of building envelopes [16].

Recent works relates to different optimization methods, followed by authors in order to optimize energy consumptions in building designs; the interactions between cooling and lighting energy use in perimeter spaces were evaluated as a function of window-to-wall ratio and shading parameters is studied in [17]. In [18] Genetic Algorithm is used to select optimal values of a comprehensive list of parameters associated with the envelope to minimize energy use for residential buildings. Proposed framework in [19] starts with a building design and optimizes it, providing to the architect many variations that minimize both energy consumption and construction cost.

Although in most of these works all objectives proposed in this chapter are not considered simultaneously or some of main conditions and limitations are not fully studied but their procedures are noticeable.

In this chapter, a new procedure is proposed in order to optimize not only the cost of building construction relates to different materials but to reduce the energy cost of the building including the energy consumption for air conditioning and lighting. Some related methodologies are applied to different parameters computation. Moreover, Genetic Algorithm is used in order to solve this multi-objective optimization which it demonstrated to be well suitable due to the non-linear nature of the proposed problem. In this chapter, all existing limitations and constraints are applied to this algorithm while the effectiveness of proposed method is illustrated in two different scenarios.

2 Mathematical Modeling and Problem Formulation

In order to calculate the heat energy transferring through each surface of the building including roof, walls and windows well know Newton's Cooling Law is used.

Newton's Law is mathematically stated by the simple first-order differential equation as follow:

$$\frac{dQ}{dt} = H.A(T_{env} - T(t)) = -H.A.\Delta T \tag{1}$$

where,

Q	Thermal energy in joules
H	Heat transfer coefficient
A	Surface area of the heat being transferred
T	Temperature of the object's surface and interior (since these are the same in this approximation)
T_{env}	Temperature of the environment

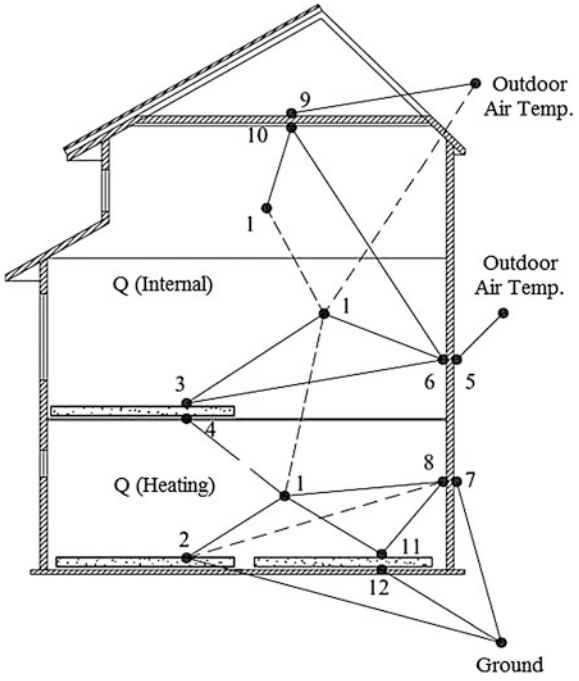

Fig. 1 A thermal network scheme for a sample building, Gaussian procedure (*Source* [20])

Moreover, $\Delta T - T(t) - T$ is the thermal gradient between environment and the object.

To make it more accurate in calculating interior temperature of the building, one can follow Gaussian procedure. Figure 1 represents a thermal network scheme for a sample building. Thermal reflection lines in Fig. 1 clearly illustrate how Gaussian Law can be used to consider the heat reflecting inside the building.

This method can also be expanded by considering some specific interior design objects such as brick walls and fireplaces or even sample furniture such as sofas for residual or desks for commercial purposes which is formal in recent building designs.

For second part of proposed optimization problem it is necessary to calculate the amount of lighting requires for each design solution, So that, the optimal solution should either provide enough lighting for the building and consumes less energy.

The amount of luminaries required to light a space to a desired average illumination level (foot candles) can be calculated knowing certain characteristics of the room and light source. The following method is the zonal cavity method of calculation average illumination level, which is widely used in this chapter:

$$\frac{Area}{Luminaire} = \frac{N \times Lumens\,per\,lamp \times CU \times MF}{E_{av}} \tag{2}$$

where,

N Number of lamps
CU Coefficient of Utilization
MF Maintenance Factor
E_{av} Recommended average illumination level

As it is clear in (2), recommended average illumination level is the result of solving the equation which it is a function of other variables such as lumens per lamp and number of lamps. This is while, for solving the proposed method this equation is used in reverse direction. It means that in proposed algorithm, recommended average illumination level is fixed during the computation process and the number of required lamps is maintained from the equation. With this definition, the Eq. (2) can be rewritten as:

$$N = \frac{Area\,per\,luminaire \times E_{av}}{Limens\,per\,lamp \times CU \times MF} \tag{3}$$

The Coefficient of Utilization CU is a factor that reflects the fact that not all the lumens produced by a luminary reach the surface. It depends on the particular light fixture used as well as the characteristics of the room in which it is placed, including the room size and the surface reflectance of the room. If the specific luminary is used, *CU* factor obtains from the manufacturer where usually included in product catalogs. Moreover, one can find it easily in standard tables for typical luminary such as in [21].

The Maintenance Factor (MF) is a fraction that represents the amount of light that will be lost due to things such as dirt on lamps, reduction of light output of a lamp over time, and similar factors. The following items are the individual components of the MF. So that MF is another factor in this equation which is fixed for each kind of product and is reachable by standard tables such as in [21].

Knowing the reflection coefficients of the ceiling, walls, window and door of the building which are mainly related to their materials, and also regarding the type of the luminary, maximum distance between each luminary, MF and CU, recommended average illumination level (E_{av}) is determined in accordance with the standards provided by Illuminating Engineering Society of North America (IESNA) such in [22] which is depending on room type.

For this purpose it is also necessary to calculate the space index for direct, semi-direct and uniform distribution light by following equation:

$$K_r = \frac{L \times W}{h \times (L + W)} \tag{4}$$

where,

K_r Space Index
L length of the room
W Width of the room
h Installation height of the light from flooring

Considering these methodologies, Genetic Algorithm is used to solve the proposed optimization problem in next steps.

3 Proposed Genetic Algorithm and Its Parameters

Genetic Algorithm (GA) was first proposed by Holland [23] in the early 1975s. This algorithm follows an adaptive method simulating the evolutionary process in nature and is based on the principle of nature selection and best survival. So that it is one of the optimization methods based on heredity and evolution [24].

Unlike traditional optimization methods, Genetic Algorithm is a robust search method requiring little information to search effectively in a large or poorly understood search space. Moreover, it has no prerequisite on the type of functions that it can handle, where the function is discrete or multimodal in nature.

The most important difference between this algorithm and most other heuristic methods is that a GA works on a population of possible solutions, while other heuristic methods use a single solution in their iterations. Meanwhile, GA is probabilistic, not deterministic. Considering all these advantages and nature of proposed optimal building design determination problem, GA can be a proper evolutionary method to well solve this type of problems. A flowchart describing main steps in basic Genetic Algorithm is illustrated in Fig. 2.

3.1 Chromosomes Coding

For proposed problem and before proceed with Genetic Algorithm to solve optimal design determination it is necessary to code the type of each building materials, their dimension, lighting aspects of the building and etc. Hence, coding of the potential solution is the first important aspect of a correct implementation of the GA, while, a proper coding will result not only in better solutions but in fast computations.

For proposed problem, a binary coding is used in order to representing the chromosomes' structure. The main propose of choosing binary coding instead of other chromosome descriptions such as decimal value encoding is that in binary coding one can easily arrange different kind of units together in a one string. For instants, an specific genomes of a binary coded chromosomes can represent an specific unit such as type of materials where another specific genomes can define dimensions. This is while, with this point of view, there would be neither any concern using units nor about nonlinear equation.

So that, the chromosomes consist of substrings are including different type of genomes, all in binary codes representing different type of units. A typical binary coded chromosome is illustrated in Fig. 3.

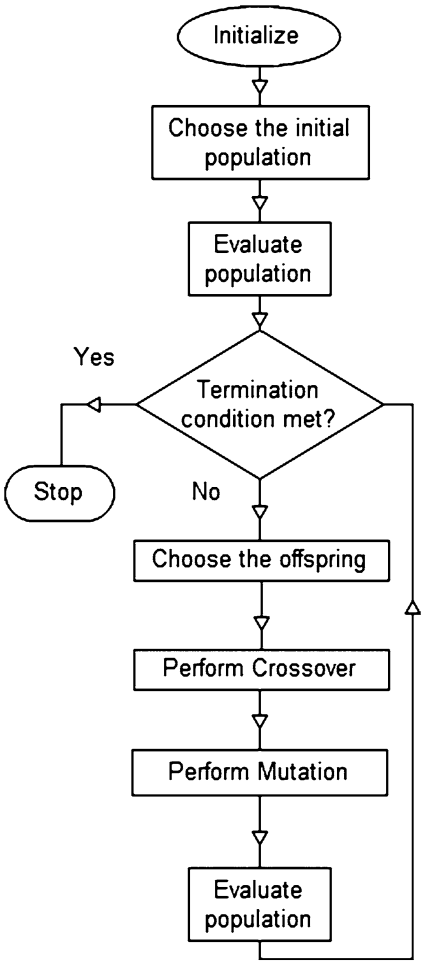

Fig. 2 Basic genetic algorithm's flowchart

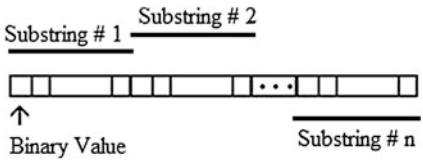

Fig. 3 A typical binary coded chromosome

3.2 Fitness Scaling

Fitness scaling converts the raw fitness scores that are returned by the fitness function to values in a range that is suitable for the selection function. The selection function uses the scaled fitness values to select the parents of the next

generation. The selection function assigns a higher probability of selection to individuals with higher scaled values.

The range of the scaled values affects the performance of the Genetic Algorithm. If the scaled values vary too widely, the individuals with the highest scaled values reproduce too rapidly, taking over the population gene pool too quickly, and preventing the Genetic Algorithm from searching other areas of the solution space. On the other hand, if the scaled values vary only a little, all individuals have approximately the same chance of reproduction and the search will progress very slowly.

Rank fitness scaling, scales the raw scores based on the rank of each individual instead of its score. The rank of an individual is its position in the sorted scores; the rank of the best fitted individual is 1, the second one is 2, and so on.

The rank scaling function assigns scaled values so that:

- The scaled value of an individual with rank n is proportional to $\frac{1}{\sqrt{n}}$.
- The sum of the scaled values over the entire population equals the number of parents needed to create the next generation

Note that Rank fitness scaling removes the effect of the spread of the raw scores.

3.3 Mutation

Although, in general, the genetic mutation probability is fixed throughout the whole search process, due to the fact that in practical application of proposed problem, a small fixed mutation probability can only result in a premature convergence, an adaptive mutation process is used to change the probability:

$$p(k+1) = \begin{cases} p(k) - p_{step} & if \quad f_{\min}(k) : unchanged \\ p(k) & if \quad f_{\min}(k) : decreased \\ P_{final} & if \quad p(k) - p_{step} < p_{final} \end{cases}$$
$$p(0) = 1.0 \qquad (5)$$
$$p_{\text{step}} = 0.001$$
$$p_{\text{final}} = 0.05$$

where,

k Generation number

p Mutation probability

Note that with this methodology the minimum mutation probability is given as 0.06 due to several experiments done for proposed solution.

3.4 Crossover

Crossover operator specifies how the Genetic Algorithm combines two individual, or parents, to form a crossover child for the next generation. Here the scattered crossover method is used which it creates a random vector and selects the genes where the vector is a 1 from the first parent, and the genes where the vector is a 0 from the second parent, and combines the genes to form the child. For example, if P1 and P2 are the parents;

P1 = [a b c d e f g h]

P2 = [1 2 3 4 5 6 7 8]

And the binary vector is [1 0 0 1 0 1 0 0], the function returns the following child:

Child 1 = [a 2 3 d 5 f 7 8]

3.5 Other Factors

In this study the population size of 150 is considered. More over the crossover factor for this population size is considered as 0.5, which demonstrates an acceptable fast convergence by means of several experimental executions. This factor determines the percentage of population which will contribute to produce crossover children.

3.6 Constraint

The proposed problem includes several constraints such as minimum size of windows, minimum and maximum area of building, maximum number of lights per each square meter, minimum average of lumens provides inside the building, minimum and maximum installation height of each construction unit and etc. all these constraint are considered in the algorithm using high penalty factors which result in elimination of corresponding child from possible solutions.

3.7 Termination

Here the termination criterion is set to stop the process at the time that no significant change occurs in fitness, for specified number of generations.

Regarding above mentioned descriptions on how to manage proposed Genetic Algorithm, this algorithm starts with initial population and continues with evaluating each reproduction. This evaluation occurs according to the fitness function

includes overall cost of building construction materials, air conditioning and lighting energy consumption as follow:

$$F_{fitness} = Min \sum_{t=0}^{\Delta T} F1(t, \alpha, \beta) + F2(t, \alpha, \beta) + F3(t, \alpha, \beta). \quad (6)$$

where, F1, F2 and F3 are objective functions of overall cost of building construction materials, air conditioning and lighting energy consumption, respectively. In this equation, "t", represents the time while Δt indicates the duration of the time under study. This is obvious that, one can easily define a short-time period or a long-term optimization by choosing a desired Δt. Moreover, above sub-functions are dependent to α and β, which represent the temperature and lighting respectively.

In order to examine the effectiveness proposed optimization method, the discussed procedure is applied to optimize the design of a hypothetical building considering above objectives. The building is assumed to be constructed in a 100 m^2 area while the construction area is limited to 60 m^2 as one of the constraints.

In this study, Installation height of the light from the ceiling is considered as a constant value during the computation process. The amount of heat generates from lights is neglected for simplification. Moreover, it is assumed that existing lights do not have any portion in lighting the building during the day times and daylight is adequate for this purpose as itself.

One can include these topics for further studies, while, it can be reachable by considering the existing lights and windows as a heating point and lighting surface respectively with specific conduction coefficients.

Table 1 provides required test data for different practical construction materials includes their technical characters and costs per square meter. Moreover, test data are available in Table 2 for two different lighting options from Philips technical catalogue implemented in further examinations, while, the cost of electric energy is assumed to be 0.0987 $/kWh.

Table 1 Test data for different practical construction materials

Item	Option	Description	Heat conduction ($W/m^2 \cdot K$)	Light reflection factor (%)	Cost ($/m^2$)
Wall	#1	White oak	0.10	31.4	52.36
	#2	White pin	0.63	27.8	41.33
Door	#1	Full wood	0.43	14.9	32.00
	#2	Beech	0.64	12.6	86.73
Window	#1	ASW-T (double layer-clear glazing)	1.80	8.4	9.23
	#2	V-cool (double layer)	1.20	9.2	11.81
Ceiling	#1	Wood with rock wool insulation	0.040	85.2	12.20
	#2	Wood with basic insulation	0.057	85.2	10.95

Table 2 Test data for different practical lighting options

Lighting option/(model number)	Description	Watts	Lumens
#1/(50/150A/WL)	Soft white	150	2,015
#2/(60G25/W/LL)	Soft white	60	700

4 Experimentations and Numerical Results

The examinations is implemented in two different scenarios; in the first scenario the only objectives of the problem is to optimize the building design considering the cost of materials as well as air conditioning energy cost, while the second one includes one more objective which is lighting energy cost.

4.1 First Scenario

In order to implement the first scenario, the air conditioning system data used for this optimization is a typical HVAC system as ones from General Electric (GE) technical data sheets.

Table 3 illustrates data performance for five typical models.

Experimental records show that the average service life of a typical HVAC unit is 10–14 years. With this assumption, the proposed method is used to optimize the building design for duration of 10 years.

The weather data are taken from meteorological data of years 2001–2011 for 10 years (As in Ref. [25]). These data are then combined to form two average annual matrixes for day/night temperatures. Where, each matrix includes 364 elements for each average days/nights temperature of one sample year. This procedure is repeated for average time of day lights and duration of nights which all data are taken from Calendar Center of Tehran University Geophysics Institute [26].

Implementing the proposed algorithm with first scenario consideration results in the construction depicted in Fig. 4.

In this construction the biggest wall in area is situated in south to north direction with 10 m long. Also there is a big size window on it where the door is situated in east side wall and opens to resulted long corridor. The resulted surfaces' dimensions as well as the materials used for each construction unit are shown in Table 4.

Table 3 Data performance for five typical HVAC models

Product number	Total capacity (kW)	Net sensible (kW)	Net latent (kW)	E.E.R.	S.E.E.R.	Sound rating (db)	CFM (L/S)
#1	5.5	4.0	1.5	12.15	14.50	74	307
#2	7.3	5.4	1.9	12.55	14.50	73	378
#3	8.6	6.2	2.4	12.85	14.50	73	484
#4	10.3	6.9	3.4	12.00	14.50	76	495
#5	14.1	9.9	4.2	12.60	15.10	76	743

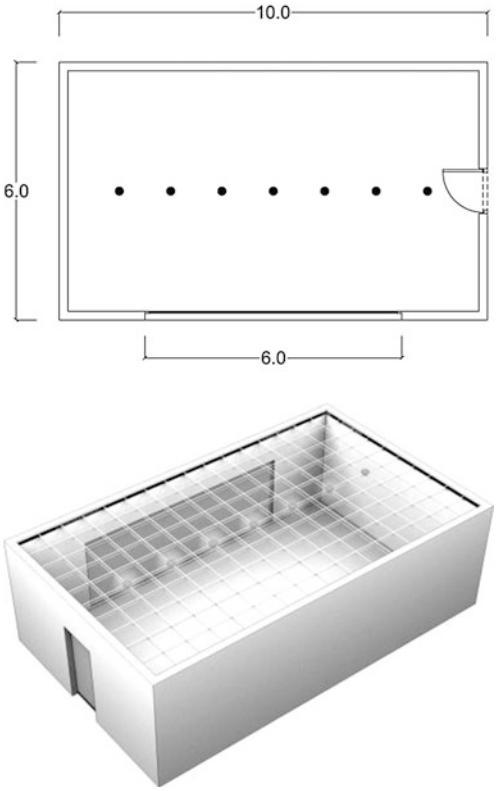

Fig. 4 Resulted construction by implementing first scenario

As it is clear from these results, since in this scenario there is no any lighting energy cost consideration, the shape of the construction is determined in a long corridor which its main side walls face to the sun directions, during more daylight times, to absorb the most heat. Also, this kind of shape shows almost less indoor heat loss while its big window south surface of the building undoubtedly has a significant impact on this result. This is while there would be seven 60 W lights which will result in high electric energy consumption with total 420 W.

Table 4 Resulted materials and their dimensions in first scenario

Item	Selected material	Length (m)	Width (m)	Installation height (m)
Wall (North)	White pine	10.0	3.1	0.0
Wall (South)		10.0	3.1	0.0
Wall (East)		6.0	3.1	0.0
Wall (West)		6.0	3.1	0.0
Door	Full wood	1.0	2.2	0.03
Window	ASW-T	6.0	2.0	0.2
Ceiling	Wood with rock wool insulation	10.0	6.0	3.1

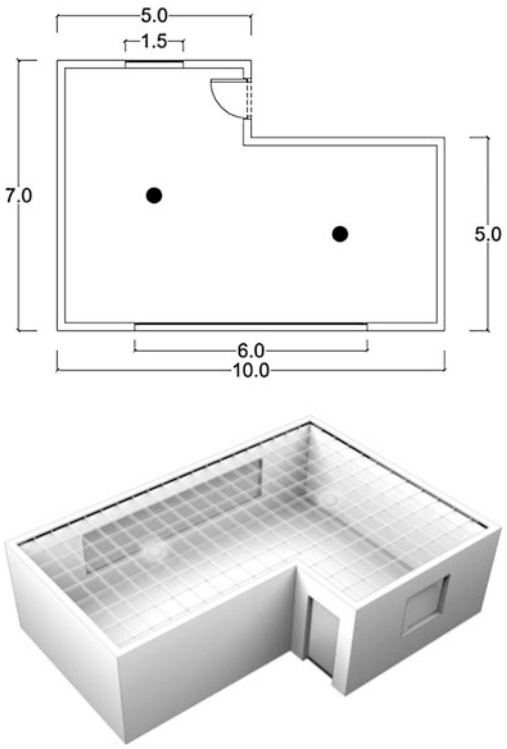

Fig. 5 Resulted construction by implementing second scenario

4.2 Second Scenario

In second scenario, previous objectives are included in proposed optimization algorithm as well as energy cost reduction for lighting. All data are same as it mentioned before.

Implementing the proposed algorithm with second scenario consideration results in the construction depicted in Fig. 5.

Again, in this construction the biggest wall in area is situated in south side with 10 m long in the same direction as in first scenario. This is while, in this optimal solution the shape of the building including two connected spaces, instead of a long corridor, is noticeable.

Again an almost big size window is satiated in the biggest side, where in this design another smaller window is on the opposite side. The door situates in east side and opens to small area section of the building.

The resulted surfaces dimensions' as well as the materials used for each construction unit are shown in Table 5.

In this design, total numbers of the required lights are decreased to total 300 W (two 150 W lights) which is resulted in total energy cost for lighting the building. Moreover, the resulted design demonstrates not only less energy loss and consumptions for air conditioning but also in construction materials cost. As it is clear

Table 5 Resulted materials and their dimensions in second scenario

Item	Selected material	Length (m)	Width (m)	Installation height (m)
Wall (North–East)	White oak	5.0	2.8	0.0
Wall (North–West)		5.0	2.8	0.0
Wall (South)		10	2.8	0.0
Wall (East)		5.0	2.8	0.0
Wall (East–North)		2.0	2.8	0.0
Wall (west)		7.0	2.8	0.0
Door	Full wood	1.0	2.2	0.3
Window (North)	V-cool	1.5	1.3	0.9
Window (South)	V-cool	6.0	1.3	0.9
Ceiling (North)	Wood with basic insulation	5.0	2.0	2.8
Ceiling (South)	Wood with basic insulation	10.0	5.0	2.8

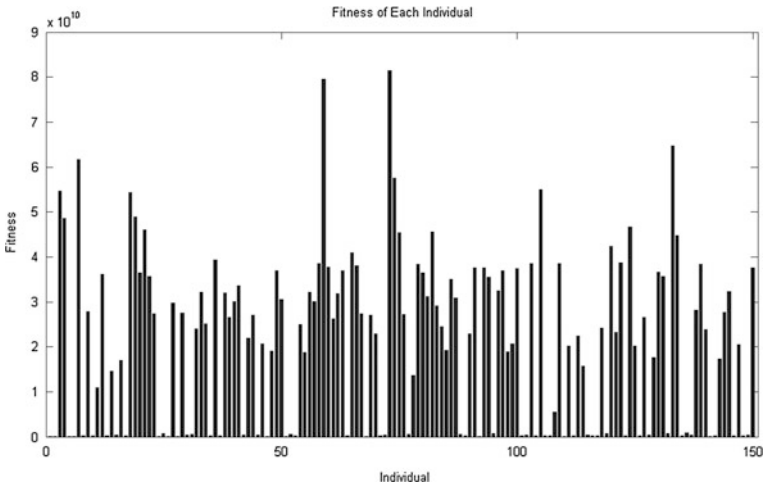

Fig. 6 Fitness diagram for 150 individuals

from these results, proposed algorithm is followed all considered objectives properly with a reasonable saving in construction and daily service costs. Figure 6 illustrates fitness of 150 individuals during the algorithm performance.

5 Conclusions

In this chapter a new procedure was proposed in order to reach optimal design for buildings. In this optimization problem, three main objectives was considered to either reduce the total cost of construction and also the energy cost of daily services; conditioning and lighting the building.

Genetic Algorithm was used to well solve the proposed problem which its advantages made it to be one of the proper and easy applying algorithms.

Fully discussed about the proposed methodology and also proposed Genetic Algorithm including its structure and operating factors, proposed procedure was implemented in two different scenarios; no energy cost of lighting was considered in first scenario and in second one the lighting energy cost was considered beside other mentioned main objectives.

In both these scenarios, experimentations demonstrated a reasonable by choosing best fitted construction materials and lights. This is while, resulted design depicts an optimal trade-off between construction costs and the total cost of energy consumption in the building including air conditioning and lighting.

For further studies, one can consider more interior and out-door design objects which will result in extra computations with same methods. Moreover, it suggested that proposed procedure to be examined with some other optimization algorithms to test the possibility of the implementation and to compare the computation speeds. Regarding to the parallel multi-objective optimization nature of the discussed problem, further studies can be done in solving the proposed method using different improved GAs such as Non-dominated Sorting Genetic Algorithm-II (NSGA-II) where it seems that desirable results can be expected like author's recent similar experiments in [27]. The last suggestion refers to applying different mathematical calculation methodologies such as the one is proposed by [28] in order to consider extra insulation units for different parts of the building which will result in more savings with heat energy loss reduction.

Acknowledgments Present chapter is a part of recent research projects by Abnieh Betonie. Authors acknowledgment financial and technical support from Abnieh Betonie Company, specially from M.Sc. Mohammad-Taghi Hassaninejad Farahani, the CEO. Faranak Ebrahimnejad Farahani's warmest acknowledgment refers to M.Sc. Armin Ebrahimi Milani for his professional support in technical evolutionary programming and computations.

References

1. Charron, R., Athienitis, A.K.: Optimization of the performance of double-façades with integrated photovoltaic panels and motorized blinds. Sol. Energy **80**, 482–491 (2006)
2. Charron, R., Athienitis, A.K.: Design and optimization of net-zero energy solar homes. ASHRAE Trans. **112**, 285–296 (2006)
3. Charron, R.: A review of design processes for low energy solar homes. Open House Int. **33**, 7–16 (2008)
4. Gero, J.S., Radford, A.D.: A dynamic programming approach to the optimum lighting problem. Eng. Optim. **3**(2), 71–82 (1978)
5. Wilcox, B.A.: Development of the envelope load equation for ASHRAE standard 90.1. ASHRAE Trans. **97**, 913–927 (1991)
6. O'Neill, J.B., Crawley, D.B., Schliesing J.S.: Using regression equations to determine the relative importance of inputs to energy simulations tools. Building Symposium'91, pp. 283–289 (1991)

7. Sander D.M., Crawley, D.B., Cornik, S., Newsham, G.R.: Development of a simple model to relate heating and cooling energy to building envelope thermal characteristics. In: 3rd International Conference of the International Building Performance Simulation Association, pp. 223–230. (1993)
8. Sullivan, R., Lee, E., Selkowitz, S.: A method for optimizing solar control and day-lighting performance in commercial office buildings. ASHRAE/DOE/BTECC Conference on the Thermal Performance of the Exterior Envelopes of Buildings (1993)
9. Baker, N., Steemers, K.: Energy and environment in architecture: A technical design guide. E&FN Spon, London (2000)
10. Dickinson, S., Bradshaw, A.: Genetic algorithm optimization and scheduling for building heating systems. Genetic Algorithms in Engineering Systems: Innovations and Applications, University of Sheffield, Conference Publication, pp. 106–111 (1995)
11. Wright, J.: HVAC optimization studies: sizing by genetic algorithm. Build. Serv. Eng. Res. Technol. **17**, 1–14 (1996)
12. Huang, W., Lam, H.: Using genetic algorithms to optimize controller parameters for HVAC systems. Energy Build. **26**, 277–282 (1997)
13. Caldas, L., Norford, L.: A genetic algorithm tool for design optimization. In: Proceedings of ACADIA'99, pp. 260–271 (1999)
14. Caldas, L., Norford, L.: Energy design optimization using a genetic algorithm. Autom. Constr. **11**, 173–184 (2000)
15. Caldas, L., Norford, L.: Architectural constrains in a generative design system: Interpreting energy consumption levels. In: Seventh International IBPSA Conference, pp. 1397–1404 (2001)
16. Caldas, L., Norford, L.: Genetic algorithms for optimization of building envelopes and the design and control of HVAC systems. Sol. Energy Eng. **125**, 343–351 (2003)
17. Tzempelikos, A., Athienitis, A.K.: The impact of shading design and control on building cooling and lighting demand. Sol. Energy **81**, 369–382 (2007)
18. Dubrow, D.T., Krarti, M.: Genetic-algorithm based approach to optimize building envelope design for residential buildings. Build. Environ. **45**, 1574–1581 (2010)
19. Fialho, A., Hamadi, Y., Schoenauer, M.: Optimizing architectural and structural aspects of buildings towards higher energy efficiency. In: 13th Annual Conference Companion on Genetic and Evolutionary Computation, pp. 727–732 (2011)
20. Chen, Y., Athienitis, Q.K., Berneche, B., Poissant, Y., Gala, K.E.: Design and simulation of a building integrated photovoltaic thermal system and thermal storage for a solar home. In: 2nd Canadian Solar Buildings Conference, pp. 1–10 (2007)
21. Hickey, R.B.: Electrical construction data book. McGraw-Hill, New York (2002)
22. Illuminating Engineering Society of North America: The IESNA lighting handbook. IESNA, USA (2011)
23. Holland, J.H.: Adaptation in natural and artificial systems: An introductory analysis with applications to biology, control and artificial intelligence. The University of Michigan Press, USA (1975)
24. Ebrahimi Milani, A., Mozafari B.: Genetic Algorithm based optimal load frequency control in two-area interconnected power systems. Global J. Technol. Optim. (GJTO), 6–10 (2011)
25. Iran Meteorological Organization. http://weather.ir
26. Calendar Center of Tehran University Geophysics Institute. http://calendar.ut.ac.ir
27. Tavakoli Shooshtari, A., Joorabian, M., Ebrahimi Milani, A.: Transmission service cost calculation with power loss and congestion considerations. Int. J. Energy Optim. Eng. (IJEOE) **1**, 39–58 (2012)
28. Taheri, S., Mammadov, M.: Solving systems of nonlinear equations using a globally convergent optimization algorithm. Global J. Technol. Optim. (GJTO), 132–138 (2012)

Mathematical Modelling of the Influence of Thermal Power Plant on the Aquatic Environment with Different Meteorological Condition by Using Parallel Technologies

Alibek Issakhov

Abstract This paper presents the mathematical model of the thermal power plant in cooling pond under different meteorological conditions, which is solved by three dimensional Navier-Stokes equations and temperature equation for an incompressible fluid in a stratified medium. A numerical method based on the projection method, which divides the problem into three stages. At the first stage it is assumed that the transfer of momentum occurs only by convection and diffusion. Intermediate velocity field is solved by method of fractional steps. At the second stage, three-dimensional Poisson equation is solved by the Fourier method in combination with tridiagonal matrix method (Thomas algorithm). At the third stage it is expected that the transfer is only due to the pressure gradient. The compact scheme was used to increase the order of approximation. Then the basic laws of the hydrothermal processes depending on different hydrometeorological conditions were determined qualitatively and quantitatively approximate.

Keywords Stratified medium · Thermal power plant · Large eddy simulation · Parallel technologies

1 Introduction

Environment—the basis of human life, as mineral resources and energy are produced from them. Moreover they are the basis of modern civilization. However, the current generation of energy cause appreciable harm to the environment, worsening living conditions. The basis of the energy—are the various types of power plants. But power generation in thermal power plants (TPP), hydro power

A. Issakhov (✉)
al-Farabi Kazakh National University, Almaty 050040, Kazakhstan
e-mail: aliisahov@mail.ru

I. Zelinka et al. (eds.), *Power, Control and Optimization*, Lecture Notes in Electrical Engineering 239, DOI: 10.1007/978-3-319-00206-4_11,

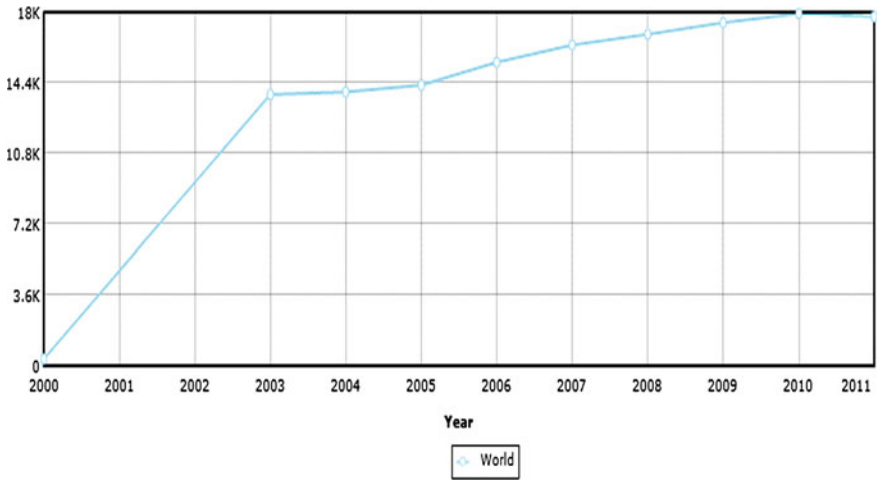

Fig. 1 Energy consumption in the world (in billion kWh)

plant (HPP) and nuclear power plants (NPP) are associated with adverse effects on the environment. The problem of the interaction of energy and the environment has taken on new features, extending the influence of the vast territory, most of the rivers and lakes, the huge volumes of the atmosphere and hydrosphere. Previously, the impact of TPP on the environment was not in first priority, as before to get electricity and heat had a higher priority. Technology of production of electrical energy from power plant is connected with a lot of waste heat released into the environment. Today the problem of influence of the nature by power is particularly acute because the pollution of the atmosphere and hydrosphere increases each year. Figure 1 shows that the energy consumption scale is increasing year by year, as a result the negative impact of energy on the environment increases too. In the terms of energy primarily guided feasibility in terms of economic were costs, but now the most important issue in the construction and operation of energy is their impact on the environment. Another problem, of TPP is thermal pollution of reservoirs or lakes. Dropping hot water—is a push chain reaction that begins reservoir overgrown with algae, it violates the oxygen balance, which in turn is a threat to the life of all its inhabitants. Thermal power plants with cooling water shed 4–7 kJ of heat for 1 kW/h electricity generation. Meanwhile, the Health Standards discharges of warm water with TPP should not raise the temperature higher than 3 °C in the summer and 5 °C in winter of the reservoir's initial temperature. As seen in Fig. 2, large proportion of electricity (81.3 %) in the world is produced by thermal power plants. Therefore, emissions of this type of power plants to the atmosphere and hydrosphere, provide the greatest amount of anthropogenic contaminants in it.

Spread of harmful emissions from TPP depends on several factors: the terrain, environmental temperature, wind speed, cloud cover, precipitation intensity. Speed

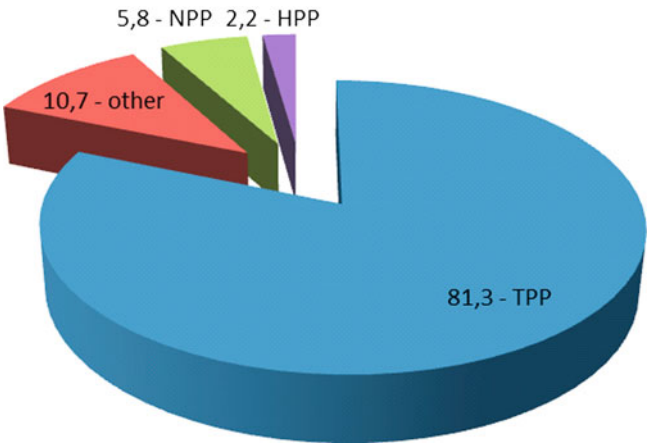

Fig. 2 Electricity production in the world by type of power plant (2010), in %

deployment and increases the thermal pollution area—are meteorology conditions. Thermal pollution of reservoirs' or lakes' water that cause multiple violations of their state is a one representation of environment danger. Thermal power plants generate energy through turbines, driven by hot steam and exhaust steam is cooled by water. Therefore, from the power plants the water flows with the temperature of 8–12 °C above the temperature of the reservoir is continuously transferred to the reservoirs or lakes itself. Large TPP shed till 90 m^3/s of heated water. For example, according to estimates of German and Swiss scientists, the possibility of rivers of Switzerland and the upper flows of the Rhine on the heating by stations heat relief have been exhausted. Hot water at any place of the river should not exceed more than 3 °C maximum temperature of the river water, which is assumed to be 28 °C. Following these conditions, the power station of Germany, constructed on the Rhine, Inna, Weser and Elbe, is limited by 35,000 MW.

Thermal pollution can lead to tragic consequences. Scientists predict changes in the characteristics of the environment in the next 100–200 years can cause large changes in the environment. Figure 3 shows the effect of TPP on the environment.

Let us consider hydrosphere pollution. Heat from TPP mainly is given to the environment from the water-cooled condenser steam turbines. The value of heat to the environment depends on the capacity of thermal power plants. Number of diverted energy to the environment is for condensing power plants from 40 % to 70 % of the thermal energy released by the combustion of fuel.

Thermal effects with through cooling water in and direct-flow-back scheme inflow and outflow water is limited by the local allowable increase in water temperature in the source water: river, lake and reservoir. Water supply system has a number of features of TPP. Almost all of the water to 95 % from total is applied to cool the condenser coils and auxiliary steam turbines. With up to 5 % of the

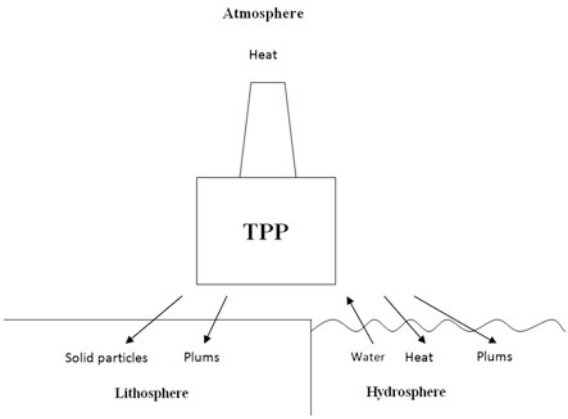

Fig. 3 TPP impact on the environment

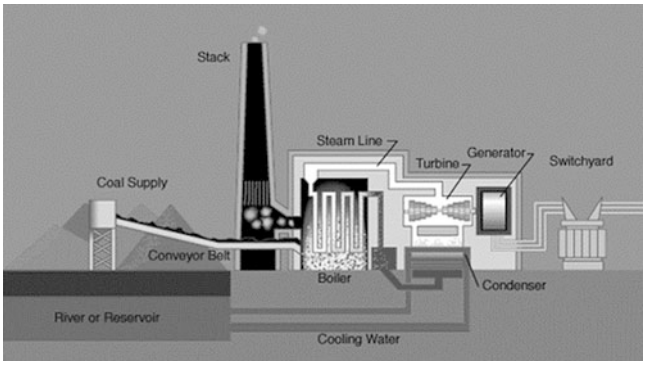

Fig. 4 Graphical scheme of cooling condensers of TPP

total value of the water supply to the thermal power plant equipment is generally irreversible consumption. As a rule, the main building of the condensing power plant is located directly at the shore line of the river, lake or reservoir-cooler. Water is supplied to the main unit of heat removal to the environment pumping stations. After heating it in condensers and heat exchangers, water is discharged to the surface water body. However, this amount of water is subject only to heating. Depending on the type of scheme water quantity of heat transfer in the once-through cooling water circuit for TPP will be minimal and some increase in the use of systems apply cooling towers. Figure 4 shows a graphical scheme of the cooling condensers of TPP with the cooling reservoir.

2 Background, Methodology and Literature Review

Often, industrial facilities, located on the shores of lakes and reservoirs disposed of warm water waste products in the form of impurities. If we consider that in the most developed countries in the cooling of thermal power plants and industrial facilities will be used by 10 % of water resources, the issues of efficient and effective use of the reservoir for cooling stations are of great importance. To solve these problems we need to be able to predict and control the temperature of the water and the spread of passive pollutants in reservoir. The distribution of temperature and passive scalar affect not only the processes of heat and mass, but also the process of density stratification. Stratification appears in connection with the difference between the density of water discharged from the density of the surrounding water in the reservoir, or the presence of impurities in the discharged water. For example, the heated water is easier, so it is in the form of a jet stretches a near the free surface. Stable density stratification of water reduces turbulent exchange between the vertical layers of fluids, especially in the area of the density jump. In general, hydrothermal regime of the reservoir is formed under the influence of uncontrollable environmental factors and factors amenable to regulation.

Strict restrictions associated with the protection of the environment were faced more often in recent years. According to the rules designer has not limit the limitation size of "zone transfer" of hot water so that it does not exceed half the width of the river and occupied no more than half of the total cross-sectional area and flow. Ignoring these rules may lead to short-term or long-term stopping of power plant, and therefore the accuracy requirements to structural analysis are very strict. In fact, emergance of the hydrodynamic problem can be described as a fully three-dimensional, with irregular boundaries, with the presence of the mass forces of buoyancy and the velocity of the main flow, which can vary by an order, sometimes it happens so fast that the important role is played by the effects of non-stationary. In addition, by certain combinations of conditions, for instance when the fault-heated water is almost drawn into the upstream region of cooling water, there are large areas of recycling. The result could be a significant loss of total operating efficiency of the system.

From the above it follows that the construction of a theoretical model relevant to real processes occurring in the water-cooler is quite big problem.

One of the first works of hydrodynamics and thermals of reservoirs—cooling was performed by Bernadskii and Proskuryakov [1]. Their method of calculation does not take into account the stratification of the environment, so hydrothermal problem was solved independently from heat. Sometimes the calculation of the hydrothermal processes reservoir—cooler part of the hydraulic calculation replace the physical simulation of flow in the reservoir. Reliable information about the reservoir, of course, give natural measurements in the field, but they are expensive, considerable difficult to hold them in the winter period. Therefore physical modeling are usually used. However, this method of study has its own difficulties,

related primarily to the conservation of the similarity criteria. Reduction of the model to tens and sometimes to hundreds times from the natural scale of the fully simulated object imposes scales. Accordingly, the greater the degree of overlapping scale there are more difference in the results of the modelling. When the simulation of overlapping scales achieve similarity of the flow this breaks the similarity of turbulent mixing, heat transfer.

Now mathematical models are based on transport equations and their numerical solution by PC [2]. The flow in the reservoir is considered as stationary, the fluid density is constant. The process of heat transfer in the water body is not fixed and it is assumed that the inertial forces, the horizontal turbulent exchange and the change in temperature with depth are negligible. This model allows us to take into account the influence of the configuration of the reservoir, the bottom topography, the position of the jet direction levees and meteorological factors, including wind. The model was used by the authors to model the flow pattern of the temperature distribution on the area of one of the specific reservoir—cooling in the U.S.

Recently, the theoretical description of phenomena in hydrothermal reservoirs—coolers are increasingly used by various schemes, taking into account the stratification. This involves using two-layer model and the model with continuous stratification depth. Two-layer models are used when the value of the local density gradient in a layer called the thermocline is large. In this case, the real picture of the bundle with a higher degree of accuracy can be schematized as a two-layer flow profile of a gap at the interface. The caused by dumping heated water in the coastal zone of the sea was studied in work [3]. Two-layer model is used to smooth the hydrothermal solutions of the problem with heat transfer to the environment, as well as the effects of buoyancy and the involvement of fluid from the lower layer at the top.

The results of mathematical modeling of hydrothermal regime of reservoirs associated with hydro accumulating power station were discussed in work [3]. The water temperature is calculated consistently for the upper and lower layer of the water reservoir at the well-known one-dimensional model. The annual cycle of temperature change with homothermy spring as initial conditions was calculated according to this model. For each horizontal layer thickness of 0.5 m average temperature is defined, but the calculations were made with an hour time step. The mathematical model includes elements like: the calculation of evaporation through the surface, selective withdrawals and outfall, the levels of the free surface, the diffusion coefficients, wind mixing and calculation of rise and the melting of the ice cover.

A two-dimensional model of vertical mathematical model for the calculation of the flow and heat transfer in a stratified reservoir has been taken in work [2]. It is based on equations of continuity, motion and heat obtained from the corresponding three-dimensional equations using formal averaging the width of the reservoir. Turbulent exchange coefficients are determined as a function of the local velocity gradients and temperature.

The most successful mathematical model of the reservoir is proposed in [4], which deals with the three-dimensional flow. The model includes the equation of turbulent motion of a thermally stratified fluid in the Boussinesq approximation. As usual, it is assumed that the distribution by vertical direction is hydrostatic.

Horizontal sharing is not considered, and a two-parameter model which contains the equations for turbulence energy and its dissipation rate is used to determine the vertical turbulent exchange coefficients. A computational algorithm using the iterative method combined with the method of fractional steps is offered for the numerical implementation of this model. Merit of the work is that the model takes into account the real borders of the reservoir, bottom relief, as well as the effect of stratification on the averaged characteristics of hydrothermal regime of the reservoir.

3 Mathematical Models

Numerical simulation was carried out on the Ekibastuz SDPP-I reservoir, located in the Pavlodar region, 17 km to the north-east of Ekibastuz city, Kazakhstan. Technical water supply of SDPP-I was carried on the back of the circuit with cooling circulating water. The surface of the reservoir is at 158.5 m, the area is 19.6 km^2, the maximum size of 4 × 6 km, the average depth of 4.6 m and a maximum depth of 8.5 m at the intake, the volume of the reservoir is 80 million cubic meters. Selective intake and spillway combined type are used in the reservoir. Waste water enters the pre-channel mixer, then through a filtration dam uniformly enters the cooling reservoir. Water intake is at a distance of 40 m from the dam at a depth of 5 m. Design flow of water 120 m^3/s, and the actual flow rate varies depending on the mode of TPP within 80–100 m^3/s. A real coastal circuit of Ekibastuz SDPP-I reservoir was constructed for the numerical simulation of this problem.

In the reservoirs—cooling spatial temperature change is small. Therefore, stratified flow in the reservoirs—cooler can be described by equations in the Boussinesq approximation. The three dimensional equations of motion, the continuity equation and the equation for the temperature are considered for the mathematical modelling. Let us consider the development of spatial turbulent stratified reservoir—cooler [5–8]. Three dimensionally model is used for distribution of temperature modelling in a reservoir [9, 10, 19]

$$\frac{\partial \overline{u_i}}{\partial t} + \frac{\partial \overline{u_j u_i}}{\partial x_j} = -\frac{\partial \overline{p}}{\partial x_i} + \nu \frac{\partial}{\partial x_j}\left(\frac{\partial \overline{u_i}}{\partial x_j}\right) + \beta g_i (T - T_0) - \frac{\partial \tau_{ij}}{\partial x_j} \tag{1}$$

$$\frac{\partial \overline{u_j}}{\partial x_j} = 0 \quad (i = 1, 2, 3). \tag{2}$$

$$\frac{\partial T}{\partial t} + \frac{\partial u_j T}{\partial x_j} = \frac{\partial}{\partial x_j}\left(\chi \frac{\partial T}{\partial x_j}\right) \tag{3}$$

where

$$\tau_{ij} = \overline{u_i u_j} - \overline{u_i}\,\overline{u_j} \tag{4}$$

g_i—the gravity acceleration, β—the coefficient of volume expansion, u_i—velocity components, χ—thermal diffusivity coefficient, T_0—the equilibrium temperature, T—deviation of temperature from the balance.

We start with regular LES corresponding to a "bar-filter" of Δx width, an operator associating the function $\overline{f}(\overline{x}, t)$. Then we define a second "test filter" tilde of large $2\Delta x$ width associating $\tilde{f}(\overline{x}, t)$. Let us first apply this filter product to the Navier-Stokes equation. The subgrid-scale tensor of the field $\tilde{\overline{u}}_i$ is obtained from Eq. (4) with the replacement of the filter bar by the double filter and tilde filter [11]:

$$\tau_{ij} = \tilde{\overline{u}}_i \tilde{\overline{u}}_j - \widetilde{\overline{u}_i \overline{u}_j} \tag{5}$$

$$l_{ij} = \tilde{\overline{u}}_i \tilde{\overline{u}}_j - \overline{u}_i \tilde{\overline{u}}_j \tag{6}$$

Now we apply the tilde filter to Eq. (4), which leads to

$$\tilde{\tau}_{ij} = \overline{u}_i \tilde{\overline{u}}_j - \widetilde{\overline{u}_i \overline{u}_j} \tag{7}$$

Adding Eqs. (6) and (7) and using Eq. (5), we obtain

$$l_{ij} = \tau_{ij} - \tilde{\tau}_{ij}$$

We use Smagorinsky model expression for the subgrid stresses related to the bar filter and tilde-filter it to get

$$\tilde{\tau}_{ij} - \frac{1}{3}\delta_{ij}\tilde{\tau}_{kk} = -2C\tilde{A}_{ij} \tag{8}$$

where $A_{ij} = (\Delta x)^2 \left|\overline{S}\right| \overline{S}_{ij}$

Further on we have to determine τ_{ij}, the stress resulting from the filter product. This is again obtained using the Smagorinsky model, which yields to

$$\tau_{ij} - \frac{1}{3}\delta_{ij}\tau_{kk} = -2CB_{ij} \tag{9}$$

where $B_{ij} = (2\Delta x)^2 \left|\tilde{\overline{S}}\right| \tilde{\overline{S}}_{ij}$

Subtraction of (8) from (9) with the aid of Germano's identity yields to

$$l_{ij} - \frac{1}{3}\delta_{ij} l_{kk} = 2CB_{ij} - 2C\tilde{A}_{ij}$$

$$l_{ij} - \frac{1}{3}\delta_{ij} l_{kk} = 2CM_{ij}$$

where

$$M_{ij} = B_{ij} - \tilde{A}_{ij} \tag{10}$$

All the terms of Eq. (10) may now be determined with the aid of $\overline{u}$. Unfortunately, there are five independent equations for only one variable C, and thus the problem is overdetermined. A first solution proposed by Germano is tensorially multiply (10) by $\overline{S}_{ij}$ to get

$$C = \frac{1}{2}\frac{l_{ij}\overline{S}_{ij}}{M_{ij}\overline{S}_{ij}}$$

This provides finally dynamical evaluation of C, which can be used in the LES of the bar field $\overline{u}$ [12, 13].

Initial and boundary conditions are defined for the non-stationary 3D equations of motion, continuity and temperature, which satisfy the equations.

4 Numerical Methods

Numerical solution of (1)–(3) is carried out on the staggered grid using the scheme against a stream of the second type and compact approximation for convective terms [14–17]. Projection method [7] is used to solve the problem in view of the above with the proposed model of turbulence. It is anticipated that at the first stage the transfer of momentum occurs only through convection and diffusion. The numerical solution of system is built on the staggered grid with usage of the scheme against a stream of the second type

$$\frac{\partial u\xi}{\partial x} = \frac{u_R\xi_R - u_L\xi_L}{\Delta x}$$

where ξ can be u,v,w

$$u_L = \frac{u_i + u_{i-1}}{2}, \quad u_R = \frac{u_{i+1} + u_i}{2}$$

$$\xi_L = \begin{cases} \xi_{i-1}, u_L > 0 \\ \xi_i, u_L < 0 \end{cases} \quad \xi_R = \begin{cases} \xi_i, u_R > 0 \\ \xi_{i+1}, u_R < 0 \end{cases}$$

and compact approximation for convective member.

$$f(x) = \frac{du}{dx}$$

$$\alpha f_{i-1} + \beta f_i + \gamma f_{i+1} = \frac{u_j - u_{j-1}}{h}$$

Factorizing the f(x) and u(x) to Taylor series we can determine α, β, γ.

For mathematical interpretation of projection method we can write like that:

1. $\frac{u^* - u^n}{\tau} = -(\nabla u^n u^* - v \Delta u^*)$
2. $\Delta p = \frac{\nabla u^*}{\tau}$
3. $\frac{u^{n+1} - u^*}{\tau} = -\nabla p.$

Intermediate field of speed is solved by using fractional steps method with the tridiagonal method (Thomas algorithm). The second stage is for pressure which is found by the intermediate field of speed from the first step. Three dimensional Poisson equations for pressure are solved by Fourier method for one coordinate in combination with the tridiagonal method (Thomas algorithm) that is applied to determine the Fourier coefficients. The numerical algorithm for three dimensional Poisson equation was parallelized on the high-performance system [18, 20].

$$p_{i,j,k} = \frac{2}{N_3} \sum_{l=0}^{N_3} \rho_l a_{i,j,k} cos \frac{\pi k l}{N_3}$$

$$-A_j \overrightarrow{a}_{j-1} + B_j \overrightarrow{a}_j - C_j \overrightarrow{a}_{j+1} = F_j$$

$$\alpha_{j+1} = (B_j - A_j \alpha_j)^{-1} C_j, \quad \alpha_1 = B_0^{-1} C_0$$

$$\beta_{j+1} = (B_j - Aj\alpha_j)^{-1} (F_j + A_j \beta_j), \quad \beta_1 = B_0^{-1} F_0$$

$$\overrightarrow{a}_j = \alpha_{j+1} \overrightarrow{a}_{j+1} + \beta_{j+1}, \quad \overrightarrow{a}_{N_2} = \beta_{N_2+1}$$

At the third stage, it is supposed that the transfer is carried out only by the pressure gradient.

5 Results of Numerical Modelling

Initial and boundary conditions were given respectively to solve these problems. The mesh of $100 \times 100 \times 100$ size was used in the numerical simulation. Figures 5 and 6 show the solved spatial contours and isolines of the temperature distribution at different times after the launch of the Ekibastuz SDPP-1, on the surface, from different angles of view. Figures 7, 8, 9, 10 show the solved spatial contour, isoline of temperature and velocity vector field at different times in the different wind directions after the launch of the Ekibastuz SDPP-1, on the surface,

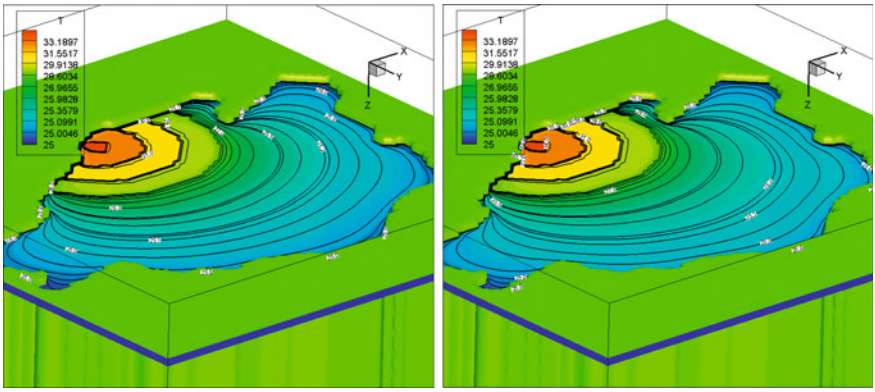

Fig. 5 Contours and isolines of the temperature distribution after 15 and 24 h after the launch of Ekibastuz SDPP-1, on the surface of the water, *the sides view*

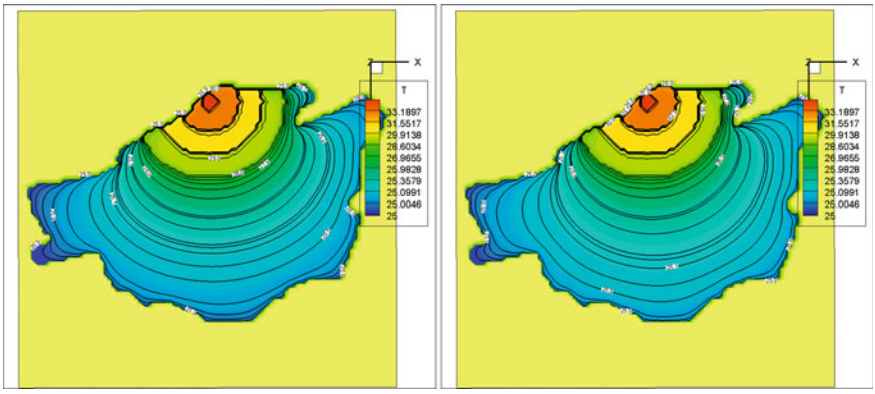

Fig. 6 Contours and isolines of the temperature distribution through 15 and 24 h after the launch of Ekibastuz SDPP-1, on the surface of the water, *the top view*

from different angles of view. In these figures we can see that temperature distribution strongly depends on wind direction and big part of heat follows in those directions.

In all figures we can see that the discharge of warm water creates a jet spreading in the longitudinal direction in the central part of the reservoir. There is a drift of recirculating flow on the surface, the lateral directions in the shallow part of the lake. The thickness of the layer of warm water and the temperature near the axis has changed slightly. At the bottom of the reservoir the most part is directed mainly towards the water intake. Current cold water is uniform in temperature. Thus, under a heavy load on the cooling reservoir and shallow enough to observe the development stratified flow. To achieve the optimal use of the reservoir for water supply power plants must have an impact on the formation of these currents.

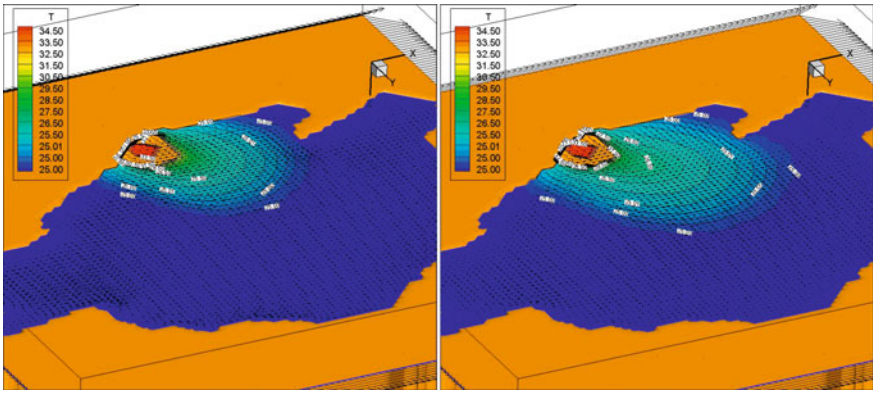

Fig. 7 Contours and isolines of temperature and velocity vector field at 15 and 24 h at the north-west wind after the launch of the Ekibastuz SDPP-1, on the surface, *the side view*

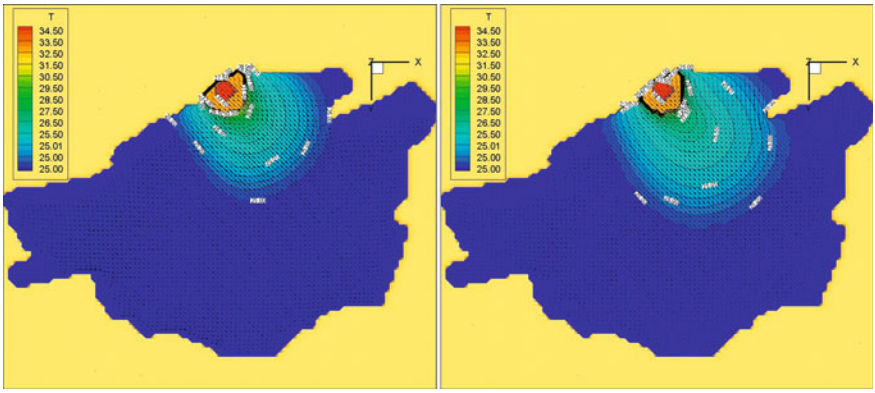

Fig. 8 Contours and isolines of temperature and velocity vector field at 15 and 24 h at the north-west wind after the launch of the Ekibastuz SDPP-1 on the surface of the water, *the top view*

6 Discussion

LES is a more universal approach to the construction of closure for large-eddy simulation models. A necessary condition for the performance of turbulent closures is the ability to "subgrid" model correctly describe the dissipation of the kinetic energy of smoothed velocity fluctuations—the ability to simulate the circuit direct energy cascade from large to small eddies. This stage is the primary mechanism for the redistribution of energy in the inertial range of three-dimensional homogeneous isotropic turbulence.

The principal advantage of the LES from RANS is that, due to the relative homogeneity and isotropy of the small-scale turbulence, plotting a subgrid model is much simpler than the construction of turbulence models for RANS, when it is

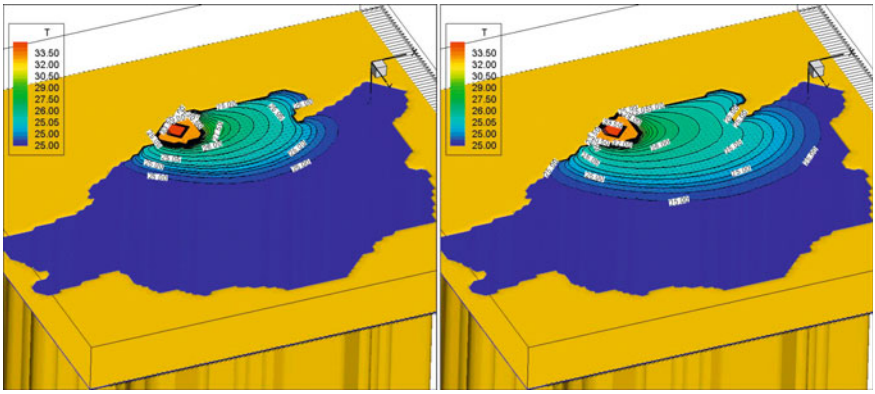

Fig. 9 Contours and isolines of temperature and velocity vector field at 15 and 24 h at the north wind after the launch of the Ekibastuz SDPP-1, on the surface, *the side view*

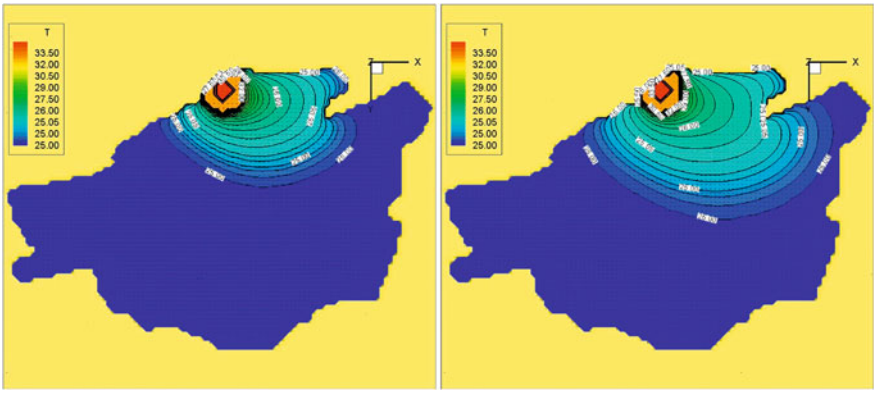

Fig. 10 Contours and isolines of temperature and velocity vector field at 15 and 24 h at the north wind after the launch of the Ekibastuz SDPP-1 on the surface of the water, *the top view*

necessary to model the full range of turbulence. For the same reason, the hope for a "universal" subgrid model for LES are much more reasonable than a similar model for RANS. Natural price to pay for these important benefits LES is a significant increase computational cost associated with the need (as in the case of DNS) of three-dimensional time-dependent calculations on sufficiently fine grids, even in cases where direct interest to the practice of the average flow is two-dimensional and stationary. On the other hand, for obvious reasons, the computational resources required to implement the LES, is much smaller than for the DNS.

The degree of influence of different processes governing the formation of stratified flows and hydrothermal conditions, the entire body of water can be divided into two zones: the first (near), directly adjacent to the water outlet structures, and the second is for the major part of the reservoir. In the near zone forming stratified flow is influenced by the processes of mixing water discharged

from the water reservoir and its possible regulation by creating a specific hydraulic regime in the outfall. In the second zone of hydrothermal regime is formed primarily by the processes of heat transfer. The propagation of heat in this part of the reservoir is more dependent on the wind (direction and speed). When you reset the heated water density jump appears in a cold environment between the upper layer of warm water and cold bottom, where there is a compensation for the direction toward the spillway. This allows the use of a combined intake and outfall instead of building costly diversion canals to the spillway. This raises the problem of optimal choice of the geometrical and operational parameters of the cooling pond for efficient power plant.

7 Conclusions

All the figures show that the temperature distribution with distance from the flow approaches the isothermal distribution. The numerical results show that the temperature distribution is distributed over a larger area of the reservoir—cooler.

Thus, using a mathematical model of three-dimensional stratified turbulent flow can be determined qualitatively and quantitatively approximate the basic laws of the hydrothermal processes occurring in the reservoirs. And we can see that distribution of temperature more depend on meteorological conditions.

References

1. Bernadksii, N., Proskuryakov, B.: Theory and Practice of Calculations of the Cooling Pond. GosEnergoizdat, Mascow (1933)
2. Harper, W.L., Waldrop W.R.: Numerical hdrodynamics of reservoir stratification and density currents. 2nd International Symposium Stratified flow. Norwegian Institute and Technology, Trondheim, pp. 1011–1020 (1980)
3. Wada, A.: Study of thermal diffusion in a two-layer sea caused by outfall of cooling water. International Symposium Stratified flow, paper 21, Novosibirsk (1972).
4. McGuirk, J.J., Rodi W.: Mathematical modelling of three dimensional heated surface jets. J. Fluid Mech., 609–633 (1979)
5. Fletcher, C.A.: Computational techniques for fluid dynamics. Special Techniques for Differential Flow Categories, vol. 2. p. 493. Springer, Berlin (1988)
6. Roache, P.J.: Computational Fluid Dynamics. p. 446. Hermosa Publications, Albuquerque, NM (1972)
7. Peyret, R., Taylor, D.Th.: Computational Methods for Fluid Flow. p. 358. Springer, Berlin, (1983)
8. Tannehill, J.C., Anderson, D.A., Pletcher, R.H.: Computational Fluid Mechanics and Heat Transfer, 2nd edn. p. 816. McGraw-Hill, New York (1997)
9. Issakhov, A.: Mathematical modeling of the influence of hydrothermal processes in the water reservoir. In: Proceedings of World Academy of Science. Engineering and Technology, Issue **69**, 632–635 (2012)

10. Issakhov, A.: Mathematical modelling of the influence of thermal power plant to the aquatic environment by using parallel technologies. In: Proceeding of Sixth Global Conference on Power Control and Optimization, p. 34. Las Vegas, USA, (2012). ISBN: 978-983-44483-56.
11. Germano, M., Piomelli, U., Moin, P., Cabot, W.H.: A dynamic subgrid-scale eddy viscosity model. Phys. Fluids. A **3**, 1760–1765 (1991)
12. Lesieur, M., Metais, O., Comte, P.: Large Eddy Simulation of Turbulence. p. 219. Cambridge University Press, New York (2005)
13. Tennekes, H., Lumley, J.L.: A First Course in Turbulence. p. 390. The MIT Press, Cambridge (1972)
14. Tolstykh, A.I.: Compact difference scheme and their applications to fluid dynamics problems. p. 230. Nauka, Mascow (1990)
15. Yanenko, N.N.: The Method of Fractional Steps. Springer, New York. In Bunch, J.B., Rose, D.J. (eds.) Space Matrix Computations. p. 168. Academics Press, New York (1979)
16. Issakhov, A.: Large eddy simulation of turbulent mixing by using 3D decomposition method. J. Phys.: Conf. Ser. 318(4), 042051 (2011)
17. Zhumagulov, B., Issakhov, A.: Parallel implementation of numerical methods for solving turbulent flows. Vestnik NEA RK **1**(43), 12–24 (2012)
18. Issakhov, A.: Parallel algorithm for numerical solution of three-dimensional Poisson equation. In: Proceedings of World Academy of Science. Engineering and Technology, Issue **64**, 692–694 (2012)
19. Issakhov, A.: Mathematical modelling of the influence of thermal power plant to the aquatic environment by using parallel technologies. AIP Conf. Proc. **1499**, 15–18 (2012). doi:http://dx.doi.org/10.1063/1.4768963
20. Issakhov, A.: Development of parallel algorithm for numerical solution of three dimensional Poisson equation. J. Commun. Comput. **9**(9), 977–980 (2012)